

Boron-Nitrogen Derivatives of Organic Reactive Intermediates

Dissertation

der Mathematisch-Naturwissenschaftlichen Fakultät

der Eberhard Karls Universität Tübingen

zur Erlangung des Grades eines

Doktors der Naturwissenschaften

(Dr. rer. nat.)

vorgelegt von

Sunanda Biswas

aus Nadia, West Bengal, India

Tübingen

2011

Tag der mündlichen Qualifikation:

30.01.2012

Dekan:

Prof. Dr. Wolfgang Rosenstiel

1. Berichterstatter:

Prof. Dr. Holger F. Bettinger

2. Berichterstatter:

Prof. Dr. Lars Wesemann

Acknowledgements

This doctoral work was carried out from September 2007 to July 2009 at Lehrstuhl für Organische Chemie II, Fakultät für Chemie and Biochemie, Ruhr-Universität Bochum, Germany and from August 2009 to November 2011 at the Institut für Organische Chemie der Mathematisch-Naturwissenschaftlichen Fakultät, Eberhard Karls Universität Tübingen, Germany, under the guidance of Professor Dr. Holger F. Bettinger.

I convey my sincere reverence and gratitude to all of them who have been closely associated with me for the last few years in some way or other and thereby enabling me to achieve this. It is my great privilege to acknowledge them.

First and foremost, I express my heartfelt thanks to Professor Holger F. Bettinger for giving me the opportunity to work on this extremely interesting and challenging project. I am grateful for his valuable discussions and suggestions which have not only helped me to solve many problems but also have enriched my knowledge. He gave me the independence in my endeavour to develop scientific skills and rationale, and also trained me to become a good human being. I convey my sincere gratitude for being such a great support throughout my work.

I thank Prof. Dr. Iris M. Oppel and Manuela Winter from Ruhr-Universität Bochum, Dr. Cécilia Maichle-Mössmer and Elke Niquet from Universität Tübingen for their great contribution in X-ray crystallography measurements.

A special recognition needs to be given to Dr. Dorothee Wistuba from Universität Tübingen for her technical assistance in many chromatographic analyses and HRMS measurements.

I express my gratitude to Assistant Professor Dr. Tapas Kar from Utah State University, USA for his helpful discussion in computational work.

I would like to thank all my friends and lab mates for their cordial support and inspiration during my study in Bochum as well as in Tübingen.

Finally, I am thankful to my beloved friend Arijit Kumar Chatterjee and to my family for their unconditional love and encouragement.

Publications

1. S. Biswas, I. M. Oppel and H. F. Bettinger, "Synthesis and Structural Characterization of 9-Azido-9-Borafluorene: Monomer and Cyclotrimer of a Borole Azide". *Inorg. Chem.*, **2010**, *49*, 4499.
2. S. Biswas, M. Müller, C. Tönshoff, K. Eichele, C. Maichle-Mössmer, A. Ruff, B. Speiser, H. F. Bettinger, "An Overcrowded Borazine Derivative of Hexabenzotriphenylene via Dehydrohalogenation" *submitted*.
3. S. Biswas, C. Maichle-Mössmer and H. F. Bettinger, "From the Borole to the Azaborine Motif via a Formal Dyotropic Rearrangement" *manuscript under preparation*.

List of Oral and Poster Presentations

1. "Structure and Reactivity of Novel Azidoboranes". A poster presentation at **IMEBORON XIII**, International Conference on Boron Chemistry, (P031) September 21st – 25th, **2008**; held at Platja d'aro, Spain.
2. "A Novel Synthetic Approach to 9-Azido-9-borafluorene and 1,2:3,4:5,6-tris-(1,2'-biphenylene)borazine (TBB)". A poster presentation at **EuroBoron5**, August 29th – September 2nd, **2010**; held at Harriot-Watt University, Edinburgh, UK.
3. "Attempt to generate 9,10-didehydroazaborine". An oral presentation at **Borchemiker-Treffen**, October 8th – 10th, **2010**; held at Hotel Krone, Hirschberg-Großsachen, Germany.

To my Parents

Abbreviations

9-BBN	9-Borabicyclo[3.3.1]nonane
BCl ₃	Boron trichloride
Bn	Benzyl
br	Broad (NMR)
CH ₂ Cl ₂	Dichloromethane
COSY	Correlation Spectroscopy
δ	Chemical shift in ppm (NMR)
d	Doublet (NMR)
EI	Electron impact
equiv	Equivalent
ESI	Electrospray Ionization
Et	Ethyl
g	gram
h	Hour(s)
HRMS	High Resolution Mass Spectrometry
HSQC	Heteronuclear Single-Quantum Correlation Spectroscopy
Hz	Hertz
<i>i</i> -Pr	Isopropyl
<i>J</i>	Coupling constant
L	liter
m	Multiplet
M	mol/L
mg	milligram
min	Minute

Abbreviations

mL	Milliliter
NMR	Nuclear magnetic resonance
NOESY	Nuclear Overhauser Effect Spectroscopy
ppm	Parts per million
py	Pyridine
R _f	Retention factor (TLC)
R _t	Retention time
RT	Room temperature
s	Singlet (NMR)
t	Triplet (NMR)
<i>t</i> -Bu	Tertiarybutyl
THF	Tetrahydrofuran
TMP	2,2,6,6-tetramethylpiperidino
TMS	Trimethylsilyl

Table of Contents

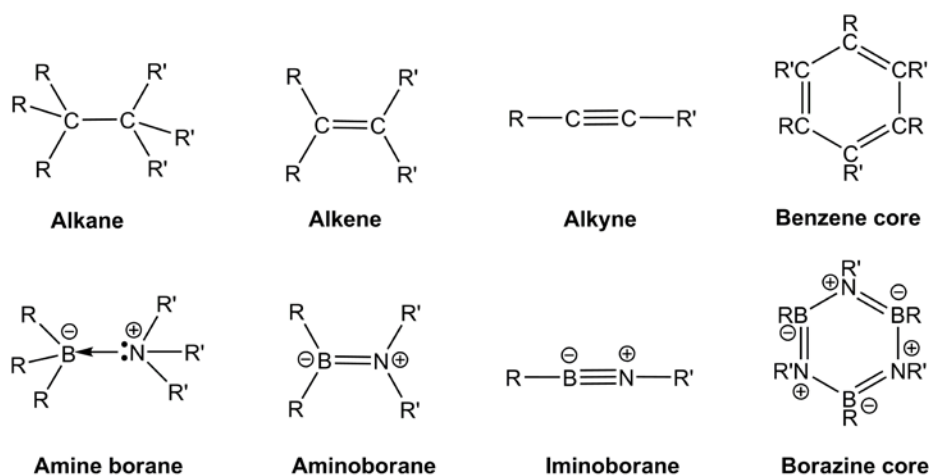
1. Introduction.....	1
1.1 Comparative Study of Isostructural CC and BN Compounds	1
1.2 BN Analogs of CC Reactive Intermediates	2
1.3 Borylnitrene	3
1.4 Aminoborylene	5
1.5 Iminoborane	8
1.6 1,2-Azaborine.....	15
2. Motivation.....	17
3. Diphenylaminoborylene	18
3.1 Matrix Isolation Technique.....	18
3.2 Synthetic Methodology.....	22
3.3 Synthesis	23
3.4 Matrix Isolation Experiment	28
4. 9,10-Didehydro-9-aza-10-boraphenanthrene.....	32
4.1 Theoretical Study	32
4.2 Synthetic Strategies.....	35
5. The Azide Route via 9-Azido-9-borafluorene	36
5.1 Introduction.....	36
5.2 Computational Analysis.....	37
5.3 Results and Discussion	39

6. Route via Silyl(silyloxy)aminoborole	58
6.1 Background Informations and Proceedings	58
6.2 Results and Discussions	62
6.3 Conclusion	75
7. Route via Dehydrohalogenation	76
7.1 Introduction.....	76
7.2 Results and Discussions.....	78
7.2.1 Dehydrohalogenation Approaches with Bases of Different Strength.....	78
7.2.2 Reactions with Trapping Agents.....	96
7.3 Conclusion	105
8. Experimental Section.....	107
8.1 General Procedure and Equipments.....	107
8.2 Computation.....	111
8.3 Synthesis	112
A. Crystallographic Data.....	124
B. Selected NMR Spectra	149
C. Bibliography	184

1. Introduction

1.1 Comparative Study of Isostructural CC and BN Compounds

The distinct behavior of the compounds containing boron-nitrogen unit, in place of carbon-carbon unit, lead the chemists to investigate their properties. The key factor in this chemistry is the empty p orbital of the boron atom which calls for the chances to tune the properties of such systems by coordination of a lone pair from the donor atom and the isoelectronic relationship between B–N and C–C units. The difference in reactivity of these two BN and CC containing compounds is attributed to the polarity difference of the B–N bond compared to that of the C–C bond. There are four classes of organic BN compounds which are comparable to the isoelectronic carbon analogs (Chart 1.1). These are: (1) amine boranes, $R_3B-NR'_3$, isoelectronic to alkanes, (2) aminoboranes, $R_2B=NR'_2$, isoelectronic to the alkenes, (3) iminoboranes, $RB\equiv NR'$, isoelectronic to the alkynes and (4) borazines, $(-RB-NR'-)_3$, isoelectronic to benzene; which have been nicely reviewed by Paetzold.^[1, 2]



R = R' or R = R'; R and R' positions are interchangeable

Chart 1.1 Different types of BN analogs of carbon compounds.

Among these four types of BN compounds, iminoboranes ($RB\equiv NR'$) are unstable towards

isolation at ambient conditions unless bulky substituents are introduced. Due to high sensitivity towards oxygen and moisture the synthesis and isolation of the boron nitrogen compounds are quite challenging. The amine boranes, aminoboranes and iminoboranes, all have vacant p_z orbitals on the boron centers and thus they are keen toward coordination by donor atoms and so for water or oxygen. Only borazines are found to be air stable. Very accurately the BN bonds should be written with a positive charge on the nitrogen atom and negative charge on the boron atom, but authors like P. Paetzold, R. Köster sometimes omitted the charges in the chemical structures which are followed throughout this dissertation.

1.2 BN Analogs of CC Reactive Intermediates

The simple C_2 reactive intermediate known is vinylidene (RRCC). Formal substitution of CC by BN provides boryl nitrene (**A**) and aminoborylene (**B**) (Chart 1.2). As mentioned earlier, iminoboranes (**C**) are only isolable under special circumstances; they can thus also be considered as reactive intermediates. Whereas benzyne (only *ortho*-benzyne has been taken into account) is well investigated, the BN analog i.e. 1,2-azaborine (**D**) is not known to exist so far (Chart 1.2, Charges on BN compounds are drawn for comparison).

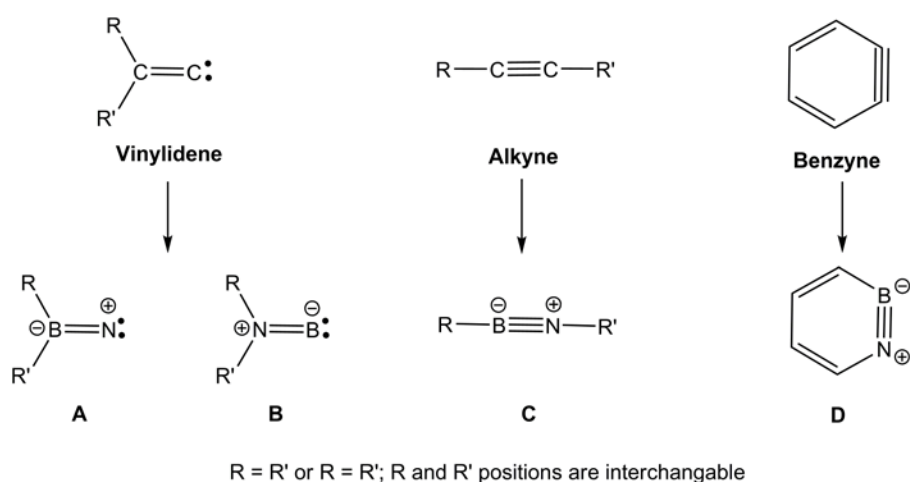
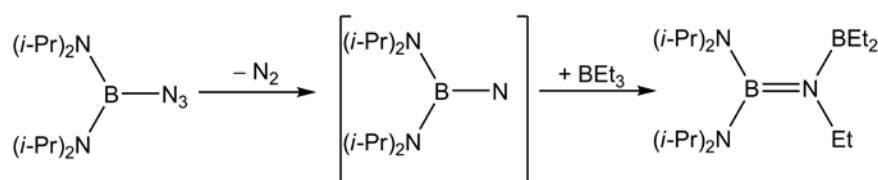


Chart 1.2 BN analogs of CC reactive intermediates.

1.3 Borylnitrene

Borylnitrene (**A**) can be obtained from photochemical and thermal decomposition of azidoboranes by eliminating one nitrogen molecule. In 1981 Pieper et al. reported the first successful trapping of a donor stabilized borylnitrene.^[3] These authors have found that the photolysis of diaminoazidoboranes, $(R_2N)_2BN_3$ ($R = i\text{-Pr}$, 2,6-dimethylpiperidino), generate the corresponding borylnitrenes and these highly reactive species immediately stabilize themselves through intramolecular reactions. The $(i\text{-Pr})_2BN$ has been trapped by ethylboration with BEt_3 according to the Scheme 1.1.

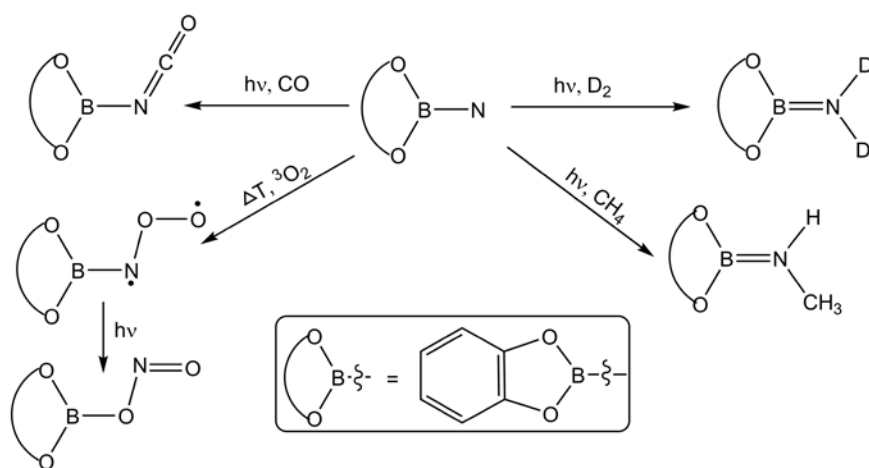


Scheme 1.1 Generation and trapping reaction of $(i\text{-Pr})_2BN$.^[3]

Nitrenes generally prefer triplet ground states.^[4] The presence of the vacant boron p-orbital located on the Lewis acidic boron center which interacts to the nitrogen atom can influence the energetic ordering of the electronic states. In the case of parent borylnitrene (**A**), the singlet state (\tilde{X}^1A_1) is favored by 12 kcal mol^{-1} over the triplet state (\tilde{A}^3B_1) according to the calculations.^[5-7] However, these computations show that the singlet state corresponds to a first order stationary point on the potential energy surface and rearranges to iminoborane (**C**)^[5, 7] if the C_{2v} symmetry constraint is removed in the geometry optimization. In the case of donor stabilized borylnitrenes, the Lewis acidity of the boron atom is reduced, and the triplet state is lower in energy than the singlet state. In 2006, the borylnitrene was characterized spectroscopically for the first time under the condition of matrix isolation by Bettinger and Bornemann.^[7] They found that nitreno-1,3,2-benzodioxaborol (catBN; cat = catecholato)

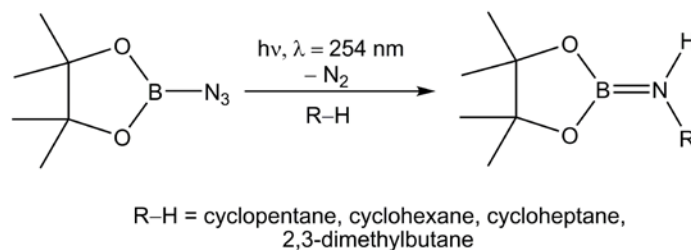
prefers the triplet state. Here, the energy difference between the triplet ground state and the lowest singlet state is 33 kcal mol⁻¹ according to the computational analysis at the CCSD(T)/cc-pVTZ level of theory. This study of catBN has shown that the electronic energy of states of a borylnitrene can be altered significantly by the substituents of the boron center.

Borylnitrenes are found to be extremely reactive even at cryogenic temperatures.^[8] The catechol derivative of borylnitrene (catBN) can split the H–H bond or functionalize the unactivated C(sp³)–H bond of methane at 10 K upon photo excitation.^[8-10] Upon annelation an oxygen doped argon matrix to 35 K catBN produces the nitroso-O-oxide that is unstable towards photoirradiation ($\lambda = 254$ nm) and rearranges to the nitritoborane (Scheme 1.2).^[7, 8] The catBN also undergoes rapid reaction with CO as well as N₂ to give the corresponding isocyanate and the catecholazidoborane, respectively, upon visible light irradiation ($\lambda > 550$ nm) (Scheme 1.2).^[7, 9] This unusual high reactivity of catBN was explained by the electronic similarity between the singlet state of catBN and difluorovinylidene (F₂CC). The latter was detected in cryogenic matrix^[11] and shows extremely high electrophilicity and inserts into methane as well as H₂ at 20 – 40 K.^[12, 13]



Scheme 1.2 Reactivity of catBN.

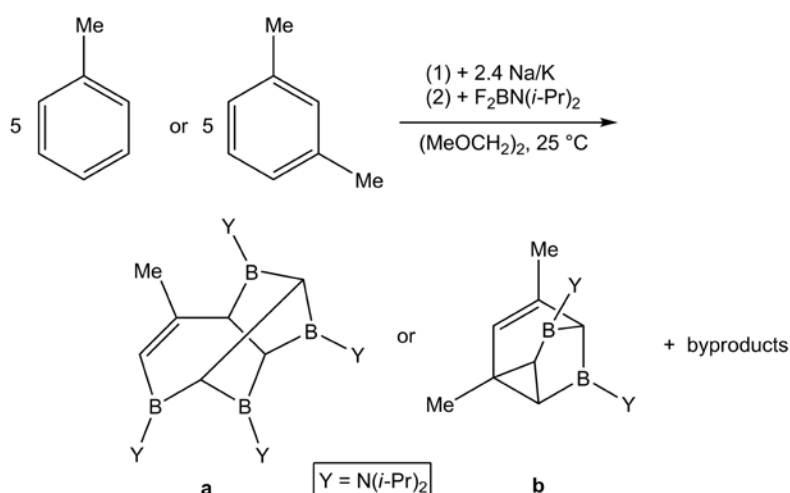
At ambient temperature the pinacol borylnitrene (PinBN) displays a profound reactivity towards C–H bonds of (cyclo)alkanes in solution.^[9] This result opens a new opportunity for a one-pot transformation of an alkane into primary amine or into amide in good yields without using any metal simply via photochemical C–H activation by borylnitrene followed by alcoholysis or acylation reaction (Scheme 1.3).^[14]



Scheme 1.3 Reactivity of pinBN in solution.

1.4 Aminoborylene

The synthesis of aminoborylene, R_2NB (**B**) basically relies on the dehalogenation of dihalo(diakylamino)borane (X_2BNR_2 , $X = F, Cl, Br$; $R = i\text{-Pr}, TMS$) by metal.^[15-18] Meller et al. have studied the reactivity of such transient species with different aromatic systems. In benzene, the aminoborylene forms $C_6H_6 \cdot xBN(i\text{-Pr})_2$ ($x = 1 - 6$) in the reaction of dichloro(diisopropylamino)borane with Na/K alloy in 1,2-dimethoxyethane according to mass spectrometric studies.^[16, 19] The reactions of $F_2BN(i\text{-Pr})_2$ with different substituted benzene rings e.g. toluene, isopropylbenzene, *t*-butylbenzene also brought the same observations under similar reaction conditions.^[16] But the addition of aminoborylene unit depends on the number of substituents on the benzene ring. With benzene up to six $BN(i\text{-Pr})_2$ units can be added,^[19] whereas for toluene and *m*-xylene the numbers are four and two, respectively (**a** & **b** Scheme 1.4).^[15, 16] The structures of **a** and **b** were confirmed by X-ray diffraction.



Scheme 1.4 Insertion reaction of $(i\text{-Pr})_2\text{NB}$ to the aromatic rings.^[15]

In contrast the carbon analog of aminoborylene i.e. vinylidene inserts only one unit into the benzene ring.^[20] The higher reactivity of this borylene than that of carbene is due to the higher electron deficiency of the boron atom. The four-electron species borene results in multiple additions to aromatic systems whereas carbene, a six-electron system, leads to only one addition.^[16]

In 1995 Andrews' group identified the parent aminoborylene species, BNH_2 in an argon matrix after co-deposition of laser ablated boron atoms with ammonia at 10 K with absorption frequencies at 1530 and 596 cm^{-1} .^[21] Very recently, Kinjo et al. have successfully characterized the parent borylene (BH) supported by two cyclic alkyl(amino)carbenes (CAACs) and demonstrated its unusual basic property.^[22] Also Braunschweig's group has reported the trapping products of the N-heterocyclic carbene (NHC) stabilized parent borylene (BH) with naphthalene recently.^[23]

It is also to be mentioned here that the borylene ligands can be stabilized by coordinating with metal(s).^[24] Many metal-borylene complexes are known with structural diversities. The borylene ligands are found to co-ordinate to the metal(s) in two fashions:

either bridging between two metal centers or in a terminal fashion with co-ordination number two. Few selected examples of metal stabilized bridged-aminoborylene^[25-28] and terminal-aminoborylene complexes^[29, 30] are shown in Figure 1.1.

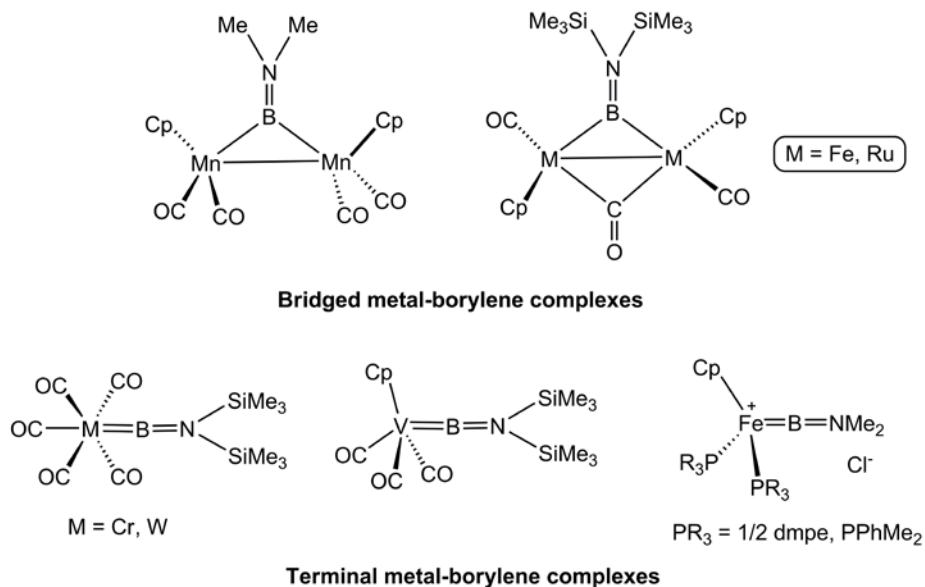
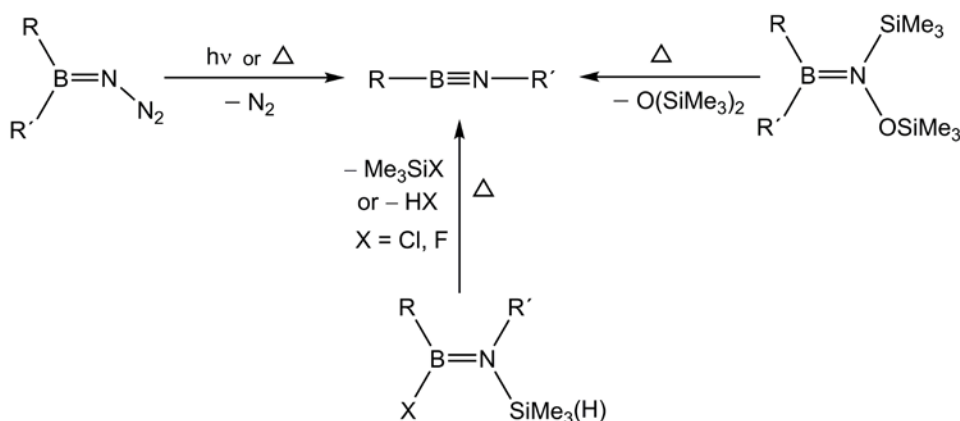


Figure 1.1 Examples of metal-aminoborylene complexes.

In earlier reports, the general route to obtain the terminal borylene complexes is the salt elimination reaction from dianionic carbonylmetallates and dihaloboranes. In 2001, Braunschweig et al. reported photochemically induced intermetallic borylene transfer as an alternative path to get both bridged and terminal metal-borylene complexes.^[31, 32] Recently, the Aldrich group has reported the spontaneous formation of cationic aminoborylene metal complex, $\text{Cp}(\text{R}_3\text{P})_2\text{Fe}=\text{B}=\text{NMe}_2^+\text{Cl}^-$ [$\text{R} = \frac{1}{2} \text{ dmpe, PPhMe}_2$] by halide ejection from the corresponding chloride, i.e. $\text{Cp}(\text{R}_3\text{P})_2\text{FeB}(\text{Cl})\text{NMe}_2$ [$\text{PR}_3 = \frac{1}{2} \text{ dmpe (1,2-bis(dimethylphosphino)ethane), PPhMe}_2$] in polar solvent like dichloromethane and/or chloroform.^[30]

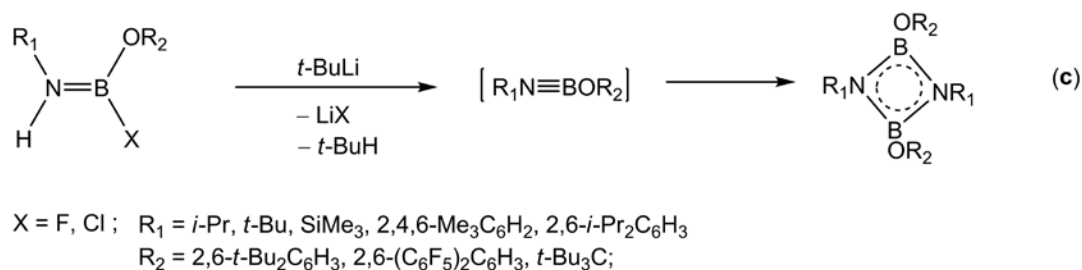
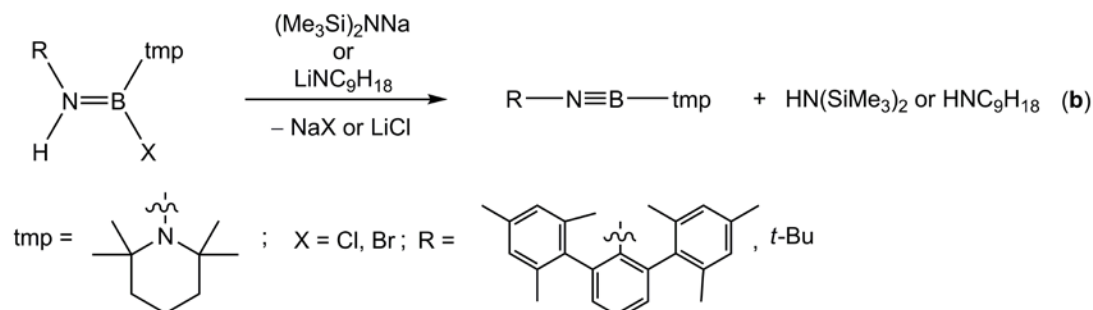
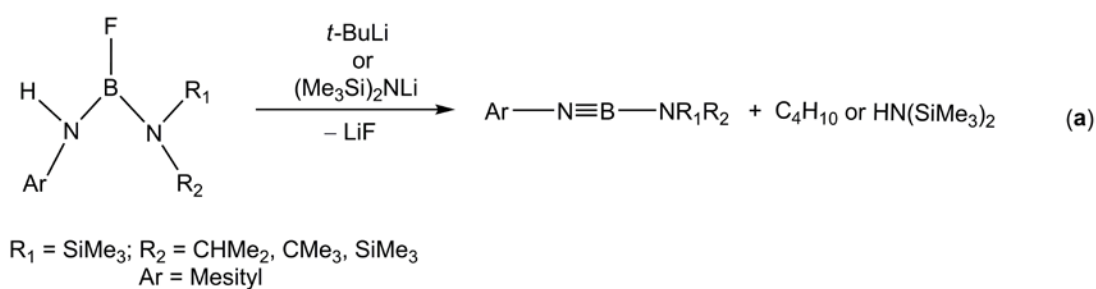
1.5 Iminoborane

In general, the iminoboranes, $\text{RB}\equiv\text{NR}'$ (**C**) are metastable species and prone to cyclooligomerization provided there are no bulky ligands that prevent oligomerization. The parent iminoborane $\text{HB}\equiv\text{NH}$ was the first iminoborane to be identified spectroscopically.^[33] This was formed as the major product by photolysis of amine-borane ($\text{H}_3\text{N}\cdot\text{BH}_3$) under matrix isolation condition. In 1979 iminoborane with two-coordinate boron, $\text{C}_6\text{F}_5\text{-B}\equiv\text{N-}t\text{-Bu}$, was first isolated and characterized.^[34] This compound can be stored and handled at low temperature ($-30\text{ }^\circ\text{C}$). Comparison of the bond lengths of $\text{C}\equiv\text{C}$ (118 pm) and $\text{B}\equiv\text{N}$ (124 pm) clearly shows that the $\text{C}\equiv\text{C}$ bond is much stronger than $\text{B}\equiv\text{N}$ bond and therefore the $\text{B}\equiv\text{N}$ bond containing compounds become more reactive than simple alkynes.^[2] Paetzold et al. have successfully synthesized a number of iminoboranes and studied their properties extensively.^[34-44] The synthetic strategy to generate iminoborane can be divided in three ways, (i) from azidoboranes by photochemical or thermal elimination of nitrogen followed by 1,2-shift of one of the substituents from the boron atom to the nitrogen atom;^[38, 45] (ii) thermolysis of silyl(silyloxy)aminoboranes, $\text{RR}'\text{B}=\text{N}(\text{SiMe}_3)(\text{OSiMe}_3)$ ($\text{R}, \text{R}' = \text{Pr}, \text{Bu}$) and elimination of hexamethyldisiloxane, $(\text{Me}_3\text{Si})_2\text{O}$ followed by migration of R or R' ;^[38, 46] and (iii) by thermal elimination of TMSX or HX [$\text{X} = \text{F}, \text{Cl}$] from $\text{R}(\text{Cl})\text{B}=\text{N}(\text{SiMe}_3)\text{R}'$,^[36, 38] $\text{R}(\text{Cl})\text{B}=\text{N}(\text{H})\text{R}'$,^[35] $\text{R}(\text{F})\text{B}=\text{N}(\text{SiMe}_3)\text{R}'$ (Scheme 1.5).^[47]



Scheme 1.5 Different synthetic approaches for iminoboranes.

Apart from these three main procedures, base induced dehydrohalogenation reaction is also reported as another successful route to iminoboranes for three special cases. The bis-(amino)(halo)boranes of the type Ar-N(H)-B(X)-NR_2 are able to produce iminoboranes upon treatment with different bases (Scheme 1.6a & b).^[48-51] In 2000 Meller et al. reported the in situ generation of organyloxy(imino)boranes, $\text{RO-B}\equiv\text{N-R}'$ from amino(halo)(organyloxy)boranes $[\text{R}_1\text{O-B(X)-N(H)R}_2]$ with $t\text{-BuLi}$.^[52] In this case the iminoboranes are unstable and form the corresponding cyclodimers (Scheme 1.6c) but the formation of iminoboranes have been detected by ^{11}B NMR studies.^[52]

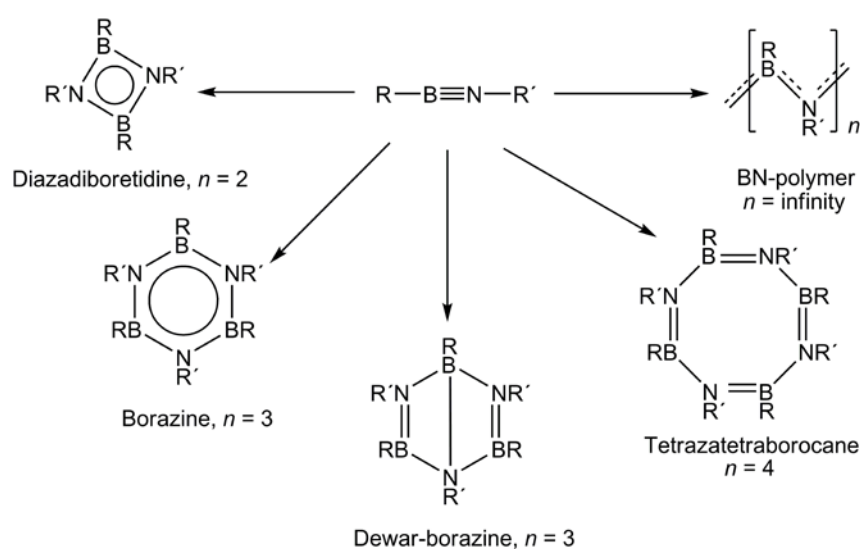


Scheme 1.6 Generation of iminoboranes by base induced 1,2-elimination reactions.

Iminoboranes ($\text{RB}\equiv\text{NR}'$) usually prefer to undergo oligomerization either thermally or catalytically in absence of trapping agent which is nicely explained by Paetzold in his review.^[1] Here, thermal refers to any temperature above or below room temperature. Depending on the size of the R and R' ligands, iminoboranes readily form higher oligomers provided the BN bond is not sterically overcrowded. For example, $t\text{-BuB}\equiv\text{N}t\text{-Bu}$ is stable at 0 °C but $\text{MeB}\equiv\text{NMe}$ is not above -110 °C.^[2, 53] The tendency towards cyclooligomerization of iminoborane is comparable to polar alkynes, e.g. $\text{FC}\equiv\text{C}t\text{-Bu}$ ^[54], which are also unstable at room temperature. Though the polarity difference, calculated or observed for iminoboranes, are found to be small (0.20 D for $t\text{-BuB}\equiv\text{N}t\text{-Bu}$),^[55] the values are high enough to form

cyclooligomers.

The thermal stabilization of iminoboranes generally favors borazine ($n = 3$) formation but different sets of R/R' are also able to stabilize diazadiboretidines ($n = 2$). There are also examples for R/R' ligand sets which are too large to allow borazine formation but not large enough to stop at the four membered BN ring. These sets of ligands (R/R' e.g. *i*-Pr/*t*-Bu,^[40] *s*-Bu/*t*-Bu,^[43] Ph/*t*-Bu^[44]) force the iminoboranes to produce Dewar borazines (Scheme 1.7).



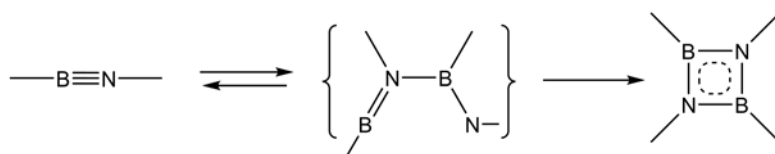
Scheme 1.7 Thermal self-oligomerization of iminoboranes.

The versatile outcome of the cyclooligomerization of iminoboranes for different sets of R/R' creates difficulty in understanding the product determining factors of such reactions. For example, the ligand sets $R/R' = i\text{-Pr}/t\text{-Bu}$, Ph/*t*-Bu form Dewar-borazines ($n = 3$) whereas the reverse sets i.e. *t*-Bu/*i*-Pr, *t*-Bu/Ph produce diazadiboretidines ($n = 2$).^[36] Likewise, $R/R' = \text{Me}/t\text{-Bu}$ yields simple borazine ($n = 3$) and the reverse set forms (*t*-BuBNMe)₄, a tetrazatetraborocane ($n = 4$), an eight-membered ring.^[1] In some cases ($R/R' = \text{Me}/t\text{-Bu}$,^[1] *i*-Pr/*i*-Pr^[56]) a reversible equilibrium was found between the cyclodimer and the cyclotetramer which can be followed by NMR methods.^[57] The eight-membered ring ($n = 4$) predominates

at room temperature but at higher temperature the cyclodimer ($n = 2$) is preferred. It can be easily understood that the eight-membered ring is energetically more favourable due to less ring strain but entropically disfavored.

In presence of a catalyst the cyclooligomerization scenario can be changed dramatically. The iminoboranes $\text{RB}\equiv\text{N}t\text{-Bu}$ ($\text{R} = \text{Et}, \text{Pr}, i\text{-Pr}, \text{Bu}$) generally prefer to form borazine or Dewar-borazine ($n = 3$) but in presence of catalytic amount of isonitrile $\text{C}\equiv\text{N}t\text{-Bu}$ the oligomerization products are diazadiboretidines ($n = 2$).^[1, 41, 42, 58, 59] Once formed catalytically, these cyclodimers are found to be thermally stable toward transformation into the corresponding borazine. Likewise, in the presence of $\eta^5\text{-(C}_5\text{H}_4\text{Me)Mn(CO)}_2\text{(THF)}$, $i\text{-PrB}\equiv\text{Ni-Pr}$ forms the cyclodimer instead of the cyclotrimer and the resulting $(i\text{-PrBNi-Pr})_2$ slowly transforms into the eight-membered ring $(i\text{-PrBNi-Pr})_4$ at room temperature.^[56]

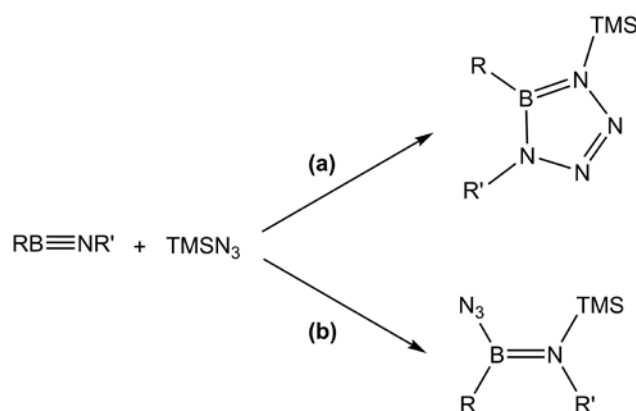
The cyclodimerization of iminoborane is an example of $[2 + 2]$ cycloaddition reaction. There is no clear evidence for the mechanism so far. Paetzold stated that a two-step mechanism would be rather unfavourable as the intermediate contains a sextet boron atom in a linear coordination (Scheme 1.8).^[1] A previous report of such a type of boron atom containing species, like aminoboron cation $[\text{C}_9\text{H}_{18}\text{N}=\text{B}-\text{Me}]^+$, also has established its instability even at low temperature.^[60] When two different iminoboranes, $i\text{-PrB}\equiv\text{Ni-Pr}$ and $(\text{TMS})(t\text{-Bu})\text{N}-\text{B}\equiv\text{N}-t\text{-Bu}$, were reacted together, then the expected cyclodimer of those two iminoboranes was formed.^[61]



Scheme 1.8 Two-steps possible mechanism for cyclodimerization.^[1]

The chemistry of iminoborans $\text{RB}\equiv\text{NR}'$ with different substrates has been well explored, and a number of interesting reaction sequences including their cycloaddition, polar addition and coordination chemistry have been discovered by Paetzold's group.^[1] Concerning this issue, it is reasonable to mention here a very important remark by Paetzold: "A reaction of a certain substrate with an iminoborane will only be possible, of course, if the oligomerization of the iminoborane proceeds slower".^[2]

Other than self-oligomerization, iminophosphanes $[\text{R}_1\text{N}=\text{P}-\text{NR}_2]$,^[62] titanethene $[\text{Cp}_2\text{Ti}=\text{CH}_2]$,^[63] hexafluoroacetone $[(\text{CF}_3)_2\text{C}=\text{O}]$ ^[61] have been reported to undergo [2 + 2] cycloaddition with iminoboranes to produce four-membered rings. Iminoboranes can react with different azides ($\text{RN}_3 = \text{Me, Et, Pr, Bu, } i\text{-Bu, } s\text{-Bu, cyclo-C}_5\text{H}_9, \text{PhCH}_2, \text{Ph, TMS}$) to give [3 + 2] cycloaddition products called tetrazaborole (Scheme 1.9a).^[36, 39, 41-43, 45] But in some cases TMSN_3 can simply perform 1,2-addition reaction with iminoboranes and yield the corresponding azidosilation products (Scheme 1.9b).^[41, 42, 45, 55, 58]

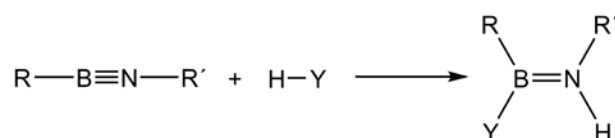


Scheme 1.9 Different reaction modes of TMSN_3 with iminoboranes.

Nitrone $[\text{PhCH}=\text{N}(\text{Me})-\text{O}]$ is also reported to form [3 + 2] cycloaddition products.^[61, 64] Unlike alkynes, iminoboranes undergo [4 + 2] cycloadditions extremely slowly due to the polarity of the $\text{B}\equiv\text{N}$ bond. Only two examples $[\text{RB}\equiv\text{N}-t\text{-Bu}; \text{R} = \text{F}_5\text{C}_6, (\text{TMS})(t\text{-Bu})\text{N}]$ have

been reported so far where iminoboranes act as simple dienophiles toward cyclopentadiene and successfully produce the [4 + 2] Diels-Alder reaction products.^[34, 61]

There are numerous examples of 1,2-addition reactions of polar molecules to the B≡N bond. Protic agents like HY [Y = Cl, OR, NR₂, (TMS)₂N] add to iminoboranes very rapidly even at low temperature to give aminoboranes (Scheme 1.10).^[65]



Scheme 1.10 1,2-Addition reactions of protic agents to iminoboranes.

The 1,2-addition reactions of X₂B–Cl [X = *i*-Bu, CH₂TMS, 3-methylboracyclopentyl],^[36, 38, 51, 61] X₂B–N₃ [X = Pr, Bu],^[61] X₂B–NR''₂ [X = Pr, R'' = N(TMS)(OTMS)],^[46] X₃B [X = Et, Bu]^[41, 42, 45, 46, 58] to the iminoboranes are also known. A different type of addition to iminoborane is that of neutral Lewis acids to the nitrogen atom. Only π-electron donating group (R) containing amino iminoborane (R₂N–B≡NR') is found to show such special property.^[66] In contrast, Lewis base stabilized iminoboranes are still unknown.

The reaction between iminoborane and metal is well explored. Like alkynes, iminoboranes are able to undergo side-on coordination (η¹), bridge two metal atoms (η²), and cyclodimerize at a metal center (η⁴). Side-on coordination of alkyne to metal is a well known property, likewise, iminoboranes also provide the analogous η¹-complex e.g. [Cp₂NbH(RB≡N*t*-Bu)] where R = *t*-Bu, N(TMS)(*t*-Bu) (**I**, Figure 1.2).^[67, 68] When *t*-BuB≡N*t*-Bu reacts with Co₂(CO)₈, it inserts into the metal complex in the same fashion as the isoelectronic alkyne, *t*-BuC≡C*t*-Bu does.^[69] The two Co atoms bridge the BN bond and form a tetrahedrane-type complex (**II**, Figure 1.2).^[70] The third type of coordination (η⁴) reaction is

preferred by iminoboranes over η^1 and η^2 coordination. In simple description, this kind of complexes are nido-clusters generated by a four-membered diazadiboretidine ring used as the base and a metal situated on the top of a tetragonal pyramid. The first example of a η^4 -complex was $\text{Cr}[(\text{BuBN}t\text{-Bu})_2]^{[59]}$; since then a number of $\text{M}[(\text{BuBN}t\text{-Bu})_2]$ ($\text{M} = \text{Mo}, \text{W}, \text{Fe}, \text{Co}$)^[1, 59, 71] complexes have been characterized by NMR and X-ray crystallography (III, Figure 1.2).

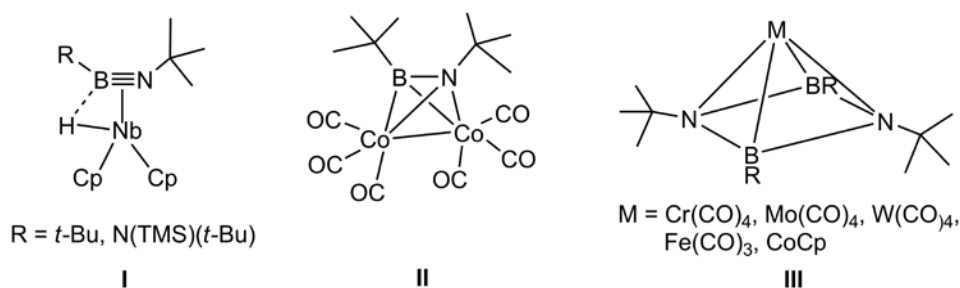


Figure 1.2 Examples of metal-coordinated iminoboranes.

1.6 1,2-Azaborine

This type of boron-nitrogen reactive intermediate, the BN derivative of *o*-benzyne, is restricted to the theoretical study so far. No experimental evidence for the existence of the cyclic iminoborane, 1,2-azaborine (**D**) is reported yet, and its synthesis remains a challenge. In 2006, Fazen and Burke have reported a comparative theoretical study on the isomers of azaborines and borazynes (Chart 1.3).^[72] They have found the triplet state of **D** to be higher in energy than the singlet state by $52.5 \text{ kcal mol}^{-1}$ at the UB3LYP/6-311++G(d,p) level of theory. The bond angles are significantly different for these two states according to UB3LYP method using 6-311++G(d,p) basis sets. Whereas the singlet state has a distorted geometry with angles of 141.6° and 109.6° at the boron and nitrogen centers, respectively, the triplet state has all the angles nearly 120° . The B–N bond is lengthened from 1.311 \AA in the singlet

state to 1.436 Å in the triplet state.

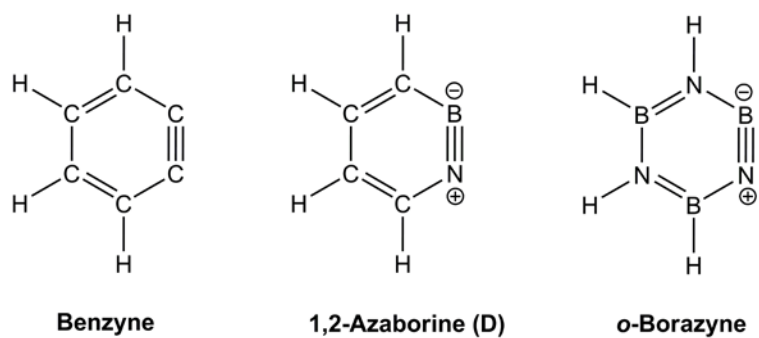


Chart 1.3 Chemical formulae of benzyne, 1,2-azaborine and *o*-borazyne.

2. Motivation

The aim of my work is to study mainly two important boron-nitrogen reactive intermediates. First is diphenylaminoborylene (Ph_2NB , **F**) and secondly 9,10-didehydro-9-aza-10-boraphenanthrene (**E**), a cyclic iminoborane which is also a dibenzo derivative of the parent 1,2-azaborine (**D**) or the BN analog of 9,10-phenanthryne (Chart 2.1).

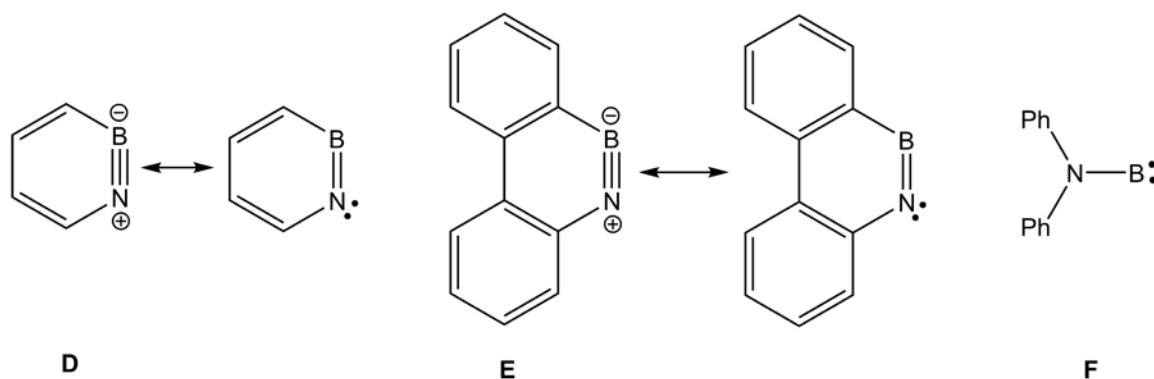


Chart 2.1

Diphenylaminoborylene (**F**) was intended to be generated by photolysis and characterized spectroscopically under matrix isolation conditions. Different approaches have been investigated to generate the 9,10-didehydro-9-aza-10-boraphenanthrene (**E**) from different starting materials in solution phase as well as to trap that with suitable trapping agents.

3. Diphenylaminoborylene

3.1 Matrix Isolation Technique

Matrix isolation is an experimental spectroscopic technique where a guest sample is isolated within the host matrix.^[73] The matrices are deposited from the gas phase by condensation on to a cold spectroscopic window. The choice of host gas depends on the choice of wanted or unwanted interaction between the host and guest molecules. The working temperature varies depending on the nature of host gas (usually 10 K or below). Usually noble gases (like argon, helium, xenon, and krypton) or nitrogen are used as host matrix in which guests like atoms, molecules, radicals, ions are trapped. Reactive hosts like CO, CO₂, CH₄ etc. can also be employed, if interaction between the host and guest is of interest. The advantage of noble gases as host material is not only their inertness to the highly reactive species such as radicals or any other reaction intermediates (guest molecule) but also their transparency throughout the IR, visible and UV regions of the electromagnetic spectrum. Also their tendency to form clear glasses at very low temperature is favourable for spectroscopic studies. Furthermore, in a rigid low temperature matrix rotations of most guest molecules are suppressed resulting very narrow IR bands ($< 1 \text{ cm}^{-1}$). The mole ratio of the host to guest is called the matrix ratio. The normal range for matrix ratio (host:guest) is 10:1 – 10,000:1 (Figure 3.1). A large matrix ratio reduces the possibility of molecular aggregation (guest-guest interaction) inside the matrix.

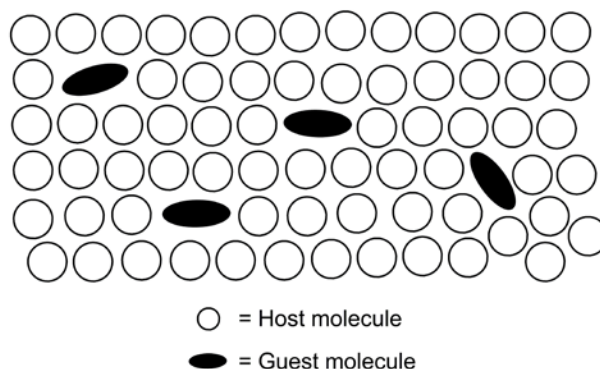


Figure 3.1 Host molecules trapped into the guest matrix.

In 1954, George Pimentel invented the technique of trapping reactive species in solidified noble gas matrix. The lowest working temperature reported in this first publication was 66 K. This allowed forming a xenon matrix, but was not sufficiently cold for neon, argon or krypton. Even at 66 K a xenon matrix was not rigid enough to give satisfactory results. Nevertheless, this idea was highly appreciated among scientists and George Pimentel is honoured as the pioneer of the matrix isolation technique.

Matrix isolation technique has attracted the chemists' attention as it opens the possibility of generation and direct characterization of reactive species by different spectroscopic techniques. From the characteristic spectroscopic data, one can identify molecular conformations, determine the structures of reactive species, investigate reaction mechanisms and study the weak interactions between species.

A simple outline of this technique is deposition of the gas mixture of guest and host onto a cold window in a vacuum chamber at a controlled flow rate followed by spectroscopic measurement. As discussed before, these guests can also be reactive species, which can be generated inside the matrices from stable precursor molecule by direct irradiation with UV-visible light, X-rays, or with an electron beam. External generation of those reactive guest

species can also be accomplished by photolysis, pyrolysis, or microwave excitation. Another possibility for matrix experiments is co-condensation of two streams of materials on to the cold window followed by reaction at the matrix surface during deposition.

Any matrix isolation system consists of a number of essential parts. These are:

(i) A cryostat: Usually helium refrigerators are used as coolant for matrix experiments. The lowest temperature attainable from a three-stage closed cycle cryostat is about 4 K. Alternatively liquid He cryostats can be used.

(ii) A sample holder: The sample holder is connected to the lower heat station of the head module of the refrigerator. The sample is deposited on a cold window (25 mm diameter) made of Caesium bromide (CsBr) or Caesium iodide (CsI) (for IR) or sapphire (for UV) which is fixed in a copper or nickel-plated copper window holder. Copper ensures the thermal conductivity between the surface of the window and the cold end of the refrigerator head module. For ESR spectroscopy, the sample holder is just a copper rod (Figure 3.2).

(iii) Vacuum chamber to enclose the sample holder: The sample holder fitted with the refrigerator head module is enclosed in a vacuum chamber or shrouds. This shroud and the refrigerator head module is attached by double O-ring seal for easy rotation. This is important because the sample deposition on the window and the spectral measurement of the sample require identical directions. For the same purpose, a pair of external windows (commonly KBr window) at the shroud is also necessary (Figure 3.2).

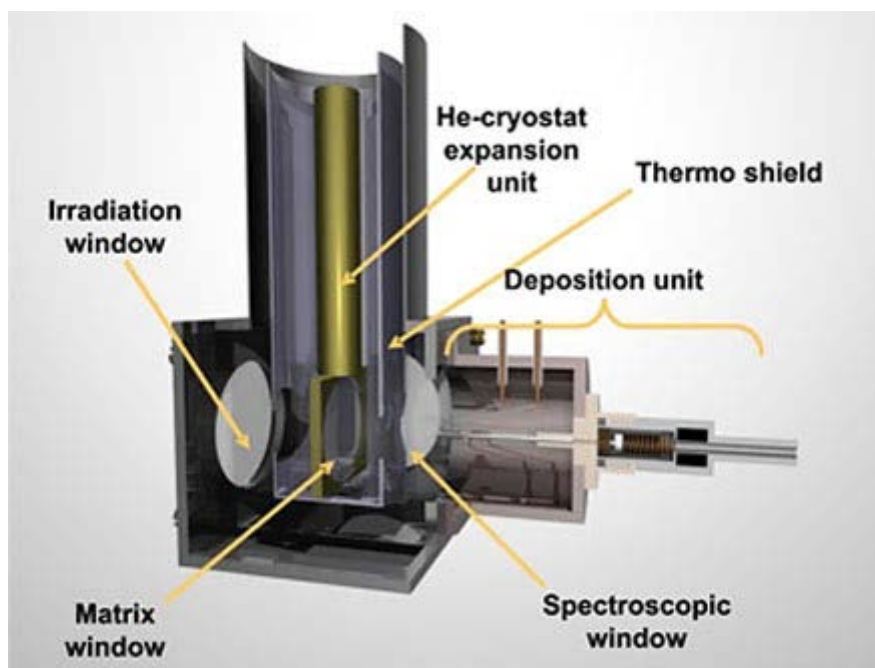


Figure 3.2 Cross section of sample deposition unit of a matrix machine for UV/IR measurement.ⁱ

(iv) Temperature measuring and controlling device: Thermocouples, silicon diodes, or hydrogen-vapour bulbs can be used as temperature measuring device. Usually the controller is attached with a heater wire which is connected to the lower heat station. By tuning the voltage power supply one can increase the matrix temperature slightly whenever needed to induce diffusion of trapped species.

(v) Vacuum-pumping system: Maintaining a continuous vacuum ($10^{-5} - 10^{-7}$ mbar) inside the shroud chamber is most important for a successful matrix isolation experiment. The shroud enclosing the head module of the refrigerator is continuously evacuated to insulate the cold sample window from warming by conduction or convection. It also prevents

ⁱ <http://www.ruhr-uni-bochum.de/oc2/matrix.html>

condensation of contaminants on top of the matrix. Two gauges are installed permanently to monitor the pressure inside the shroud and the pressure provided by the backing pump ($\sim 10^{-3}$ mbar).

(vi) Gas handling and flow controller system: High purity gasses are always used for matrix study. A regulator is installed to control the flow rate of the host gas to the vacuum chamber. Mixing of different host gases is also possible with appropriate equipments.

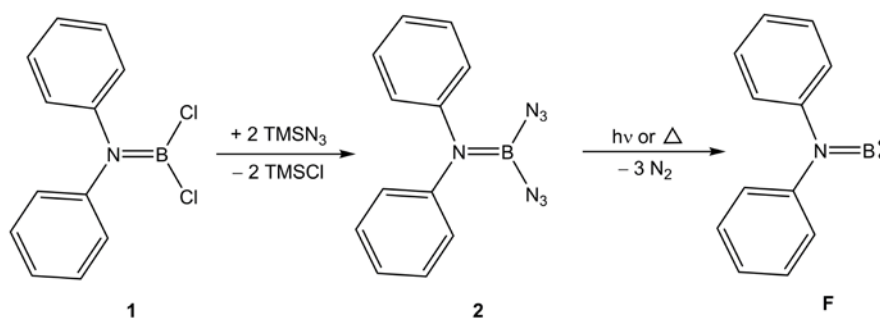
(vii) Devices for UV-irradiation or pyrolysis: Different light sources can be utilized in matrix studies. These include high pressure mercury lamps or mercury-xenon arc for complete UV-visible region, argon-plasma arc lamps for 210-260 nm with greater output intensity, low pressure mercury lamp to produce essentially monochromatic light at 254 nm. Filters are also used to allow wavelengths above or below the desired wavelength. Lasers, (O)LEDs are also important tools for irradiation. For pyrolysis, a special pyrolysis tube is prepared which is installed in the junction of sample container and the shroud.

(viii) Data analysing device (usually spectrometers): For data collection different types of spectrophotometers like IR, UV-visible, EPR are combined with the matrix isolation machines. Other than these Raman, Fluorescence spectroscopic measurements are also viable.

3.2 Synthetic Methodology

Based on the earlier discovery that boryl nitrenes can be generated from corresponding azidoboranes by means of photolysis or thermolysis, a synthetic scheme has been designed for the diphenyl aminoborylene [$\text{Ph}_2\text{N-B:}$, **F**] from the unknown bisazido(diphenylamino)borane [$(\text{Ph}_2\text{NB}(\text{N}_3)_2$]. In 2006, Bettinger has identified phenyl

borylene [Ph-B:] generated photochemically from bisazidophenylborane [PhB(N₃)₂] along with the rearranged nitrene [Ph-N=B-N] as major photoproduct in an inert gas matrix.^[74] Likewise, the bisazido(diphenylamino)borane, Ph₂NB(N₃)₂ (**2**) is expected to eliminate three molecules of nitrogen upon photoirradiation and produce the target intermediate, diphenylaminoborylene **F**. The diphenylamino group can stabilize the free borylene sterically and electronically by sharing the lone pair of electrons of the nitrogen atom. The bisazidoborane (**2**) can be obtained from the corresponding dichloride, i.e. Ph₂NBCl₂ (**1**) by treatment with trimethylsilylazide (TMSN₃) as shown in Scheme 3.1.



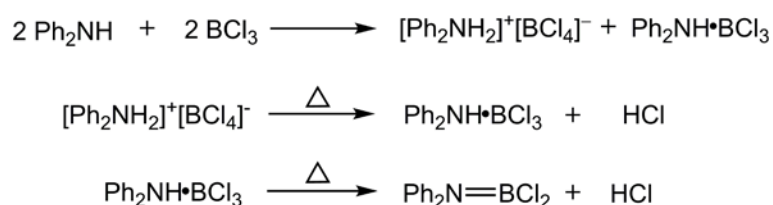
Scheme 3.1 Synthetic design for diphenyl aminoborylene (Ph₂NB, **F**).

The bisazidoborane (**2**) is expected to be sublimed easily to the cold window of the matrix head along with an inert gas as host.

3.3 Synthesis

The diphenylaminoboron dichloride (Ph₂NBCl₂, **1**) was prepared from diphenylamine (Ph₂NH) and boron trichloride (BCl₃) according to the procedure reported by Becher^[75] in 1957 with little modification. Becher mentioned that the 1:1 amine-boronhalide adduct was the main primary product after the addition of dichloromethane solution of diphenylamine to the solution of boron trichloride in the same solvent. Later on, Gerrard et al. found that

initially the diphenylammonium tetrachloroborate $\{[\text{Ph}_2\text{NH}_2]^+[\text{BCl}_4]^-; \nu(\text{N-H}) = 3135 \text{ cm}^{-1}\}$ was the major product mixed with little amount of 1:1 complex $[\text{Ph}_2\text{NH}\cdot\text{BCl}_3; \nu(\text{N-H}) = 3145 \text{ cm}^{-1}]$ and diphenylaminoboron dichloride (Ph_2NBCl_2 , **1**).^[76, 77] Upon boiling in benzene this tetrachloroborate complex decomposes to the 1:1 adduct, and further decomposition of that adduct produces **1** by eliminating HCl according to the following equations.



Scheme 3.2 Formation of **1** via different complexes.

In the present work, ^{11}B NMR investigations at different stages of this reaction showed that before refluxing in benzene the white solid mixture had two ^{11}B NMR signals; one sharp signal at 8.8 ppm as the major one and a small, comparatively broader peak at 32.7 ppm. The latter one is assigned to **1** according to the literature.^[78] After boiling in benzene the 33 ppm peak turned into the major component. During purification it was observed in a few trials that the compound with 8.8 ppm ^{11}B shift is also subliming along with **1** at $65 \text{ }^\circ\text{C}/10^{-5}$ mbar. Therefore, it can be assumed that the second compound is an adduct of amine and chloroborane (e.g. $\text{BCl}_3\cdot\text{NEt}_3$ $\delta^{11}\text{B} = 10$ ppm, $\text{BCl}_3\cdot\text{Py}$ $\delta^{11}\text{B} = 8$ ppm)^[79] rather than an ionic complex like $[\text{Ph}_2\text{NH}_2]^+[\text{BCl}_4]^-$. A resublimation at $42 \text{ }^\circ\text{C}/4 \times 10^{-5}$ mbar produced pure diphenylaminoboron dichloride (Ph_2NBCl_2 , **1**) which was characterized by NMR and IR spectroscopy. The ^{11}B (in CD_2Cl_2) chemical shift of 32.4 ppm^[78] is in the range as expected for a tricoordinated boron center attached to nitrogen atom/s. In the IR, this compound has a strong band at 1387 cm^{-1} which is assigned to the B–N bond stretching vibration by comparison with the literature.^[75, 77] Comparison of the B–N bond stretching frequencies of

different dialkylaminoboron dichlorides (R_2NBCl_2 ; $R = Me$, 1526 cm^{-1} ;^[80] $R = Et$, 1505 cm^{-1} ;^[81] $R = i\text{-Pr}$, 1486 cm^{-1})^[77] and Ph_2NBCl_2 (1387 cm^{-1}) shows an increasing B=N double bond character with increase of electron-releasing property of the substituents ($Me < Et < i\text{-Pr} < Ph$). The crystal structure of **1** shows that the B–N bond length is 1.380 \AA and confirms that the boron and nitrogen atoms are connected by a double bond.^[82]

The conventional procedure to synthesize an azidoborane is the treatment of the corresponding chloroborane with trimethylsilylazide ($TMSN_3$). Usually azidoboranes are sensitive to heat, electrostatic discharge and/or mechanical shock. But electron donating groups attached to the boron atom can reduce the electron deficiency of the latter to a certain extent and make the azidoborane stable enough for safe handling. Detailed investigations of the explosive properties of azidoboranes have been reported in the literature.^[83]

The synthesis of the bisazido(diphenylamino)borane, $Ph_2NB(N_3)_2$ (**2**) has been done by adding two equivalents of $TMSN_3$ to the chloroborane (**1**) in CD_2Cl_2 . The reaction was monitored by $^{11}B\{^1H\}$ NMR of the reaction mixture over time and an interesting outcome was observed. Within 10 minutes after the addition, the reaction mixture showed the peak for chloroborane (**1**, $\delta^{11}B = 32.3\text{ ppm}$) along with a new peak arising at 28.2 ppm . Within 15 mins the 32.3 ppm peak disappeared and an additional peak was found developing at 23.7 ppm which started to grow with time. But surprisingly, after $2\frac{1}{2} - 3\text{ h}$ the 28.2 ppm peak was increasing again associated with the gradual decrease of the new peak at 23.7 ppm (Figure 3.3).

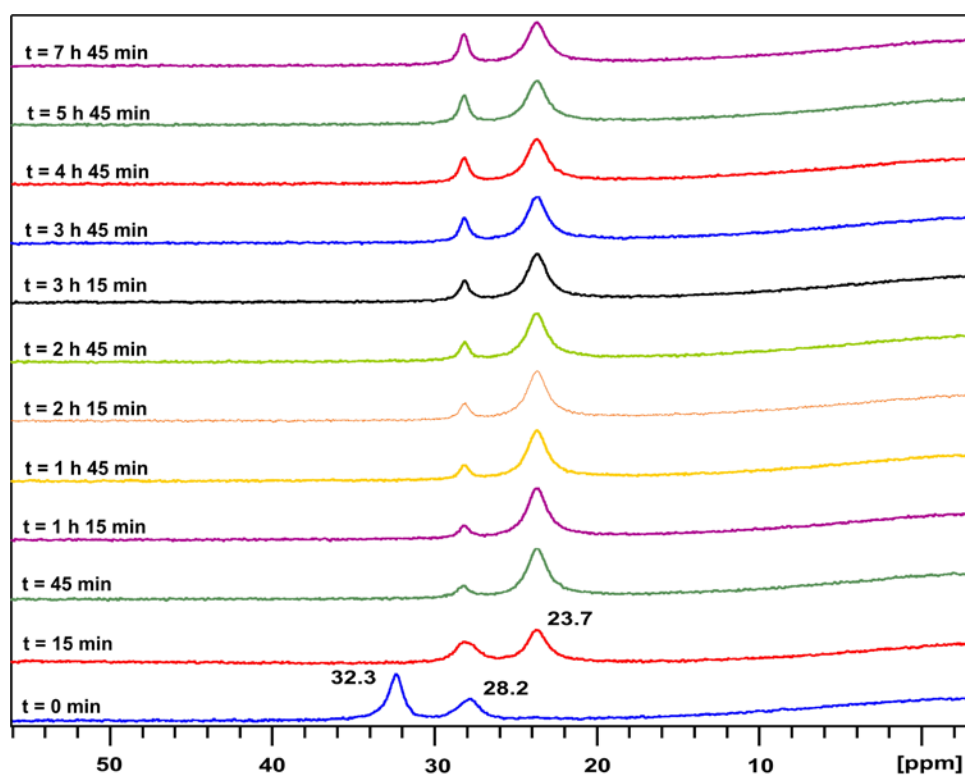
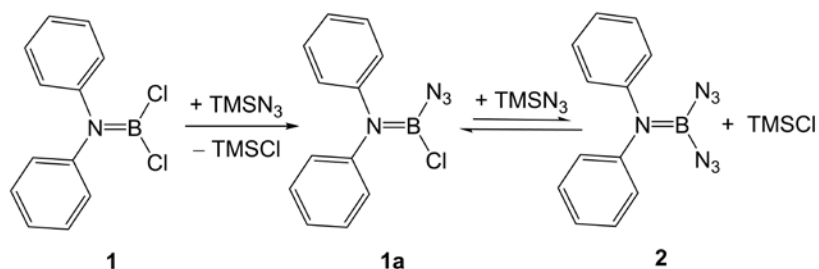


Figure 3.3 $^{11}\text{B}\{^1\text{H}\}$ NMR study for the gradual formation of **2** from **1** via **1a** in CD_2Cl_2 .ⁱⁱ

This experiment indicates stepwise formation of the bis-azide from the dichloride **1**. A plausible reaction pathway could be the initial formation of mono-azide (**1a**) followed by conversion into bis-azide (**2**) by another molecule of TMSN_3 according to Scheme 3.3. The difference in ^{11}B chemical shift between the dichloroborane and the bisazidoborane is quite similar to that of tmpBCl_2 ($\delta^{11}\text{B} = 33.0$ ppm in C_6D_6)^[51] and $\text{tmpB}(\text{N}_3)_2$ (tmp = 2,2,6,6-tetramethylpiperidino, $\delta^{11}\text{B} = 23.0$ ppm in C_6D_6).^[83]

ⁱⁱ Time delay to bring the sample from laboratory to the spectrometer is roughly 10 min.



Scheme 3.3 Stepwise formation of bisazido(diphenylamino)borane (**2**).

Though the $\text{tmpB}(\text{N}_3)_2$ is stable at ambient temperature, the bisazidoborane (**2**) seems not to be stable enough under experimental conditions. Compound **2** slowly decomposed into **1a**. But there was no complete conversion of **2** to **1a** over time; rather an equilibrium was attained as shown in Scheme 3.3. Even after a week the same sample was a 4:1 mixture of **1a** and **2** at room temperature.

For comparison, the nuclear shielding values were calculated for the compounds **1**, **1a** and **2** at the B3LYP/6-311+G(d,p) level of theory using B3LYP/6-31+G(d) optimized geometries. Table 3.1 shows the chemical shifts. The absolute nuclear shielding constants $\sigma(^{11}\text{B})$ were converted to $\delta^{11}\text{B}$ data using the experimental chemical shift of B_2H_6 (18 ppm vs $\text{BF}_3 \cdot \text{OEt}_2$) and its computed isotropic shielding value 84.1. The $\delta^{11}\text{B}$ chemical shift (22.3 ppm) for **2** is found to be matching reasonably well with the experimental value (23.7 ppm). The computed ^{11}B shift for the monoazido compound **1a** is 5.3 ppm downfield compared to **2** and thus 29.0 ppm would be the expected value, in good agreement with the measurement (Figure 3.3). But for the dichloride **1** the computed value ($\delta^{11}\text{B} = 36.4$ ppm) shows a 4.1 ppm difference from the experimental value ($\delta^{11}\text{B} = 32.3$ ppm).

Table 3.1 Computed [B3LYP/6-311+G(d,p)//B3LYP/6-31+G(d) level of theory] and experimental chemical shifts.

Compounds	Calculated chemical shifts (in ppm, referenced to BF ₃ •OEt ₂)	Experimental chemical shifts (in ppm, referenced to BF ₃ •OEt ₂)
1	36.4	32.3
1a	27.6	28.2
2	22.3	23.7

To overcome this equilibrium, excess TMSN₃ (2.5 equiv) was used for complete conversion of the dichloroborane **1** to **2**. After working up the reaction mixture a white sticky material was obtained which had only one ¹¹B signal at 23.7 ppm in CD₂Cl₂. This compound was transferred to a rigorously dried flask fitted via VCR connections with a membrane valve under argon atmosphere. This tube was attached to the sample line of the matrix head (Figure 3.2).

3.4 Matrix Isolation Experiment

Once the sample tube was attached and the matrix isolation machine was brought to the proper condition [vacuum = 1.6 x 10⁻⁶ mbar; matrix window temperature = 16 K], a reference background IR spectra was measured. For deposition of the sample onto the matrix window, the temperature was increased to 30 K and sample tube was slowly opened to the matrix head and the deposition was started with argon at a flow rate of 2.0 sccm/min. The deposition was continued for 1 h 30 min. In Figure 3.4, the curves (A) and (C) display the FTIR spectra of the deposited sample. The peaks at 2135 and 1146 cm⁻¹ are assigned to HN₃

and the peaks at 1608 and 1624 cm^{-1} to water. The peaks at 2157, 1358 and 1103 cm^{-1} are similar to those reported by Mulinax et al. for $\text{B}(\text{N}_3)_3$.^[84]

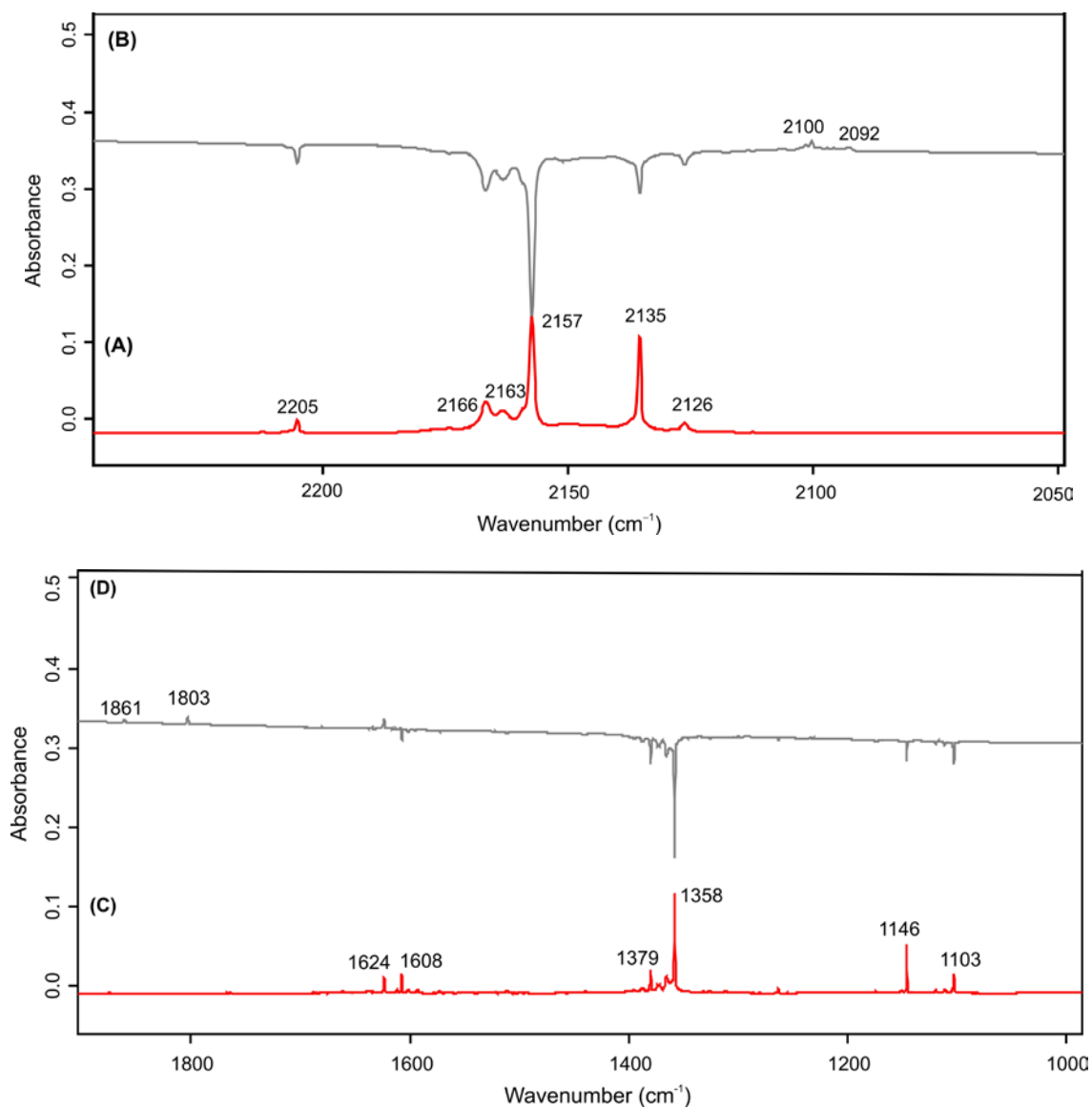


Figure 3.4 Expanded regions of the FTIR spectrum: (A) and (C) the absorption spectra after deposition of sample; (B) and (D) are difference spectra after photolysis at 254 nm.

The generation of $B(N_3)_3$ could not be avoided even after several trials. According to the Mulinax group, the $B(N_3)_3$ behaves as '*a relatively short-lived species at room temperature*' and they had observed a gradual decrease of the relative absorbance of $B(N_3)_3$ with time due to decomposition to N_2 and species which were deposited on the walls.^[84] But in the present study there was no indication for the decomposition of $B(N_3)_3$ under the experimental conditions over time and also deposition from the same sample tube at different times did not alter the spectra as shown in the Figure 3.4 (A) & (C). All the spectra discussed here were acquired at 16 K.

The matrix isolated $B(N_3)_3$ was irradiated using a Grätzel lamp (254 nm) with 225 nm cut-off filter. After 1 min of irradiation the major peaks at 2157, 1358 and 1103 cm^{-1} were decreasing. They were completely bleached within 16 min. This is shown in Figure 3.4 curves (B) and (D) by bands pointing down. Simultaneously a group of new peaks at 2100, 1861 and 1803 cm^{-1} appeared. These were previously assigned to NNBN by Gilbert group who studied the photolysis of $B(N_3)_3$.^[85] They prepared $B(N_3)_3$ in the gas phase by mixing BCl_3 and HN_3 in a 1:3 ratio and performed a low-temperature photolysis in an Ar matrix. They have identified the NNBN product and assigned the peaks based on computational data as well as previous reports on B_xN_y species by Andrews et al.^[86]

Azidoboranes are known to be extremely moisture sensitive and susceptible towards heat and mechanical shock. According to Smith, a nitrogen content of more than 25 % in any azidoborane causes the material to be highly explosive.^[87] Thus $B(N_3)_3$ is a very dangerous material to handle and needs utmost precautions and equipments for any experiment. Due to the unknown origin of continuous evolution of $B(N_3)_3$ and its dangerous nature no further experiment was done.

Paetzold's more stable $\text{tmpB}(\text{N}_3)_2$ was not investigated. Because the photodecomposition of $\text{tmpB}(\text{N}_3)_2$ is expected to involve a transient borylnitrene. Experiments in our group have shown that intramolecular CH insertions of boraylnitrene are facile.^[88]

4. 9,10-Didehydro-9-aza-10-boraphenanthrene

4.1 Theoretical Study

To shed light on the energy and structure of the reactive intermediate, 9,10-didehydro-9-aza-10-boraphenanthrene (**E**), a computational study at the B3LYP/6-31G(d) level of theory was performed. For comparison, the 1,2-azaborine and the carbon analogs were also investigated. The frequency calculations show that all the structures are at the minima of the potential energy hypersurface. For clarity, the optimized structures have been marked as **C-I** (benzyne), **C-II** (1,2-azaborine), **C-III** (phenanthryne) and **C-IV** (9,10-didehydro-9-aza-10-boraphenanthrene) (Figure 4.1). Several computational studies have been reported previously for benzyne (**C-I**) with respect to its structure,^[72, 89-91] vibrational frequencies,^[92, 93] electronic transition spectra,^[94] aromaticity.^[89-91] Here, the triplet states for **C-I**, **C-II**, **C-III** and **C-IV** are found to be energetically higher compared to their singlet states by 29.07, 50.41, 44.46 and 45.76 kcal mol⁻¹ respectively. As found by Fazen and Burke for **C-II**,^[72] the angle at B is larger in the singlet (142.9°) than the triplet (121.4°) state of **C-IV**. The angle at N is smaller in the singlet (110.3°) than in the triplet state (118.8°). In the **C-IV** triplet state all angles in the central ring are nearly 120°. The BN bond length increases from 1.288 Å in the singlet to 1.430 Å in triplet state. In the case of singlets, the dibenzoannulation of the parent azaborine (**C-II**) shows a decrease in the BN bond length to 1.288 Å in **C-IV** from 1.316 Å whereas this has nearly no effect for the geometries of the triplet states.

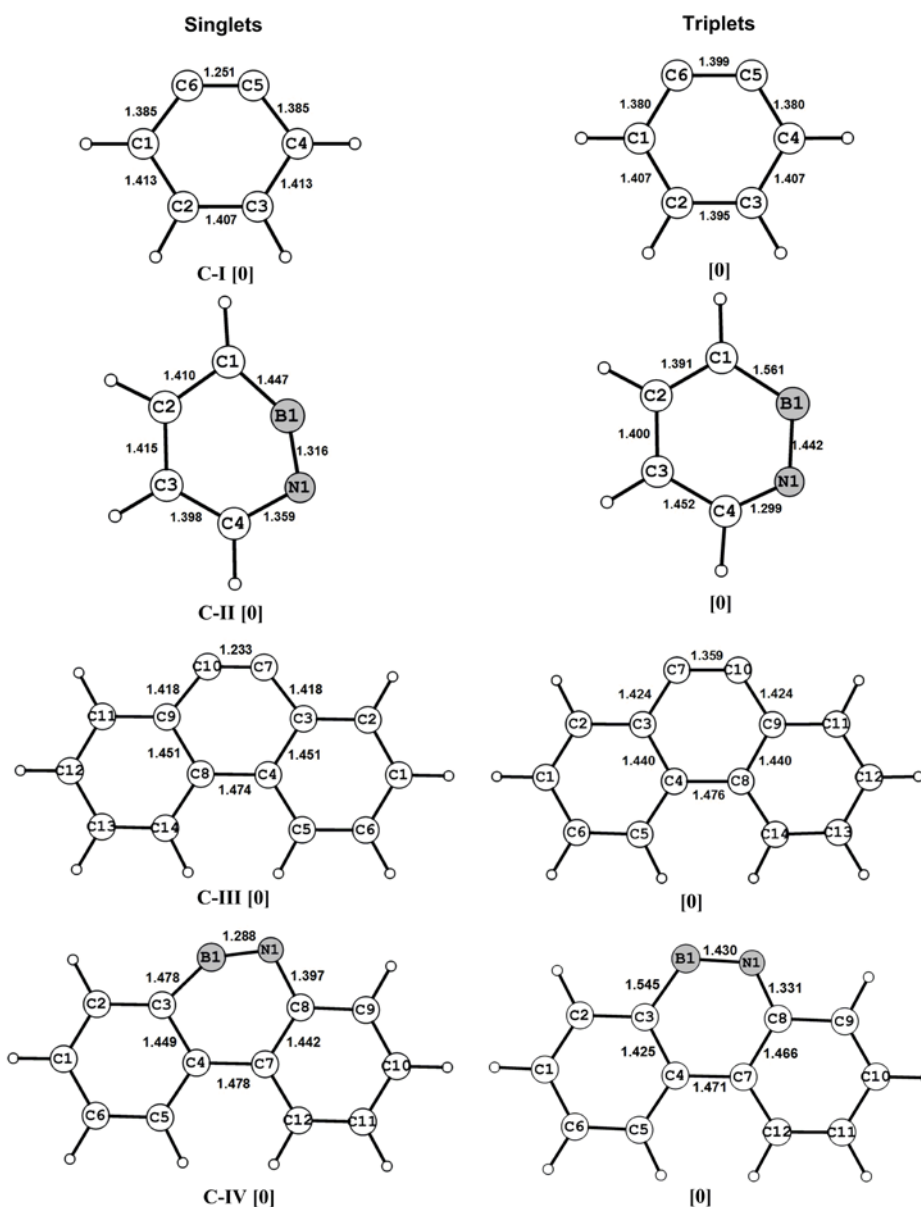


Figure 4.1 Optimized geometries of **C-I**, **C-II**, **C-III** and **C-IV** computed at the B3LYP/6-31G(d) level of theory and the number of imaginary frequency is shown in parentheses.

The vibrational frequency calculations show that the BN stretching vibration ($\nu_{\text{BN}} = 1814 \text{ cm}^{-1}$, uncorrected) in **C-IV**-singlet is blue shifted by 93 cm^{-1} compared to the parent azaborine, **C-II**-singlet ($\nu_{\text{BN}} = 1721 \text{ cm}^{-1}$, uncorrected). This shift is similar to that in the carbon analogs, i.e., benzyne ($\nu_{\text{C5-C6}} = 2027 \text{ cm}^{-1}$, uncorrected) and phenanthryne ($\nu_{\text{C7-C10}} = 2117 \text{ cm}^{-1}$, uncorrected).

As the triplet states are energetically higher than the singlets, further analysis is done only on the singlet states. The HOMO-LUMO gaps in the BN-substituted reactive intermediates are higher compared to their corresponding carbon derivatives as shown in the Figure 4.2.

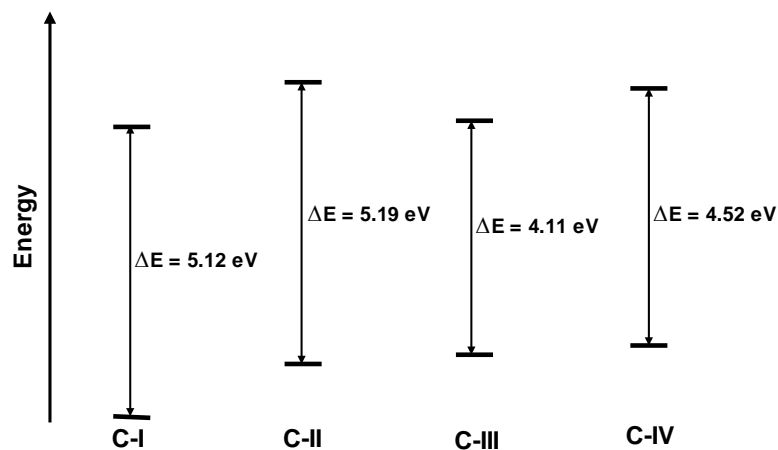


Figure 4.2 HOMO-LUMO energy gaps in **C-I**, **C-II**, **C-III** and **C-IV** for the singlet states.

The dibenzo systems have smaller HOMO-LUMO energy gaps than their parent structures, as expected. For **C-II** as well as **C-IV**, the LUMOs shift to higher energies compared to the carbon analogs **C-I** and **C-III**. The LUMOs of **C-II** and **C-IV** can be considered as sp^2 hybrid orbitals located on the boron atoms and thus the compounds would readily be attacked by nucleophiles at the boron atoms (Figure 4.3).

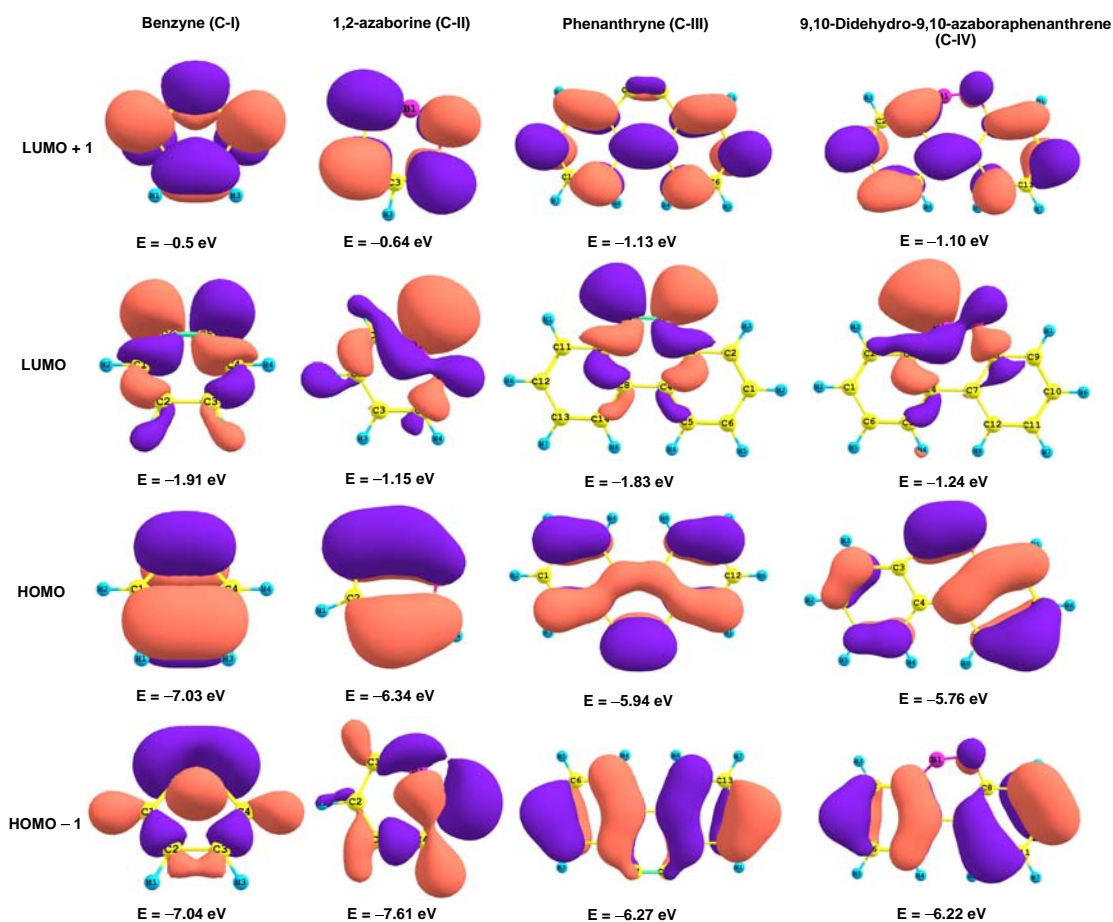


Figure 4.3 The first two HOMOs and LUMOs of C-I, C-II, C-III and C-IV obtained at B3LYP/6-31G(d) level of theory and the corresponding energies are given at the bottom of each MO picture.

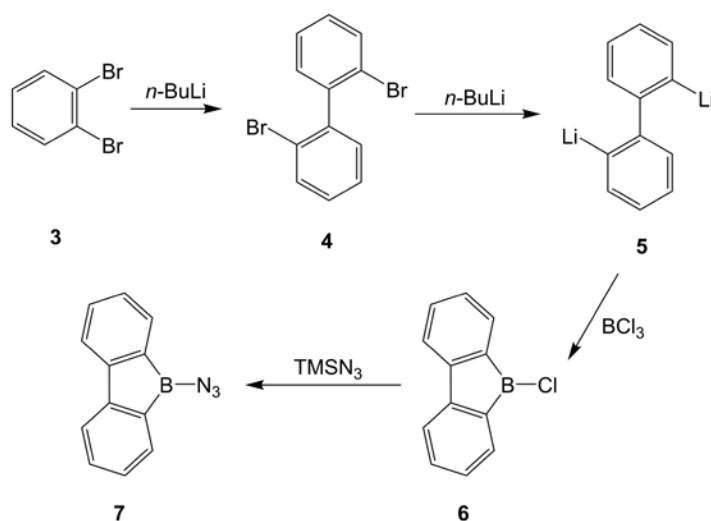
4.2 Synthetic Strategies

The generation of 9,10-didehydro-9-aza-10-boraphenanthrene (**E**) was attempted by three different routes as introduced in Chapter 1 (Section 1.5); (i) from azidoborane via generation of boryl nitrene, (ii) from silyl(silyloxy)aminoborole and (iii) by base induced dehydrohalogenation from suitable precursors. The results are discussed in the following chapters.

5. The Azide Route via 9-Azido-9-borafluorene

5.1 Introduction

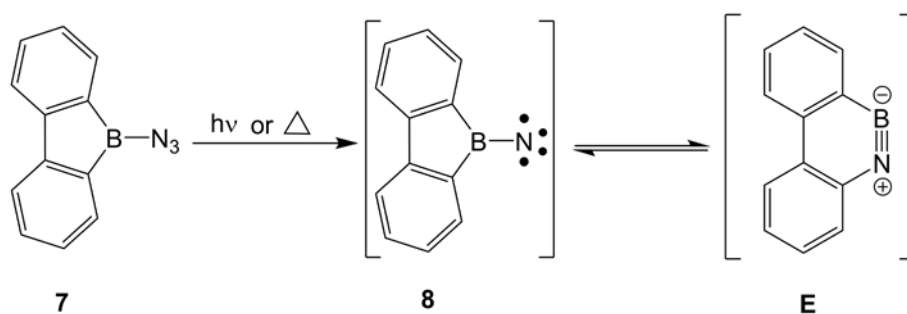
As reviewed in Chapter 1 azidoboranes are good precursors to generate borylnitrenes ($\text{RRB}=\text{N}$) by photolysis or thermolysis and thereafter formation of iminoborane ($\text{RB}\equiv\text{NR}$) via rearrangement/migration of substituent (R) from the boron center to the nitrogen center. Accordingly the obvious choice for the 9,10-didehydro-9-aza-10-boraphenanthrene (**E**) is the unknown 9-azido-9-borafluorene (**7**). The azide should be accessible from the corresponding chloroborane, i.e. 9-chloro-9-borafluorene (**6**), by reaction with TMSN_3 . The preparation of **7** was performed as shown in the Scheme 5.1; the chloride **6** can be prepared by salt elimination from 2,2'-dilithiobiphenyl (**5**) according to earlier reports.^[95,96]



Scheme 5.1 Synthetic outline for 9-azido-9-borafluorene (**7**).

After the synthesis of the azide (**7**) the nitrene should be available under suitable photolytic conditions. The nitrene (**8**) is expected to be unstable towards rearrangement and would produce the 9,10-didehydro-9-aza-10-boraphenanthrene (**E**) in an energetically favourable fashion according to the computation analysis, discussed in the following section (Scheme

5.2).



Scheme 5.2 Expected rearrangement from **8** to **E**.

5.2 Computational Analysis

The optimized geometries were obtained at the B3LYP/6-31G(d) level of theory (Figure 5.1). The boron center in the optimized structure of the 9-azido-9-borafluorene (**C-V**) has a planar configuration, as expected. The C(2)–B(1)–C(1) (105.7°) bond angle is much smaller than that of a sp^2 -hybridised atom. The B(1)–C(1) (1.558 Å), B1–C2 (1.567 Å), C(1)–C(4) (1.420 Å), C(4)–C(6) (1.489 Å) and C(6)–C(2) (1.422 Å) bond lengths signify a prominent bond length alternation inside the five membered borole ring. The N(1)–N(2) (1.236 Å) and N(2)–N(3) (1.138 Å) bond lengths are in the expected range of N=N and N≡N bonds respectively. The N(1)–N(2)–N(3) angle is slightly bent with an angle of 172.3° and the computed asymmetric stretching frequency for the azide group is at 2284 cm^{-1} (uncorrected).

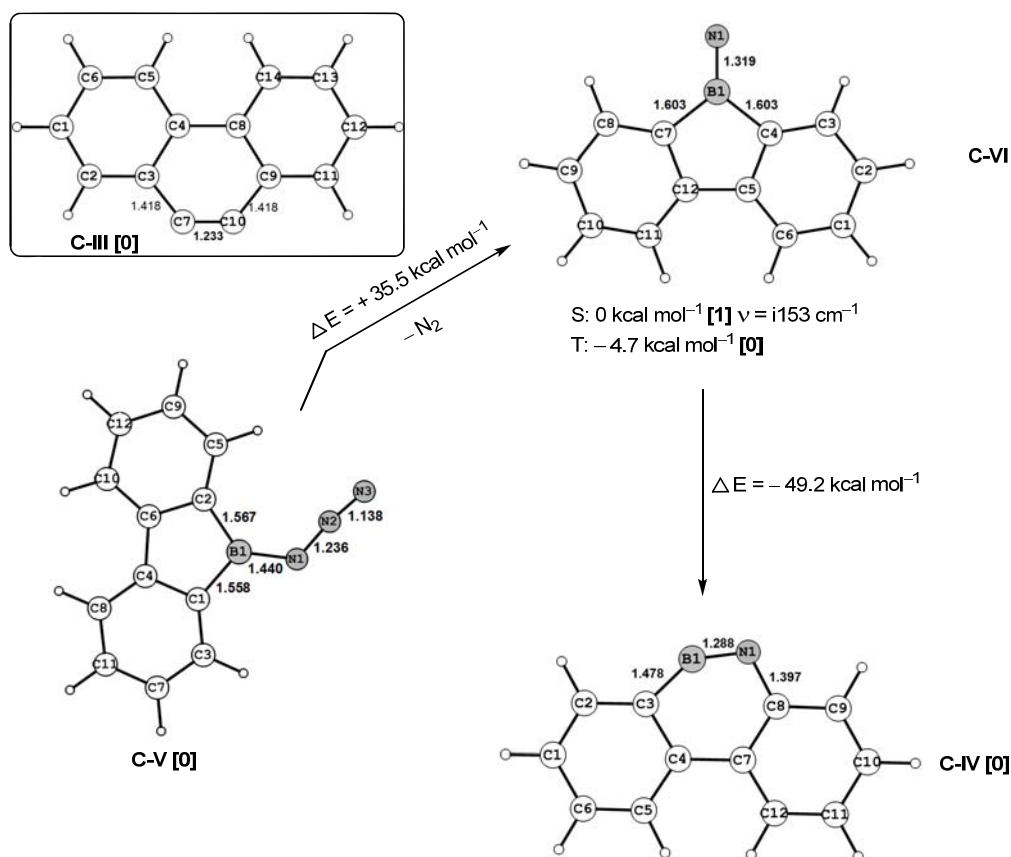


Figure 5.1 Energy profile diagram for 9,10-didehydro-9-aza-10-boraphenanthrene from 9-azido-9-borafluorene. The optimized geometries were obtained at the B3LYP/6-31G (d) level of theory with ZPE corrections. Numbers of imaginary frequencies are given in the parentheses.

According to this computational work, the borylnitrene (**C-VI**, S: Singlet) obtained from the 9-azido-9-borafluorene (**C-V**) does not correspond to a minimum on the potential energy surface in singlet state, showing an in-plane vibration of the BN bond ($\tilde{\nu} = i153 \text{ cm}^{-1}$) and hence this singlet borylnitrene **C-VI** does not correspond to an observable intermediate. Rather, it rearranges to the cyclic iminoborane (**C-IV**) releasing $49.5 \text{ kcal mol}^{-1}$ of energy. The triplet state of the nitrene **C-VI** is energetically favored by $\sim 5 \text{ kcal mol}^{-1}$ over **C-VI S**.

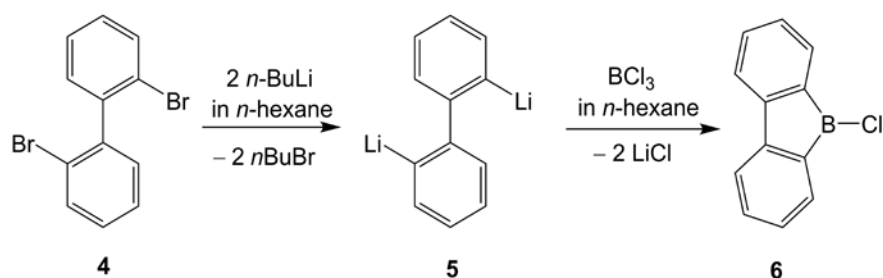
According to the computational investigation, the formation of 9,10-didehydro-9-aza-

10-boraphenanthrene (**C-IV**) is a feasible reaction thermodynamically from 9-azido-9-borafluorene (**C-V**).

The instability of borylnitrene has been experimentally proved by Paetzold et al. for related diaryl and dialkyl derivatives. They found that the thermolysis of dialkyl or diaryl azidoboranes (R_2BN_3)^[64] and *N*-trimethylsilyl-*N*-(trimethylsilyloxy)aminoboranes [$R_2BN(TMS)(OTMS)$] produced the rearranged iminoboranes without forming detectable borylnitrene intermediates.^[46, 65]

5.3 Results and Discussion

According to the reaction outline shown in Scheme 5.1, 2,2'-dibromobiphenyl (**4**) was synthesized with ease as described in the literature.^[95, 96] The 9-chloro-9-borafluorene (**6**), was first synthesized by Köster and Benedikt in 1963^[97, 98] by thermolysis of 2-biphenyl-dialkylborane. Later, this compound was synthesized either by transmetallation or by salt elimination. Narula and Nöth^[99] reported a high yielding (75 %) transmetallation procedure using a mercury containing precursor. To avoid the highly toxic mercury compound the salt elimination procedure, reported by Hong and Chung, is found to be a more convenient source of **6**.^[100] The reaction was carried out in dry diethylether (Et₂O) as described in the literature, but even after several trials it was not possible to get clean 9-chloro-9-borafluorene (**6**). The chloride [$\delta^{11}B$ (CDCl₃) = 63.7 ppm] was always mixed with a minor impurity having an ¹¹B chemical shift at 37.3 ppm. Also the overall yield was poor. But a simple modification not only gave pure **6**, but also improved the yield considerably from 36 %, reported by Hong and Chung.^[100] Carrying out the dilithiation of 2,2'-dibromobiphenyl in *n*-hexane^[101] rather than in ether produced **6** in 90 % yield with respect to 2,2'-dibromobiphenyl (Scheme 5.3).^[102]



Scheme 5.3 Synthesis of 9-chloro-9-borfluorene (**6**).

The chloride **6** was purified by distillation at 90 °C/10⁻³ mbar. During distillation the yellow liquid of **6** rapidly formed nice yellow needle shaped crystals upon contact with the cold trap (0 °C). These were suitable for X-ray analysis.

9-Chloro-9-borfluorene **6** crystallizes in the monoclinic space group $P2_1/c$ with four formula units in the unit cell. Figure 5.2 shows the projection of the molecule. The molecule is planar having a sum of bond angles around the boron atom of 359.9°. The B–Cl bond length [1.752(3) Å] is in the usual range.^[103-105] The B–C bond lengths [B(9)–C(9A) 1.547(4) Å and C(8A)–B(9) 1.536(4) Å] are shorter than typical B–C_{aryl} bonds in other three-coordinated boranes [e.g., 1.589(5) and 1.571(3) in Ph₃B,^[106] 1.579(2) and 1.580(3) in Mes₃B^[107]] and slightly shorter than in other 9-borfluorene compounds [e.g., 1.549(3) in F₈C₁₂B(C₆F₅) (Figure 5.3. **I**),^[108] 1.556(7) and 1.573(6) in 1-(4-*t*-butylphenyl)-7-*t*-butyl-9-(bis-2,6-(4-*t*-butylphenyl)phenyl)-9-borfluorene (Figure 5.3. **II**).^[109]

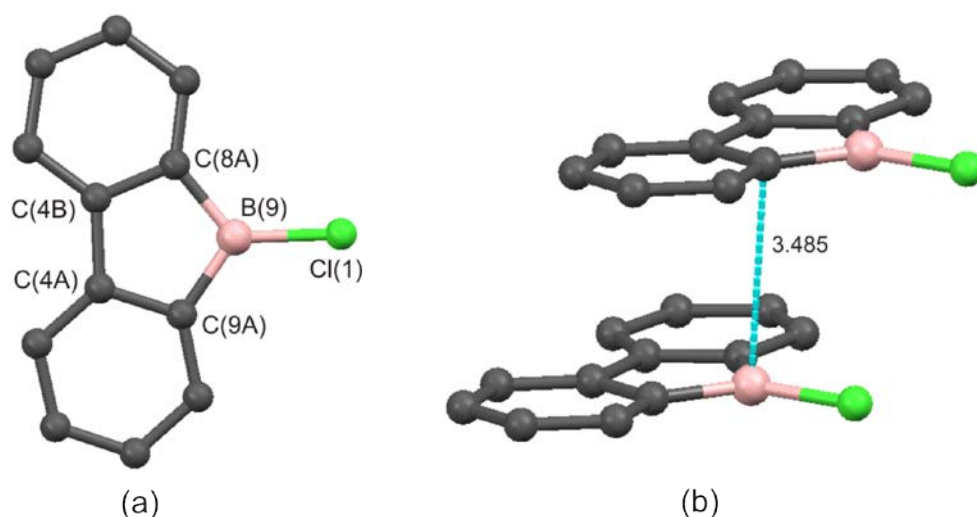


Figure 5.2 (a) Molecular structure of **6**. Selected bond lengths [\AA] and angles [$^\circ$]: B(9)–Cl(1) 1.752(3), B(9)–C(9A) 1.547(4), C(8A)–B(9) 1.536(4), C(4A)–C(9A) 1.409(3), C(4A)–C(4B) 1.481(3), C(4B)–C(8A) 1.416(3); Cl(1)–B(9)–C(8A) 126.3(2), C(8A)–B(9)–C(9A) 105.9(2), B(9)–C(8A)–C(4B) 106.8(2), C(8A)–C(4B)–C(4A) 110.2(2); (b) Dimeric subunit in the crystal lattice of **6**. The intermolecular B(9)···C(9A) distance is 3.485 \AA . Hydrogen atoms are omitted for clarity.

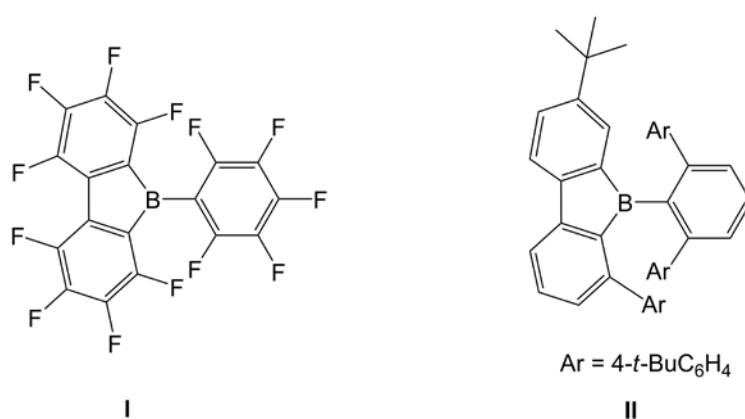


Figure 5.3 Structures of $\text{F}_8\text{C}_{12}\text{B}(\text{C}_6\text{F}_5)$ (**I**) and 1-(4-*t*-butylphenyl)-7-*t*-butyl-9-(bis-2,6-(4-*t*-butylphenyl)phenyl)-9-borafluorene (**II**).

The B–C bond lengths in **6** are shorter than its pyridine adduct **6•py** that was prepared and structurally characterized by Narula and Nöth previously.^[110] Likewise, the unusually long

B–Cl bond in **6•py** [1.900(2) average] shortens significantly in free **6** to 1.752(3) Å. The lengths of the C(4A)–C(9A) [1.409(3) Å] and C(4B)–C(8A) [1.416(3) Å] bonds are also similar to those of **6•py** [1.404(3) and 1.408(3) Å] and in agreement with an aromatic six membered ring system (1.40 Å). The distance between C(4A)–C(4B) [1.481(3) Å] bond is slightly shorter than the C–C single bond between two sp²-hybridized carbon atoms (1.49 Å) and similar to the corresponding length in **6•py**.

To achieve the planar geometry, the bond angles inside the five membered ring also become smaller by 10–15° than the value expected for sp² hybridized atoms. This induces some strain that is relieved upon pyramidalization. This issue was previously discussed by Narula and Nöth in the context of the X-ray structure of the pyridine adduct of 9-chloro-9-borafluorene, **6•py**.^[110] The crystal packing of **6** reveals the intermolecular interaction between the boron atom and the π system of a neighboring molecule. The shortest intermolecular B···C distance is 3.485 Å (Figure 5.2b) which is shorter than that of pentasubstituted borole compounds reported earlier.^[111, 112] An even shorter intramolecular distance between a boron center of a borafluorene and an aromatic ring was observed by Hoefelmeyer et al.^[113]

Depending on the purity of **6**, crystallization can either be retarded or not be observed at all. In one instance a by-product **6a** [2,2′-bis(9-borafluoren-9-yl)biphenyl] was isolated as deep red crystals. These grew from the yellow oil after standing for an extended period of time without interruption (Figure 5.4).

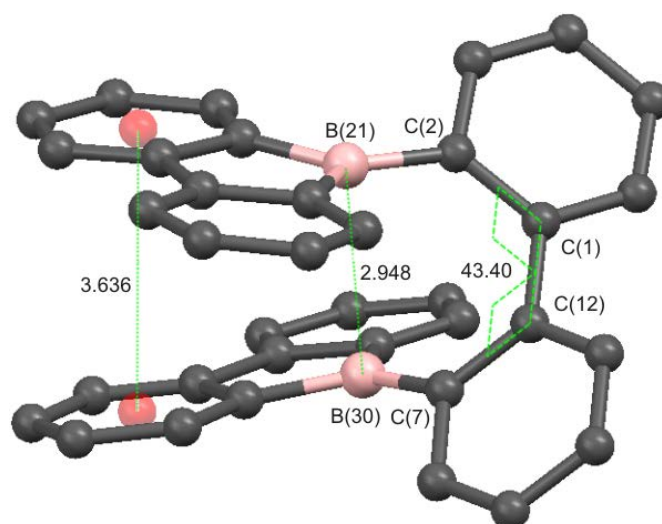


Figure 5.4 Molecular structure of **6a**. Hydrogen atoms are omitted for clarity. The red dots mark the center of rings. Selected bond lengths [Å] and angles [°]: B(21)–C(2) 1.558(5), C(2)–C(1) 1.414(4), C(1)–C(12) 1.480(5), C(12)–C(7) 1.415(5) and C(7)–B(30) 1.551(5); B···B 2.948; Selected dihedral angle [°]: C(2)–C(1)–C(12)–C(7) 43.40.

Compound **6a** crystallizes monoclinically in the space group $P2_1/c$ with $Z = 4$. The planar dibenzoborole units have comparable bond lengths and angles. The syn orientation of the two dibenzoborole units in **6a** is unexpected in view of their size and results in a dihedral angle C(2)–C(1)–C(12)–C(7) of 43.4° . This is rather small compared to the value of this particular dihedral angle in 1,1'-binaphthyl-2,2'-diboronic acid (96.65°).^[114] In the syn conformation these two 9-borafluorene units have a short distance of 3.636 Å between the centers of six membered rings indicative of π - π interaction between two dibenzoborole units. The boron-boron distance [2.948 Å] is similar to that of 1,8-bis(diphenylboryl)naphthalene [3.002 Å] indicating a significant overlap of p_z orbitals of the two boron centers as described by Hoefelmeyer and Gabbai.^[115] The average distances between B–C_{biphenyl} (1.555 Å) and in the borole units B–C (1.566 Å) are in the range of regular B–C(sp²) distances.

The synthesis of the target compound 9-azido-9-borafluorene **7** was started with a

conventional procedure of adding trimethylsilyl azide (TMSN_3) to the dichloromethane solution of **6** at $-78\text{ }^\circ\text{C}$. It was found that the crude yellow reaction mixture has one intense ^{11}B signal at δ 50.2 ppm which is expected for a typical three coordinated monomeric azidoborane **7a**. Interestingly after removal of all volatiles from the reaction mixture followed by redissolution in CD_2Cl_2 , the sample shows an additional signal in the ^{11}B NMR spectrum at δ 5.0 ppm along with δ 50.3 ppm. This new signal at δ 5.0 ppm lies in the region of tetracoordinated boron centers and is assigned to an oligomer **7b** which appears to be formed in the solid state and that persists in solution thereafter (Figure 5.5a & b).

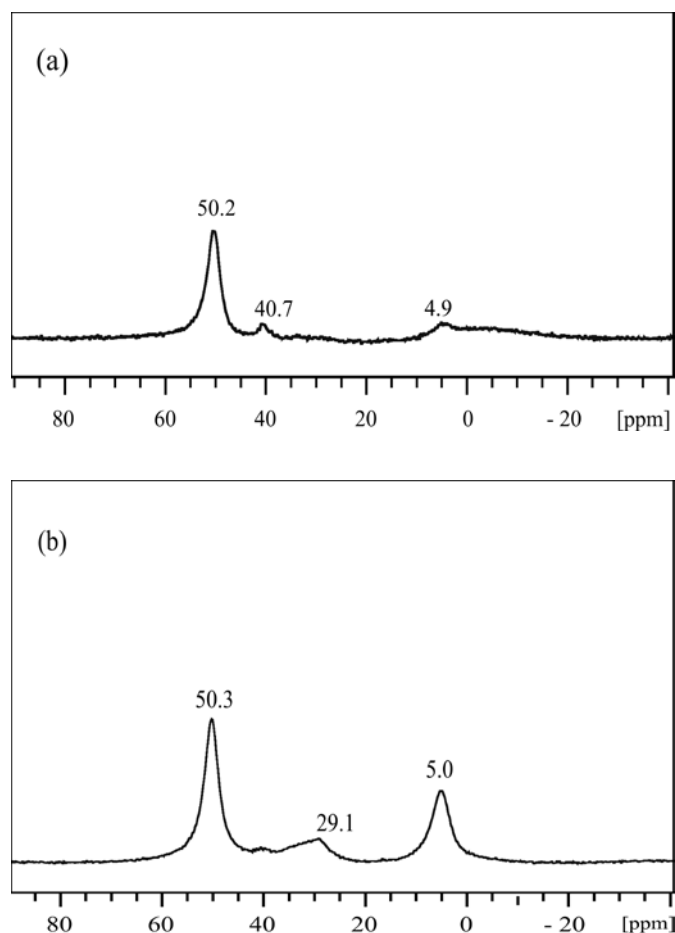
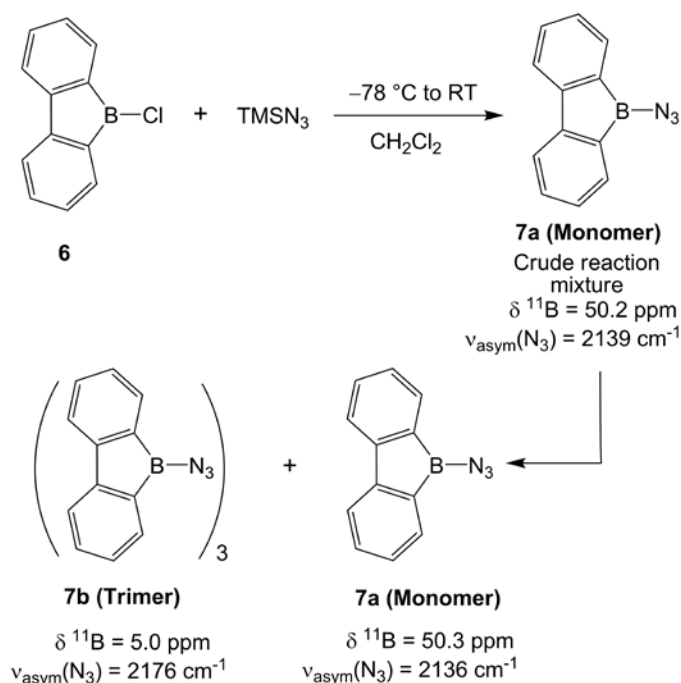


Figure 5.5 (a) Crude reaction mixture in CH_2Cl_2 ; (b) After removal of all volatiles followed by redissolution in CD_2Cl_2 .

For further understanding, the IR spectra were measured for the crude reaction mixture as well as for the redissolved crude solid. Whereas the former shows a strong absorption at 2139 cm^{-1} , the later has two absorptions in the asymmetric stretching region of azides: one is at 2136 cm^{-1} and another one is blue shifted to 2176 cm^{-1} in dichloromethane solution. This frequency shift to higher wave number is in agreement with an oligomer **7b** of monomeric 9-azido-9-borafluorene (**7a**) (Scheme 5.4). The typical range for the asymmetric stretching frequency of monomeric azidoboranes is $2100\text{--}2200\text{ cm}^{-1}$ ^[64] and that for higher oligomers like $(\text{BF}_2\text{N}_3)_3$ (2236 cm^{-1}),^[116, 117] $(\text{BCl}_2\text{N}_3)_3$ (2210 cm^{-1})^[118, 119] and $[(\text{C}_6\text{F}_5)_2\text{BN}_3]_2$ (2209 cm^{-1})^[120] clearly show that the N–N stretching vibration of bridging azides are always shifted to higher wave number compared to that of monomeric free azides.



Scheme 5.4 Synthesis of 9-azido-9-borafluorene (**7**).

9-Azido-9-borafluorene **7** is the first example of an azidoborole of type **J** (Chart 5.1). Since Wiberg and Michaud^[121] reported the first azidoborane in 1954, $[\text{B}(\text{N}_3)_3]$, many acyclic azidoboranes of type **G** (R_2BN_3 ; R = alkyl, aryl, oxo, amino)^[3, 45, 64, 122-125] have been

reported. A number of heterocyclic azidoboranes of type **H** are also known,^[3, 9, 125, 126] but only two examples of stable carbocyclic azidoboranes of type **I** have been described.^[38]

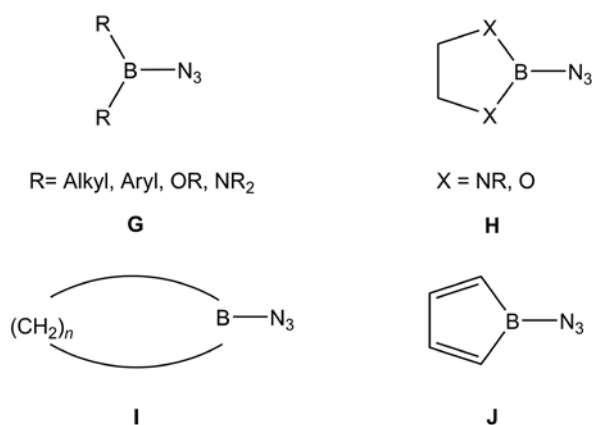


Chart 5.1 Different types of azidoboranes.

Most of the known azidoboranes are monomeric in solution and in the solid state.^[52, 124, 126] But the tendency to aggregate strongly depends on the Lewis acidity of the boron center that is controlled by electronic effects as well as by steric effects.^[38, 127] When R is small (type **G**), the azide forms oligomers. A typical example is Me₂BN₃^[123] that was found by Paetzold to show temperature dependent oligomer formation in solution. Likewise, the small and electron withdrawing halogens of dihaloazidoboranes [BX₂N₃ (X = F, Cl, Br)] result in the formation of trimers (BX₂N₃)₃.^[116, 118, 119, 128] Klapötke et al. reported the NMR data for the known (BF₂N₃)₃ in 2000.^[117] Since then only three additional aggregated azidoboranes have been structurally characterized in the solid state by Klapötke et al.: the trimer [C₆F₅B(N₃)₂]₃,^[117] and the dimers [(C₆F₅)₂BN₃]₂^[120] and [(C₆H₃F₂)₂BN₃]₂.^[124] An oligomeric structure is also likely for solid [C₆H₃F₂B(N₃)₂] based on vibrational spectroscopy.^[124] Whereas all of these azides are oligomeric only in the solid state and transform completely into monomers in solution, the 9-azido-9-borofluorene **7** (type **J**) has shown a distinct behavior of co-existence of monomer and dimer in solution. On the other

hand, spectroscopic data for $(\text{BX}_2\text{N}_3)_3$ [$\text{X} = \text{F}, \text{Cl}, \text{Br}$] show evidence only for trimeric azides in the solid state as well as in solution.^[116-119, 128]

The stability of carbocyclic azidoboranes of Type **I** appears to depend on the ring size. 1-Azido-3-methylboracyclopentane ($n = 4$) undergoes ring expansion at room temperature while carbocyclic azidoboranes with $n = 6, 7$ are found to be stable at room temperature.^[38] An attempt to synthesize 9-BBN- N_3 failed as reported by Nöth et al.^[126]

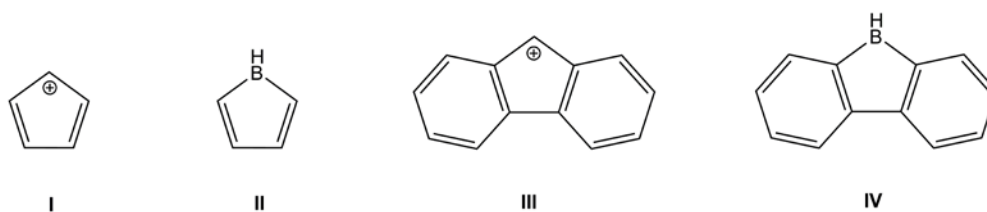


Chart 5.2 Isoelectronic structures of borole, cyclopentadienyl cation and their corresponding dibenzoderivatives.

This observation brings an insight to the antiaromatic nature of the unsaturated five membered borole ring. The parent borole (**II**, Chart 5.2) is isoelectronic to the cyclopentadienyl cation (**I**) (Chart 5.2). A quantitative comparison of unsaturated five membered ring systems based on geometric, energetic, and magnetic criteria has been convincingly interpreted by Schleyer et al.^[129] in terms of the aromatic and antiaromatic nature of these species. Recently Braunschweig et al.^[111] observed that in the solid state structure of pentaphenyl borole PhBC_4Ph_4 , the bond length alteration (BLA) in the BC_4 ring is significantly smaller than computed for the antiaromatic species in the gas phase. This was ascribed to result from intermolecular interactions that reduce the Lewis acidity of the boron center and induce the observed changes in bond lengths. Piers et al. could not identify intermolecular interactions in the solid state of the highly symmetric perfluorinated

pentaphenylborole and ascribed the apparently reduced BLA to crystallographic disorder.^[130] Yamaguchi and co-workers also noticed π interaction as judged by intermolecular distances in less symmetric boroles [$\text{Ph}_4\text{C}_4\text{BAr}$, $\text{Ar} = p\text{-MeC}_6\text{H}_4$, $p\text{-Me}_3\text{SiC}_6\text{H}_4$, $p\text{-FC}_6\text{H}_4$]. However, still significant bond length alternation was present in the BC_4 unit.^[112]

Dibenzoborole or 9-H-9-borafluorene, **IV**, is isostructural with the fluorenyl cation, **III**, whose antiaromaticity is still a matter of debate. Efforts to generate this fluorenyl cation as a long lived species in strong acid were unsuccessful.^[131] Numerous rate measurements^[131-135] display a rate retardation in forming the fluorenyl carbocation compared to the benzhydryl system, and calculations indicate that carbocation **III** is 8-10 kcal mol⁻¹ less stable than benzhydryl system.^[135-137] Excitation energy calculations^[138] propose antiaromatic character in **III**, i.e., the longest wavelength absorption of cyclopentadienyl cation increases upon annulation going to indenyl and fluorenyl cation. Already in 1966, Armstrong and Perkins^[139] have compared the calculated (using the semiempirical PPP Hamiltonian) and experimental absorption spectra of borafluorene systems with suitable models. They concluded that neutral borafluorene (**IV**) has very small π charge on boron and that the presence of the bond connecting the two phenyl rings at ortho positions “effectively cuts off π electron conjugation *via* boron.”^[139] This suggests that in borafluorenes the boron center is a strong electron acceptor. Piers et al. reported that the boron center in the perfluorinated dibenzannulated borole is more Lewis acidic than the open perfluorinated diarylborane systems.^[108]

The crystallization of the 9-azido-9-borafluorene^[102] **7** is very difficult. Still few yellow crystal blocks grown at -20 °C from dichloromethane solution of **7** confirm that the oligomer **7b** is trimeric in nature in the solid state as shown in X-ray crystallography analysis.

Unfortunately, the crystal data is not of sufficiently good quality to discuss the geometry parameters (Figure 5.6). The crystals are extremely air and moisture sensitive and even covered with oil at 100 K they decompose quite rapidly on the diffractometer. Nevertheless the data set was good enough to confirm the connectivity of **7b**.

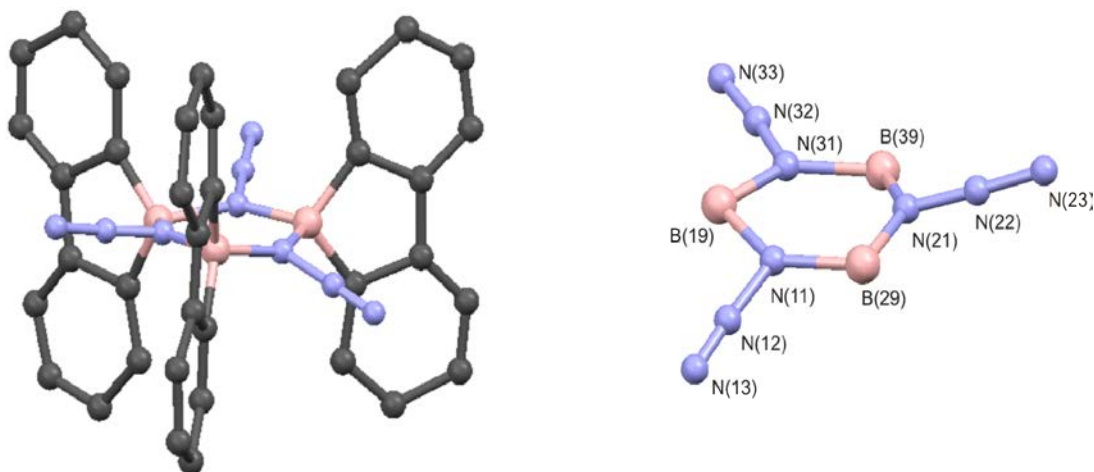
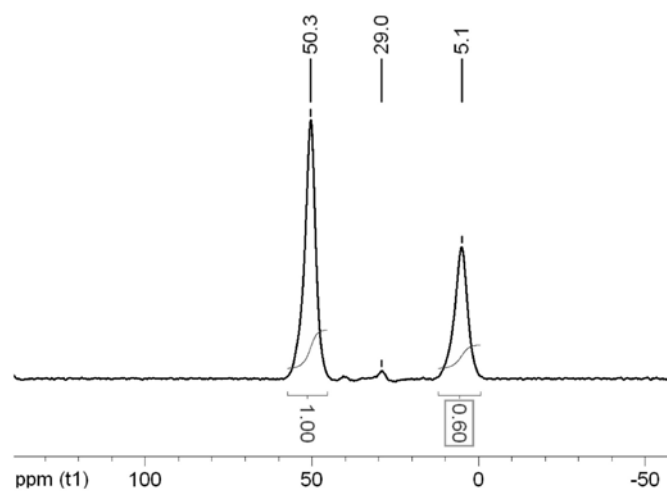
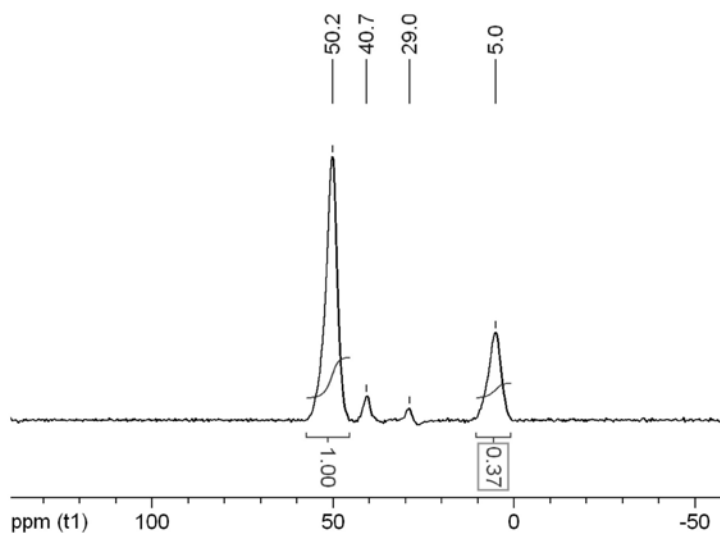


Figure 5.6 Molecular structure of **7b** (left) and depiction of its $B_3(N_3)_3$ core (right). Two dichloromethane solvent molecules and hydrogen atoms are omitted for clarity. pale yellow crystal, $0.22 \times 0.20 \times 0.10 \text{ mm}^3$, triclinic, $P\bar{1}$, $a = 11.069(4) \text{ \AA}$, $b = 11.233(3) \text{ \AA}$, $c = 16.894(5) \text{ \AA}$, $\alpha = 90.44(2)^\circ$, $\beta = 91.11(3)^\circ$, $\gamma = 118.21(3)^\circ$, $V = 1850(1) \text{ \AA}^3$, $Z = 2$, $\rho_{\text{calc}} = 1.240 \text{ g/cm}^3$, $\theta_{\text{max}} = 23.7^\circ$, $\lambda (\text{Mo K}\alpha) = 0.71073 \text{ \AA}$, $T = 110(2) \text{ K}$, 5621 independent reflections, 2223 [$I > 2\sigma(I)$], 237 parameter, $R = 0.216$, $wR = 0.537$ (for all data).

The aggregation behavior of **7** was explored by slightly increasing the temperature (Figures 5.7a & 5.7b) of its solution in CD_2Cl_2 . After keeping the temperature at 40°C for 3 hours the intensity of the signal at $\delta 5.1 \text{ ppm}$ decreased compared to the signal at $\delta 50.3 \text{ ppm}$ as expected for a monomer-oligomer equilibrium. However, an additional weak signal at $\delta 40.7 \text{ ppm}$ was observed after warming which could be due to an unknown decomposition product of the azide.



(a) At ambient temperature



(b) After warming at 40 °C for 3 hours

Figure 5.7 Temperature effect on the oligomerization of 9-azido-9-borfluorene (**7**) in CD_2Cl_2 .

The azide **7** is soluble in benzene, toluene and dichloromethane but decomposes in chloroform. Its stability in dichloromethane solution is still limited though as it slowly decomposes to a greenish compound even at $-20\text{ }^\circ\text{C}$ after a few days. Because of the

instability of this azide, the isolation and purification is very difficult. Although the nitrogen content is below the commonly accepted critical value of 25 %, sensitivity also depends on other parameters.^[87] Paetzold has stated that the formation of oligomers turn the corresponding azides into labile and dangerous compounds.^[38] The strongly Lewis acidic boron center could potentially catalyze the (spontaneous) decomposition of this azide. Due to this dangerous nature and the observed thermal instability, separation of these two compounds (**7a** & **7b**) was not possible for further matrix experiment.

The azide **7** is extremely sensitive towards degradation. In the presence of trace amount of water the yellow solid azide turns into a colorless solid that has an ^{11}B shift at 45.6 ppm. But addition of a drop of water on purpose immediately shows another peak in the ^{11}B NMR at ~ 30 ppm along with a small peak at 46 ppm. Narula and Nöth reported the ^{11}B chemical shift of 9-methoxy-9-borafluorene to be 46 ppm.^[99] So it can reasonably be assumed that the compound with the 46 ppm peak could be due to a hydrolysis product 9-hydroxy-9-borafluorene [$\text{C}_{12}\text{H}_8\text{B}-\text{OH}$]. The product with ^{11}B chemical shift at ~ 30 ppm might have a 2-biphenyl-boryl group, formed under more rigorous condition. X-ray crystallography confirms that the sample exposed to air underwent cleavage of the borole ring and 1,3,5-tris(2-biphenyl)cyclotriboroxane **8** has been formed (Figure 5.8). The colorless compound **8** crystallizes in a triclinic space group $P-1$ ($Z = 4$) with two independent enantiomeric molecules in the asymmetric unit that have equal lengths of equivalent bonds. The B_3O_3 ring is nearly planar with B–O bond distances from 1.364(15) to 1.385(15) Å and the boroxin ring angles are close to 120° with the B–O–B angles slightly larger [$120.9(9)$ – $121.6(9)^\circ$] than the O–B–O angles [$118.4(10)$ – $118.9(10)^\circ$]. This is similar to boroxin crystals investigated earlier.^[140-143]

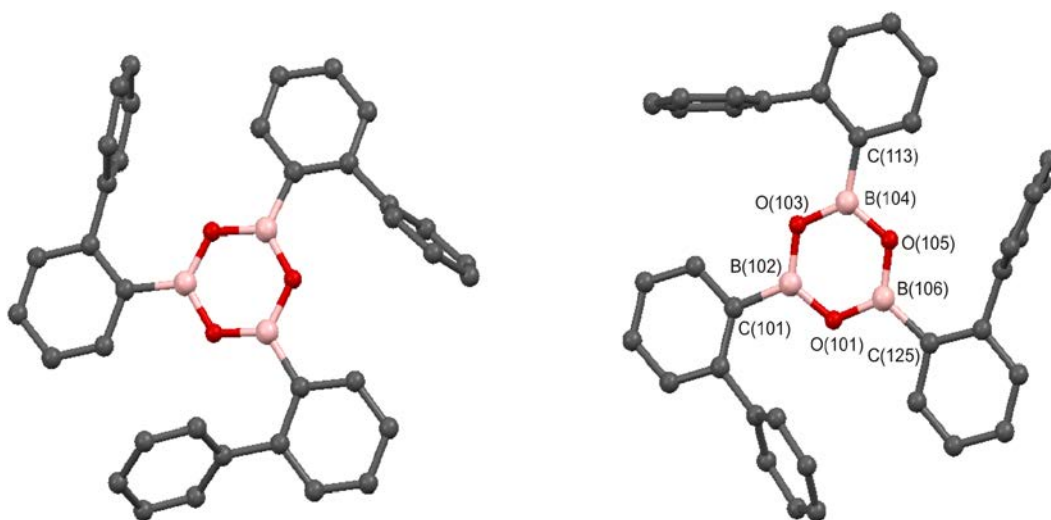


Figure 5.8 Molecular structure of **8**. Hydrogen atoms are omitted for clarity. Selected bond length lengths [Å] and angles [°] in one enantiomer: O(101)–B(102) 1.376(15), O(101)–B(106) 1.381(14), O(103)–B(102) 1.377(15), O(103)–B(104) 1.378(15), O(105)–B(106) 1.364(15), O(105)–B(104) 1.385(15), B(102)–C(101) 1.562(17), B(104)–C(113) 1.557(17), B(106)–C(125) 1.563(17); B(102)–O(101)–B(106) 121.4(10), B(102)–O(103)–B(104) 120.9(9), B(106)–O(105)–B(104) 121.6(9), O(101)–B(102)–O(103) 118.9(10), O(101)–B(102)–C(101) 121.6(11), O(103)–B(102)–C(101) 119.4(10), O(103)–B(104)–O(105) 118.7(11), O(103)–B(104)–C(113) 124.3(11), O(105)–B(104)–C(113) 117.0(10), O(105)–B(106)–O(101) 118.4(10).

Note that Wehmschulte et al. have reported that the sterically encumbered boraffluorene compounds 1-(4-*tert*-butylphenyl)-7-*tert*-butyl-9-(bis-2,6-(4-*tert*-butylphenyl)phenyl)-9-boraffluorene (**II**) and 1-(3,5-dimethylphenyl)-6,8-dimethyl-9-(bis-2,6-(3,5-dimethylphenyl)phenyl)-9-boraffluorene are air and moisture stable (**III**, Figure 5.9).^[109] Exposure of the pyridine adduct of 1-(4-*tert*-butylphenyl)-7-*tert*-butyl-9-(bis-2,6-(4-*tert*-butylphenyl)phenyl)-9-boraffluorene to concentrated aqueous HCl for one week in the presence of air led to cleavage of one of the B–C bonds of the boraffluorene unit (**IV**, Figure

5.9). The splitting pattern is similar for the highly stable compound of Wehmschulte et al.^[109] and the labile 9-azido-9-borafluorene **7**.

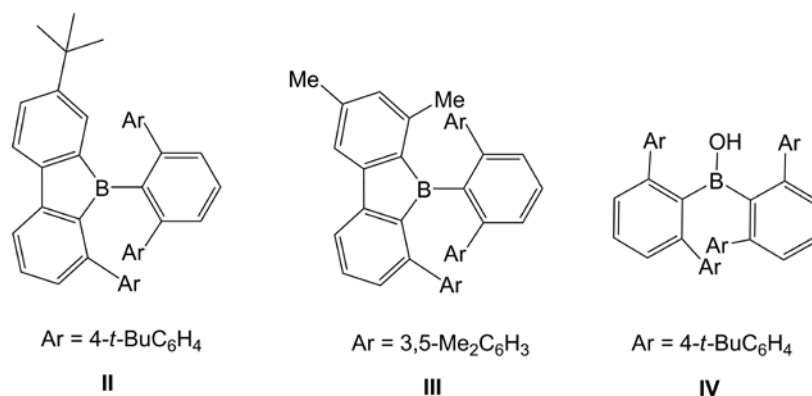
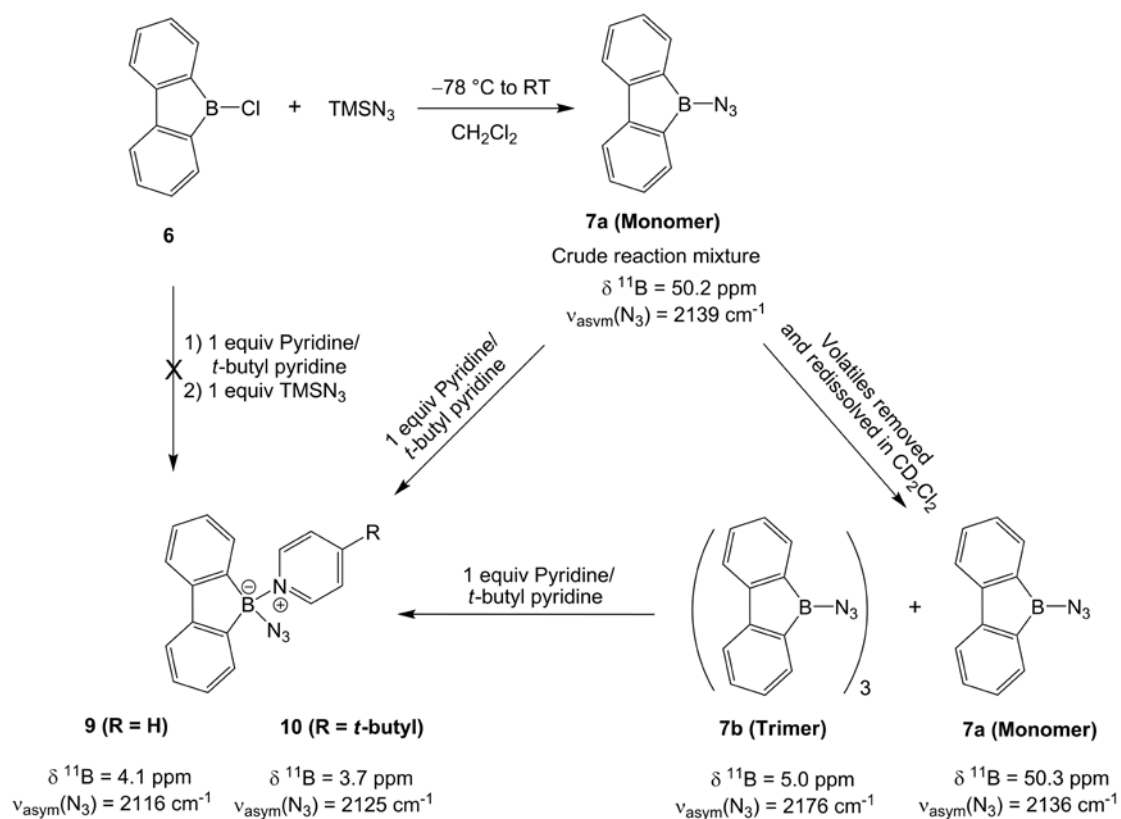


Figure 5.9 Structures of **II**, **III** and **IV**.

Addition of pyridine or 4-*t*-butylpyridine (mentioned as *t*-butyl pyridine throughout the following discussion) to 9-azido-9-borafluorene (**7a**) (the crude reaction mixture) as well as to the redissolved product (**7a** & **7b**) in dichloromethane, in separate experiments, produced the identical colorless stable pyridine adducts of 9-azido-9-borafluorene **7** (**9** & **10** Scheme 5.5). Compound **9** and **10** showed the $\delta^{11}\text{B}$ chemical shift at 4.1 and 3.7 ppm respectively. And the azide groups were identified by the strong absorption bands at 2116 (for **9**) and 2125 cm^{-1} (for **10**) in the IR vibrational spectra. This red shift of the asymmetric stretching vibration of azide is well known for pyridine adducts of different azidoboranes as reported earlier for catBN_3 (2169 cm^{-1}) and $\text{catBN}_3\cdot\text{py}$ (2132 cm^{-1}) [cat = catechol];^[126] $[(\text{C}_6\text{F}_5)_2\text{BN}_3]_2$ (2202 cm^{-1}) and $(\text{C}_6\text{F}_5)_2\text{BN}_3\cdot\text{py}$ (2137 cm^{-1});^[120] $[\text{C}_6\text{F}_5\text{B}(\text{N}_3)_2]_3$ (2200/2180/2142 cm^{-1}) and $\text{C}_6\text{F}_5\text{B}(\text{N}_3)_2\cdot\text{py}$ (2146/2130 cm^{-1}).^[117]



Scheme 5.5 Coordination reaction of **7** with pyridines.

Attempts to synthesize **9** or **10** from their corresponding pyridine adducts of the 9-chloro-9-borofluorene, i.e. **6•py** & **6•*t*-butyl py** (**6b**), by reacting with TMSN_3 were unsuccessful. The starting materials were recovered completely [**6•py** ($\delta^{11}\text{B} = 5.6\text{ ppm}$, CD_2Cl_2) and **6•*t*-butyl py** (**6b**) ($\delta^{11}\text{B} = 5.5\text{ ppm}$, CD_2Cl_2)]. The electron pair from the coordinating nitrogen atom saturates the boron center electronically and thus no substitution could take place thereafter.

Slow evaporation of solvent from the CH_2Cl_2 solution of compound **9** produces colorless needle shaped crystals. The crystal structure of compound **9** (Figure 5.10) confirms the existence of monomeric azide **7a** in the reaction mixture. This compound crystallizes triclinically in the *P*-1 space group with eight formula units in the unit cell and four molecules in the asymmetric unit. The boron atom is tetrahedrally arranged and bonded to pyridine with a B–N dative bond (average length B–N_{py} 1.61 Å). Comparing this distance

with earlier investigated crystal structures of pyridine adducts of azidoboranes, i.e. 9-BBN-N₃•py (1.637 Å) [prepared from 9-BBN-Cl with TMSN₃ in presence of pyridine]^[126] or (2-FC₆H₄)₂BN₃•py (1.621 Å),^[124] suggests that the boron center in dibenzoborole is slightly more acidic and acts as a better acceptor towards the pyridine donor. The azide group attached to boron is slightly bent [N_α-N_β-N_γ 174-176°] in all molecules **9**. The B-N_α bond length of 1.562 Å (avg.) is a little shorter than a typical B-N single bond (1.59 Å). The N_β-N_γ (avg. 1.136 Å) is shorter than N_α-N_β (avg. 1.192 Å) and these bond distances have lengths between those of a N-N double (1.24 Å) and a triple bond (1.10 Å).^[126]

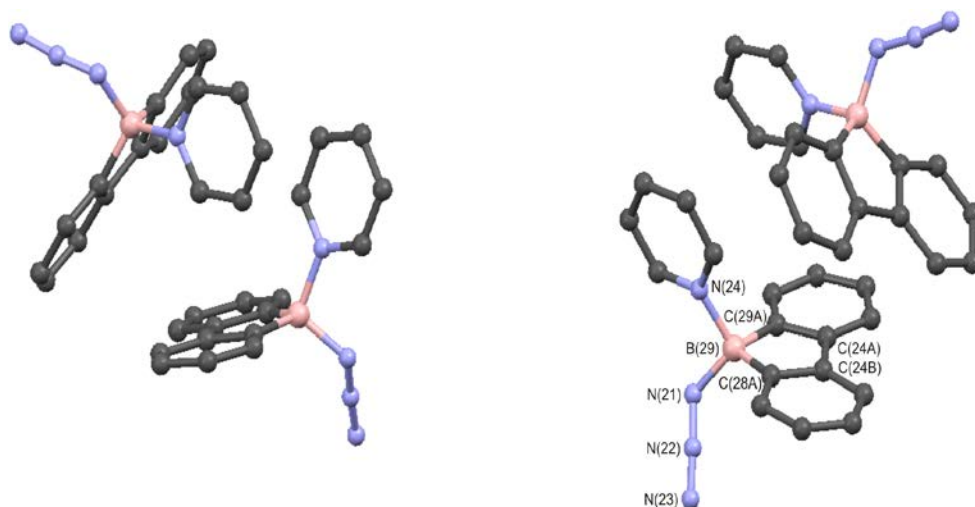


Figure 5.10 Molecular structure of **9** in an asymmetric unit. Hydrogen atoms are omitted for clarity. Selected bond length lengths [Å] and angles [°] in single molecule: N(21)-B(29) 1.559(3), N(21)-N(22) 1.201(2), N(22)-N(23) 1.136(2), N(24)-B(29) 1.619(2), C(28A)-B(29) 1.610(3), C(29A)-B(29) 1.598(3), C(24B)-C(28A) 1.406(2), C(24A)-C(24B) 1.485(2), C(24A)-C(29A) 1.409(2); N(21)-N(22)-N(23) 175.9(2), B(29)-N(21)-N(22) 119.99(17), C(29A)-B(29)-C(28A) 101.12(16), C(24B)-C(28A)-B(29) 108.58(17), C(24A)-C(29A)-B(29) 108.93(16), C(28A)-C(24B)-C(24A) 110.68(16), C(29A)-C(24A)-C(24B) 110.54(17).

The trapping reaction of **7** was also carried out with *t*-butyl pyridine producing 9-azido-9-borofluorene•*t*-butyl py **10**. After washing with pentane the colorless, crystalline, moisture sensitive pure product was obtained. Addition of *t*-butyl pyridine shifts the ^{11}B NMR signal upfield to δ 3.7 ppm and the IR stretching frequency to lower frequency ($\nu_{\text{asym}}\text{N}_3$ 2125 cm^{-1}) compared to the free azide **7**. The single crystal X-ray analysis confirms the structure of **10** as depicted in Figure 5.11.

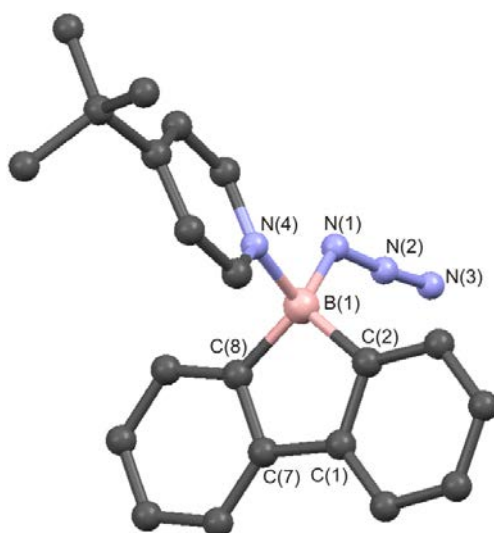


Figure 5.11 Molecular structure of **10**. Hydrogen atoms are omitted for clarity. Selected bond

length lengths [\AA] and angles [$^\circ$]: B(1)–C(2) 1.611(19), B(1)–C(8) 1.617(2), C(2)–C(1) 1.413(17), C(1)–C(7) 1.485(18), C(7)–C(8) 1.410(17), N(1)–N(2) 1.208(14), N(2)–N(3) 1.138(15), B(1)–N(1) 1.548(16), B(1)–N(4) 1.608(17); N(1)–N(2)–N(3) 174.4(13), B(1)–N(1)–N(2) 121.7(11), B(1)–C(2)–C(1) 109.1(11), C(2)–C(1)–C(7) 110.8(11), C(1)–C(7)–C(8) 110.6(11), C(7)–C(8)–B(1) 109.1(11), C(2)–B(1)–C(8) 100.5(10).

Compound **10** crystallizes in the monoclinic space group $P2_1/c$ with $Z = 4$. It shows tetrahedral coordination geometry around the boron atom. Again, the azide group is slightly bent at N(2) [N(1)–N(2)–N(3) 174.4 $^\circ$] and the N(2)–N(3) bond (1.138 \AA) is shorter than the N(1)–N(2) bond (1.208 \AA). The B(1)–N(1) (1.548 \AA) and B(1)–N(4) (1.608 \AA) distances are

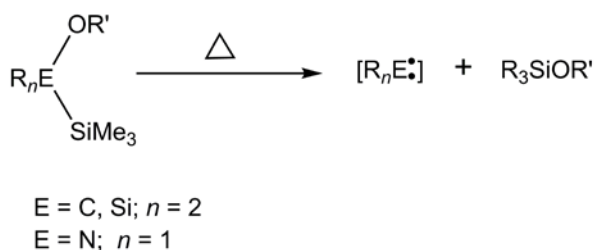
comparable to those of pyridine adduct **9**. The bond lengths in the BC_4 unit, B(1)–C(2) 1.611 Å, B(1)–C(8) 1.617 Å are in the range that is typical for B–C(sp^3) single bonds for tetrahedral boron center 1.60–1.64 Å.^[144] The bond lengths C(2)–C(1) 1.413 Å, C(1)–C(7) 1.485 Å and C(7)–C(8) 1.410 Å resemble to the structural parameters found in 9-chloro-9-borafluorene. Thus it can be concluded that these bond lengths have little dependence on the coordination number of the boron center.

To summarize, a new type of azidoborane of the borole system (type **J**) has been achieved through these experiments for the first time. The extremely Lewis acidic boron center in the 9-azido-9-borafluorene **7** made the azidoborane highly unstable to isolate and thus compound **7** transformed into a higher oligomer. The azide **7** existed as a monomer **7a** in solution just after its synthesis, but once the cyclotrimer **7b** was formed in the solid state, that coexisted with the monomer **7a** after redissolution. Due to the spontaneous decomposition of the 9-azido-9-borafluorene monomer at room temperature continuation of any further experiment was not possible; but the azide was trapped as pyridine adducts. These were characterized completely by multinuclear NMR spectroscopy and X-ray crystallography.

6. Route via Silyl(silyloxy)aminoborole

6.1 Background Informations and Proceedings

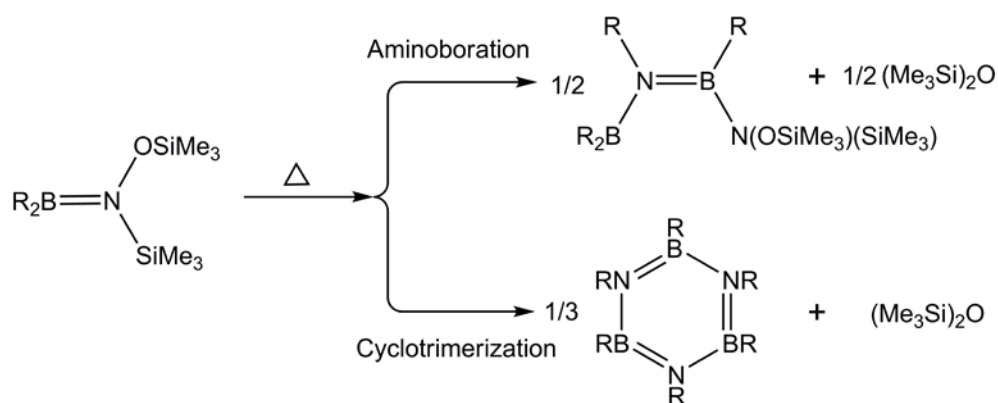
In 1974, Tsui et al. reported the synthesis of phenyl nitrene (PhN) via α -deoxysilylation process from hydroxylamine derivatives according to Scheme 6.1.^[145, 146] This pyrolysis process was already known to result in α -elimination at carbon^[147, 148] or silicon centers.^[149-151] Later on these pyrolysis reactions for the generation of nitrenes have been explored with variety of organosilylated hydroxylamine derivatives like $R_nE(OR)(SiMe_3)$ [$E = N$; $R = COOEt, ArCO, ArSO_2, Me, H$ and $R' = SiMe_3, SiMe_2t-Bu, C(O)Ph$].^[152]



Scheme 6.1 α -Deoxysilylation process for group IV and V elements at the elimination center (E).^[145]

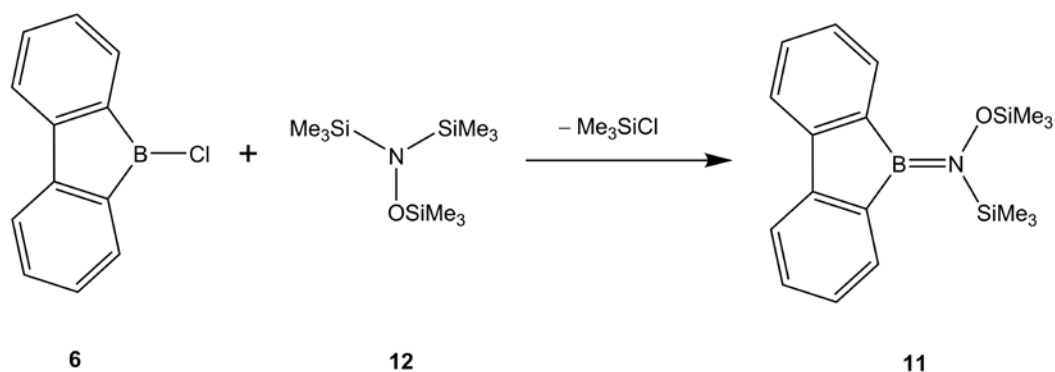
The α -deoxysilylation process increases the synthetic flexibility to generate boryl nitrene by using $R_2B-N(TMS)(OR)$ as a precursor. In 1981, Paetzold first reported the synthesis of iminoborane ($R-B\equiv N-R', C$) from the dialkyl[(trimethylsilyl)(trimethylsilyloxy)amino]boranes, $R_2B-N(OTMS)(TMS)$ by thermally induced α -deoxysilylation.^[46] Only a handful of examples of *N*-trimethylsilyl(*N*-trimethylsilyloxy)aminoboranes are known so far that have been successfully prepared and characterized. These are $R_2B-N(OTMS)(TMS)$ [$R = Me, Et, Pr, Bu, i-Pr, i-Bu,$

$-\text{CH}_2-\text{CH}(\text{CH}_3)-\text{CH}_2-\text{CH}_2-$, 9-BBN].^[38, 46, 53, 65, 153] When these aminoboranes are thermolized in the liquid phase or in the gas phase, elimination of $(\text{Me}_3\text{Si})_2\text{O}$ and mixtures of $(\text{R}-\text{B}\equiv\text{N}-\text{R})_3$, $\text{R}_2\text{B}-\text{NR}-\text{BR}-\text{N}(\text{OTMS})(\text{TMS})$ have been obtained (Scheme 6.2).^[46, 53, 65] The gas phase thermolysis of the compounds $\text{R} = \text{Et}, \text{Pr}$ at $270\text{ }^\circ\text{C}$ produce polymeric material along with the trimers of the corresponding iminoboranes.^[46]



Scheme 6.2 Thermolysis reaction products of $\text{R}_2\text{BN}(\text{OTMS})(\text{TMS})$.^[46]

As it was shown by Paetzold that thermolysis of *N*-trimethylsilyl(*N*-trimethylsilyloxy)aminoboranes is a plausible route to generate iminoboranes, similarly 9-[trimethylsilyl(trimethylsilyloxy)amino]-9-borafluorene (**11**) was considered as a precursor for 9,10-didehydro-9-aza-10-boraphenanthrene (**E**). The compound **11** should be accessible from the corresponding chloride i.e. 9-chloro-9-borafluorene **6** by reacting with tris(trimethylsilyl)hydroxylamine $[(\text{TMS})_2\text{N}(\text{OTMS})]$, **12** according to following Scheme 6.3.

Scheme 6.3 Synthetic design for **11**.

Reports on aminoboroles are relatively scarce. The only five aminoboroles^[99, 154-156] reported so far are shown in Chart 6.1. In **a**, **b** and **c**, the borole units are surrounded by bulky substituents which stabilize those aminoboroles for characterization, but the parent aminoborole $[\text{H}_4\text{C}_4\text{B}=\text{NH}_2]$ is still unknown. Herberich et al. succeeded in isolating the dilithio salts of a few aminoboroles **f**.^[157, 158] Herberich and Ohst have observed that upon oxidation with SnCl_2 the lithium-[1-(diisopropylamino)borolenediide], $\text{Li}_2[\text{H}_4\text{C}_4\text{B}=\text{N}(\textit{i}\text{-Pr})_2]$ results in the Diels-Alder dimer of the corresponding aminoborole (Scheme 6.4).^[159] Apart from these compounds, two more examples of dibenzoaminoboroles **d** and **e** are known where dibenzoannulation of the borole rings provide the structural stability for those aminoboroles.

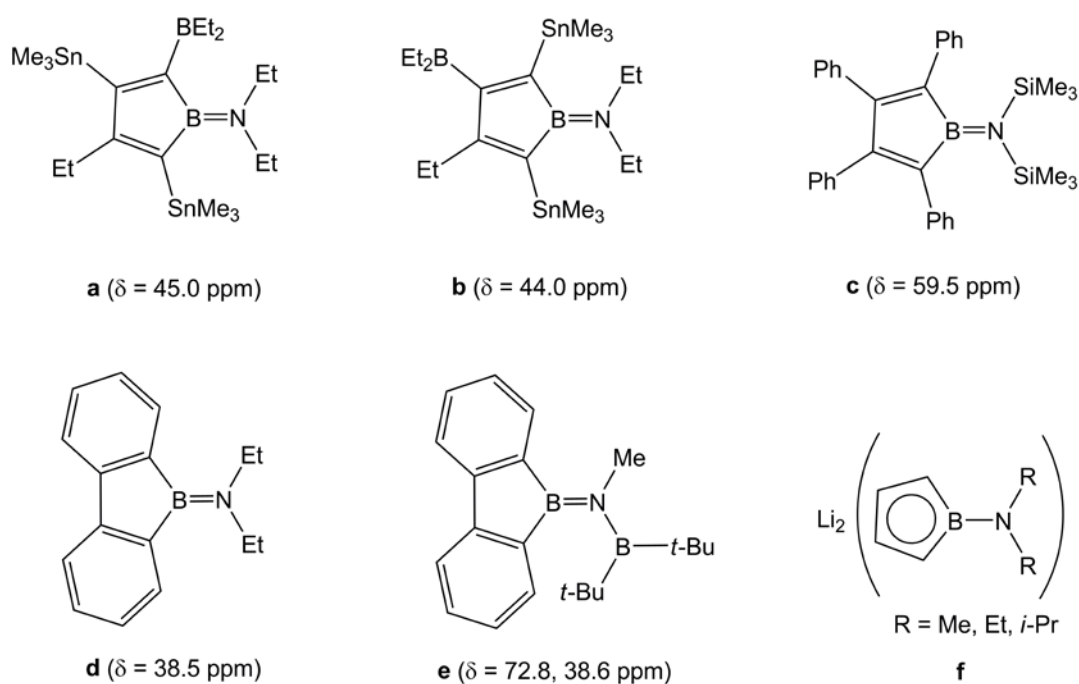
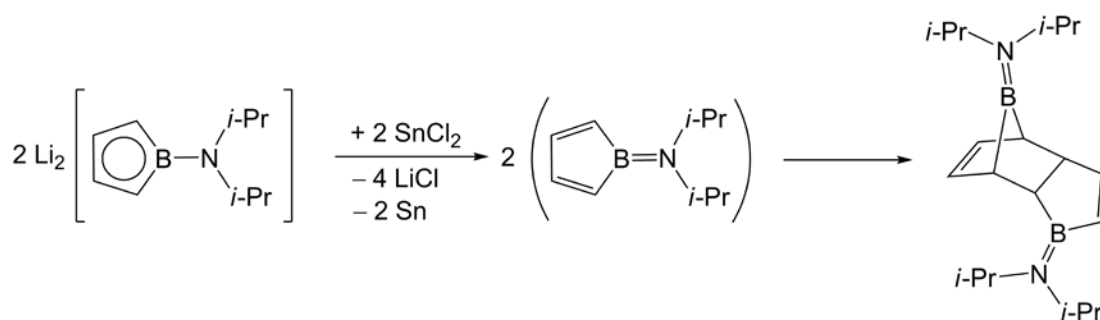


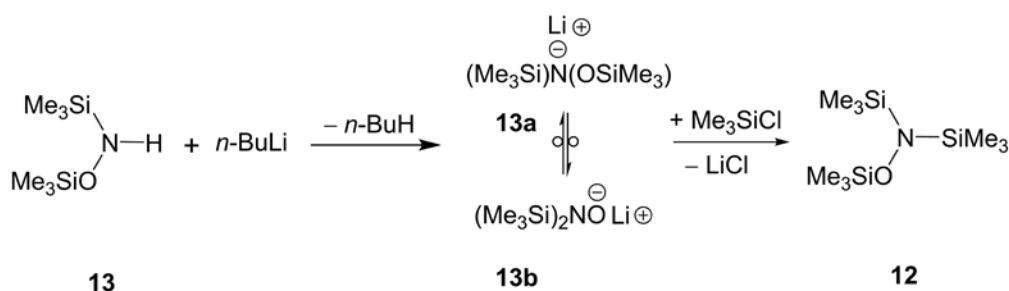
Chart 6.1 Reported aminoboroles; $\delta^{11}\text{B}$ chemical shifts are given in parentheses.



Due to the instability of the free boroles as 4π antiaromatic systems^[111, 129] they are particularly challenging to synthesize. But the dilithio salts of different boroles (Chart 6.1 **f**) react with various types of metal compounds to produce a large variety of metal complexes e.g. sandwich compounds $(\eta^5\text{-C}_4\text{H}_4\text{BR})_2\text{M}$ [$\text{M} = \text{Ni}$, $\text{R} = \text{H}$, Me , Bu , $t\text{-Bu}$, Ph ,^[160] F , Cl , Br , I , OH , OMe , OCH_2Ph , NMe_2 , Ni-Pr_2 ^[159]],^[161] mono or dinuclear complexes $(\eta^5\text{-C}_4\text{H}_4\text{B}=\text{Ni-Pr}_2)\text{ML}$ [$\text{ML} = \text{Ru}(\text{C}_6\text{Me}_6)$, $\text{Rh}(\text{C}_5\text{Me}_5)$] and $(\eta^5\text{-C}_4\text{H}_4\text{B}=\text{Ni-Pr}_2)(\text{ML})_2$ [$\text{ML} = \text{Rh}(\text{C}_2\text{H}_4)_2$, $\text{Rh}(\text{COD})$].^[159]

6.2 Results and Discussions

In 1968, Witke et al. reported the synthesis of the amine **12** by silylation of hydroxylammonium sulfate.^[162] Since then hydroxylamines have attracted attention due their interesting properties toward anionic, radical and thermal neutral intramolecular rearrangements.^[163-170]



Scheme 6.5 Synthesis of tris(trimethylsilyl)hydroxylamine **12**.

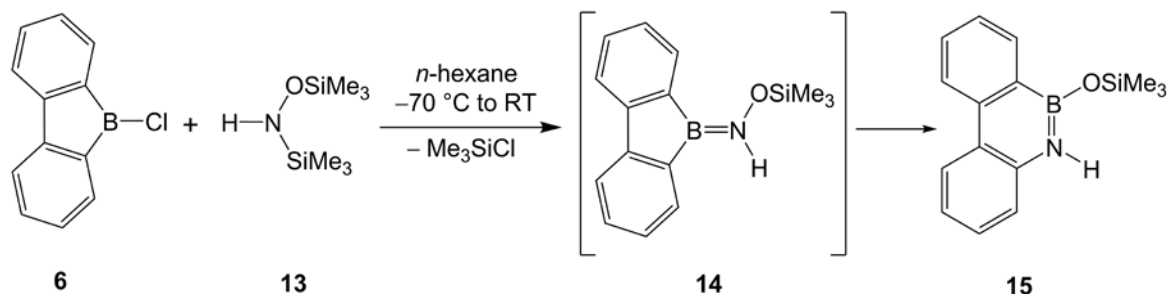
West et al. reported that upon treatment of **13** with base an equilibrium is formed between the anions **13a** and **13b**. Later, the migratory aptitude of organosilicon groups has been investigated in detail by the same group.^[170, 171] The derivatization reactions of a number of deprotonated organosilylhydroxylamines produce an isomeric distribution of products depending on the derivatizing agents used, and this implicates the existence of an equilibrium between the isomeric anions.^[171]

In the present work, the tris(trimethylsilyl)hydroxylamine, (TMS)₂N(OTMS) **12**, was prepared by lithiation of the *N,O*-bis(trimethylsilyl)hydroxylamine [HN(TMS)(OTMS), **13**] followed by addition of trimethylsilylchloride (TMSCl) according to the reported procedure (Scheme 6.5).^[172] The product was characterized by ¹H,^[172, 173] ¹³C and ²⁹Si NMR. The purity was also checked by GC-MS analysis where **12** eluted at 13.5 min and ~ 8 % starting material **13** was also identified as contamination (R_t = 6.9 min).

Amine **12** was added to the bright yellow *n*-hexane solution of 9-chloro-9-borafluorene at -78 °C. No immediate color change was observed but with increase of temperature the color fades and at approximately 10 °C precipitation of a solid was observed. Then the faint yellow solution was decanted under inert atmosphere to separate the slightly yellow precipitate. This isolated solid is insoluble in *n*-pentane, *n*-hexane, dichloromethane and chloroform but soluble in THF. Unfortunately, no defined product could be identified from the solid precipitate. The solid was found to be non-volatile under EI mass spectrometric conditions. Removal of the solvent from the decanted solution produced a slightly brown solid that was examined by mass spectrometry and also by GC-MS analysis. The complex mass spectra showed no indication for the presence of the desired product 9-[trimethylsilyl(trimethylsiloxy)amino]-9-borafluorene (**11**) or of any other rearranged products of **11**. Notably, the reverse addition of the reagents did not change the outcome.

Paetzold et al. reported that the trimethylsilyl(trimethylsiloxy)aminoboranes $[\text{R}_2\text{B}=\text{N}(\text{OTMS})(\text{TMS})]$ are very susceptible towards high temperature, and in three cases $[\text{R} = i\text{-Pr}, i\text{-Bu}, -\text{CH}_2-\text{CH}(\text{CH}_3)-\text{CH}_2-\text{CH}_2-]$ ^[38, 65] the products show complete decomposition upon attempted distillation. According to their reports, during the synthesis of $(i\text{-Bu})_2\text{B}=\text{N}(\text{OTMS})(\text{TMS})$ and $9\text{-BBN}=\text{N}(\text{OTMS})(\text{TMS})$ they also have observed formation of unidentified solid.^[38, 65] These experimental studies indicate that the reaction between chloroborane and tris(trimethylsilyl)amine **12** is not merely an elimination of TMSCl , but more complex. Furthermore, the borafluorene unit may additionally limit the stability. Note, for example, that the alkylideneamino-borane $\text{Ph}_2\text{C}:\text{N}-\text{BPh}_2$ is monomeric whereas the borafluorene derivative forms polymeric material $(\text{Ph}_2\text{C}:\text{N}-\text{BC}_{12}\text{H}_8)_n$, as reported by Summerford and Wade.^[174]

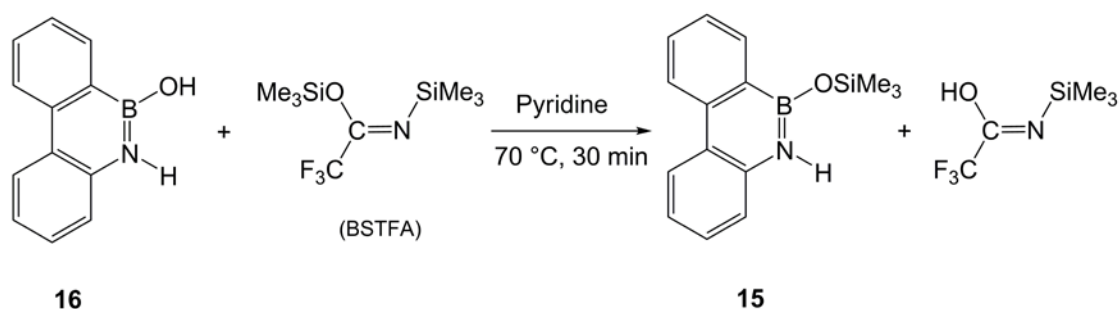
For further understanding, a reaction was performed between 9-chloro-9-boraphluorene **6** and *N,O*-bis(trimethylsilyl)hydroxylamine **13** in *n*-hexane and surprisingly a rearranged product **15** was obtained instead of the expected aminoborole **14** (Scheme 6.6). This is the first example of an aminoborole to 1,2-dihydro-1,2-azaborine rearrangement.^[175]



Scheme 6.6 Aminoborole to 1,2-dihydro-1,2-azaborine rearrangement.

Upon treating **13** with one equivalent of **6** in *n*-hexane at $-70\text{ }^{\circ}\text{C}$ immediate formation of a colorless precipitate was observed. That precipitate started to dissolve at around $-20\text{ }^{\circ}\text{C}$ and a colorless solution remained at room temperature. A colorless solid product was obtained by precipitation from the concentrated reaction mixture at $-18\text{ }^{\circ}\text{C}$ within a few days. According to high resolution electron impact mass spectrometry the product has the stoichiometry of **14** or **15** but the ^{11}B NMR shift, 27 ppm, is at higher field than expected for an aminoborole ($\delta^{11}\text{B} > 35\text{ ppm}$, Chart 6.1). This chemical shift is rather similar to the boron center that is coordinated by two hetero atoms as in **15**. The eleven signals observed in the aromatic region of the ^{13}C NMR spectrum are in agreement with **15**, assuming that the carbon atom bonded to boron is not detected; whereas only ten signals are expected for **14** assuming a hindered BN bond rotation. The GC-MS analysis of **15** and the product derived from derivatization of known **16** with *N,O*-bis(trimethylsilyl)trifluoroacetamide (BSTFA) (Scheme 6.7) show identical retention times and mass spectra, in support of an assignment to a 9-aza-10-boraphenanthrene system (see page 109). Compound **16** was prepared according to

procedure reported by Harris et al.^[176]



Scheme 6.7 Derivatization reaction of **16** with BSTFA.

Finally the assignment based on the spectral data was confirmed by a single crystal X-ray crystallographic analysis. The colorless crystals were grown by slow evaporation of dichloromethane solvent. Figure 6.1 shows the molecular structure of compound **15**. The B–N [1.420(3) Å], C–N [1.399(3) Å], B–C [1.547(3) Å], all bond distances and C–B–N [115.3(2)°], B–N–C [124.5(2)°] bond angles are similar to related oxy-substituted 9-aza-10-boraphenanthrene systems.^[176-178] One unit cell consists of four molecules of **15**. The molecules have a regular π -stacking in the crystal packing with a shortest distance of 3.62 Å between one boron atom and an aromatic ring of the adjacent molecule (Figure 6.2). Harris et al. have also reported π - π stacking between adjacent molecules in the solid state structure of 9-hydroxy-9-aza-10-boraphenanthrene **16** but the distance is longer than 3.6 Å.^[176]

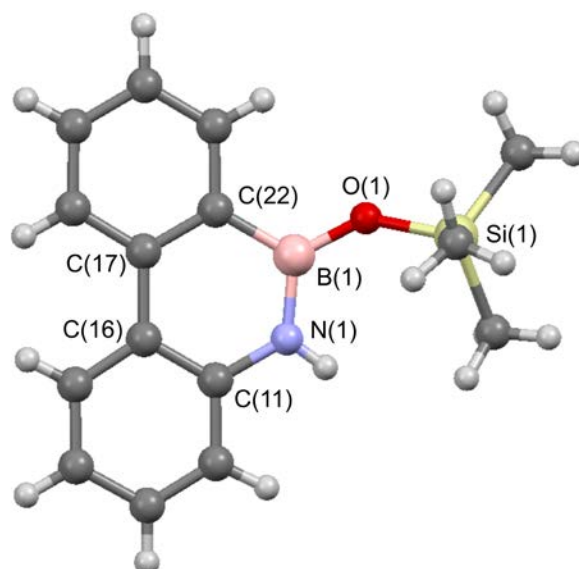


Figure 6.1 Molecular structure of **15**. Selected bond length lengths [\AA] and angles [$^\circ$]:
B(1)–C(22) 1.547(3), B(1)–N(1) 1.420(3), B(1)–O(1) 1.368(3), O(1)–Si(1) 1.6398(16),
C(11)–N(1) 1.399(3), C(11)–C(16) 1.409(3), C(16)–C(17) 1.480 (3), C(17)–C(22) 1.412(3);
C(22)–B(1)–N(1) 115.3(2), B(1)–N(1)–C(11) 124.5(2), B(1)–O(1)–Si(1) 138.68(15),
N(1)–C(11)–C(16) 120.24(19), C(11)–C(16)–C(17) 120.34(19), C(16)–C(17)–C(22)
119.39(19), C(17)–C(22)–B(1) 119.99(19); Dihedral angle Si(1)–O(1)–B(1)–N(1) 30.46(27).

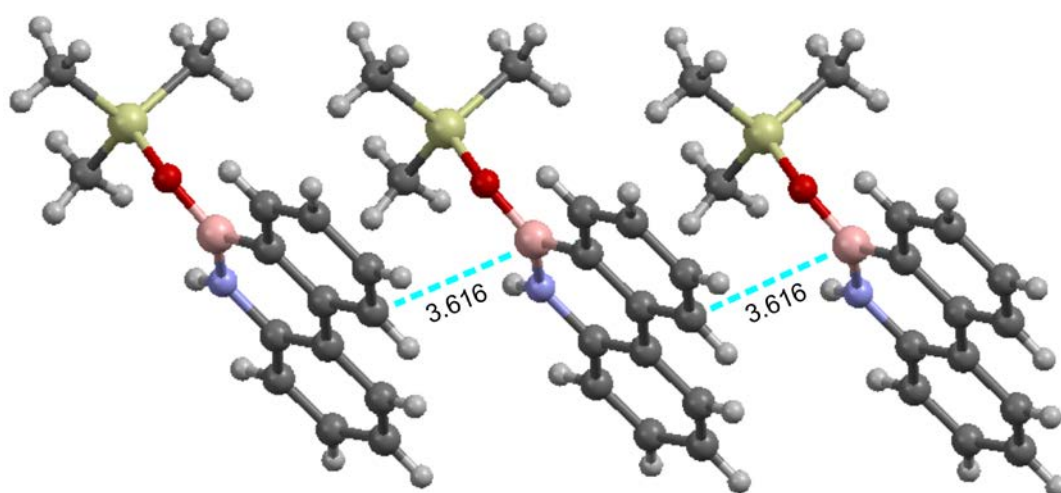


Figure 6.2 A depiction of the regular π -stacking arrangement of **15** in crystal packing.

To investigate if the expected aminoborole would have formed at lower temperature, the reaction was followed by $^{11}\text{B}\{^1\text{H}\}$ NMR spectroscopy between $-10\text{ }^\circ\text{C}$ and $26\text{ }^\circ\text{C}$ in a quartz NMR tube using $[\text{D}_6]$ -benzene as the locking solvent (Figure 6.3). Formation of the precipitate after addition of the amine **13** to the chloride **6** precluded NMR investigation at lower temperature. After dissolution of the precipitate at $-10\text{ }^\circ\text{C}$ two compounds with chemical shifts at 9.5 and 2.7 ppm were dominating. Based on the chemical shifts these compounds are believed to be tetracoordinated boron systems. With increasing temperature, these two signals decreased while one at 37.7 ppm increased and dominated at $26\text{ }^\circ\text{C}$.

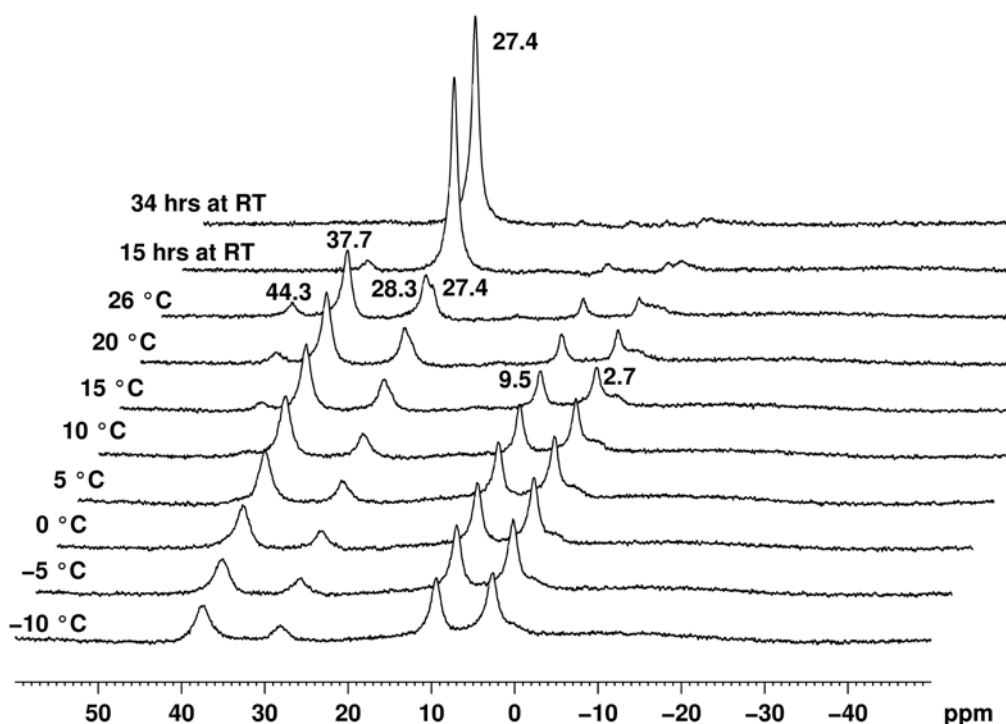


Figure 6.3 Variable temperature $^{11}\text{B}\{^1\text{H}\}$ NMR (160 MHz) investigation of the reaction of **6** with **13** between $-10\text{ }^\circ\text{C}$ to $26\text{ }^\circ\text{C}$. The temperature was increased after the measurements in five degree steps and kept constant for 5 min before the measurements.

In a separate experiment when the temperature of the reaction mixture was decreased from $15\text{ }^\circ\text{C}$ to $-10\text{ }^\circ\text{C}$, the signals at 9.5 and 2.7 ppm were found increasing with

simultaneous decrease of the signal at 37.7 ppm. The signal at 28 ppm did not change in intensity. This suggests the existence of an equilibrium between the compounds responsible for the signals at 9.5, 2.7 and 37.7 ppm. Though no experimental evidence is obtained yet, it is reasonable to assume that the signals at 9.5 and 2.7 ppm may be due to two higher oligomers (e.g. dimer/trimer) of the aminoboroles **14** or **11** (Chart 6.2).

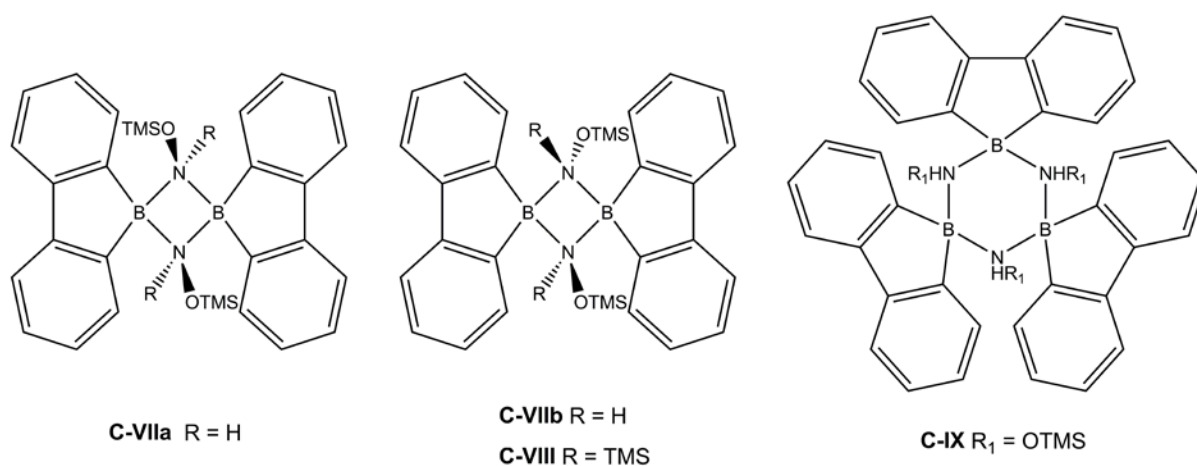


Chart 6.2 Possible dimers of the aminoboroles **14**, **11** and trimer of **14**.

To aid in an assignment of these experimental chemical shifts, DFT computation were performed. The gas-phase structures of the compounds (Table 6.1) were optimized by quantum chemical calculations at the B3LYP/6-31G(d) level of theory. Using those optimized structures, ^{11}B NMR calculations were performed at the B3LYP/6-311+G(d,p) level of theory. The ^{11}B chemical shifts were first computed using B_2H_6 as reference. Finally those shifts were referenced to $\text{BF}_3\cdot\text{OEt}_2$ [$\sigma(\text{B}_2\text{H}_6) = 84.1$, $\delta^{11}\text{B}(\text{B}_2\text{H}_6) = 18$ ppm vs $\text{BF}_3\cdot\text{OEt}_2$] and the results are summarised in Table 6.1.

Table 6.1 Computed [B3LYP/6-311+G(d,p)//B3LYP/6-31G(d)] and experimental chemical shifts of compounds **6**, **11**, **14**, **15**, **C-VIIa**, **C-VIIb** and **C-VIII**.

Compounds	Calculated chemical shifts (in ppm, referenced to BF ₃ •OEt ₂)	Experimental chemical shifts (in ppm, referenced to BF ₃ •OEt ₂)
6	64.5	63.6
11	43.6	-
14	36.6	-
15	25.0	27.3
C-VIIa (<i>cis</i> -Dimer)	3.1	-
C-VIIb (<i>trans</i> -Dimer)	4.3	-
C-VIII (<i>trans</i> -Dimer)	8.4	-

According to these computations, for the aminoborole **14** a downfield shift of 11.6 ppm compared to the 10-trimethylsilyloxy-9-aza-10-boraphenanthrene **15** is expected; thus 38.9 ppm assuming a similar error as in the calculation of **15**. So the signal developing at 37.7 ppm, seen in the NMR experiment, can be assigned to the aminoborole **14** (Scheme 6.6) which dominates at 26 °C. Compound **11** is computed to resonate at 43.6 ppm and thus the signal at 44.3 ppm is tentatively assigned to **11** (Scheme 6.3). The dimer and the trimer of the aminoborole **14** can acquire two different isomeric forms depending on the orientations of the substituents of the bridging ligand [–NH(OTMS)–]. The signal at 2.7 ppm is possibly due to one of the dimeric forms of **14** that are computed to resonate at 3.1 ppm (**C-VIIa** *cis*-dimer) and 4.3 ppm (**C-VIIb** *trans*-Dimer). The ¹¹B chemical shift of the dimer of **11** (**C-VIII** Chart

6.2) is computed at 8.4 ppm, in reasonable agreement with the measurement (9.5 ppm, Figure 6.3). With increase of temperature these dimers convert into the monomers i.e. compound **11** and **14**. The aminoboroles **11** and **14** are unstable under experimental conditions and thus formation of the rearranged product **15** already sets in above 0 °C. After stirring the reaction mixture for 15 hours at room temperature all signals except for that of **15** disappeared almost completely. The corresponding ^1H NMR measured at 26 °C under identical experimental conditions shows clean formation of **15** along with TMSCl signal. Notably, in this reaction both elimination of TMSCl or HCl is conceivable. But Nöth and Storch observed that at lower temperature TMSCl elimination is preferred in the reaction of chloroboranes with $\text{HN}(\text{TMS})_2$.^[179]

A further observation supports involvement of aminoborole dimers: the reaction between the 9-chloro-9-borafluorene **6** and $\text{HN}(\text{TMS})_2$ in *n*-hexane produced a cyclo dimer **17** of 9-amino-9-borafluorene that was identified by X-ray crystallography (Figure 6.4). The colorless crystals were obtained from the dichloromethane solution of the solid reaction mixture. The mechanism of the formation of **17** is not clear, but **17** is the first example of a 1,3,2,4-diazadiboretane compound associated with borole rings. This structure also supports the possible formation of such cyclo dimers for the aminoboroles **14** or **11** which are mentioned in the foregoing discussion. Similarly, formation of the cyclo trimer from the 9-azido-9-borafluorene **7** was also experienced as discussed in Chapter 5.^[102] Dimerization of a closely related aminoborane $[(\text{C}_6\text{F}_5)_2\text{BN}(\text{H})\text{TMS}]$ ($\delta^{11}\text{B} = 38.2$ ppm in C_6D_6) was observed by Galsworthy et al. in the reaction of $(\text{C}_6\text{F}_5)_2\text{BCl}$ with $\text{HN}(\text{TMS})_2$ and the ^{11}B NMR chemical shift of $[(\text{C}_6\text{F}_5)_2\text{BN}(\text{H})\text{TMS}]_2$ was reported at -2.8 ppm in C_6D_6 .^[180]

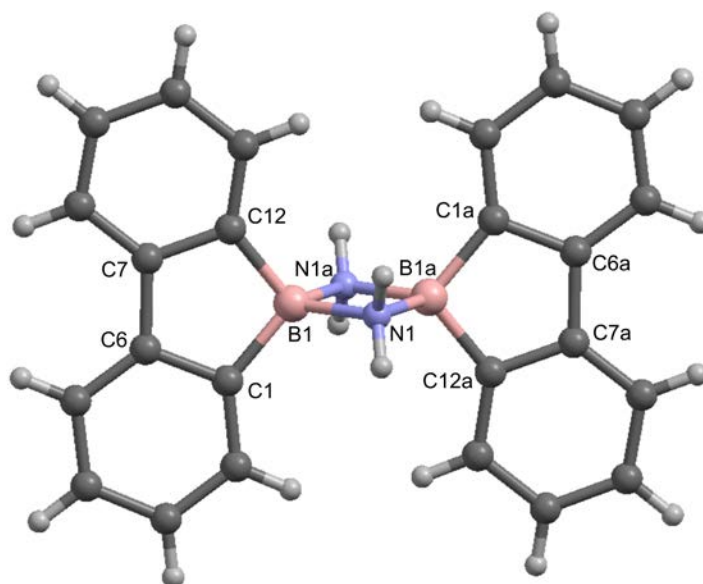
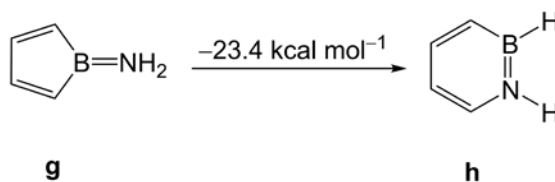


Figure 6.4 Molecular structure of **17**. Selected bond lengths [\AA] and bond angles [$^\circ$]:
 B1–N1 1.5959(16), B1–C1 1.6108(16), C1–C6 1.4160(15), C6–C7 1.4763(16), C7–C12
 1.4108(15), C12–B1 1.6075(16); B1–N1–B1a 89.23(8), N1–B1–N1a 90.77(8), C1–B1–C12
 101.07(9), B1–C1–C6 108.12(9), C1–C6–C7 111.00(9), C6–C7–C12 110.79(9), C7–C12–B1
 108.50(9).

The compound **17** crystallises in the orthorhombic space group $Pbca$ with four formula units in the unit cell. The crystal shows an inversion center and thus the structural parameters for the two borafluorene units replicate each other. The B1–N1 and B1–N1a have equal length of 1.5959(16) \AA . The B1–C1 [1.6108(16) \AA] and B1–C12 [1.6075(16) \AA] bonds are slightly longer compared to that of 9-chloro-9-borafluorene **6** (1.547 and 1.536 \AA) but similar to B–C bonds found in the tetracoordinated borafluorene systems e.g. pyridine adducts of 9-azido-9-borafluorene **9** (1.610 and 1.598 \AA) and **10** (1.611 and 1.617 \AA) (Chapter 5). The characteristic of the bond length alternation in the BC_4 ring i.e. C1–C6 [1.4160(15) \AA], C6–C7 [1.4763(16) \AA], C7–C12 [1.4108(15) \AA] and C12–B1 [1.6075(16) \AA] are also noticeable in this structure alike compound **6**, **9** and **10**. The $(BN)_2$ ring in **17** has a

nearly perfect square shape with angles of $90.77(8)^\circ$ and $89.23(8)^\circ$ at the boron and nitrogen centers respectively. All other bond angles in the borafluorene units of **17** are comparable to the structures discussed previously in Chapter 5.

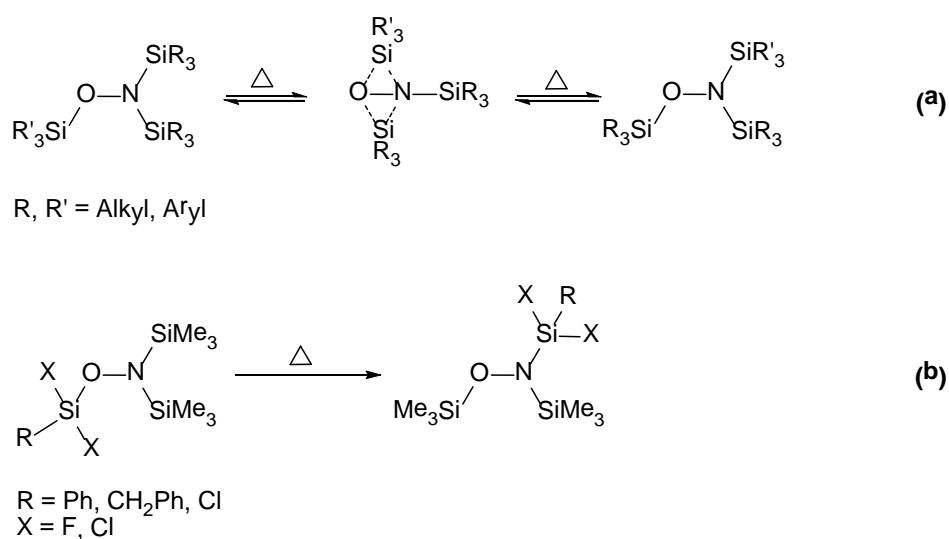
According to the computational investigations, the reaction between 9-chloro-9-borafluorene **6** and bis(trimethylsilyl)hydroxylamine **13** is found to be strongly exothermic releasing $21.1 \text{ kcal mol}^{-1}$ energy in gas-phase to form the aminoborole **14**, computed at B3LYP/6-31G(d) level of theory (Scheme 6.6). The isolated product i.e. 10-trimethylsilyloxy-9-aza-10-boraphenanthrene **15** is thermodynamically more stable compared to the structural isomer **14** and the conversion is highly exothermic ($\mathbf{14} \rightarrow \mathbf{15}$, $\Delta_{\text{R}}H = -82.6 \text{ kcal mol}^{-1}$). Additionally, the exothermicity computed at the same level of theory for the parent aminoborole **g** to 1,2-dihydro-1,2-azaborine **h** is found to be $-23.4 \text{ kcal mol}^{-1}$ (Scheme 6.8).



Scheme 6.8 Rearrangement of aminoborole (**g**) to 1,2-dihydro-1,2-azaborine (**h**) computed at B3LYP/6-31G(d) level of theory.

Although the reaction of 9-chloro-9-borafluorene **6** with bis(trimethylsilyl)hydroxylamine **13** may not provide the desired precursor aminoborole **11** to generate the 9,10-didehydro-9-aza-10-boraphenanthrene (**E**, Chart 2.1), the interesting outcome of this reaction demands more focus on it. This reaction provides the first example of isomerisation of **g** into **h** structural unit. But the available data do not provide insight into the mechanism of the rearrangement; thermal *neutral* dyotropic rearrangements of silylated

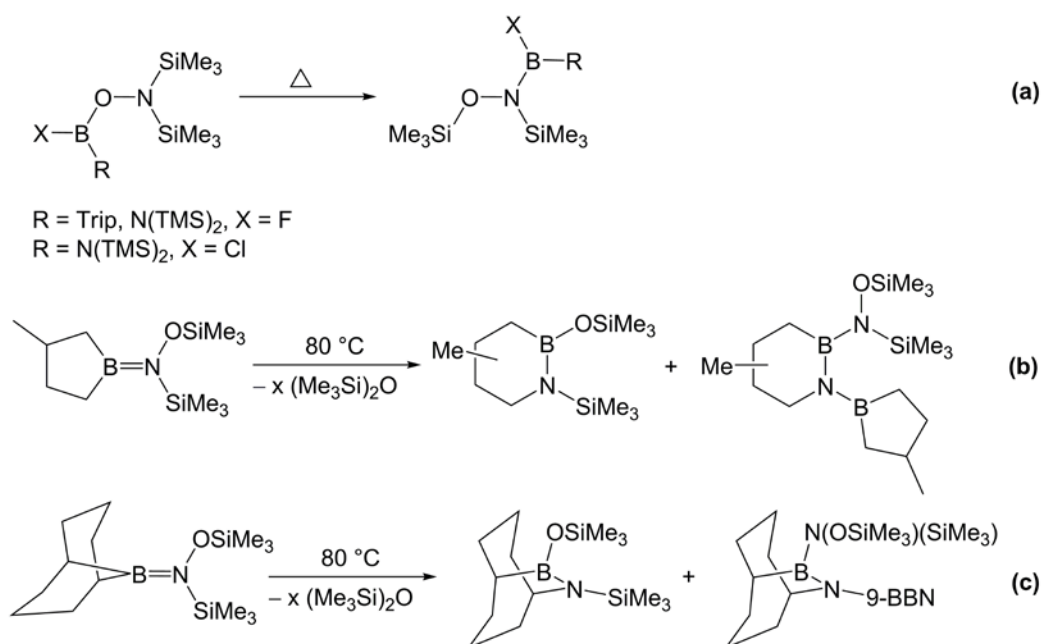
hydroxylamines are well documented since 1973 when Frainnet and Nowakowski described an exchange of trialkylsilyl groups in bis(organosilyl)hydroxylamines.^[181] Later, West et al. found thermal reversible positional exchange of organosilicon groups on nitrogen and oxygen atoms in tris(organosilyl)hydroxylamines via a dyotropic transition state^[182, 183] (Scheme 6.9a)^[164, 173] whereas for halogen-functionalized tris(organosilyl)hydroxylamines Wolfgramm et al. have observed an irreversible positional exchange (Scheme 6.9b).^[166, 167, 184]



Scheme 6.9 Thermal neutral isomerization of tris(organosilyl)hydroxylamine.

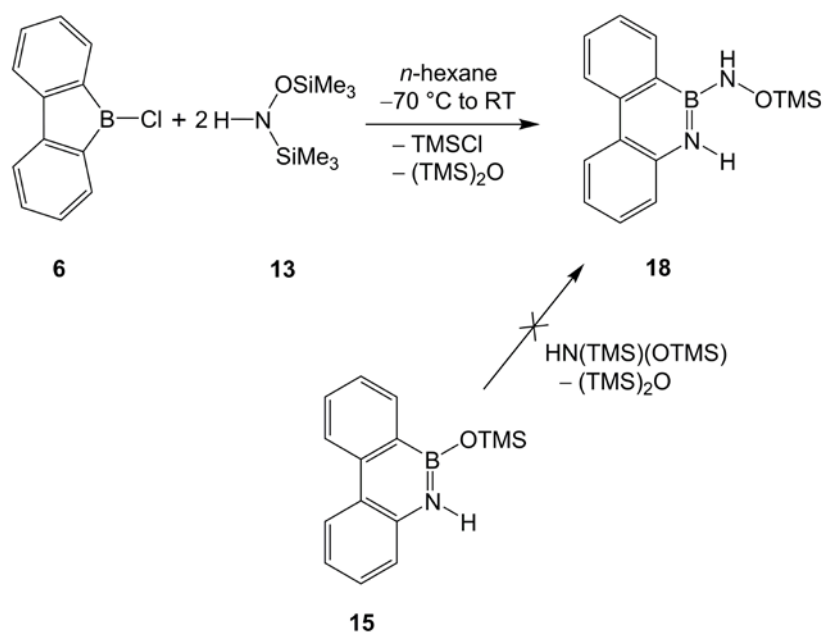
In 1999, Albrecht et al. has reported a dyotropic rearrangement of B-halogeno-boryl-hydroxylamines, R–B(X)ON(TMS)₂ [X = F; R = 2,4,6-triisopropylphenyl (trip), N(TMS)₂ and X = Cl, R = N(TMS)₂] as depicted in the following Scheme 6.10a.^[185] The rearrangement has a strong dependence on the substituents of the boron atom as the related compound (TMS)(Dip)N–B(F)ON(TMS)₂ [Dip = 2,6-diisopropylphenyl] shows no isomerization even after heating at 250 °C and (Me₂CH)₂N–B(F)ON(TMS)₂ decomposes upon heating at 100 °C but no isomerized product was identified. Münster et al. also have found dyotropic rearrangement of aminoboranes, R₂B=N(OTMS)(TMS) [R = –CH₂–CH(CH₃)–CH₂–CH₂–, 9-

BBN] upon thermolysis reactions at 80 °C (Scheme 6.10b & c).^[38]



Scheme 6.10 Dyotropic rearrangement of boryl-bis(silyl)hydroxylamines.

Running the reaction of 9-chloro-9-borafluorene **6** with two equivalents of amine **13**, to learn if a second equivalent of base may facilitate the HCl elimination, produced a new product **18** (76 %) along with a minor amount of **15** (Scheme 6.11). The compound **18** was characterized by multinuclear (¹¹B, ¹H, ¹³C, ²⁹Si) NMR and HR-MS data. To explain this fact one could assume that the primary product **14** might have formed a coordination complex with another molecule of amine followed by elimination of one disiloxane molecule [(TMS)₂O] which was identified in the ¹H NMR of the reaction mixture. This statement was further strengthened when **15** was found inert towards the amine **13** even after a week.



Scheme 6.11 Reaction of **6** with two equivalents of amine **13**.

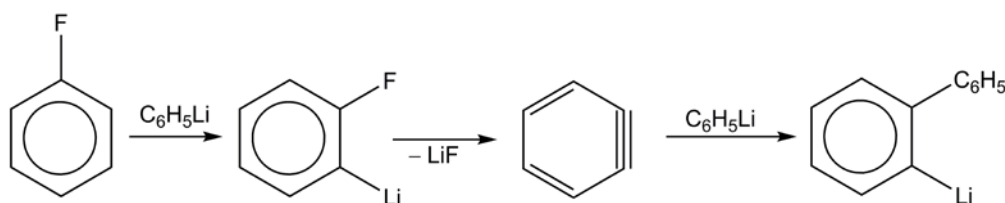
6.3 Conclusion

This work brings in a new route to obtain 9-aza-10-boraphenanthrene analogs from the borafluorene compounds. The formation of 10-trimethylsilyloxy-9-aza-10-boraphenanthrene **15** from 9-chloro-9-borafluorene **6**, by addition of suitable amine, is the first example of isomerization of borole to azaborine fragment via a formal dyotropic rearrangement.

7. Route via Dehydrohalogenation

7.1 Introduction

Dehydrohalogenation is one of the successful processes known to generate *ortho*-benzyne which is also called 1,2-didehydrobenzene or simply dehydrobenzene. Hoffmann has nicely reviewed the history of the development of the concept of dehydrobenzene in his book named “*Dehydrobenzene and Cycloalkynes*”.^[186] In 1940 Wittig et al.^[187] found that fluorobenzene reacts faster with phenyl-lithium to yield biphenyl than any other halogenobenzene. Later on in 1942, Wittig explained the outcome to be due to the unusual high acidity of the *ortho*-hydrogens of fluorobenzene as shown in Scheme 7.1.^[188, 189]



Scheme 7.1 Reaction between fluorobenzene and phenyl-lithium.^[188, 189]

In another approach the formation of many rearranged products during the amination of aryl halides by metal amides in liquid ammonia also triggered the issue of the participation of dehydrobenzene in these reactions. In 1953 Roberts et al. have undoubtedly proven the existence of *dehydrobenzene*, acting as the reactive intermediate in these amination reactions. They set up a reaction between [1-¹⁴C]-chlorobenzene and potassium amide in liquid ammonia and equal amounts of [1-¹⁴C]-aniline and [2-¹⁴C]-aniline were obtained (Scheme 7.2).^[190] Afterwards Huisgen’s reports^[191] on the dehydroaromatic nature of the intermediates involved in the reaction of aryl halides with phenyllithium and the successful trapping of dehydrobenzene via Diels-Alder reactions by Wittig^[189] are milestones in the

development of organic chemistry.

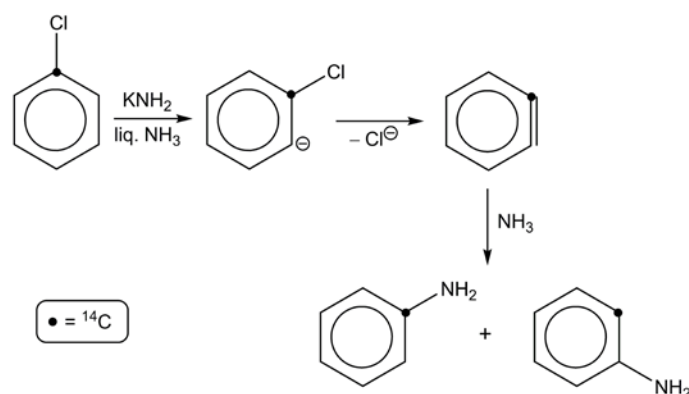
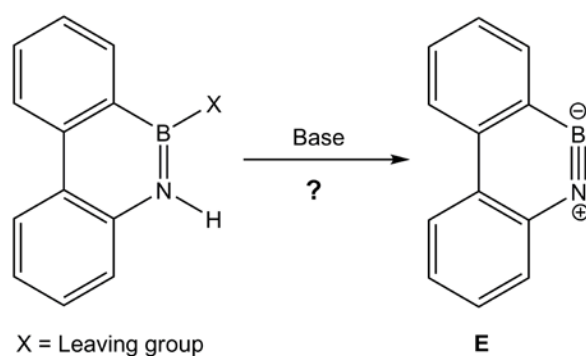


Figure 7.2 ^{14}C -labeling reaction of chlorobenzene with base.^[190]

Inspired by these dehydrohalogenation reactions, a similar approach has been attempted to generate the 9,10-didehydro-9-aza-10-boraphenanthrene (**E**) from suitable precursors according to the following scheme.



Scheme 7.3 Proposed dehydrohalogenation reaction.

In this case due to the involvement of boron and nitrogen, a number of limitations arise because of the Lewis acidity of boron. And therefore a number of precautions have to be taken into account with respect to the following issues;

(i) **Type of base:** As boron is an electron deficient element, strong nucleophilic bases (e.g. MeLi, *n*-BuLi, NaOH, KOH, KO^tBu) are expected to preferably undergo nucleophilic

addition at the boron center. So a suitably strong non-nucleophilic base is necessary to work with.

(ii) **Solvents:** Solvents containing donor atoms (e.g. Et₂O, THF, acetone, acetonitrile, DMSO, pyridine etc.) may destroy the starting materials or could coordinate to the boron center and possibly form ionic salts. To perform the dehydrohalogenation reaction at the boron-nitrogen system, a chemically inert solvent needs to be employed.

(iii) **Inert atmosphere:** This is a very basic requirement to work with such systems. Starting materials need to be protected from oxygen and moisture in order to avoid decomposition due to hydrolysis. This also limits the range of chemical reagents to be used.

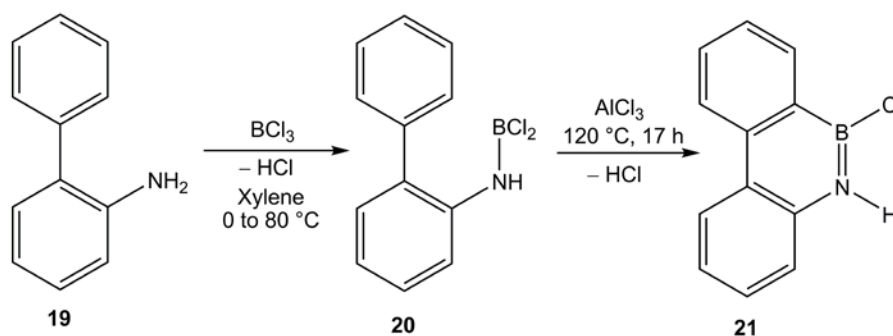
(iv) **Trapping agents:** The trapping reactions of highly unstable iminoboranes are done by in situ generation of iminoboranes in the presence of trapping agents. In contrast, stable iminoboranes can be synthesized independently and then be treated directly with various types of reagents. In the present study, it can be assumed that the target cyclic iminoborane (**E**) would be extremely reactive and thus an in situ generation and trapping is necessary. So a careful choice of trapping agents for this base induced elimination reaction is required; i.e. only those reagents are useful that do not coordinate to the boron atom in the precursors and that are inert towards the base being used.

7.2 Results and Discussions

7.2.1 Dehydrohalogenation Approaches with Bases of Different Strength

The starting material 10-chloro-9-aza-10-boraphenanthrene **21** (X = Cl, Scheme 7.4) was prepared according to the procedure reported by Dewar et al.^[192, 193] and the multinuclear

NMR spectroscopy data [^{11}B (34.6 ppm in C_6D_6), ^1H , ^{13}C] are identical to literature data (Scheme 7.4).^[194]



Scheme 7.4 Synthesis of 10-chloro-9-aza-10-boraphenanthrene **21**.

To choose the appropriate solvent for the 1,2-elimination reaction a number of tests were performed. In *n*-hexane, toluene, benzene or dichloromethane the starting material **21** dissolved well and remained intact. But after dissolving the chloroborane in THF, within 15 min a new NMR peak appeared at 28.7 ppm along with the chloroborane **21** ($\delta^{11}\text{B} = 34.4$ ppm) which slowly increased over time and after 16 h the initial signal completely disappeared and only the new peak remained [here C_6D_6 was used as locking solvent] (Figure 7.1).

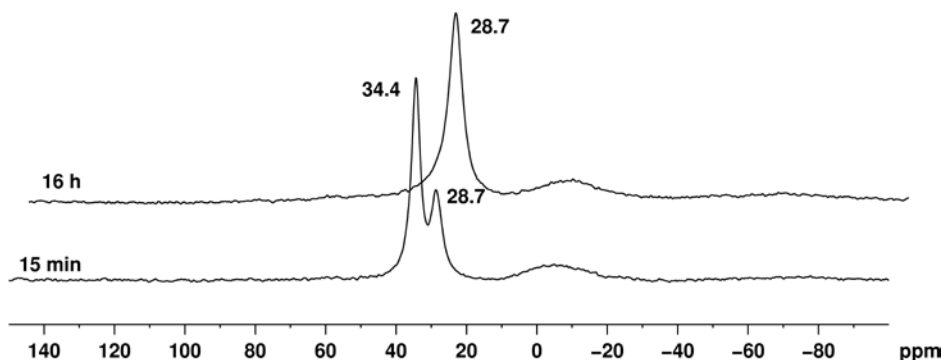
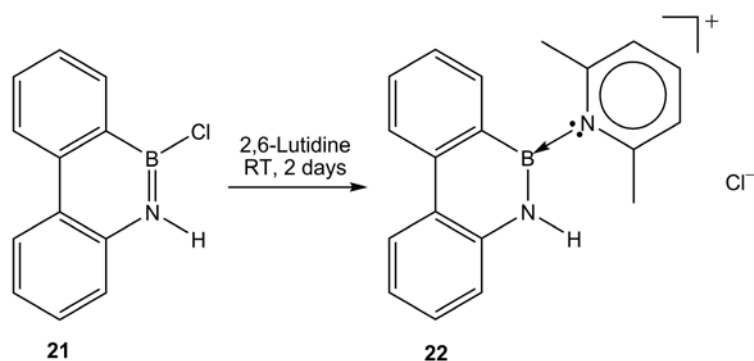


Figure 7.1 Gradual change of $^{11}\text{B}\{^1\text{H}\}$ chemical shift of **21** in THF [C_6D_6 as lock].

The ^{11}B chemical shift (28.7 ppm) is in the region of tri-coordinated boron centers

that are attached to one or two heteroatom/s. Haloboranes are known to be coordinating to donor solvents and they can also cleave the C–O bond of cyclic ethers.^[195-198] When chloroborane **21** was reacted with 2,6-lutidine, the ¹¹B chemical shift was found at 28.3 ppm which indicated formation of a tricoordinated boron compound [typical range of $\delta^{11}\text{B}$ for amine-ligated borenium salts is 25 to 30 ppm)^[199] rather than the expected tetra coordinated salt (Scheme 7.5). The compound **22** was isolated as a colorless solid and characterized by NMR spectroscopy. Liu's group similarly observed the formation of cation of 1,2-dihydro-1,2-azaborine compounds upon treatment of different types pyridines on 1-ethyl-2-trifluoromethanesulfonyl-1,2-dihydro-1,2-azaborine.^[200]



Scheme 7.5 Coordination reaction of **21** with 2,6-lutidine.

When one equivalent of pyridine was added to a benzene solution of **21** the ¹¹B NMR ([D₆]-benzene, locking solvent) showed two signals; one at 34.1 ppm which was the starting chloroborane, and another signal at 7.3 ppm with low intensity (Figure 7.2a). Regular measurements of this sample did not display any change in the chemical shifts even after 10 days. No indication was found for a tricoordinated borenium salt **23** (Scheme 7.6). When a huge excess of pyridine was added into that solution, immediately, a bright yellow solution was obtained showing only one ¹¹B NMR signal at 8.1 ppm (Figure 7.2b). This suggests that the boron center has a tetrahedral coordination environment i.e. a boronium species has

formed. The chemical shift also falls in the usual range of a ^{11}B signal observed for a boronium ion (0 to 15 ppm) as reported in the literature.^[199] Additionally no such boronium species has been observed upon use of excess 2,6-lutidine.

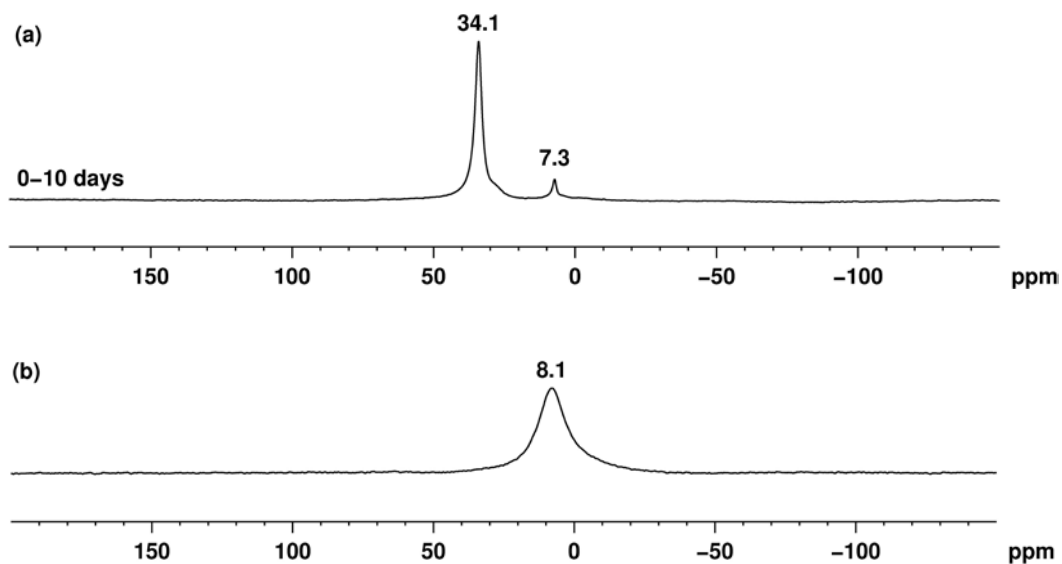
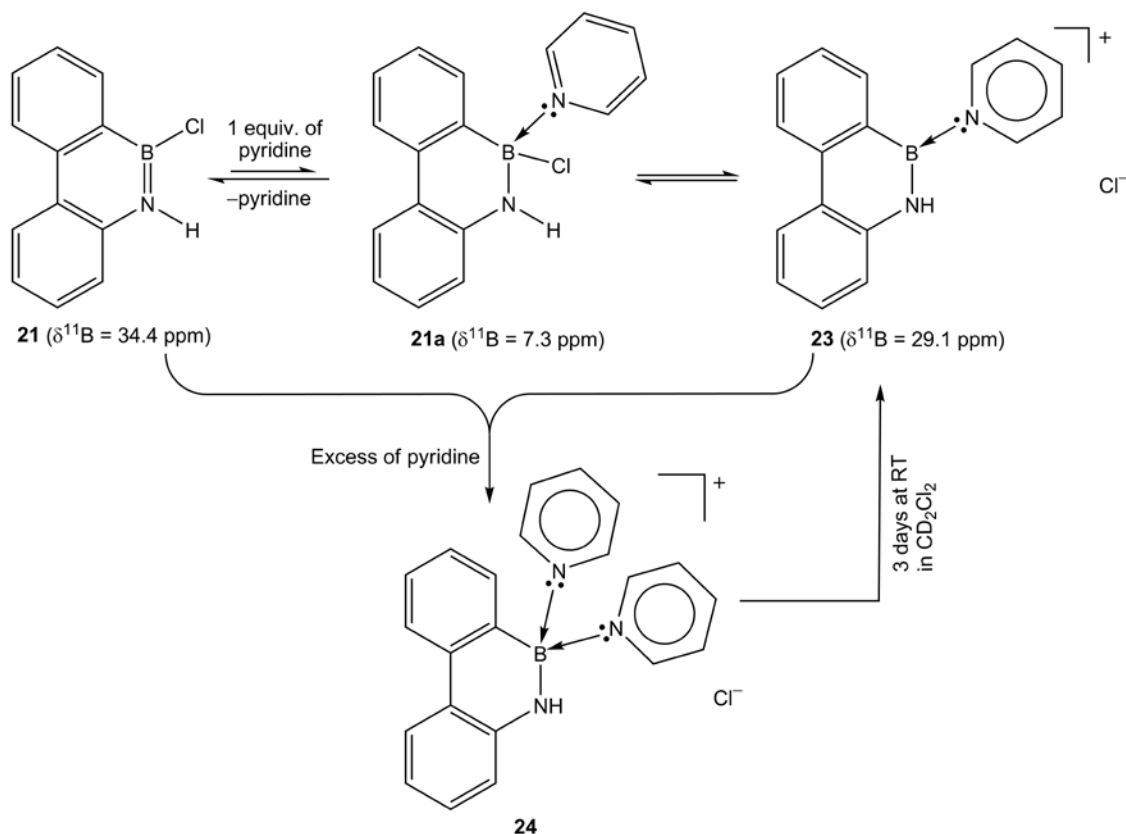


Figure 7.2(a) Reaction of **21** with 1 equiv of pyridine in C_6D_6 ; **(b)** $^{11}\text{B}\{^1\text{H}\}$ chemical shift upon using excess of pyridine in C_6D_6 .

The ^1H NMR spectrum of the bright yellow solid product shows the required 4:5 ratio for the protons of borazarophenanthrene unit to the py-H signals. And the ^{13}C NMR spectrum displays 14 carbon signals that can be expected for a structure like **24** shown in Scheme 7.6 (provided the carbon attached to the boron center is not detected). During the electron impact mass spectrometry measurement the pyridine molecules were found to be labile as they were rapidly cleaved from **24** upon heating. Accordingly the remaining BN-phenanthrene unit of **24** combined with the chloride anion to form 10-chloro-9-aza-10-boraphenanthrene **21** and the corresponding $[\text{M}^+]$ (213 amu) peak was clearly observed. In CD_2Cl_2 the compound **24** slowly converted to another colorless compound **23** ($\delta^{11}\text{B} = 29.1$ ppm) which was assigned according to multinuclear NMR spectroscopy data.

The ^{11}B NMR study of the pyridine reaction with **21** indicates a possible formation of 10-chloro-9-aza-10-boraphenanthrene•py (21a $\delta^{11}\text{B} = 7.3$ ppm, Figure 7.2a) in the first step. This is in equilibrium with the starting material **21** and possibly with **23** and upon using excess of pyridine this mixture completely converts into **24** (Scheme 7.6).



Scheme 7.6 Reaction between pyridine and chloroborane **21**.

Coordination of two pyridine molecules to the boron center in compound **24** was finally confirmed by X-ray crystallography as depicted in Figure 7.3. Bright yellow crystal blocks were grown from a benzene and pyridine mixture. The compound crystallizes triclinically in the space group $P-1$ with $Z = 2$ in unit cell.

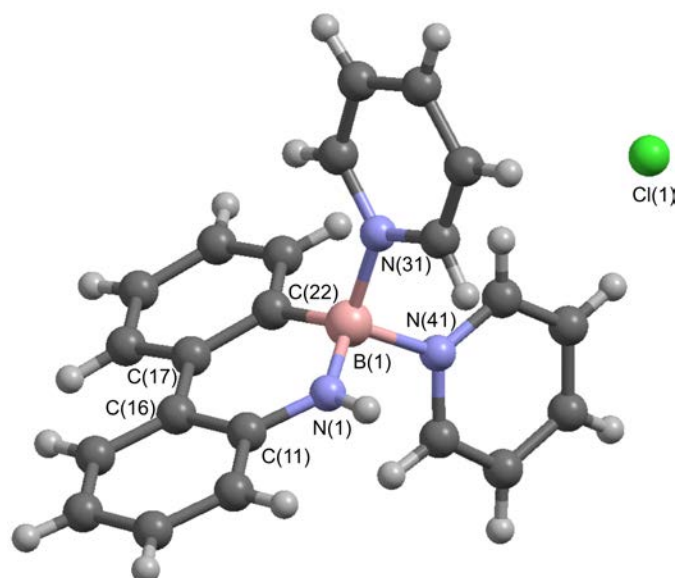


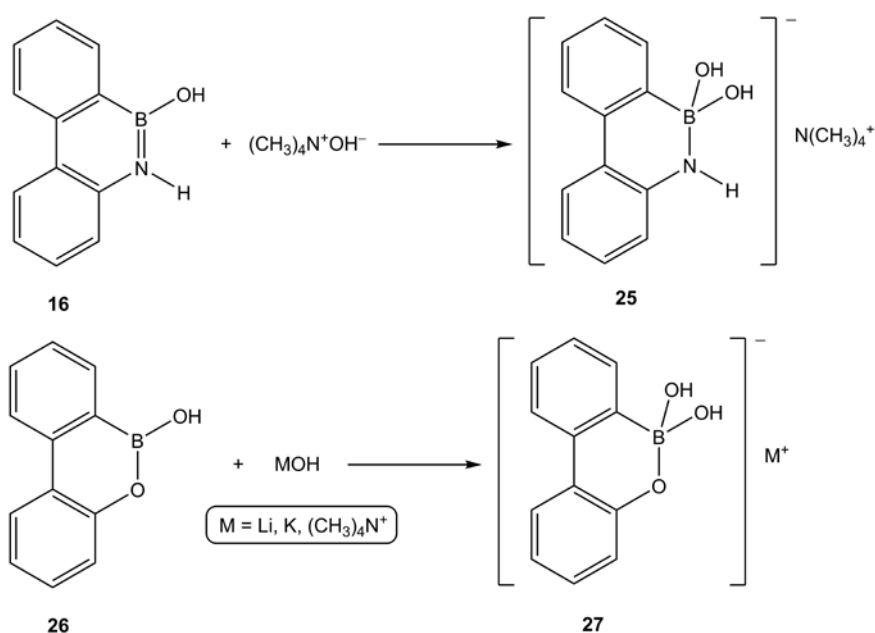
Figure 7.3 Molecular structure of **24**. Selected bond length lengths [Å] and angles [°]:

B(1)–N(31) 1.628(2), B(1)–N(41) 1.640(2), B(1)–N(1) 1.472(2), N(1)–C(11) 1.3709(19),
 C(11)–C(16) 1.413(2), C(16)–C(17) 1.474(2), C(17)–C(22) 1.418(2), C(22)–B(1) 1.592(2);
 N(31)–B(1)–N(41) 103.91(11), N(41)–B(1)–N(1) 108.51(12), N(1)–B(1)–N(31) 109.92(12),
 N(1)–B(1)–C(22) 112.23(13), C(22)–B(1)–N(31) 114.00(12), C(22)–B(1)–N(41)
 107.78(12), B(1)–N(1)–C(11) 125.19(13), N(1)–C(11)–C(16) 121.58(14),
 C(11)–C(16)–C(17) 119.68(13), C(16)–C(17)–C(22) 120.42(13), C(17)–C(22)–B(1)
 119.95(13).

The B(1)–N(31) [1.628(2) Å] and B(1)–N(41) [1.640(2) Å] bond lengths in **24** are similar to the boronium ions reported earlier e.g. [H₆C₅B•2L, L = Py],^[201] (2,2′-bipyridyl-*N,N*′-(bicyclo[3.3.1]nonane-*C*¹,*C*⁵)-boronium trifluoromethanesulfonate,^[202] C₂₅H₂₂BN₂⁺BF₄⁻.^[203] The B(1)–C(22) and B(1)–N(1) bonds are longer in **24** [1.592(2) Å and 1.472(2) Å respectively] compared to those found in the tricoordinated boron centers in related BN-phenanthrene structures like bis-(10,9-borazarophenanthryl)ether [1.540 and 1.408 Å],^[176] 10-hydroxy-9-aza-10-boraphenanthrene **16** [1.541 and 1.413 Å],^[176] 10-

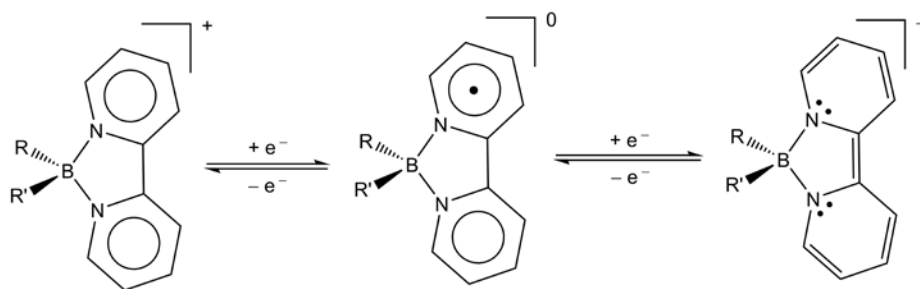
hydroxy-6-nitro-9-aza-10-boraphenanthrene [1.535 and 1.427 Å],^[177] 10-hydroxy-8-nitro-9-aza-10-boraphenanthrene [1.537 and 1.428 Å]^[177] and 10-trimethylsilyloxy-9-aza-10-boraphenanthrene (compound **15**, 1.547(3) and 1.420(3) Å]. The angle N(1)–B(1)–C(22) [112.23(13)°] is slightly narrower than those found in the compounds mentioned above (~116°). All other C–C bond lengths are in the expected region.

Mikhailov and Kuimova found that 10-hydroxy-9-aza-10-boraphenanthrene **16** produced tetrahedral (Lewis) borate-type salt **25** [$\delta^{11}\text{B} = -1.7$ to 4.3 ppm depending on the solvent used] with tetramethylammonium hydroxide [$\text{Me}_4\text{N}^+\text{OH}^-$] (Scheme 7.7).^[204] But it did not react with LiOH or KOH in aqueous media and also not with ammonium hydroxide [$\text{H}_4\text{N}^+\text{OH}^-$]. The corresponding oxygen derivative, i.e. 10-hydroxy-10,9-boroxaphenanthrene **26**, reacted faster with [$\text{Me}_4\text{N}^+\text{OH}^-$] as well as with those alkali hydroxides to form tetrahedral salts like **27** (Scheme 7.7).^[204] But no report has been recorded so far for the BN-phenanthrene analogs to produce borenium or boronium salts upon addition of Lewis bases.



Scheme 7.7 Formation of tetrahedral borate type compounds.

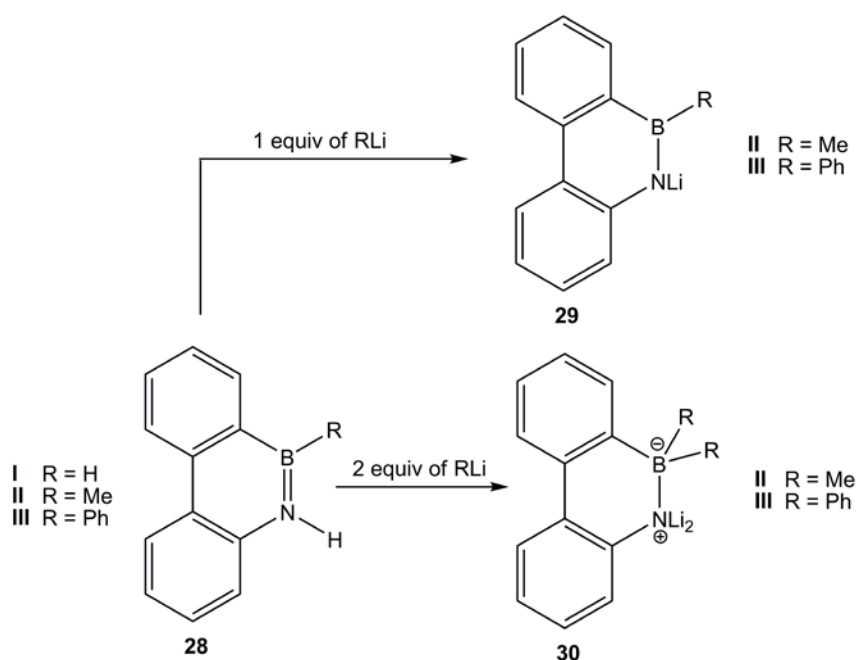
Boronium ions are reported to have interesting chemical properties as reported by Hünig and Wehner.^[205] They have observed that the 2,2'-bipyridylboronium ions are reversible two-step redox systems according to Scheme 7.8. The reversibility, however, greatly depends on the substituents present on the boron atom as well as on the solvent used.^[205] Later on, Wagner's group has modified this 2,2'-bipyridylboronium ion by attachment of ferrocene and in this way obtained a novel five-step redox system.^[206] The boronium species **24** synthesized here may be used as a redox active species; the 2,2'-bipyridyl derivative, not yet synthesized, could also considerably tune the electron transport property due to aromatic rings attached to boron center. Very recently Vedejs et al. have reported the exceptional electrophilicity of the 9-BBN-*N,N*-1,8-bis(dimethylamino)naphthalene boronium species which carries out borylation of nitrogen heterocycles in excellent yield.^[207]



Scheme 7.8 2,2'-bipyridylboronium ion, a reversible two-step redox system.

Due to close resemblance of 9-aza-10-boraphenanthrene compounds **28** to the isoconjugate derivatives of phenanthrene in electron absorption spectra Dewar and his group suggested that these 9-aza-10-boraphenanthrene compounds are aromatic and that the dipolar resonance structure with a boron-nitrogen double bond contributes significantly towards aromaticity and the hydrolytic stability.^[192, 208] This indicates that the proton attached to the nitrogen atom should be acidic. But the methylation reaction of **28II** (Scheme 7.9) with

dimethyl sulphate in presence of alkali and that with diazomethane failed.^[209] Later on Dewar et al. found that upon treatment of methyllithium or phenyllithium to **28II** and **28III**, the N–H proton was abstracted and the corresponding N-lithio derivatives **29** were formed (Scheme 7.9). When two equivalents of MeLi or PhLi were used then the second molecule of base simply added to the B–N bond and the corresponding 9,9-dilithio-10,10-dimethyl or 9,9-dilithio-10,10-diphenyl-9-aza-10-boraphenanthrene **30** were obtained.^[209]



Scheme: 7.9 Reactions of **28** with MeLi and PhLi.

Successful generation of iminoboranes by base induced dehydrohalogenation reactions are reported only for two cases; these are bis-(amino)(halo)boranes $[\text{Ar}-\text{N}(\text{H})-\text{B}(\text{X})-\text{NR}_2]$ and amino(halo)(organyloxy)borane $[\text{R}_1\text{O}-\text{B}(\text{X})-\text{N}(\text{H})\text{R}_2]$ containing bulky substituents with heteroatoms, as cited in Chapter 1.5 (Scheme 1.6).^[48, 50, 52] In 2007 Rivard et al. has synthesized a stable iminoborane which contains very large aromatic ligand like terphenyl to prevent the oligomerization.^[49] When they treated one equivalent of sodium bis(trimethylsilyl)amide $[\text{NaHMDS}]$ with $\text{Ar}'-\text{N}(\text{H})-\text{B}(\text{X})-\text{tmp}$ $[\text{Ar}' = \text{C}_6\text{H}_3-2,6-(\text{C}_6\text{H}_2-$

2,4,6-Me₃); X = Cl, Br; tmp = 2,2,6,6-tetramethylpiperidino], the corresponding iminoborane Ar'-N≡B-tmp was obtained as colorless crystals. The extremely bulky aromatic group attached to the nitrogen atom greatly stabilizes the monomeric iminoborane as it shows no reaction with dimethylaminopyridine (DMAP).

In the present study, the dehydrohalogenation reactions of 10-chloro-9-aza-10-boraphenanthrene **21** were tested with different strong or weak non-nucleophilic bases. As pyridine, also known as a weak base (pK_a of conjugate acid = 5.3),^[210, 211] was found to displace the chloride easily from the boron atom, only non-nucleophilic bases were used and strong nucleophilic bases like MeLi, PhLi, *n*-BuLi, *t*-BuLi were avoided. When weak bases like *N,N*-diisopropylethylamine, known as Hünig base (pK_a of conjugate acid = 10.5)^[212] and 1,8-diazabicyclo[5.4.0]undec-7-ene, DBU (pK_a of conjugate acid = 13.4)^[213] were reacted with the starting chloroborane **21**, the deprotonation of the N-H proton did not occur i.e. no cyclooligomer or any other products of the cyclic iminoborane were detected (**E**, Scheme 7.3). However, the change in the ¹¹B NMR chemical shift to 28-29 ppm from that of starting material (34.4 ppm) indicated the displacement of the chloride ion by the base. The compounds are extremely sensitive towards hydrolysis. These borenium salts were too unstable for complete characterization. Crystallization also was not possible. Only a hydrolysis product, bis(10,9-borazarophenanthryl)ether **31**, could be structurally characterized by X-ray analysis (Figure 7.4B). The ¹¹B chemical shift of **31** is found at 28.6 ppm in CD₂Cl₂ and also the ¹H, ¹³C NMR data are consistent with the previous reports.^[176, 194] Notably, throughout this study it was found that the NMR (mainly ¹H NMR) chemical shifts and pattern of the 9-aza-10-boraphenanthrene compounds strongly depend on the nature of the solvent used.

The crystal structure of the compound **31** was earlier reported by the Philip group^[176] who found that the crystal has monoclinic space group $C2/c$ with $Z = 8$. But the compound **31** obtained in this work crystallizes as needles in the monoclinic system but the space group is $P2_1/c$ and the cell constants are determined as, $a = 14.1998(19) \text{ \AA}$, $b = 5.5331(4) \text{ \AA}$, $c = 27.016(4) \text{ \AA}$ and $\alpha = 90.00^\circ$, $\beta = 120.079(9)^\circ$, $\gamma = 90.00^\circ$, $V = 1836.8(4) \text{ \AA}^3$ with $Z = 4$. In literature the authors found the cell dimensions were $a = 50.749(5) \text{ \AA}$, $b = 5.4547(5) \text{ \AA}$, $c = 13.502(2) \text{ \AA}$ and $\beta = 92.274(2)^\circ$, $V = 3734.5(7) \text{ \AA}^3$. The molecules are also found here to form homochiral π -stacked columns along the b axis (Figure 7.4A).^[176] The bond lengths and bond angles of the structure found here are comparable to the reported one. The B–N (1.413 and 1.406 \AA), B–O (1.367 and 1.379 \AA), B–C (1.542 and 1.551 \AA) bonds and other CC bond lengths, are very similar to the previous structure or differs slightly by 0.01–0.02 \AA . The angle between B–O–B is 139.49° , much wider than expected for a sp^2 -hybridized oxygen atom, indicates transfer of electron density from oxygen towards the boron centers. A closer look at the BN-phenanthrene units shows that the two C_6 containing rings are not completely planar but slightly bent with dihedral angles of 1.56° for the C(42)–B(20)–N(21)–C(31) plane and -4.29° for the C(2)–B(1)–N(6)–C(5) plane. The dihedral angles between N(21)–B(20)–O(1)–B(1) and N(6)–B(1)–O(1)–B(20) are -121.14° and -154.05° , respectively.

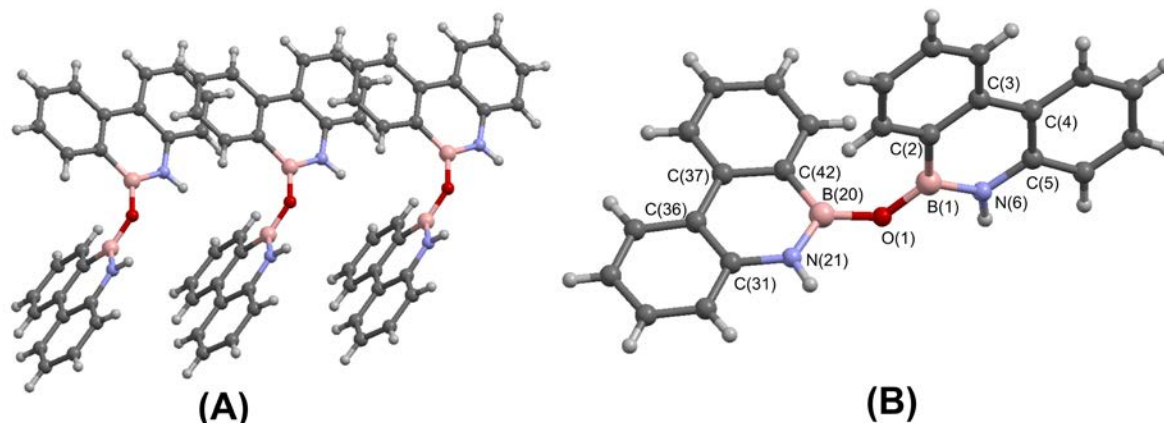


Figure 7.4 (A) Molecular structure of **31**. Selected bond length lengths [\AA] and angles [$^\circ$]: B(1)–N(6) 1.413(3), B(20)–N(21) 1.406(3), B(1)–O(1) 1.367(3), B(20)–O(1) 1.379(3), B(1)–C(2) 1.551(3), B(20)–C(42) 1.542 (3), N(6)–C(5) 1.394(3), C(31)–N(21) 1.395(3); B(1)–O(1)–B(20) 139.49(18), N(6)–B(1)–C(2) 115.87(18), O(1)–B(1)–C(2) 125.81(19), O(1)–B(1)–N(6) 118.3(2), O(1)–B(20)–N(21) 118.3(2), N(21)–B(20)–C(42) 125.0(2), O(1)–B(20)–N(21) 118.3(2), N(21)–B(20)–C(42) 116.59(18); (B) partial view of the adjacent molecules in π -stacking along b-axis.

It is clear that stronger bases than Hünig base or DBU is necessary in order to deprotonate the N–H, so potassium bis(trimethylsilyl)amide (KHMDS, pK_a of conjugate acid = 26) was used for further investigation. When one equivalent of KHMDS base was added to the *n*-hexane solution of the chloride **21** at -50°C , immediately a colorless solid formed (Scheme 7.10a). The reaction mixture was allowed to come to room temperature slowly with continuous stirring overnight. Next day an appreciable amount of colorless precipitate was obtained which was extracted into toluene to separate the insoluble potassium chloride and other insoluble materials. After removal of toluene a slightly brown solid was obtained which was further purified by precipitation from a 1:1 mixture of dichloromethane and *n*-hexane at -20°C . A fine colorless powder (compound **33**) was obtained after drying under vacuum in

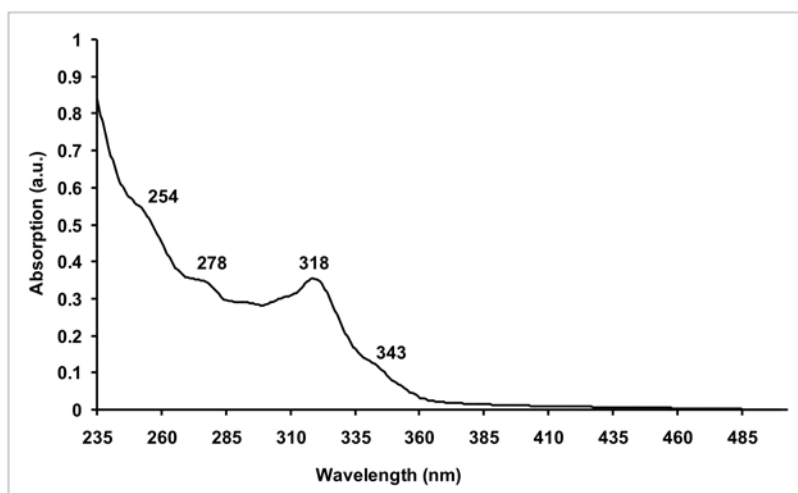
approximately 30 % yield.^[214] The colorless solid is stable in air and is fairly soluble in dichloromethane, THF, benzene, toluene, methanol but remains insoluble in non polar solvents like *n*-pentane, *n*-hexane. According to the high resolution mass spectrometry (ESI) the molecular ion peak (531 amu) fits to the mass of the trimer of the 9,10-didehydro-9-aza-10-boraphenanthrene (**E**, Scheme 7.3) i.e. 1,2:3,4:5,6-tris-(2,2'-biphenylene)borazole (TBB, **33**).

The signals in ¹H NMR of the colorless solid, measured in CD₂Cl₂, are integrated to eight protons and have no broad signal for N–H. The correlations found in the ¹H–¹H COSY spectrum can be explained for the protons of a BN-phenanthrene unit. The ¹³C NMR spectrum has eleven signals and the carbon atom bound to the boron center is not observed. In the ¹¹B spectra the compound shows a very broad signal at ~ 36 ppm. In the infrared spectra a very strong band is found at 1366 cm⁻¹ which is a characteristic of B=N stretching of a borazine core and the bands at 785 cm⁻¹ and 761 cm⁻¹ also indicate an *o*-disubstitued benzene ring.^[215, 216]

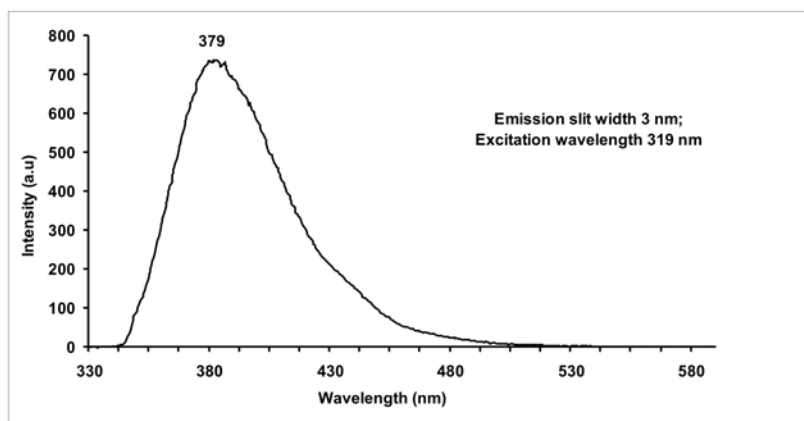
To facilitate the elimination, the chloride group was replaced by a triflate group (–OTf). The triflate compound **32** was obtained from the chloroborane **21** by reacting with silver trifluoromethanesulfonate (AgOTf). Addition of AgOTf to the *n*-hexane solution of the chloroborane **21** immediately resulted in formation of a colorless precipitate which was removed by filtration after 4 h of stirring at room temperature. The colorless filtrate was used for the next step (Scheme 7.10b). After workup, as described in Scheme 7.10a, the TBB **33** was obtained in higher yield (~ 40 %).

The UV-visible spectrum of **33** [Figure 7.5(A)], measured in dichloromethane, is comparable to that of 14,16,18-tribora-13,15,17-triazarotriphenylene.^[217] Compound **33** also

displays a blue fluorescence with an emission maximum at 379 nm measured in the same solvent upon excitation at 319 nm [Figure 7.5(B)]. In the solid state the emission maximum is slightly shifted to 383 nm.

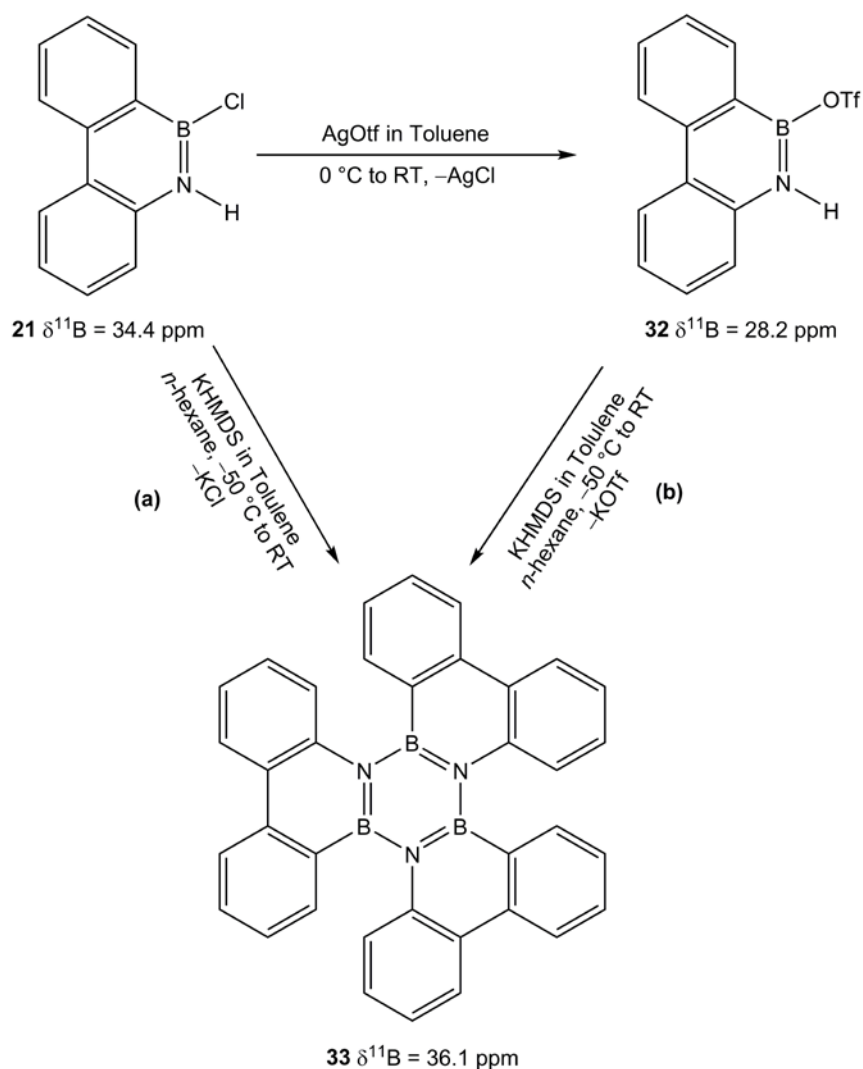


(A)



(B)

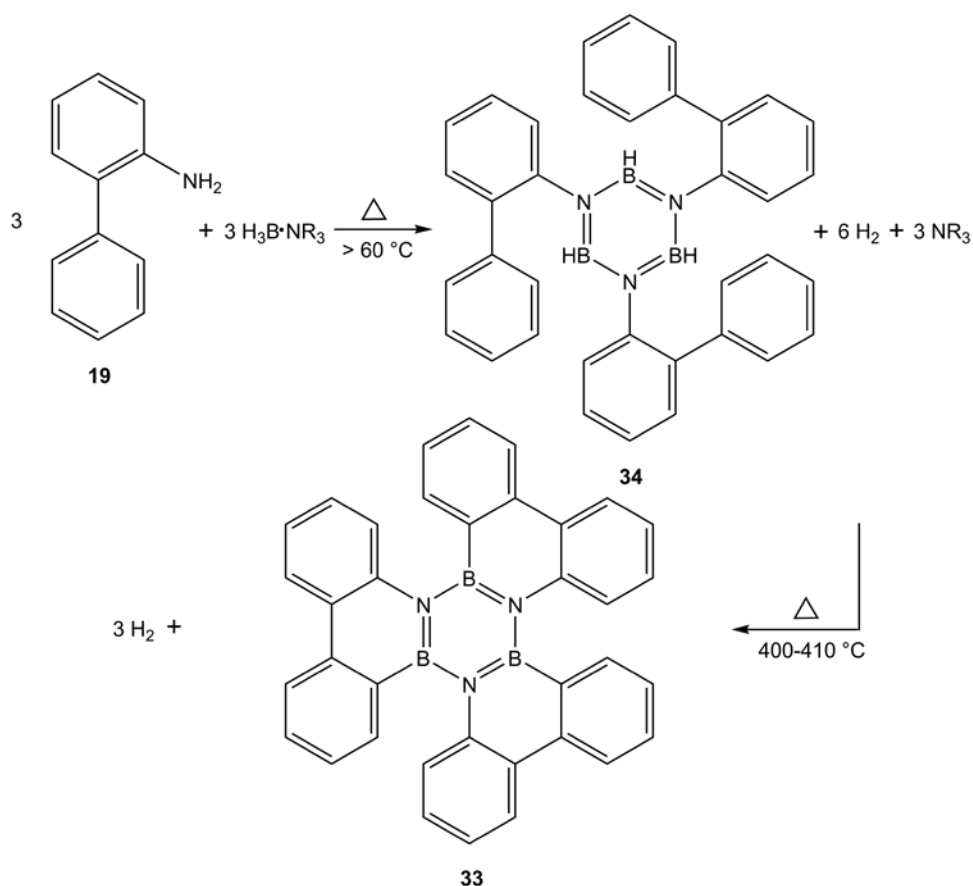
Figure 7.5 (A) UV-Vis and (B) Fluorescence spectra for TBB **33** in dichloromethane.



Scheme 7.10 Synthesis of TBB **33** from chloroborane **21** by base induced elimination reactions.

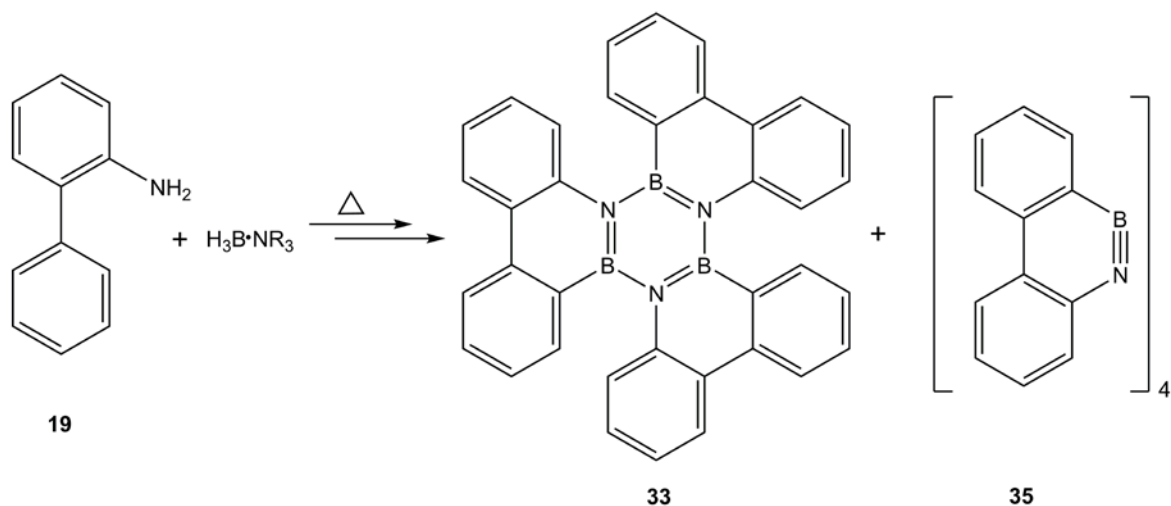
All the analytical data are consistent with structure of TBB **33**. Köster et al. synthesized the borazine compound **33** already in 1965 from *N,N',N''*-tris-(2-biphenyl)borazole via dehydrogenation at 400-410 °C (Scheme 7.11).^[215, 218] They found the B=N stretching vibration at 1362 cm⁻¹ in the infrared spectrum and also reported the mass. But according to Köster et al. compound **33** is insoluble and thus no further analytical data was reported.^[218] Later Robert et al. published the crystal structure of **33** in 1974.^[219] To confirm the assignment of the colorless powder **33**, obtained from this base induced

elimination reactions (Scheme 7.10), a powder X-ray diffraction analysis was performed. The pattern obtained was identical to the previous single crystal X-ray data. This undoubtedly proves the characterization of compound **33** as TBB. Compound **33** can also be purified by column chromatography with 1:1 dichloromethane:*n*-hexane with a R_f value 0.64 over silica. The trimer **33** can be identified on LC-MS by an elution time 23.2 min with H₂O/MeOH solvent mixture (see page 110 for the conditions) and the corresponding electron spray ionization mass spectrum shows $[M + H^+]$ (532 amu), $[M + H^+ + \text{MeOH}]$ (564 amu) and $[M + \text{Na}^+ + \text{MeOH}]$ (586 amu) ion peaks.



Scheme 7.11 Reported synthetic scheme for **33**.^[218]

Upon re-examination of the product mixture, obtained according to the procedure reported by the Köster group,ⁱⁱⁱ an interesting observation was made. The mixture was not completely soluble in CD_2Cl_2 ; still the NMR data acquired from the suspension was identical to that of the product **33**. The mixture had the BN stretching at 1363 cm^{-1} . When the mixture was repeatedly sonicated and centrifuged with dichloromethane, a very fine colorless powder remained insoluble. This has a strong IR band for ν_{BN} at 1362 cm^{-1} which is slightly shifted to lower wave number in comparison with **33** ($\nu_{\text{BN}} = 1366\text{ cm}^{-1}$). The compound isolated from the dichloromethane washings in the solution phase was only the trimer **33** with its BN-stretching at 1366 cm^{-1} , in agreement with the IR of the samples obtained via the elimination route. The insoluble material has a high resolution mass that is in agreement with the tetramer of 9,10-didehydro-9-aza-10-boraphenanthrene (**E**), **35** (Scheme 7.12).^[214]

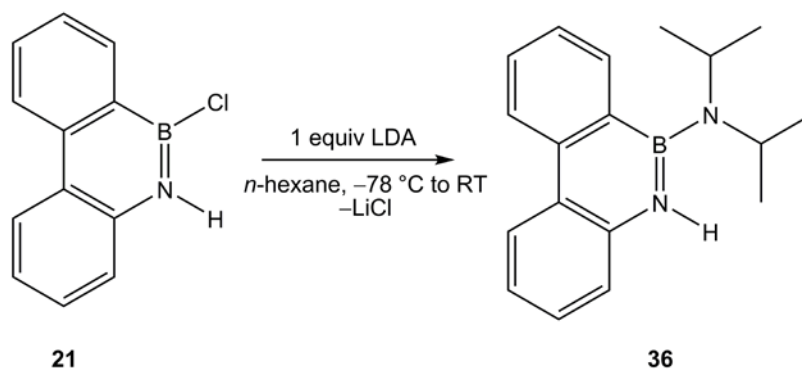


Scheme 7.12 Formations of borazine (**33**) and tetrazatetraborocane (**35**).

ⁱⁱⁱ The dehydrogenation reaction (Köster's procedure) was done by my colleague Matthias Müller and I express my gratitude for his kindness to provide me 20 mg of crude reaction mixture.

This simply implies that the dehydrogenation reaction described by Köster et al. does not only produce the trimer (**33**, TBB) but also the tetramer (**35**) which is a completely insoluble compound. And in contrast to Köster's statements, the trimer is adequately soluble to get the analytical data (Scheme 7.12).

The stronger non-nucleophilic base like lithium diisopropylamide (LDA, $pK_a = 35.7$)^[220] was also applied for the dehydrohalogenation reaction. Treatment of the chloroborane **21** with LDA resulted mainly in 10-diisopropylamino-9-aza-10-boraphenanthrene (**36**) (Scheme 7.13). The compound **36** can be sublimed at $65\text{ °C}/10^{-3}\text{ mbar}$ as a colorless moisture sensitive solid and in few trials $< 3\%$ of trimer was also isolated. The compound **36** was completely characterized by multinuclear NMR spectroscopy and HR-MS.



Scheme 7.13 Reaction of LDA with chloroborane **21**.

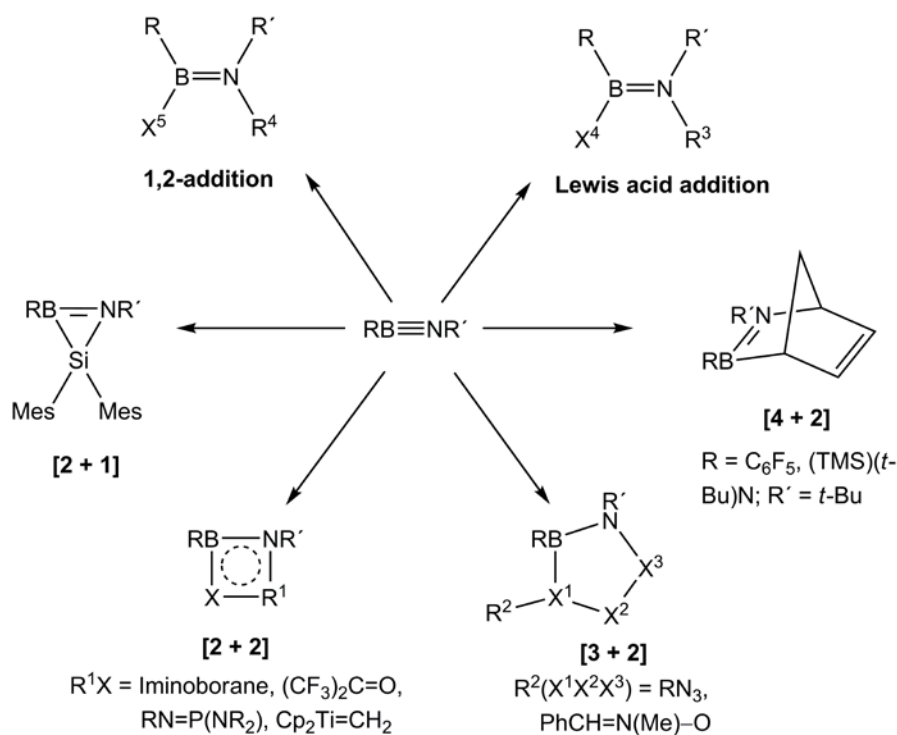
Another strong base, lithium tetramethylpiperidide, (LiTMP, $pK_a = 37.3$)^[221] which was prepared from 2,2,6,6-tetramethylpiperidine (HTMP) and *n*-BuLi in THF at 0 °C according to the reported procedure, was also attempted.^[222] Though LiTMP is known as the least nucleophilic base, the yield of **33** was not improved compared to the reaction with KHMDS.

To investigate the mechanism of the cyclotrimerization reaction, many trapping

reactions were performed with different types of trapping agents and those are discussed in the following section.

7.2.2 Reactions with Trapping Agents

Several types of trapping reactions of iminoboranes are known, like 1,2-polar addition, [2 + 1], [2 + 2], [3 + 2], [4 + 2] cycloadditions. Among these, [2 + 1] and [4 + 2] cycloaddition reactions are not very common. In Chapter 1, Section 1.5 these reactions are mentioned and the 1,2-addition reactions are described briefly (Scheme 1.10). Here all of those cycloaddition reactions have been summarized (Scheme 7.14) and the results of the attempted trapping reactions in present study are discussed in the light of those known examples.



Scheme 7.14 Different types of trapping reactions of iminoboranes.

The only example of a [2 + 1] cycloaddition reaction known is the reaction of

dimesitylsilylene with $t\text{-BuB}\equiv\text{N}t\text{-Bu}$ cited by Paetzold.^[2] The [2 + 2] reactions are very rapid; the four membered rings, diazadiboretidines, are available from dimerization or cross coupling of two iminoboranes, e.g. $i\text{-PrB}\equiv\text{N}i\text{-Pr}$ and $(\text{TMS})(t\text{-Bu})\text{N}-\text{B}\equiv\text{N}-t\text{-Bu}$ (Chart 7.1a). In the presence of aldehydes or ketones ($\text{RR}'\text{C}=\text{O}$), the reactions with iminoboranes are more complicated. In absence of an enolic proton in the oxo-compounds, [2 + 2] cycloaddition products are obtained with iminoboranes (Chart 7.1b). Sometimes formation of boroxins $(\text{RBO})_3$, i.e. complete cleavage of the $\text{B}\equiv\text{N}$ bond, are also reported.^[1] When the oxo-compound contains an enolic proton then an open-chain product is formed as shown in the Chart 7.1c.^[1] Imines $[\text{RN}=\text{CR}'\text{R}']$ are found to react with iminoboranes in a similar way as observed for $\text{O}=\text{CRR}'$ depending on the substituent present on the imine nitrogen atom (Chart 7.1d & e).^[1, 34] Formation of four-membered rings with iminoboranes and iminophosphanes $[\text{RN}=\text{P}(\text{NR}'_2)]$ have also been reported (Chart 7.1f)^[62] and one example of an alkylidenephosphane reaction product is known (Chart 7.1h).^[1]

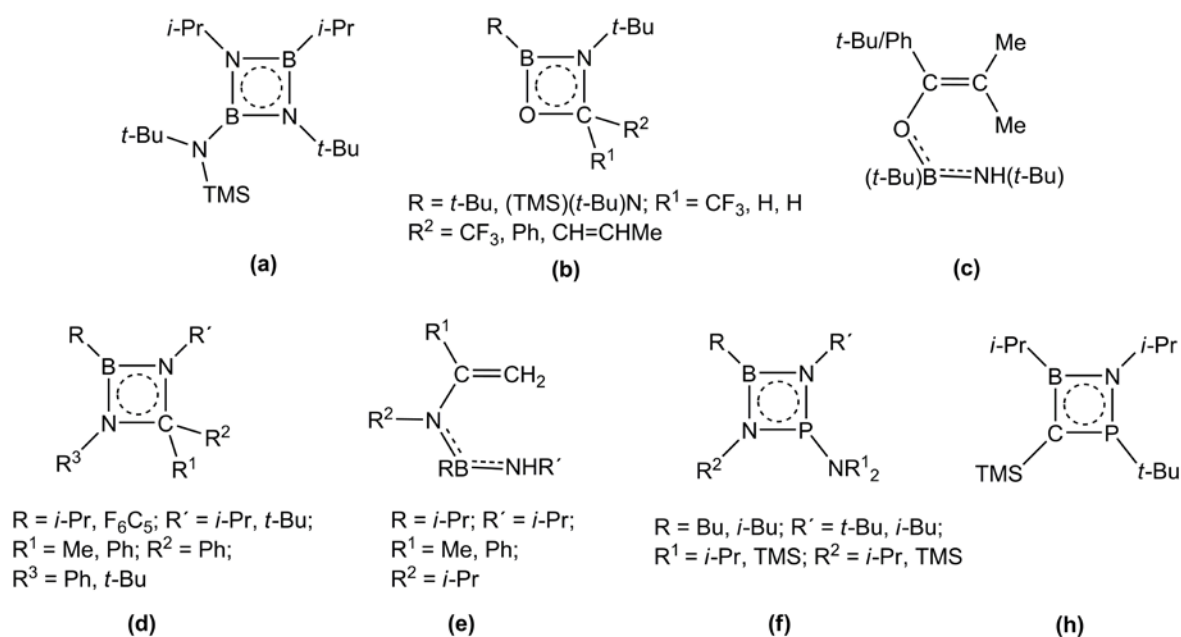


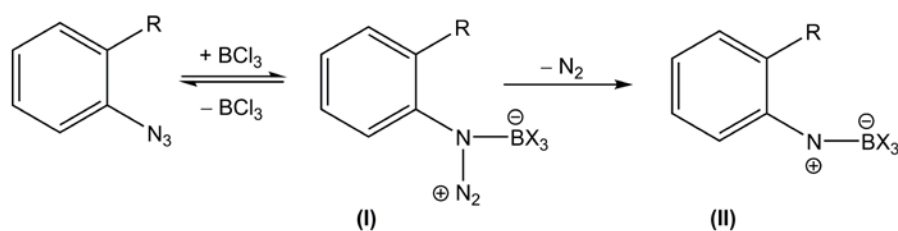
Chart 7.1 Examples of reaction products of iminoboranes with different types of 'ene' compounds.

As these ene compounds contain heteroatoms they can be assumed to react with the starting materials, either with the base or with the chloroborane **21**, and thus they have been avoided in this present study.

The [3 + 2] cycloaddition reactions of iminoboranes with azides (RN_3) or with nitrone [$\text{R}^1\text{R}^2=\text{N}(\text{R}^3)-\text{O}$] are common. The $\text{B}\equiv\text{N}$ bond in the iminoboranes pertain some polarity and thus the reactions with 1,3-dipoles are facile. Several alkyl or aryl azides are known to form tetrazaboroles with iminoboranes as mentioned in Chapter 1. The $t\text{-BuB}\equiv\text{N}t\text{-Bu}$ is a very good example as it forms tetrazaborole with ten different alkyl azides ($\text{R} = \text{Me, Et, Pr, Bu, s-Bu, i-Bu, n-C}_5\text{H}_9, \text{sec-C}_6\text{H}_{11}, \text{PhCH}_2$)^[1, 39] and also with arylazides where $\text{R} = \text{Ph, Mes}$.^[64] Diaryliminoboranes like $\text{MesB}\equiv\text{NMes}$, $\text{F}_5\text{C}_6\text{B}\equiv\text{NC}_6\text{F}_5$ produce tetrazaboroles exclusively with azides.^[64] The $t\text{-BuB}\equiv\text{N}t\text{-Bu}$ is also reported to react with a diazomethane derivative [$t\text{-BuCH}=\text{N}_2$] to give the corresponding five-membered ring product.^[39]

When the chloroborane **21** and phenyl azide, prepared according to literature,^[223] were mixed together at room temperature and cooled to $-78\text{ }^\circ\text{C}$, interestingly, the mixture acquired a deep red color. This slowly disappeared with increasing temperature and reappeared upon cooling. This indicates some interaction between the azide and the chloroborane at low temperature. Upon addition of the potassium bis(trimethylsilyl)amide (KHMDS) to this mixture at $-50\text{ }^\circ\text{C}$, no cycloaddition product was identified. It is noteworthy to mention here that Spagnolo and Zanirato observed reactions between boron trihalide and aryl azides.^[224, 225] They found that various phenyl azides react with $\text{BF}_3\cdot\text{OEt}_2$ at $60\text{ }^\circ\text{C}$ in methylated benzene (toluene, *p*-xylene, *m*-xylene, mesitylene) to produce *N*-benzylanilines or diarylamines.^[224] Later on they observed that boron trichloride (BCl_3) rapidly reacts with 2-azidobiphenyl at $25\text{ }^\circ\text{C}$ to produce carbazole in high yield followed by aqueous workup.^[225]

They treated BCl_3 with different types of organic azides and obtained various types of products, depending on the electronic nature of the substituent/s of the azides. They suggested formation of azide- BX_3 complexes or nitrenium- BX_3 complexes by loss of nitrogen [Scheme 7.15 (I) & (II) respectively], which were the activated species for further reaction/s.^[225] It is reasonable to assume that the chloroborane **21** and phenyl azide may also have a dative interaction between them at lower temperature and that coordinated complex shows a red color which is destroyed upon warming.



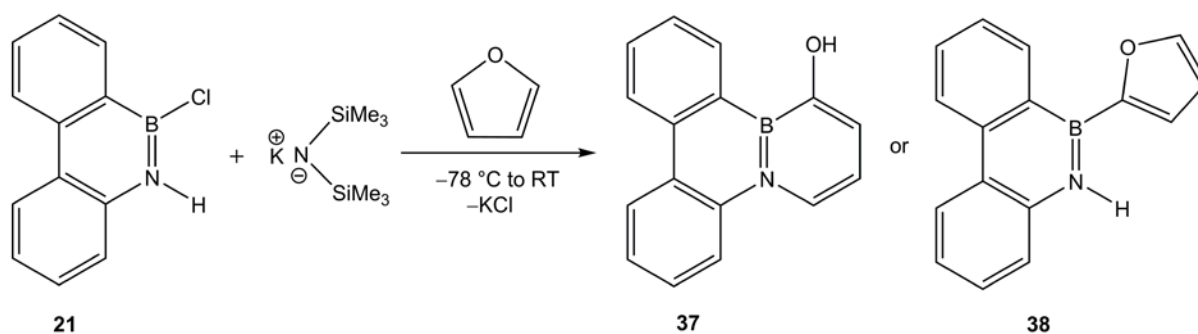
Scheme 7.15 Complex formation between azides and trihaloboranes.^[225]

Paetzold mentioned that the [4 + 2] cycloaddition reactions are ‘‘notoriously’’ slow.^[2] Accordingly only two Diels-Alder products of iminoboranes are known. These are formed in the reactions of a dienophile, $\text{RB}\equiv\text{N}t\text{-Bu}$ [$\text{R} = \text{C}_6\text{F}_5, \text{TMS}(t\text{-Bu})\text{N}$] and cyclopentadiene (Scheme 7.14) but these reveal an important property of iminoboranes. According to the computational analysis by Gilbert, the [2 + 2] dimerization is favoured over [4 + 2] cycloaddition due to lower barrier.^[226] From the detailed study performed on various types of iminoboranes, $\text{RB}\equiv\text{NR}'$ [$\text{R} = \text{H}, \text{Me}, \text{CF}_3, \text{C}_6\text{F}_5, t\text{-Bu}$; $\text{R}' = \text{H}, \text{Me}, t\text{-Bu}$], he concluded that the [4 + 2] cycloaddition is favored over [2 + 2] dimerization with increase of the Lewis acidity of the boron center by electron withdrawing substituents, more bulky groups on boron and nitrogen centers, and also by a less strained diene. This theoretical study provides helpful informations to choose appropriate diene for a certain iminoborane to perform the desired cycloaddition reaction.

To learn if the desired cyclic iminoborane (**E**) may be involved in the formation of the trimer **33**, the dehydrohalogenation reaction with KHMDS was carried out in presence of anthracene; only the trimer **33** was isolated and the anthracene remained unreacted. When 2,3-dimethyl-1,3-butadiene was used as diene, no trimer was observed but a yellow oily material was found after removal of volatiles. Unfortunately no defined product could be characterized from the reaction mixture. Another diene selected for the trapping reaction was *N*-methylpyrrole as it was found not to coordinate to 10-chloro-9-aza-10-boraphenanthrene **21**. However, it reacted vigorously with KHMDS and immediately a dark red solution formed. The spiro[2,4]hepta-4,6-diene (1,1-cyclopropylcyclopentadiene, CPCP), prepared from cyclopentadiene and 1,2-dibromoethane by reacting with sodium nitrite in presence of benzyltriethylammonium chloride (Et₃NBnCl) as phase transfer agent,^[227] also reacted with the base KHMDS rapidly resulting in a brown solution.

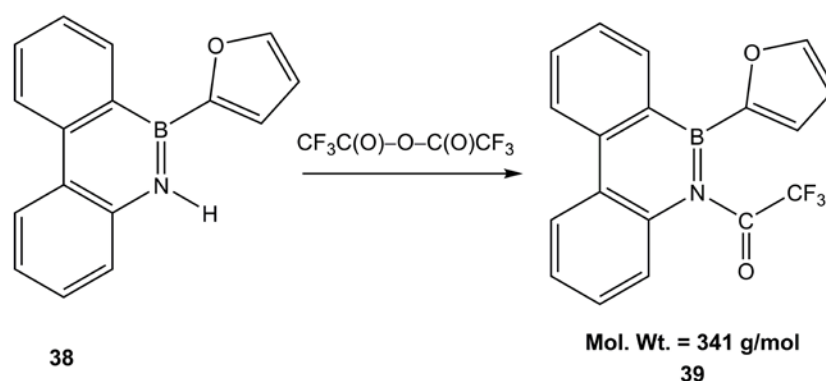
Furan is known to be a reactive diene towards several alkynes in Diels-Alder reactions, so it was also employed as trapping agent. Furan was dried over calcium hydride (CaH₂) and distilled at 48 °C (bath temperature). The starting chloroborane **21** was dissolved in furan and the ¹¹B chemical shift (34 ppm) did not change, so adduct formation can be excluded. The complete reaction of the chloroborane with KHMDS was then carried out in furan as reaction medium. The base dissolved in furan was added to the furan solution of chloroborane at -60 °C. Slowly the mixture turned to opaque and the next day the precipitate was separated by filtration under ambient atmosphere. After removal of furan from the filtrate a dirty brown solid mixture was obtained. The electron impact mass spectrum of the crude mixture shows molecular ion peaks for the trimer **33** (531 amu), sometimes tetramer **35** (708 amu) and 245 amu as most abundant peak. The brown reaction product mixture was purified by column chromatography over silica with 4:1 dichloromethane and *n*-hexane mixture. A

colorless solid (R_f value 0.81), was isolated in 39 % yield. This compound has an ^{11}B chemical shift at 30.3 ppm which indicates a tricoordinated boron center. The ^1H NMR contains 12 protons along with a broad signal which could be either due to a $-\text{NH}$ or $-\text{OH}$ group. The ^{13}C NMR spectrum has 14 carbons; these data suggest a structure containing a BN-phenanthrene unit attached to a furan molecule like **37** or **38** as shown in Scheme 7.16. For the structure **37**, at least two ^1H - ^1H NOESY correlations should be present between the furan skeleton and BN-phenanthrene protons but the spectrum exhibits only one correlation which excludes **37** and allows assignment for the structure **38**.



Scheme 7.16 Reaction of chloroborane **21** with KHMDS in furan.

The LC-MS measurement showed that the compound **38** elutes with water-acetonitrile (mixed with 10 % of THF) mixture at 15.1 min (see experimental section, page 110). The compound also was identified on GC-MS having the retention time 23.2 min. Under identical condition the derivatized product of **38** with trifluoroacetic anhydride (TFAA) was identified at 25.8 min with mass of 341 amu as required for **39** (Scheme 7.17) but in case of BSTFA no derivatization product was observed.



Scheme 7.17 Derivatization reaction of **38** with TFAA.

When two equivalents of KHMDS were treated with the chloroborane **21** in furan under identical experimental conditions, an interesting outcome was observed. Following a similar work up procedure, a colorless compound **40** was separated having an R_f value of 0.17 over silica column with 4:1 dichloromethane and *n*-hexane mixture.

The ^1H NMR spectrum shows 16 protons; among them eight protons can be correlated to each other as depicted by the ^1H - ^1H COSY spectrum and other sets of 4 signals for 8 protons are correlated to each other. The ^{13}C spectrum contains 14 carbons signals and carbon attached to the boron is not visible. In the electron impact mass spectrum, the $[\text{M}^+]$ peak was found at 313 amu. This is the sum of the masses of one BN-phenanthrene unit and two furan molecules. The compound has a $^{11}\text{B}\{^1\text{H}\}$ chemical shift at -8.4 ppm. When the ^{11}B NMR spectrum of this compound was regularly measured, the chemical shift slowly changed from -8.4 to 30.3 ppm in CD_2Cl_2 . The final ^1H NMR spectrum was identical to that of **38** (Figure 7.6).

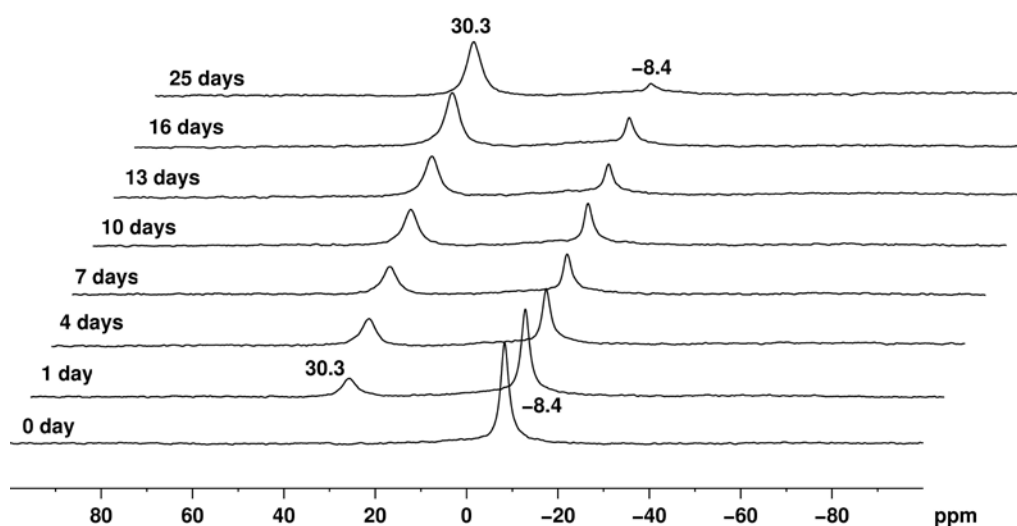
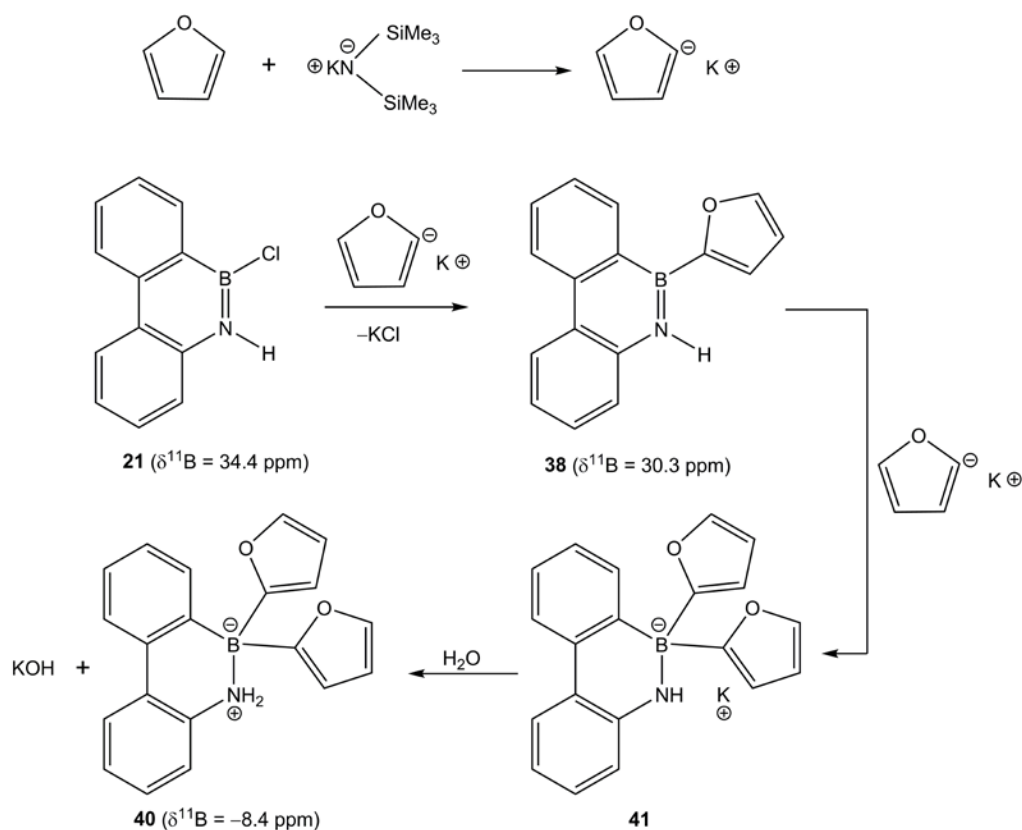


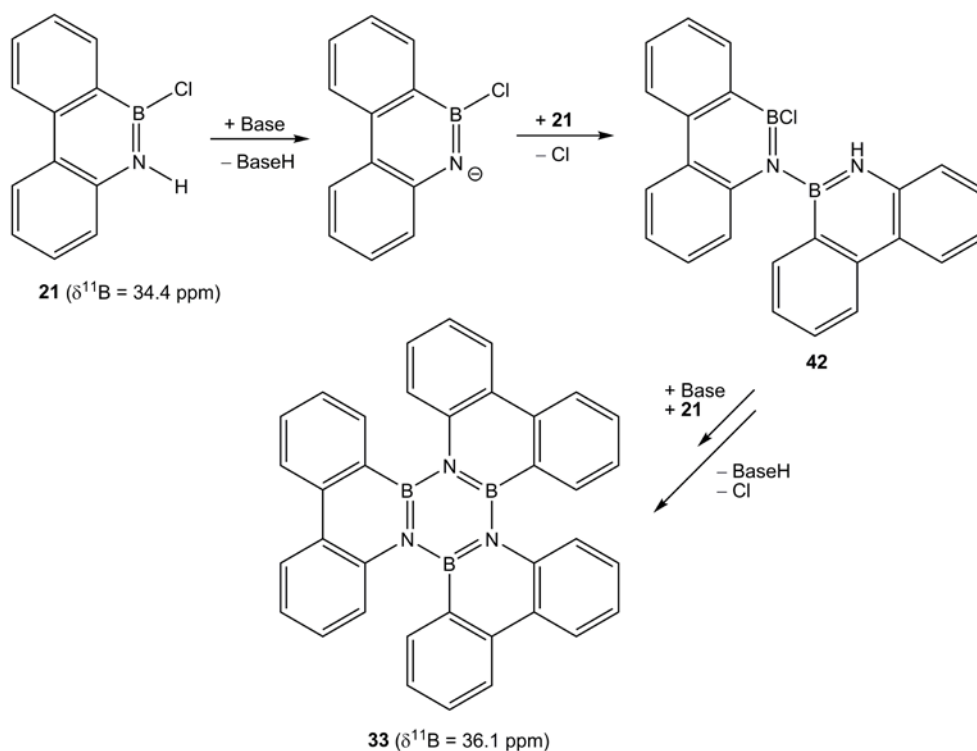
Figure 7.6 Gradual conversion of **40** to **38** in CD_2Cl_2 over time.

The structure of the product **40** is expected to be very similar to **38** according to these analytical data. The broad signal in the ^1H NMR spectrum of **40** integrates to two H's that are due to the two N–H protons. A possible reaction pathway could be formation of the 2-furyl anion by KHMDS that attacks the boron center and produces the initial product **38** via nucleophilic substitution (Scheme 7.18). The second furyl anion then attacks the boron center again and results in the salt **41** which converts to **40** upon exposure to moisture. The compound **40** gradually loses furan and transforms into **38**.



Scheme 7.18 Possible reaction pathway of chloroborane **21** with 2 equivalents of KHMDS in furan.

The attempted trapping reactions do not provide any evidence for the existence of the 9,10-didehydro-9-aza-10-boraphenanthrene (**E**). Possibly the cyclotrimerization occurred via deprotonation of the chloroborane **21** with base to afford the primary anion which could further react with another molecule of **21** to produce **42** and that might undergo a similar reaction to result in the formation of the trimer **33** as shown in Scheme 7.19.



Scheme 7.19 Possible reaction mechanism of the cyclotrimerization reaction.

7.3 Conclusion

The base induced dehydrohalogenation study reveals many interesting properties of the 9-aza-10-boraphenanthrene compounds. They are able to form borenium and boronium salts with different Lewis bases. These salts may be important in terms of electrochemical properties and could be promising agents for further chemical transformations.

This study also showed that 9-aza-10-boraphenanthrene compounds may undergo dehydrohalogenation reactions with appropriate bases. Though these reactions are very challenging, the formation of the 1,2:3,4:5,6-tris-(2,2'-biphenyllylene)borazole, TBB **33**, established a new route to obtain sterically overcrowded hexabenzotriphenylene derivative in higher yield and higher purity. TBB was completely characterized for the first time. Comparison with the products obtained from the original TBB synthesis by Köster et al.,

shows that an previously overlooked tetramer i.e. 1,2:3,4:5,6:7,8-tetrakis-(2,2'-biphenylene)-1,3,5,7-tetraza-2,4,6,8-tetraborocane **35**, is also formed. Several trapping reactions attempted in this work to identify the possible reactive intermediate 9,10-didehydro-9-aza-10-boraphenanthrene (**E**) were not successful. These suggest that the 9,10-didehydro-9-aza-10-boraphenanthrene (**E**) may not be involved in this base induced dehydrohalogenation reaction but a stepwise nucleophilic attack by the primary amide anion produced from **21** has more preference in this reaction as revealed in Scheme 7.19.

Additionally the reaction in furan with the chloroborane **21** in presence of base produced a novel compound **40** with two furyl groups on the boron and that was isolated and characterized completely.

8. Experimental Section

8.1 General Procedure and Equipments

All the reactions carried out under inert atmosphere of argon gas using standard Schlenk techniques and the reaction flasks were pre-dried by heat gun under high vacuum. All the moisture sensitive compounds were stored in an M-Braun Unilab glove box unless or otherwise mentioned. Solvents *n*-pentane, *n*-hexane, toluene, THF, CH₂Cl₂ were collected from an M-Braun solvent purification system (SPS) just before use. Benzene and xylene were dried over sodium and phosphorous pentoxide (P₂O₅) respectively prior to use. 1,2-dibromobenzene, *n*-BuLi (1.6M in *n*-hexane), BCl₃ (1M in *n*-hexane), BCl₃ (1M in CH₂Cl₂), trimethylsilyl azide (TMSN₃), pyridine, 4-*t*-butylpyridine, 2,6-lutidine, *N,O*-bis(trimethylsilyl)hydroxylamine, trimethylsilyl chloride (TMSCl), 2-aminobiphenyl, aluminium chloride (AlCl₃), *N,N*-diisopropylethylamine (Hünig Base), 1,8-diazabicyclo[5.4.0]undec-7-ene (DBU), silver trifluoromethanesulfonate, potassium bis(trimethylsilyl)amide, lithium diisopropylamide (LDA) [1.8M in THF/heptane/ethylbenzene], 2,2,6,6-tetramethylpiperidine (HTMP), anthracene, 2,3-dimethyl-1,3-butadiene, *N*-methylpyrrole, cyclopentadiene, sodium nitrite, 1,2-dibromoethane, benzyltriethylammonium chloride, furan, calcium hydride (CaH₂), sodium azide, sodium sulfate purchased from Acros, Fluka and Aldrich were used as received without any modification if or unless mentioned. Solvents used for chromatography were purchased in specific chromatography grade.

NMR Spectroscopy

All the NMR spectra were recorded on a Bruker DRX 250 MHz, 400 MHz and AMX 600

MHz spectrometers at 295 K. The variable temperature ^{11}B NMR spectra were recorded on a Bruker AVANCE II+ 500 MHz operating at 160 MHz (^{11}B). Chemical shifts were calibrated to residual proton and carbon resonance of the solvents: C_6D_6 ($\delta^1\text{H} = 7.16$ ppm, $\delta^{13}\text{C} = 128.06$ ppm), CD_2Cl_2 ($\delta^1\text{H} = 5.32$ ppm, $\delta^{13}\text{C} = 53.84$ ppm)^[228] and externally [^{11}B : $\text{BF}_3\cdot\text{OEt}_2$, ^{14}N : CH_3NO_2 , ^{29}Si : $\text{Si}(\text{CH}_3)_4$]. The solvents for NMR measurements were purchased from Deutero GmbH, dried over 4 Å molecular sieves and were Argon saturated before use.

Fourier Transform-Infrared (FT-IR) Spectroscopy

Except for the Matrix-Isolation experiments all other Fourier transform infrared spectra (FT-IR) were measured on a Bruker TENSOR 27 FT-IR spectrometer at room temperature. The samples palettes were prepared by mixing with dry potassium bromide (KBr). For the moisture sensitive azides, the samples were prepared inside the glove box with Nujol (dried before use) using KBr disk and were measured immediately after taking the samples outside of the glove box.

Ultraviolet-Visible (UV-Vis) and Fluorescence Spectroscopy

The UV-Vis spectra were recorded on a PerkinElmer LAMBDA 1050 UV/Vis/NIR spectrometer in commercially available spectroscopy grade dichloromethane solvent purchased from Acros. The *n*-Hexane was collected from the SPS system. The fluorescence spectra were obtained on a PerkinElmer LS 55 Fluorescence spectrometer.

Mass Spectrometry

Mass spectra were measured on a Finnigan Triple-Stage-Quadrupole Spectrometer (TSQ-70) from Finnigan-Mat and the high-resolution mass spectra were obtained from a MAT 95 from

the same company. The ionization method used was electron-impact (EI, 70 eV). The HR-FT-ICR-mass was measured on an APEX 2 spectrometer from Bruker Daltonic with electrospray ionization method (ESI).

Chromatographic Methods

(i) GC-MS:

The gas chromatography mass spectroscopy measurements were performed on an Agilent HP 6890 Series with a mass selective detector 5973.

Compound **12**, in *n*-pentane, stationary phase: J+W DB-5MS, 30 x 0.25 mm; $d_f = 0.25 \mu$; temperature program = 50 °C (3 min) to 250 °C; temperature increasing rate = 6 °C/min; injection temperature = 250 °C, split method; flow rate = 1.2 mL min⁻¹; mass (EI) at 70 eV; mobile phase: helium; $t_R = 6.9$ min.

Compounds **15** & **16**, stationary Phase: J+W DB-5MS, 15 x 0.25 mm; $d_f = 0.1 \mu$; temperature program = 80 °C (2 min) to 320 °C, temperature increasing rate = 6 °C/min; injection temperature = 300 °C, split method; flow rate = 1.1 mL min⁻¹; mass (EI) at 70 eV; mobile phase: helium. Compound **15** in dichloromethane, $t_R = 19.33$ min, and the derivatized product of **16** with BSTFA, in dichloromethane, $t_R = 19.39$ min.

Compounds **38**, stationary Phase: J+W DB-5MS, 15 x 0.25 mm; $d_f = 0.1 \mu$; temperature program = 100 °C (2 min) to 320 °C, temperature increasing rate = 6 °C/min; injection temperature = 300 °C, split method; flow rate = 1.1 mL min⁻¹; mass (EI) at 70 eV; mobile phase: helium, $t_R = 23.2$ min for **38**; and the derivatized product of **38** with TFAA i.e. compound **39**, in dichloromethane, $t_R = 25.8$ min.

(ii) LC-MS

Liquid chromatography-mass spectroscopy measurements were carried out on an Agilent 1100 series LC machine coupled with an Esquire 3000 plus mass machine from Bruker Daltonics. The data analysis was done using ChemStation (for LC) and EsquireControl (for mass) software.

Compound **33**, in Dichloromethane, Stationary Phase: NUCLEODUR 100-5 C₁₈ EC 125/4; Wavelength used = 210 nm, Injection volume = 20 μ l, Column temperature = RT, Flow rate = 0.5 mL min⁻¹, Mass (ESI) at 70 eV; Mobile Phase: H₂O (A)/MeOH (B), Elution time = 23.2 min at room temperature; Solvent gradient: starting from 30 %, the percentage of B was increased to 100 % within 20 min and held that condition up to 59 min. At 60 min the gradient returned to the initial condition.

Compound **38**, in Dichloromethane, Stationary Phase: EC 125/4 NUCLEODUR 100-5 C₁₈EC 125/4; Wavelength used = 248 nm, Injection volume = 10 μ l, Column temperature = RT, Flow rate = 0.5 mL min⁻¹, Mobile Phase: H₂O (A)/(CH₃CN + 10 % THF) (B); Elution time = 15.1 min; Solvent gradient: starting from 40 %, the solvent B reached 80 % at 20 min and then again gradually increased to 100 % within next 10 min. These conditions were kept constant till 34 min and then within 1 min the gradient changed back to the initial condition.

(iii) Column Chromatography

Compound **33**, Stationary phase: Silica gel = 0.035-0.07 mesh, Mobile phase: 1:1 Dichloromethane:*n*-hexane solvent mixture, R_f = 0.64.

Compound **38**, Stationary phase: Silica gel = 0.035-0.07 mesh, Mobile phase: 4:1

Dichloromethane:*n*-hexane solvent mixture, $R_f = 0.81$.

Compound **40**, Stationary phase: Silica gel = 0.035-0.07 mesh, Mobile phase: 4:1

Dichloromethane:*n*-hexane solvent mixture, $R_f = 0.17$.

CAUTION: Azides described here may be explosive; appropriate safety precautions were taken.

X-ray Crystallography

The intensity data for the crystals **6**, **6a**, **8**, **9** and **10** were collected on an Oxford Diffraction Xcalibur2 diffractometer with a Sapphire2 CCD. The crystal structures were solved by direct methods using SHELXS-97^[229] and refined with SHELXL-97.^[229] The intensity data for the crystals **15**, **24** and **31** were collected on Stoe IPDS II diffractometer and for **17** APEX II Diffractometer was used. The structures were solved by using SHELXS-90^[230] and refined with SHELXL-97.^[229] For refinement details see crystallographic data (page 124).

8.2 Computation

Optimization of the structures, calculation of harmonic vibrational frequencies and nuclear shieldings were carried out with the standard defaults in the Gaussian09 series of programs^[231] using 6-31G(d)^[232, 233], 6-31G+(d) and 6-311+(d,p)^[234] basis sets in the DFT calculations.^[235-237] For NMR calculations, the computed $\sigma(^{11}\text{B})$ were data were converted to $\delta^{11}\text{B}$ data (vs $\text{BF}_3\cdot\text{OEt}_2$) following the equation, $\delta^{11}\text{B} = \sigma(^{11}\text{B})[\text{B}_2\text{H}_6] - \sigma(^{11}\text{B}) + 18$, where $\sigma(^{11}\text{B})[\text{B}_2\text{H}_6] = 84.1$, $\delta^{11}\text{B} [\text{B}_2\text{H}_6] = 18.0$ and $\delta^{11}\text{B}[\text{BF}_3\cdot\text{OEt}_2] = 0$.

8.3 Synthesis

Compound 1: Diphenylaminoboron dichloride. Diphenylamine (3 g, 17.7 mmol) dissolved in 10 mL dry CH₂Cl₂ was slowly added to a cooled (−78 °C) BCl₃ solution (1.1 equiv, 19.6 mL of 1M CH₂Cl₂ solution) in 20 mL dry CH₂Cl₂. After 1 h the cooling bath was removed and all volatiles were removed leaving a colorless solid. This solid was washed with *n*-hexane (2 x 10 mL) and then suspended in 20 mL dry benzene. The suspension was heated at 70 °C for 18 h and then a colorless solid mixture was obtained after removal of benzene. The pure diphenylaminoboron dichloride (**1**) was sublimed at 42 °C/10^{−5} mbar as colorless solid (2.1 g, 48 %). ¹H NMR (250 MHz, CD₂Cl₂): δ = 7.23 – 7.39 (m) ppm; ¹³C{¹H} NMR (62.9 MHz, CD₂Cl₂): δ = 146.5, 129.6, 127.8, 127.3 ppm, C directly bonded to boron was not detected; ¹¹B{¹H} NMR (80.3 MHz, CD₂Cl₂): δ = 32.3 (s, *h*_{1/2} = 77.7 Hz) ppm.

Compound 2: Bisazido(diphenylamino)borane. The diphenylaminoboron dichloride (**1**) (0.040 mg, 0.161 mmol) was dissolved in 8 ml dry CH₂Cl₂ and brought to −78 °C. Then 2.2 equiv of TMSN₃ (0.353 mmol, 0.046 mL) was added to the chloride solution and left for stirring overnight. Then all reaction volatiles were removed at room temperature under vacuum to get a colorless solid (0.032 g, 76 %). ¹H NMR (250 MHz, CD₂Cl₂): δ = 7.37 – 7.13 (m) ppm; ¹³C{¹H} NMR (62.9 MHz, CD₂Cl₂): δ = 145.5, 129.7, 127.5, 126.5 ppm; ¹¹B{¹H} NMR (80.3 MHz, CD₂Cl₂): δ = 23.8 (s, *h*_{1/2} = 115.5 Hz) ppm.

Compound 6: 9-Chloro-9-borafluorene.^[100] To a cooled solution (0 °C) of 3 g (9.6 mmol) 2,2'-dibromobiphenyl in 150 mL *n*-hexane, 12.1 mL *n*-BuLi (19.2 mmol, 1.6M in *n*-hexane) was added dropwise. After complete addition, the ice bath was removed and the colorless suspension was stirred for 3 days at ambient temperature. After removal of the solvent *in*

vacuo, the remaining colorless solid was washed with *n*-hexane (3 x 100 mL). Then a slurry was made in 150 mL *n*-hexane by vigorous stirring and 9.6 mL BCl₃ (1M in *n*-hexane, 9.6 mmol) was added slowly to it at 0 °C. After stirring over night, the bright yellow solution was filtered from the colorless precipitate and concentrated to ~ 5 mL. This remaining oily liquid was distilled at 90 °C/10⁻³ mbar to give (1.72 g, 8.6 mmol, 90 % relative to 2,2'-dibromobiphenyl) pure 9-chloro-9-borafluorene as bright yellow needle shape crystals that were good for X-ray measurement. m.p. 52 °C; ¹H NMR (250 MHz, CD₂Cl₂): δ = 7.55 (d, *J*_{HH} = 7.0 Hz, 2H), 7.39 – 7.37 (m, 4H), 7.19 – 7.16 (m, 2H) ppm; ¹³C{¹H} NMR (62.9 MHz, CD₂Cl₂): δ = 153.5, 135.7, 132.9, 129.0 and 120.2 ppm, the carbon atom directly attached to boron was not detected; ¹¹B{¹H} NMR (80.3 MHz, CD₂Cl₂): δ = 63.6 (s, *h*_{1/2} = 246.5 Hz) ppm.

Compound 6b: 9-Chloro-9-borafluorene-4-*t*-butyl py. 1 equivalent of 4-*t*-butylpyridine (0.252 mmol, 0.037 mL) was added to the 5 mL dichloromethane solution of 9-chloro-9-borafluorene **6** (0.05 g, 0.252 mmol) at 10 °C. Immediately the yellow color of the chloride solution disappeared and the colorless reaction mixture was stirred for 3 h. Then all the volatiles were removed under vacuum. The remaining colorless solid was washed with *n*-pentane and dried to get 0.072 g of clean **6b**. Yield: 86 %. ¹H NMR (250 MHz, CD₂Cl₂): δ = 8.82 (d, *J*_{HH} = 6.7 Hz, 2H), 7.64 – 7.56 (m, 4H), 7.44 (d, *J*_{HH} = 7.0 Hz, 2H), 7.27 (t, *J*_{HH} = 7.4 Hz, 2H), 7.19 – 7.14 (m, 2H), 1.33 (s, 9H) ppm; ¹³C{¹H} NMR (62.9 MHz, CD₂Cl₂): δ = 206.2, 180.3, 175.1, 155.7, 153.6, 152.2, 146.8, 141.9, 22.3 ppm, C directly attached to the boron was not detected; ¹¹B{¹H} NMR (80.3 MHz, CD₂Cl₂): δ = 5.5 (s, *h*_{1/2} = 168.4 Hz) ppm.

Compound 7: 9-Azido-9-borafluorene. A solution of 0.1 g (0.5 mmol) 9-chloro-9-borafluorene **6** in 10 mL CH₂Cl₂ was treated with 0.067 mL (0.5 mmol) trimethylsilyl azide

at $-78\text{ }^{\circ}\text{C}$. The reaction mixture was gradually warmed to room temperature after stirring over night. The resulting crude bright yellow solution was monitored by ^{11}B NMR showing complete conversion of the chloride **6** into monomeric boron azide **7a**. $^{11}\text{B}\{^1\text{H}\}$ NMR (80.3 MHz, CD_2Cl_2): $\delta = 50.2$ ppm; IR (nujol + CH_2Cl_2): 2139 vs $[\nu_{\text{asym}}(\text{N}_3)]\text{ cm}^{-1}$.

After complete removal of all volatile products, the remaining pale yellow solid product showed two signals for **7a** and **7b** in ^{11}B NMR. $^{11}\text{B}\{^1\text{H}\}$ NMR (80.3 MHz, CD_2Cl_2): $\delta = 50.3$ and 5.0 ppm; IR (nujol + CH_2Cl_2): 2176 s and 2136 vs $[\nu_{\text{asym}}(\text{N}_3)]\text{ cm}^{-1}$.

Compound 9: 9-Azido-9-borafluorene•py. Trimethylsilyl azide (0.067 mL, 0.5 mmol) was added to a solution of 0.1 g (0.5 mmol) 9-chloro-9-borafluorene **6** dissolved in 10 mL CH_2Cl_2 at $-78\text{ }^{\circ}\text{C}$. The reaction mixture was allowed to come to the room temperature slowly and stirred over night. Then 0.04 mL (0.5 mmol) pyridine was added to the reaction mixture subsequently. After that the solvent was removed *in vacuo* leaving a white solid that was purified by trituration with *n*-pentane from dichloromethane solution and dried at ambient temperature under reduced pressure to produce pure product **9**. Slow evaporation of the CH_2Cl_2 solvent from the solution of the product produced colorless crystals which were found to be suitable for X-ray crystallography. Yield 0.131 g (91 %), mp $176\text{--}178\text{ }^{\circ}\text{C}$ (decomp.). ^1H NMR (250 MHz, CD_2Cl_2): $\delta = 8.68$ (d, $J_{\text{HH}} = 6.8$ Hz, 2H), 8.07 (t, $J_{\text{HH}} = 8.1$ Hz, 1H), 7.68 (d, $J_{\text{HH}} = 7.4$ Hz, 2H), $7.63\text{--}7.57$ (m, 2H), $7.33\text{--}7.27$ (m, 4H), $7.18\text{--}7.12$ (m, 2H); $^{13}\text{C}\{^1\text{H}\}$ NMR (62.9 MHz, CD_2Cl_2): $\delta = 149.3, 144.7, 142.2, 129.9, 128.8, 127.4, 126.5, 120.0$ ppm, C directly bonded to the boron was not observed; $^{11}\text{B}\{^1\text{H}\}$ NMR (80.3 MHz, CD_2Cl_2): $\delta = 4.1$ (s, $h_{1/2} = 115.5$ Hz) ppm; ^{14}N NMR (28.9 MHz, CD_2Cl_2): $\delta = -74.7$ (N-py), -138.4 (β -N), -210.9 (γ -N) ppm, α -N not detected; IR (nujol + CH_2Cl_2): ν (cm^{-1}) = 2929 w, 2854 m, 2116 vs $[\nu_{\text{asym}}(\text{N}_3)]$, 1620 vs, 1457 vs, 1377 m, 1158 sw, 1058 w, 919 m, 874 s, 830 sw, 743 vs,

690 m, 690 s, 653 s, 619 s.

Compound 10: 9-Azido-9-borofluorene-4-*t*-butyl py. Compound **10** was prepared similarly as described for compound **9** using 0.07 mL (1 equivalent of 0.1 g of chloroborane **6**) 4-*t*-butylpyridine. After removal of all volatile residues by vacuum evaporation, colorless compound was obtained by trituration process as described above for **9**. This compound was crystallized from CH₂Cl₂. Then the white needle shaped crystals were washed with *n*-pentane to get pure product. Yield 0.152 g (88 %), mp 204-206 °C (decomp.). ¹H NMR (250 MHz, CD₂Cl₂): δ = 8.56 (d, *J*_{HH} = 6.7 Hz, 2H), 7.69 (d, *J*_{HH} = 7.4 Hz, 2H), 7.57 (d, *J*_{HH} = 6.7 Hz, 2H), 7.37 – 7.29 (m, 4H), 7.20 – 7.14 (m, 2H), 1.35 (s, 9H, –C(CH₃)₃); ¹³C{¹H} NMR (62.9 MHz, CD₂Cl₂): δ = 168.0, 149.4, 144.2, 130.0, 128.7, 127.3, 123.6, 119.9, 36.0, 30.2 ppm, C attached to the boron was not observed; ¹¹B{¹H} NMR (80.3 MHz, CD₂Cl₂): δ = 3.7 (s) ppm; ¹⁴N (28.9 MHz, CD₂Cl₂): δ = –73.0 (N-py), –135.8 (β-N), –207.6 (γ-N) ppm, α-N not detected; IR (nujol + CH₂Cl₂): ν (cm⁻¹) = 3050 s, 2956 vs, 2925 vs, 2854 vs, 2125 vs [*v*_{asym} (N₃)], 1632 vs, 1596 m, 1504 m, 1432 vs, 1352 s, 1221 s, 1151 sw, 1083 s, 929 s, 873 s, 851 s, 829 s, 742 vs, 707 m, 681 s.

Compound 12: Tris(trimethylsilyl)hydroxylamine.^[173] To the solution of *N,O*-bis(trimethylsilyl)hydroxylamine (1 mL, 4.679 mmol) in 10 mL of *n*-hexane, 1 equiv of *n*-BuLi (2.92 mL, in 1.6 M in *n*-hexane) was added at room temperature. The mixture was allowed to stir overnight and next day colorless solid formation was observed. Then TMSCl (0.59 mL, 4.679 mmol) was added to the suspension at 0 °C and left for stirring overnight. Finally the LiCl was separated by filtration through a 0.2 μm polytetrafluoroethylene (PTFE) filter. The clear colorless oily product **12** was obtained by removal of all volatiles from the filtrate at 5 °C/10⁻¹ mbar. Yield 0.613 g (52 %). ¹H NMR (400 MHz, C₆D₆): 0.22 (s, 9H,

–OSiMe₃), 0.19 (s, 18H, –N(SiMe₃)₂) ppm; ¹³C{¹H} NMR (100.6 MHz, C₆D₆): 1.23, 0.96 ppm; ²⁹Si NMR: (49.7 MHz, C₆D₆): 27.0 (s, –OSiMe₃), 7.2 (s, –N(SiMe₃)₂) ppm.

Compound 15: 10-trimethylsilyloxy-9-aza-10-boraphenanthrene. The bright yellow 9-chloro-9-borafluorene **6** (80 mg, 0.403 mmol) was dissolved in 10 mL of *n*-hexane in a Schlenk tube and brought to –78 °C. Then 0.088 mL (0.411 mmol, 1.02 equivalents) amine **13** was slowly added to the chloride solution. Immediate formation of colorless solid was observed. After complete addition of amine the yellow color of the chloride solution disappeared completely and the reaction mixture turned into thick white slurry. Then the mixture was allowed to come to the room temperature slowly. The precipitate started to dissolve above –20 °C and a colorless and clear the solution was obtained at room temperature. Colorless solid precipitation was observed within a week from the concentrated *n*-hexane reaction mixture at –18 °C. The precipitate was collected and quickly washed with 1 mL cold *n*-hexane for two times and dried under vacuum to get 78 mg compound (73 %). ¹H NMR (600 MHz, CD₂Cl₂): δ = 8.33 (d, *J*_{HH} = 8.16 Hz, 1H), 8.28 (d, *J*_{HH} = 8.0 Hz, 1H), 8.07 (d, *J*_{HH} = 7.50 Hz, 1H), 7.67 – 7.69 (m, 1H), 7.46 (t, *J*_{HH} = 7.35 Hz, 1H), 7.33 – 7.35 (m, 1H), 7.12 – 7.15 (m, 1H), 7.1 (dd, *J*_{HH} = 8.07, 1.05 Hz, 1H), 6.48 (s, br, N–H), 0.36 (s, –C(CH₃)₃, 9H) ppm; ¹³C{¹H} NMR (150.9 MHz, CD₂Cl₂): δ = 141.0, 140.6, 133.1, 131.1, 128.5, 126.3, 124.2, 122.4, 122.3, 120.7, 118.8, 1.8 ppm, C directly attached to the boron was not detected; ¹¹B{¹H} NMR (80.3 MHz, CD₂Cl₂): δ = 27.3 (s, *h*_{1/2} = 239 Hz) ppm; ²⁹Si NMR (49.7 MHz, CD₂Cl₂): δ = 11.4 ppm; UV-Vis (in *n*-hexane): λ_{max}(log ε) = 223(4.786), 228(4.764), 249(4.505), 269(4.402), 298(4.133), 311(4.19), 324(4.181) nm; HRMS(EI) (C₁₅H₁₈BNOSi): 267.12677 amu, Calc'd 267.125072 amu found.

Compound 18: 10-trimethylsilyloxyamino-9-aza-10-boraphenanthrene. The bright yellow 9-chloro-9-boraflluorene (80 mg, 0.403 mmol) was dissolved in 10 mL of *n*-hexane in a Schlenk tube and brought to $-78\text{ }^{\circ}\text{C}$. Then 0.175 mL (0.818 mmol, 2.03 equivalents) amine was added dropwise to the chloride. Immediate formation of white solid was observed. After complete addition of amine the yellow color of the chloride solution disappeared completely and turned into thick solid slurry which started to dissolve above $-20\text{ }^{\circ}\text{C}$. Then the mixture was allowed to come to the room temperature slowly. At ambient condition the reaction mixture was completely clear. Colorless precipitate was obtained from the concentrated reaction mixture at $-20\text{ }^{\circ}\text{C}$. Then the colorless solid was washed quickly with 1 mL cold *n*-hexane for 2 times and dried properly under vacuum to get 86 mg product (76 %). ^1H (400 MHz, C_6D_6): 8.16 (d, $J_{\text{HH}} = 8.16\text{ Hz}$, 1H), 8.12 (d, $J_{\text{HH}} = 7.99\text{ Hz}$, 1H), 7.40 – 7.43 (m, 1H), 7.35 (dd, $J_{\text{HH}} = 7.38, 0.96\text{ Hz}$, 1H), 7.18 (td, $J_{\text{HH}} = 7.25, 0.88\text{ Hz}$, 1H), 7.11 – 7.13 (m, 1H), 6.97 – 7.0 (m, 1H), 6.74 (s, br, 1H), 6.60 – 6.61 (m, 1H), 6.41 (s, br, 1H), 0.17 (s, 9H) ppm; $^{13}\text{C}\{^1\text{H}\}$ (100.6 MHz, C_6D_6): 140.4, 139.8, 130.6, 130.58, 128.5, 126.0, 124.4, 123.0, 122.4, 120.2, 118.5, -1.2 ppm, C directly bonded to the boron was not observed; $^{11}\text{B}\{^1\text{H}\}$ (80.3 MHz, C_6D_6): $\delta = 28.3$ (s, $h_{1/2} = 296\text{ Hz}$) ppm; ^{29}Si (49.7 MHz, C_6D_6): $\delta = 25.5$ ppm; UV-Vis (in *n*-hexane): $\lambda_{\text{max}}(\log \epsilon) = 226(4.579), 250(4.287), 271(4.181), 298(3.877), 312(3.948), 325(3.949)\text{ nm}$; HRMS(EI) ($\text{C}_{15}\text{H}_{19}\text{BN}_2\text{OSi}$): 282.13914 amu, Calc'd 282.135971 amu.

Compound 22: 10-(2,6-lutidin-1-yl)-9-aza-10-boraphenanthryl chloride. The 10-chloro-9-aza-10-boraphenanthrene **21** (80 mg, 0.374 mmol) was dissolved in 10 mL toluene. Then 2,6-lutidine (1 equiv, 0.374 mmol, 0.043 mL) was added dropwise to the clear solution at room temperature. Colorless solid formation was observed within a minute and continued stirring at room temperature for 16 h. After 2 days the clear supernatant was decanted via syringe and the remaining white precipitate was dried properly to get 0.071 g (67 %) of **22**.

^1H (400MHz, CD_2Cl_2): 8.40 (d, $J_{\text{HH}} = 8.24$ Hz, 1H), 8.34 (d, $J_{\text{HH}} = 8.04$ Hz, 1H), 8.09 (dd, $J_{\text{HH}} = 7.52, 1.08$ Hz, 1H), 8.01 (t, $J_{\text{HH}} = 7.92$ Hz, 1H), 7.73 – 7.69 (m, 1H), 7.41 – 7.35 (m, 4H), 7.25 – 7.22 (m, 2H), 7.21 – 7.17 (m, 1H), 2.90 (s, 6H) ppm; $^{13}\text{C}\{^1\text{H}\}$ (100.6 MHz, CD_2Cl_2): 154.3, 144.5, 141.3, 140.4, 133.1, 131.5, 128.6, 126.4, 124.8, 124.2, 122.6, 122.5, 121.0, 119.1, 19.5 ppm, C attached to the boron was not detected; $^{11}\text{B}\{^1\text{H}\}$ (80.3 MHz, CD_2Cl_2): $\delta = 28.3$ (s, $h_{1/2} = 366.8$ Hz) ppm; m. p. = decomposed above 220 °C.

Compound 23: 10-(pyridine-1-yl)-9-aza-10-boraphenanthryl chloride. ^1H (600 MHz, CD_2Cl_2): 8.77 (br, 2H), 8.31 (d, $J_{\text{HH}} = 8.01$ Hz, 1H), 8.27 (t, $J_{\text{HH}} = 7.83$ Hz, 1H), 8.23 (d, $J_{\text{HH}} = 8.16$ Hz, 1H), 8.13 (dd, $J_{\text{HH}} = 7.47, 1.11$ Hz, 1H), 7.79 (t, $J_{\text{HH}} = 6.60$ Hz, 2H), 7.68 – 7.65 (m, 1H), 7.44 (td, $J_{\text{HH}} = 7.32, 0.84$ Hz, 1H), 7.30 – 7.27 (m, 1H), 7.26 (s, br, 1H), 7.12 (dd, $J_{\text{HH}} = 7.95, 1.11$ Hz, 1H), 7.09 – 7.07 (m, 1H) ppm; $^{13}\text{C}\{^1\text{H}\}$ (150.9 MHz, CD_2Cl_2): 144.9, 142.4, 140.74, 140.71, 132.2, 131.1, 128.5, 127.1, 126.2, 124.1, 122.4, 121.9, 120.2, 118.7 ppm; $^{11}\text{B}\{^1\text{H}\}$ (80.3 MHz, CD_2Cl_2): $\delta = 29.2$ (s, $h_{1/2} = 250.5$ Hz) ppm.

Compound 24: 10,10-bis(pyridine-1-yl)-9-aza-10-boraphenanthryl chloride. The 10-chloro-9-aza-10-boraphenanthrene **21** (30 mg, 0.141 mmol) was dissolved in 2 mL of dry benzene in a Schlenk tube and slowly 1 mL of pyridine was added to it at room temperature. Immediately bright yellow solid was formed which was washed with *n*-pentane and dried under vacuum for 3 h to get 46 mg (88 %). ^1H (600 MHz, CD_2Cl_2): 8.62 – 8.61 (m, 4H), 8.44 (d, $J_{\text{HH}} = 8.04$ Hz, 1H), 8.39 (d, $J_{\text{HH}} = 8.22$ Hz, 1H), 8.23 (d, $J_{\text{HH}} = 7.50$ Hz, 1H), 7.85 (s, br, 1H), 7.80 – 7.77 (m, 1H), 7.76 – 7.73 (m, 1H), 7.57 – 7.54 (m, 1H), 7.46 – 7.43 (m, 1H), 7.35 – 7.33 (m, 4H), 7.29 – 7.27 (m, 2H) ppm; $^{13}\text{C}\{^1\text{H}\}$ (150.9 MHz, CD_2Cl_2): 149.3, 139.7, 138.9, 137.3, 134.4, 132.3, 128.9, 128.7, 127.0, 124.5, 123.2, 122.7, 122.3, 119.2 ppm, C attached to the boron was not observed; $^{11}\text{B}\{^1\text{H}\}$ (80.3 MHz, $\text{C}_6\text{D}_6 + \text{Py}$): $\delta = 8.1$ (s) ppm.

Compound 32: 10-trifluoromethanesulfonato-9-aza-10-boraphenanthrene. The triflate synthesis was carried out in dark. The chloride **21** (0.085 g, 0.398 mmol) was dissolved in 30 mL of 1:1 mixture of *n*-hexane:toluene in a 100 mL Schlenk flask. Silver triflate (AgOTf) (0.105 g, 0.410 mmol, 1.03 equiv, dried under vacuum for 30 min at 40 °C) was dissolved in 2 mL of toluene and then was added to the chloride solution at 0 °C under argon atmosphere. An immediate formation of colorless precipitate was observed. After complete addition of silver triflate solution, the reaction mixture was kept stirring for 4 h at room temperature. Then the colorless precipitate was removed by filtration and the filtrate containing **32** was used for the next step as described for the dehydrochlorination of **21**.

Compound 33: 1,2:3,4:5,6-tris-(2,2'-biphenylene)borazole (TBB). Potassium bis(trimethylsilyl)amide (KHMDs) (0.087 g, 0.438 mmol), dissolved in minimum amount of toluene (~3 mL), was added to the *n*-hexane solution of 10-chloro-9-aza-10-boraphenanthrene **21** (0.085 g, 0.398 mmol) at -50 °C. Next day a colorless solid was formed which was filtered out under air and extracted the solid with toluene. The toluene extract was collected and a white solid was obtained after removal of toluene from the filtrate. This white solid was washed with 20 mL of *n*-hexane and little amount of acetone (1 – 2 mL). Then 0.025 g of pure TBB was recovered after drying under vacuum. Yield: 35 %. m. p. > 401 °C. ¹H (400 MHz, CD₂Cl₂): 8.26 (d, *J*_{HH} = 6.56 Hz, 2H), 7.64 – 7.59 (m, 2H), 7.50 (d, *J*_{HH} = 7.60 Hz, 1H), 7.32 (t, *J*_{HH} = 7.50 Hz, 1H), 7.16 (t, *J*_{HH} = 7.50 Hz, 1H), 7.10 (t, *J*_{HH} = 7.38 Hz, 1H) ppm.; ¹³C{¹H} (100.6 MHz, CD₂Cl₂): 141.1, 140.7, 134.7, 131.8, 127.5, 127.3, 126.3, 126.2, 125.2, 123.7, 123.6 ppm, C directly attached to the boron was not observed; ¹¹B{¹H} (80.3 MHz, CD₂Cl₂): δ = 36 (brs, *h*_{1/2} = 690.1 Hz) ppm; IR (KBr): 3440(w), 3060(m), 1601(m), 1578(m), 1555(m), 1482(m), 1445(m), 1366 (vs, *ν*_{BN}), 1319(m), 1294(m), 1264(m), 1163(m), 1043(m), 785(m), 761(s), 735(s), 687 (m) cm⁻¹; UV-Vis (in dichloromethane): λ (log ε) =

343(4.207), 318 (4.671), 293(4.584), 276(4.665), 254(4.846) nm; MS (EI), m/z: 531 ($[M^{+}]$), 525, 514, 263, 257, 249, 244, 237, 171; HRMS (ESI) for $C_{36}H_{24}B_3N_3$ (M^{+}) [$M + H^{+}$]: 532.229585 amu, calc'd 532.234104 amu, for [$M + H^{+} + MeOH$]: 564.255179 amu, calc'd 564.2589654 amu.

Compound 35: 1,2:3,4:5,6:7,8-tetrakis-(2,2'-biphenylene)-1,3,5,7-tetraza-2,4,6,8-tetraborocane. The crude reaction mixture (15 mg) obtained from the thermolysis reaction of 2-aminobiphenyl and amine-borane complex, was taken in a screw capped glass vial with 2 mL dichloromethane solvent and was sonicated for 15 min. Then the suspension was transferred into a micro tube and centrifuged for 10 min. After that the supernatant was decanted and repeated the sonication with fresh dichloromethane. After six times of consecutive washings with dichloromethane, the remaining insoluble colorless powder was dried under vacuum. IR (KBr): 3442(w), 3059(m), 3021(m), 1603(m), 1577(m), 1553(m), 1494(s), 1483(s), 1446(m), 1434(m), 1380(m), 1362 (vs, ν_{BN}), 1329(m), 1298(m), 1261(m), 752(s), 723(s), 619(m) cm^{-1} ; MS (EI), m/z: 708 ($[M^{+}]$), 354, 177, 168; HRMS (EI) for $C_{48}H_{32}B_4N_4$ [M^{+}]: 708.30259 amu, calc'd 708.299921 amu.

Compound 36: 10-diisopropylamino-9-aza-10-boraphenanthrene. The base lithium diisopropylamide (LDA, 1.8M in THF/heptane/ethylbenzene) (0.191 mL, 0.344 mmol, 1.05 equiv) was added to the 10 mL of *n*-hexane solution of 10-chloro-9-aza-10-boraphenanthrene **21** (0.07 g, 0.328 mmol) which was cooled down to -50 °C. The colorless suspension became faint yellow within few minutes of addition and at room temperature the reaction mixture turned to slightly brown with a precipitation. The volatiles were removed under vacuum leaving a brown solid mixture. The compound **36** was sublimed at 65 °C/ 10^{-3} mbar as a colorless solid (0.031 g). Yield: 34 %. 1H (400 MHz, CD_2Cl_2): 8.26 (d, $J_{HH} = 8.12$ Hz, 1H),

8.15 (d, $J_{\text{HH}} = 7.72$ Hz, 1H), 8.06 (d, $J_{\text{HH}} = 7.76$ Hz, 1H), 7.56 (t, $J_{\text{HH}} = 8.32$ Hz, 1H), 7.38 – 7.35 (m, 1H), 7.26 (t, $J_{\text{HH}} = 8.18$ Hz, 1H), 6.98 (t, $J_{\text{HH}} = 7.76$ Hz, 2H), 6.36 (br, s, 1H), 4.02 (heptet, $J_{\text{HH}} = 6.84$ Hz, 2H), 1.39 (d, $J_{\text{HH}} = 6.84$ Hz, 12H) ppm.; $^{13}\text{C}\{^1\text{H}\}$ (150.9 MHz, CD_2Cl_2): 141.0, 140.7, 134.0, 129.6, 128.5, 125.7, 124.0, 123.1, 121.5, 119.2, 117.8, 46.9, 24.0 ppm, C next to the boron center was not observed; $^{11}\text{B}\{^1\text{H}\}$ (80.3 MHz, CD_2Cl_2): $\delta = 28.4$ (s, $h_{1/2} = 243.2$ Hz) ppm; MS (EI), m/z : 278 [$\text{M}^{+\bullet}$], 263, 221, 178, 151; HRMS (EI) for $\text{C}_{18}\text{H}_{23}\text{BN}_2$ [$\text{M}^{+\bullet}$]: 278.19579 amu, calc'd 278.195430 amu.

Compound 38: 10-(2-furyl)-9-aza-10-boraphenanthrene. Drying of Furan: Furan ($\geq 99\%$), purchased from Sigma-Aldrich, was predried with dry sodium sulfate and distilled over CaH_2 at $48\text{ }^\circ\text{C}$ (oil bath temperature) under argon atmosphere. Argon was bubbled through the distilled furan for 10 min and preserved at low temperature over molecular sieves (4 \AA).

Potassium bis(trimethylsilyl)amide (KHMDs) (0.103 g, 0.515 mmol, 1.1 equivalents of chloroborane **21**) was dissolved in 10 mL of furan and brought to $-60\text{ }^\circ\text{C}$. Then 10-chloro-9-aza-10-boraphenanthrene **21** (100 mg, 0.468 mmol), dissolved in 6 mL of furan separately, was added dropwise to the base solution at $-60\text{ }^\circ\text{C}$. After complete addition of chloride solution to the base, the reaction mixture became opaque. Next day a brown solid was formed. This solid was filtered out under air and filtrate was collected. After removal of furan, brown solid remained. This mixture was purified by chromatography with 4:1 mixture of dichloromethane and *n*-hexane over silica gel to give **38** ($R_f = 0.81$) as colorless solid (0.045 g). Yield: 39%. ^1H (400 MHz, CD_2Cl_2): δ 8.63 (dd, $J_{\text{HH}} = 7.7, 1.1$ Hz, 1H), 8.51 (d, $J_{\text{HH}} = 8.30$ Hz, 1H), 8.44 (dd, $J_{\text{HH}} = 8.1, 0.5$ Hz, 1H), 8.21 (br, s, 1H), 7.84 (d, $J_{\text{HH}} = 1.6$ Hz, 1H), 7.81 – 7.77 (m, 1H), 7.60 – 7.56 (m, 1H), 7.48 – 7.44 (m, 1H), 7.43 (d, $J_{\text{HH}} = 3.4$ Hz, 1H), 7.38 (dd, $J_{\text{HH}} = 7.8, 1.1$ Hz, 1H), 7.30 – 7.26 (m, 1H), 6.64 (dd, $J_{\text{HH}} = 3.4, 1.7$ Hz, 1H)

ppm; $^{13}\text{C}\{^1\text{H}\}$ (150.9 MHz, CD_2Cl_2): 146.7, 139.6, 139.1, 135.3, 131.5, 128.7, 126.6, 124.3, 123.6, 122.8, 122.0, 121.7, 119.5, 111.4 ppm, 2 C's attached to the boron were not observed; $^{11}\text{B}\{^1\text{H}\}$ (80.3 MHz, CD_2Cl_2): $\delta = 30.3$ (s, $h_{1/2} = 287.1$ Hz) ppm; IR (KBr): 3440 (w), 3059 (w), 2960 (m), 2924 (m), 2853 (m), 1606 (m), 1570 (m), 1514 (m), 1491 (m), 1446 (m), 1437(m), 1421(m), 1334 (w), 1324 (w), 1286 (m), 1261 (m), 1223 (m), 1224 (m), 1183 (w), 1153 (w), 1084 (w), 1047 (w), 1014 (w), 931 (w), 878 (w), 802 (w), 752 (m), 727 (m); UV-Vis (in dichloromethane): λ (log ϵ) = 249 (4.03), 268 (3.92), 309 (3.52), 324 (3.58), 338(3.56) nm; HRMS (EI) for $\text{C}_{16}\text{H}_{12}\text{BNO}$ [M^+]: 245.10193 amu, calc'd 245.10119 amu.

Compound 40: 10,10-bis(2-furyl)-9,9-dihydro-9-aza-10-boraphenanthrene. 2.1 equivalents of potassium bis(trimethylsilyl)amide (KHMDS) (0.157 g, 0.787 mmol) was dissolved in 15 mL of furan and brought to -60 °C. Then furan solution of 10-chloro-9-aza-10-boraphenanthrene **21** (0.08 g, 0.375 mmol) (5 mL) was added slowly to the base solution at -60 °C. After complete addition of chloride solution to the base solution, the reaction mixture became slightly yellowish. During warming up the mixture was slightly orange and then next day brown solid formation was observed. This solid was filtered out under air and filtrate was collected. After removal of furan, the remaining brown solid was purified by chromatography with 4:1 mixture of dichloromethane and *n*-hexane over silica gel to give **40** as white solid (0.017 g). [This purification was done very quickly with a small silica column due to its gradual decomposition to **38** in solution.] Yield: 14 %. ^1H (400 MHz, CD_2Cl_2): δ 7.87 (dd, $J_{\text{HH}} = 7.8, 1.0$ Hz, 1H), 7.80 (d, $J_{\text{HH}} = 7.8$ Hz, 1H), 7.47 (dd, $J_{\text{HH}} = 1.8, 0.4$ Hz, 2H), 7.41 (td, $J_{\text{HH}} = 7.6, 1.2$ Hz, 1H), 7.37 – 7.33 (m, 1H), 7.27 – 7.20 (m, 1H), 7.12 (d, $J_{\text{HH}} = 7.7$ Hz, 1H), 6.25 (dd, $J_{\text{HH}} = 3.1, 1.7$ Hz, 2H), 6.08 (dd, $J_{\text{HH}} = 3.0, 0.4$ Hz, 2H), 5.99 (br, s, 2H) ppm; $^{13}\text{C}\{^1\text{H}\}$ (100.6 MHz, CD_2Cl_2): 178.2, 143.8, 135.5, 133.5, 130.9, 129.5, 128.5, 127.8, 127.6, 126.7, 124.0, 123.8, 115.4, 109.8 ppm, C's attached to the boron were not observed;

$^{11}\text{B}\{^1\text{H}\}$ (80.3 MHz, CD_2Cl_2): $\delta = -8.3$ (s, $h_{1/2} = 181.5$ Hz) ppm; MS (EI), m/z : 313 [$\text{M}^{+\bullet}$], 245, 177, 169.

A. Crystallographic Data

Table A1.1 Crystal data and structure refinement for C₁₂H₈BCl (**6**).

Empirical formula	C ₁₂ H ₈ BCl
Formula weight [g mol ⁻¹]	198.44
Temperature [K]	103(2)
Wavelength [Å]	0.71073
Crystal system, space group	Monoclinic, P2 ₁ /c
a [Å]	3.8570(5)
b [Å]	14.0680(17)
c [Å]	17.495(3)
α [°]	90
β [°]	95.237(15)
γ [°]	90
Volume [Å ³]	945.3(2)
Z	4
Calculated density [Mg/m ³]	1.394
Absorption coefficient [mm ⁻¹]	0.350
F(000)	408
Crystal size [mm ³]	0.435 x 0.063 x 0.054
Theta range for data collection [°]	2.90 to 27.65
Limiting indices	-2 ≤ h ≤ 5, -11 ≤ k ≤ 18, -22 ≤ l ≤ 21
Reflections collected / unique	4325 / 2139 [R _(int) = 0.0768]
Completeness to theta = 27.65	98.0 %
Absorption correction	None
Refinement method	Full-matrix least-squares on F ²
Data / restraints / parameters	2139 / 0 / 127
Goodness-of-fit on F ²	0.959
Final R indices [I > 2σ(I)]	R ₁ = 0.0397, wR ₂ = 0.0472 [800 refs]
R indices (all data)	R ₁ = 0.1368, wR ₂ = 0.0573
Largest diff. peak and hole [e.Å ⁻³]	0.221 and -0.261

Table A1.2 Atomic coordinates ($\times 10^4$) and equivalent isotropic displacement parameters ($\text{\AA}^2 \times 10^3$) for $\text{C}_{12}\text{H}_8\text{BCl}$ (**6**). $U(\text{eq})$ is defined as one third of the trace of the orthogonalized U_{ij} tensor.

	x	y	z	U(eq)
Cl(1)	-12(2)	5868(1)	3683(1)	33(1)
C(1)	4161(6)	3720(2)	4408(2)	24(1)
C(2)	5791(6)	2855(2)	4577(2)	25(1)
C(3)	6450(6)	2241(2)	3999(2)	26(1)
C(4)	5532(6)	2459(2)	3229(2)	22(1)
C(4A)	3910(6)	3322(2)	3057(2)	18(1)
C(4B)	2560(6)	3705(2)	2299(2)	19(1)
C(5)	2724(6)	3312(2)	1581(2)	24(1)
C(6)	1217(6)	3807(2)	939(2)	28(1)
C(7)	-386(6)	4673(2)	1019(2)	29(1)
C(8)	-514(6)	5070(2)	1745(2)	24(1)
C(8A)	967(6)	4600(2)	2388(2)	20(1)
B(9)	1318(7)	4822(2)	3251(2)	23(1)
C(9A)	3204(6)	3957(2)	3646(2)	20(1)

Table A2.1 Crystal data and structure refinement for C₃₆H₂₄B₂ (**6a**).

Empirical formula	C ₃₆ H ₂₄ B ₂
Formula weight [g mol ⁻¹]	478.17
Temperature [K]	108(2)
Wavelength [Å]	0.71073
Crystal system, space group	Monoclinic, P2 ₁ /c
a [Å]	17.6344(17)
b [Å]	10.2537(9)
c [Å]	14.1172(13)
α [°]	90
β [°]	103.205(9)
γ [°]	90
Volume [Å ³]	2485.1(4)
Z	4
Calculated density [Mg/m ³]	1.278
Absorption coefficient [mm ⁻¹]	0.071
F(000)	1000
Crystal size [mm ³]	0.27 x 0.24 x 0.18
Theta range for data collection [°]	2.96 to 25.25
Limiting indices	-21 ≤ h ≤ 20, -12 ≤ k ≤ 12, -16 ≤ l ≤ 16
Reflections collected / unique	27172 / 4498 [R _(int) = 0.1124]
Completeness to theta = 25.25	99.8 %
Absorption correction	None
Refinement method	Full-matrix least-squares on F ²
Data / restraints / parameters	4498 / 0 / 343
Goodness-of-fit on F ²	1.133
Final R indices [I > 2σ(I)]	R ₁ = 0.0797, wR ₂ = 0.1691 [3285 refs]
R indices (all data)	R ₁ = 0.1014, wR ₂ = 0.1749
Largest diff. peak and hole [e.Å ⁻³]	0.227 and -0.229

Table A2.2 Atomic coordinates ($\times 10^4$) and equivalent isotropic displacement parameters ($\text{\AA}^2 \times 10^3$) for $\text{C}_{36}\text{H}_{24}\text{B}_2$ (**6a**). $U(\text{eq})$ is defined as one third of the trace of the orthogonalized U_{ij} tensor.

	x	y	z	U(eq)
C(1)	4190(2)	6624(3)	4194(2)	24(1)
C(2)	3626(2)	6944(3)	4725(2)	24(1)
C(3)	3817(2)	7928(3)	5432(2)	27(1)
C(4)	4521(2)	8560(4)	5631(3)	33(1)
C(5)	5075(2)	8223(4)	5111(3)	36(1)
C(6)	4903(2)	7262(4)	4407(2)	32(1)
C(7)	3317(2)	5624(3)	2700(2)	25(1)
C(8)	3199(2)	4615(4)	2012(2)	29(1)
C(9)	3759(2)	3691(4)	1985(2)	34(1)
C(10)	4466(2)	3746(4)	2660(2)	34(1)
C(11)	4598(2)	4706(4)	3361(2)	33(1)
C(12)	4033(2)	5651(3)	3399(2)	25(1)
C(13)	1848(2)	8269(3)	4698(2)	26(1)
C(14)	1072(2)	8627(4)	4644(2)	28(1)
C(15)	511(2)	7668(4)	4576(2)	30(1)
C(16)	703(2)	6353(4)	4575(2)	28(1)
C(16A)	1474(2)	6008(3)	4650(2)	23(1)
C(16B)	1808(2)	4681(3)	4641(2)	24(1)
C(17)	1453(2)	3496(4)	4655(2)	29(1)
C(18)	1882(2)	2361(4)	4643(3)	34(1)
C(19)	2658(2)	2425(4)	4602(2)	31(1)
C(20)	3019(2)	3628(4)	4594(2)	28(1)
C(20A)	2607(2)	4777(3)	4617(2)	23(1)
B(21)	2829(2)	6254(4)	4662(2)	23(1)
C(21A)	2050(2)	6968(3)	4700(2)	22(1)
C(22)	3332(2)	9088(4)	2668(3)	36(1)
C(23)	3186(3)	10412(4)	2552(3)	42(1)
C(24)	2431(3)	10869(4)	2300(3)	46(1)

128 A. Crystallographic Data

C(25)	1807(2)	10017(4)	2162(3)	38(1)
C(25A)	1950(2)	8698(4)	2273(2)	31(1)
C(25B)	1382(2)	7607(4)	2151(2)	28(1)
C(26)	581(2)	7670(4)	1948(2)	36(1)
C(27)	157(2)	6506(4)	1878(2)	39(1)
C(28)	531(2)	5313(4)	2005(2)	35(1)
C(29)	1341(2)	5250(4)	2214(2)	29(1)
C(29A)	1774(2)	6396(4)	2290(2)	28(1)
B(30)	2670(2)	6678(4)	2560(3)	26(1)
C(30A)	2718(2)	8205(4)	2529(2)	28(1)

Table A3.1 Crystal data and structure refinement for $C_{36}H_{27}B_3O_3$ (**8**).

Empirical formula	$C_{36}H_{27}B_3O_3$
Formula weight [$g\ mol^{-1}$]	540.01
Temperature [K]	108(2)
Wavelength [\AA]	0.71073
Crystal system, space group	Triclinic, P-1
a [\AA]	13.0852(5)
b [\AA]	13.3035(6)
c [\AA]	19.6082(7)
α [$^\circ$]	70.466(4)
β [$^\circ$]	74.187(3)
γ [$^\circ$]	61.449(4)
Volume [\AA^3]	2799.41(22)
Z	4
Calculated density [Mg/m^3]	1.281
Absorption coefficient [mm^{-1}]	0.078
F(000)	1128
Crystal size [mm^3]	0.58 x 0.55 x 0.23
Theta range for data collection [$^\circ$]	3.06 to 27.50
Limiting indices	$-16 \leq h \leq 16, -15 \leq k \leq 17, -24 \leq l \leq 25$
Reflections collected / unique	25207 / 12695 [$R_{(int)} = 0.0199$]
Completeness to theta = 27.50	98.6 %
Absorption correction	None
Refinement method	Full-matrix least-squares on F^2
Data / restraints / parameters	12695 / 0 / 757
Goodness-of-fit on F^2	0.882
Final R indices [$I > 2\sigma(I)$]	$R_1 = 0.0360, wR_2 = 0.0789$
R indices (all data)	$R_1 = 0.0591, wR_2 = 0.0821$
Largest diff. peak and hole [$e.\text{\AA}^{-3}$]	0.305 and -0.220

Table A3.2 Atomic coordinates ($\times 10^4$) and equivalent isotropic displacement parameters ($\text{\AA}^2 \times 10^3$) for $\text{C}_{36}\text{H}_{27}\text{B}_3\text{O}_3$ (**8**). $U(\text{eq})$ is defined as one third of the trace of the orthogonalized U_{ij} tensor.

	x	y	z	U(eq)
O(101)	1539(1)	-1730(1)	4026(1)	23(1)
O(103)	-14(1)	191(1)	3927(1)	21(1)
O(105)	-315(1)	-1377(1)	3828(1)	21(1)
B(102)	1139(1)	-565(1)	4019(1)	19(1)
B(104)	-749(1)	-199(1)	3820(1)	20(1)
B(106)	824(1)	-2143(1)	3914(1)	19(1)
C(101)	1940(1)	-96(1)	4153(1)	20(1)
C(102)	3158(1)	-740(1)	4190(1)	21(1)
C(103)	3736(1)	-264(1)	4405(1)	28(1)
C(104)	3150(1)	836(1)	4556(1)	30(1)
C(105)	1969(1)	1485(1)	4502(1)	29(1)
C(106)	1373(1)	1019(1)	4306(1)	24(1)
C(107)	3891(1)	-1893(1)	3986(1)	22(1)
C(108)	3958(1)	-1995(1)	3289(1)	26(1)
C(109)	4704(1)	-3045(1)	3082(1)	31(1)
C(110)	5398(1)	-4008(1)	3571(1)	33(1)
C(111)	5331(1)	-3924(1)	4265(1)	31(1)
C(112)	4585(1)	-2876(1)	4474(1)	27(1)
C(113)	-2039(1)	609(1)	3666(1)	21(1)
C(114)	-2612(1)	1850(1)	3537(1)	22(1)
C(115)	-3769(1)	2435(1)	3393(1)	31(1)
C(116)	-4370(1)	1824(1)	3377(1)	36(1)
C(117)	-3813(1)	616(1)	3486(1)	31(1)
C(118)	-2670(1)	26(1)	3625(1)	26(1)
C(119)	-2063(1)	2622(1)	3517(1)	21(1)
C(120)	-1910(1)	2753(1)	4152(1)	26(1)
C(121)	-1523(1)	3578(1)	4119(1)	28(1)

C(122)	-1284(1)	4275(1)	3458(1)	28(1)
C(123)	-1428(1)	4152(1)	2823(1)	29(1)
C(124)	-1819(1)	3334(1)	2853(1)	26(1)
C(125)	1380(1)	-3463(1)	3883(1)	19(1)
C(126)	810(1)	-4006(1)	3715(1)	22(1)
C(127)	1441(1)	-5169(1)	3648(1)	32(1)
C(128)	2600(1)	-5805(1)	3761(1)	36(1)
C(129)	3166(1)	-5295(1)	3939(1)	29(1)
C(130)	2563(1)	-4140(1)	3994(1)	23(1)
C(131)	-455(1)	-3421(1)	3610(1)	22(1)
C(132)	-1314(1)	-3427(1)	4212(1)	26(1)
C(133)	-2476(1)	-2980(1)	4118(1)	29(1)
C(134)	-2795(1)	-2533(1)	3425(1)	31(1)
C(135)	-1947(1)	-2531(1)	2822(1)	32(1)
C(136)	-786(1)	-2970(1)	2916(1)	27(1)
O(201)	4524(1)	9915(1)	1316(1)	24(1)
O(203)	6489(1)	8516(1)	1131(1)	25(1)
O(205)	4940(1)	8083(1)	1122(1)	22(1)
B(202)	5701(1)	9606(1)	1258(1)	21(1)
B(204)	6134(1)	7754(1)	1045(1)	20(1)
B(206)	4130(1)	9125(1)	1300(1)	20(1)
C(201)	6204(1)	10398(1)	1345(1)	19(1)
C(202)	5536(1)	11494(1)	1528(1)	21(1)
C(203)	6112(1)	12083(1)	1619(1)	29(1)
C(204)	7327(1)	11610(1)	1533(1)	31(1)
C(205)	7989(1)	10545(1)	1345(1)	26(1)
C(206)	7433(1)	9951(1)	1255(1)	22(1)
C(207)	4220(1)	12081(1)	1629(1)	20(1)
C(208)	3576(1)	11960(1)	2319(1)	26(1)
C(209)	2365(1)	12569(1)	2414(1)	28(1)
C(210)	1782(1)	13307(1)	1820(1)	28(1)
C(211)	2410(1)	13425(1)	1129(1)	29(1)
C(212)	3623(1)	12810(1)	1036(1)	25(1)
C(213)	7000(1)	6521(1)	908(1)	19(1)

132 A. Crystallographic Data

C(214)	8240(1)	6086(1)	774(1)	18(1)
C(215)	8914(1)	4903(1)	752(1)	21(1)
C(216)	8405(1)	4171(1)	817(1)	24(1)
C(217)	7192(1)	4601(1)	919(1)	25(1)
C(218)	6508(1)	5752(1)	978(1)	23(1)
C(219)	8874(1)	6840(1)	614(1)	19(1)
C(220)	9763(1)	6523(1)	1012(1)	23(1)
C(221)	10405(1)	7183(1)	833(1)	26(1)
C(222)	10163(1)	8169(1)	256(1)	26(1)
C(223)	9282(1)	8498(1)	-146(1)	25(1)
C(224)	8646(1)	7833(1)	32(1)	22(1)
C(225)	2796(1)	9435(1)	1540(1)	19(1)
C(226)	2252(1)	8698(1)	1618(1)	18(1)
C(227)	1079(1)	9031(1)	1934(1)	22(1)
C(228)	434(1)	10080(1)	2152(1)	25(1)
C(229)	954(1)	10814(1)	2073(1)	25(1)
C(230)	2118(1)	10486(1)	1775(1)	22(1)
C(231)	2841(1)	7587(1)	1360(1)	19(1)
C(232)	3208(1)	7617(1)	621(1)	23(1)
C(233)	3666(1)	6597(1)	380(1)	29(1)
C(234)	3765(1)	5542(1)	868(1)	32(1)
C(235)	3412(1)	5494(1)	1605(1)	31(1)
C(236)	2950(1)	6516(1)	1848(1)	25(1)

Table A4.1 Crystal data and structure refinement for C₁₇H₁₃BN₄ (**9**).

Empirical formula	C ₁₇ H ₁₃ BN ₄
Formula weight [g mol ⁻¹]	284.12
Temperature [K]	113(2)
Wavelength [Å]	0.71073
Crystal system, space group	Triclinic, P-1
a [Å]	9.7657(3)
b [Å]	17.5892(8)
c [Å]	18.4303(9)
α [°]	68.734(4)
β [°]	89.620(3)
γ [°]	81.217(3)
Volume [Å ³]	2911.5(2)
Z	8
Calculated density [Mg/m ³]	1.296
Absorption coefficient [mm ⁻¹]	0.079
F(000)	1184
Crystal size [mm ³]	0.36 x 0.32 x 0.21
Theta range for data collection [°]	2.64 to 25.25
Limiting indices	-8 ≤ h ≤ 11, -20 ≤ k ≤ 21, -22 ≤ l ≤ 22
Reflections collected / unique	24852 / 10505 [R _(int) = 0.0427]
Completeness to theta = 25.25	99.5 %
Absorption correction	None
Refinement method	Full-matrix least-squares on F ²
Data / restraints / parameters	10505 / 0 / 793
Goodness-of-fit on F ²	0.819
Final R indices [I > 2σ(I)]	R ₁ = 0.0380, wR ₂ = 0.0640 [5174 refs]
R indices (all data)	R ₁ = 0.0906, wR ₂ = 0.0692
Largest diff. peak and hole [e.Å ⁻³]	0.256 and -0.184

Table A4.2 Atomic coordinates ($\times 10^4$) and equivalent isotropic displacement parameters ($\text{\AA}^2 \times 10^3$) for $\text{C}_{17}\text{H}_{13}\text{BN}_4$ (**9**). $U(\text{eq})$ is defined as one third of the trace of the orthogonalized U_{ij} tensor.

	x	y	z	U(eq)
N(11)	3505(1)	8621(1)	5659(1)	35(1)
N(12)	3153(2)	8641(1)	6270(1)	36(1)
N(13)	2713(2)	8673(1)	6832(1)	80(1)
N(14)	4948(1)	8457(1)	4614(1)	25(1)
C(11)	6498(2)	9342(1)	5782(1)	31(1)
C(12)	7609(2)	9443(1)	6190(1)	33(1)
C(13)	8452(2)	8755(1)	6701(1)	33(1)
C(14)	8213(2)	7966(1)	6807(1)	32(1)
C(14A)	7122(2)	7871(1)	6385(1)	27(1)
C(14B)	6684(2)	7096(1)	6410(1)	30(1)
C(15)	7348(2)	6286(1)	6794(1)	41(1)
C(16)	6758(2)	5640(1)	6751(1)	47(1)
C(17)	5502(2)	5785(1)	6337(1)	43(1)
C(18)	4850(2)	6590(1)	5946(1)	35(1)
C(18A)	5434(2)	7254(1)	5966(1)	28(1)
C(19A)	6229(2)	8562(1)	5868(1)	26(1)
B(19)	5003(2)	8240(1)	5538(1)	28(1)
C(110)	6037(2)	8673(1)	4180(1)	30(1)
C(111)	6015(2)	8785(1)	3404(1)	36(1)
C(112)	4862(2)	8672(1)	3055(1)	36(1)
C(113)	3749(2)	8445(1)	3502(1)	37(1)
C(114)	3817(2)	8345(1)	4273(1)	32(1)
N(21)	11364(2)	6682(1)	3777(1)	57(1)
N(22)	12445(2)	6247(1)	4060(1)	48(1)
N(23)	13496(2)	5851(2)	4284(1)	87(1)
N(24)	8850(2)	6701(1)	4043(1)	31(1)

C(21)	9651(2)	8597(1)	3549(1)	33(1)
C(22)	9432(2)	9358(1)	3625(1)	35(1)
C(23)	9608(2)	9415(1)	4349(1)	34(1)
C(24)	10032(2)	8710(1)	4999(1)	28(1)
C(24A)	10247(2)	7950(1)	4919(1)	24(1)
C(24B)	10667(2)	7121(1)	5536(1)	26(1)
C(25)	11059(2)	6939(1)	6310(1)	29(1)
C(26)	11399(2)	6119(1)	6798(1)	36(1)
C(27)	11377(2)	5496(1)	6520(1)	43(1)
C(28)	11007(2)	5677(1)	5740(1)	45(1)
C(28A)	10644(2)	6496(1)	5233(1)	32(1)
C(29A)	10037(2)	7879(1)	4193(1)	26(1)
B(29)	10269(2)	6922(2)	4309(1)	36(1)
C(210)	7856(2)	6461(1)	4546(1)	37(1)
C(211)	6608(2)	6333(1)	4310(1)	42(1)
C(212)	6359(2)	6460(1)	3537(1)	40(1)
C(213)	7363(2)	6713(1)	3021(1)	40(1)
C(214)	8594(2)	6829(1)	3289(1)	36(1)
N(31)	9765(2)	3165(1)	1344(1)	52(1)
N(32)	10799(2)	3420(1)	1105(1)	41(1)
N(33)	11814(2)	3655(2)	917(1)	82(1)
N(34)	7261(2)	3291(1)	1014(1)	34(1)
C(31)	8915(2)	1327(1)	1460(1)	34(1)
C(32)	9028(2)	582(1)	1346(1)	37(1)
C(33)	9194(2)	562(1)	604(1)	39(1)
C(34)	9288(2)	1286(1)	-24(1)	35(1)
C(34A)	9170(2)	2026(1)	94(1)	30(1)
C(34B)	9235(2)	2857(1)	-490(1)	32(1)
C(35)	9496(2)	3079(1)	-1277(1)	39(1)
C(36)	9522(2)	3902(2)	-1722(1)	46(1)
C(37)	9304(2)	4498(2)	-1390(1)	48(1)
C(38)	9051(2)	4273(2)	-601(1)	46(1)
C(38A)	9008(2)	3449(1)	-141(1)	37(1)
C(39A)	8954(2)	2058(1)	839(1)	32(1)

136 A. Crystallographic Data

B(39)	8784(2)	3001(2)	768(1)	37(1)
C(310)	6190(2)	3607(1)	486(1)	47(1)
C(311)	4884(2)	3838(2)	689(1)	59(1)
C(312)	4666(2)	3738(2)	1456(1)	53(1)
C(313)	5752(2)	3398(1)	1998(1)	44(1)
C(314)	7029(2)	3178(1)	1762(1)	37(1)
N(41)	2805(1)	1404(1)	-654(1)	32(1)
N(42)	2465(2)	1395(1)	-1271(1)	37(1)
N(43)	2032(2)	1372(1)	-1832(1)	80(1)
N(44)	4151(1)	1550(1)	393(1)	23(1)
C(41)	3057(2)	3432(1)	-926(1)	32(1)
C(42)	3248(2)	4237(1)	-1346(1)	39(1)
C(43)	4382(2)	4388(1)	-1804(1)	40(1)
C(44)	5332(2)	3736(1)	-1850(1)	34(1)
C(44A)	5135(2)	2932(1)	-1434(1)	26(1)
C(44B)	5994(2)	2151(1)	-1408(1)	25(1)
C(45)	7138(2)	2058(1)	-1845(1)	30(1)
C(46)	7807(2)	1269(1)	-1736(1)	33(1)
C(47)	7342(2)	582(1)	-1212(1)	32(1)
C(48)	6187(2)	678(1)	-788(1)	29(1)
C(48A)	5493(2)	1460(1)	-878(1)	24(1)
C(49A)	3995(2)	2765(1)	-959(1)	25(1)
B(49)	4098(2)	1779(1)	-531(1)	26(1)
C(410)	2963(2)	1601(1)	756(1)	31(1)
C(411)	2939(2)	1492(1)	1527(1)	37(1)
C(412)	4170(2)	1318(1)	1958(1)	36(1)
C(413)	5385(2)	1267(1)	1585(1)	42(1)
C(414)	5349(2)	1385(1)	807(1)	33(1)

Table A5.1 Crystal data and structure refinement for C₂₁H₂₁BN₄ (**10**).

Empirical formula	C ₂₁ H ₂₁ BN ₄
Formula weight [g mol ⁻¹]	340.23
Temperature [K]	110(2)
Wavelength [Å]	0.71073
Crystal system, space group	Monoclinic, P2 ₁ /c
a [Å]	10.7761(5)
b [Å]	13.7559(7)
c [Å]	12.5533(5)
α [°]	90
β [°]	96.300(4)
γ [°]	90
Volume [Å ³]	1849.60(15)
Z	4
Calculated density [Mg/m ³]	1.222
Absorption coefficient [mm ⁻¹]	0.073
F(000)	720
Crystal size [mm ³]	0.52 x 0.43 x 0.41
Theta range for data collection [°]	2.96 to 25.24
Limiting indices	-12 ≤ h ≤ 12, -15 ≤ k ≤ 16, -14 ≤ l ≤ 15
Reflections collected / unique	9125 / 3300 [R _(int) = 0.0218]
Completeness to theta = 25.24	98.7 %
Absorption correction	None
Refinement method	Full-matrix least-squares on F ²
Data / restraints / parameters	3300 / 0 / 238
Goodness-of-fit on F ²	0.945
Final R indices [I > 2σ(I)]	R ₁ = 0.0351, wR ₂ = 0.0855 [2449 refs]
R indices (all data)	R ₁ = 0.0504, wR ₂ = 0.0890
Largest diff. peak and hole [e.Å ⁻³]	0.215 and -0.176

Table A5.2 Atomic coordinates ($\times 10^4$) and equivalent isotropic displacement parameters ($\text{\AA}^2 \times 10^3$) for $\text{C}_{21}\text{H}_{21}\text{BN}_4$ (**10**). $U(\text{eq})$ is defined as one third of the trace of the orthogonalized U_{ij} tensor.

	x	y	z	$U(\text{eq})$
B(1)	3152(1)	7485(1)	8746(1)	22(1)
N(1)	4247(1)	7660(1)	8067(1)	27(1)
N(2)	4691(1)	7006(1)	7590(1)	28(1)
N(3)	5178(1)	6444(1)	7117(1)	49(1)
C(1)	2160(1)	6000(1)	9355(1)	24(1)
C(2)	3258(1)	6564(1)	9544(1)	23(1)
C(3)	4174(1)	6272(1)	10350(1)	27(1)
C(4)	4003(1)	5446(1)	10955(1)	31(1)
C(5)	2916(1)	4905(1)	10764(1)	33(1)
C(6)	1989(1)	5175(1)	9960(1)	29(1)
C(7)	1295(1)	6425(1)	8475(1)	23(1)
C(8)	1812(1)	7274(1)	8074(1)	22(1)
C(9)	1142(1)	7767(1)	7229(1)	25(1)
C(10)	-23(1)	7423(1)	6791(1)	29(1)
C(11)	-524(1)	6592(1)	7199(1)	31(1)
C(12)	130(1)	6087(1)	8039(1)	28(1)
N(4)	3074(1)	8484(1)	9399(1)	20(1)
C(13)	3497(1)	9338(1)	9068(1)	23(1)
C(14)	3286(1)	10197(1)	9577(1)	24(1)
C(15)	2613(1)	10216(1)	10460(1)	19(1)
C(16)	2211(1)	9317(1)	10803(1)	24(1)
C(17)	2445(1)	8485(1)	10267(1)	24(1)
C(18)	2267(1)	11144(1)	11018(1)	23(1)
C(19)	2790(1)	11104(1)	12208(1)	31(1)
C(20)	2779(1)	12052(1)	10515(1)	30(1)
C(21)	830(1)	11205(1)	10908(1)	28(1)

Table A6.1 Crystal data and structure refinement for C₁₅H₁₈BNOSi (**15**).

Empirical formula	C ₁₅ H ₁₈ BNOSi
Formula weight [g mol ⁻¹]	267.20
Temperature [K]	173(2)
Wavelength [Å]	0.71073
Crystal system, space group	Monoclinic, P2 ₁ /n
a [Å]	15.288(2)
b [Å]	5.8962(5)
c [Å]	16.276(2)
α [°]	90
β [°]	94.042(11)
γ [°]	90
Volume [Å ³]	1463.5(3)
Z	4
Calculated density [Mg/m ³]	1.213
Absorption coefficient [mm ⁻¹]	0.151
F(000)	568
Crystal size [mm ³]	0.40 x 0.10 x 0.10
Theta range for data collection [°]	2.67 to 27.10
Limiting indices	-19 ≤ h ≤ 19, -7 ≤ k ≤ 7, -20 ≤ l ≤ 20
Reflections collected / unique	21898 / 3229 [R _(int) = 0.0898]
Completeness to theta = 27.10	99.9 %
Absorption correction	None
Refinement method	Full-matrix least-squares on F ²
Data / restraints / parameters	3229 / 0 / 244
Goodness-of-fit on F ²	1.233
Final R indices [I > 2σ(I)]	R ₁ = 0.0597, wR ₂ = 0.1169
R indices (all data)	R ₁ = 0.0751, wR ₂ = 0.1231
Largest diff. peak and hole [e.Å ⁻³]	0.335 and -0.261

Table A6.2 Atomic coordinates ($\times 10^4$) and equivalent isotropic displacement parameters ($\text{\AA}^2 \times 10^3$) for $\text{C}_{15}\text{H}_{18}\text{BNOSi}$ (**15**). $U(\text{eq})$ is defined as one third of the trace of the orthogonalized U_{ij} tensor.

	x	y	z	$U(\text{eq})$
C(1)	8782(2)	-1882(4)	1073(2)	37(1)
C(2)	6793(2)	-1376(4)	805(2)	33(1)
C(3)	7860(2)	2202(4)	1767(2)	37(1)
C(11)	6203(1)	4846(4)	-1028(1)	28(1)
C(12)	5285(2)	4777(5)	-1084(2)	35(1)
C(13)	4806(2)	6446(5)	-1496(2)	39(1)
C(14)	5229(2)	8227(5)	-1861(2)	37(1)
C(15)	6135(2)	8281(4)	-1820(1)	32(1)
C(16)	6650(1)	6611(4)	-1405(1)	25(1)
C(17)	7620(1)	6649(4)	-1360(1)	24(1)
C(18)	8087(2)	8348(4)	-1750(1)	31(1)
C(19)	8995(2)	8352(4)	-1697(2)	34(1)
C(20)	9464(2)	6669(5)	-1261(2)	34(1)
C(21)	9018(1)	4987(5)	-879(1)	31(1)
C(22)	8094(1)	4939(4)	-915(1)	25(1)
N(1)	6672(1)	3171(3)	-576(1)	30(1)
B(1)	7601(2)	3099(4)	-453(1)	26(1)
Si(1)	7865(1)	138(1)	899(1)	24(1)
O(1)	8029(1)	1553(3)	56(1)	33(1)

Table A7.1 Crystal data and structure refinement for C₂₄H₂₀B₂N₂ (**17**).

Empirical formula	C ₂₄ H ₂₀ B ₂ N ₂
Formula weight [g mol ⁻¹]	358.04
Temperature [K]	173(2)
Wavelength [Å]	0.71073
Crystal system, space group	Orthorhombic, Pbc _a
a [Å]	6.6199(2)
b [Å]	14.9242(6)
c [Å]	18.4745(7)
α [°]	90
β [°]	90
γ [°]	90
Volume [Å ³]	1825.22(11)
Z	4
Calculated density [Mg/m ³]	1.303
Absorption coefficient [mm ⁻¹]	0.075
F(000)	752
Crystal size [mm ³]	0.3 x 0.2 x 0.3
Theta range for data collection [°]	2.20 to 32.27
Limiting indices	-9 ≤ h ≤ 9, -22 ≤ k ≤ 21, -27 ≤ l ≤ 23
Reflections collected / unique	69624 / 3224 [R _(int) = 0.0324]
Completeness to theta = 27.10	99.7 %
Absorption correction	Empirical
Refinement method	Full-matrix least-squares on F ²
Data / restraints / parameters	3224 / 0 / 132
Goodness-of-fit on F ²	1.121
Final R indices [I > 2σ(I)]	R ₁ = 0.0527, wR ₂ = 0.1310
R indices (all data)	R ₁ = 0.0725, wR ₂ = 0.1483
Largest diff. peak and hole [e.Å ⁻³]	0.483 and -0.214

Table A7.2 Atomic coordinates ($\times 10^4$) and equivalent isotropic displacement parameters ($\text{\AA}^2 \times 10^3$) for $\text{C}_{24}\text{H}_{20}\text{B}_2\text{N}_2$ (**17**). $U(\text{eq})$ is defined as one third of the trace of the orthogonalized U_{ij} tensor.

	x	y	z	$U(\text{eq})$
B(1)	6448(2)	398(1)	5023(1)	20(1)
N(1)	4072(1)	638(1)	5081(1)	22(1)
C(1)	7654(2)	911(1)	4389(1)	21(1)
C(2)	7486(2)	933(1)	3637(1)	27(1)
C(3)	8750(2)	1480(1)	3220(1)	31(1)
C(4)	10187(1)	2018(1)	3555(1)	31(1)
C(5)	10398(1)	2008(1)	4303(1)	25(1)
C(6)	9154(2)	1454(1)	4714(1)	20(1)
C(7)	9191(2)	1326(1)	5507(1)	20(1)
C(8)	10432(2)	1753(1)	6009(1)	25(1)
C(9)	10296(2)	1512(1)	6733(1)	30(1)
C(10)	8950(2)	854(1)	6952(1)	32(1)
C(11)	7668(2)	446(1)	6448(1)	28(1)
C(12)	7750(2)	681(1)	5721(1)	21(1)

Table A8.1 Crystal data and structure refinement for C₂₅H₂₂BClN₃ (**24**).

Empirical formula	C ₂₅ H ₂₂ BClN ₃
Formula weight [g mol ⁻¹]	410.72
Temperature [K]	173(2)
Wavelength [Å]	0.71073
Crystal system, space group	Triclinic, P-1
a [Å]	8.6073(10)
b [Å]	9.0504(12)
c [Å]	15.7240(19)
α [°]	82.847(10)
β [°]	87.678(10)
γ [°]	61.321(9)
Volume [Å ³]	1066.0(2)
Z	2
Calculated density [Mg/m ³]	1.280
Absorption coefficient [mm ⁻¹]	0.196
F(000)	430
Crystal size [mm ³]	0.4 x 0.2 x 0.2
Theta range for data collection [°]	4.81 to 29.17
Limiting indices	-11 ≤ h ≤ 11, -12 ≤ k ≤ 12, -21 ≤ l ≤ 21
Reflections collected / unique	19479 / 5728 [R _(int) = 0.0518]
Completeness to theta = 29.17	99.1 %
Absorption correction	None
Refinement method	Full-matrix least-squares on F ²
Data / restraints / parameters	5728 / 0 / 343
Goodness-of-fit on F ²	1.125
Final R indices [I > 2σ(I)]	R ₁ = 0.0507, wR ₂ = 0.1058
R indices (all data)	R ₁ = 0.0658, wR ₂ = 0.1115
Largest diff. peak and hole [e.Å ⁻³]	0.301 and -0.281

Table A8.2 Atomic coordinates ($\times 10^4$) and equivalent isotropic displacement parameters ($\text{\AA}^2 \times 10^3$) for $\text{C}_{25}\text{H}_{22}\text{BClN}_3$ (**24**). $U(\text{eq})$ is defined as one third of the trace of the orthogonalized U_{ij} tensor.

	x	y	z	$U(\text{eq})$
C(01)	972(3)	598(4)	366(1)	52(1)
C(02)	-699(3)	1716(3)	15(1)	53(1)
C(03)	1660(3)	-1106(3)	353(1)	51(1)
C(11)	2784(2)	11723(2)	2316(1)	24(1)
C(12)	1999(3)	13504(2)	2220(1)	33(1)
C(13)	2585(3)	14356(3)	1616(1)	44(1)
C(14)	3956(3)	13454(3)	1085(1)	47(1)
C(15)	4711(2)	11713(3)	1159(1)	37(1)
C(16)	4159(2)	10793(2)	1768(1)	26(1)
C(17)	4917(2)	8935(2)	1834(1)	25(1)
C(18)	6125(2)	7995(3)	1227(1)	34(1)
C(19)	6862(3)	6251(3)	1292(1)	42(1)
C(20)	6401(3)	5383(3)	1949(1)	43(1)
C(21)	5172(2)	6291(2)	2538(1)	35(1)
C(22)	4424(2)	8057(2)	2508(1)	25(1)
C(31)	5407(2)	7436(2)	4389(1)	31(1)
C(32)	6045(2)	7152(2)	5217(1)	39(1)
C(33)	4929(3)	8013(2)	5841(1)	38(1)
C(34)	3181(3)	9160(2)	5616(1)	37(1)
C(35)	2622(2)	9438(2)	4775(1)	30(1)
C(41)	1318(2)	7348(2)	3741(1)	25(1)
C(42)	98(2)	6800(2)	3628(1)	29(1)
C(43)	-1023(2)	7481(2)	2917(1)	30(1)
C(44)	-957(2)	8750(3)	2358(1)	35(1)
C(45)	269(2)	9262(2)	2506(1)	30(1)
B(1)	2986(2)	9086(2)	3176(1)	23(1)

Cl(1)	9002(1)	3483(1)	4117(1)	33(1)
N(1)	2189(2)	10933(2)	2943(1)	27(1)
N(31)	3715(2)	8582(2)	4166(1)	22(1)
N(41)	1414(2)	8552(2)	3183(1)	21(1)

Table A9.1 Crystal data and structure refinement for C₂₄H₁₈B₂N₂O (**31**).

Empirical formula	C ₂₄ H ₁₈ B ₂ N ₂ O
Formula weight [g mol ⁻¹]	372.02
Temperature [K]	173(2)
Wavelength [Å]	0.71073
Crystal system, space group	Monoclinic, P2 ₁ /c
a [Å]	14.1998(19)
b [Å]	5.5331(4) A
c [Å]	27.016(4)
α [°]	90
β [°]	120.079(9)
γ [°]	90
Volume [Å ³]	1836.8(4)
Z	4
Calculated density [Mg/m ³]	1.345
Absorption coefficient [mm ⁻¹]	0.081
F(000)	776
Crystal size [mm ³]	0.5 x 0.1 x 0.05
Theta range for data collection [°]	4.55 to 26.37
Limiting indices	-17 ≤ h ≤ 17, -6 ≤ k ≤ 6, -33 ≤ l ≤ 33
Reflections collected / unique	25108 / 3721 [R _(int) = 0.0894]
Completeness to theta = 26.37	99.5 %
Absorption correction	None
Refinement method	Full-matrix least-squares on F ²
Data / restraints / parameters	3721 / 0 / 262
Goodness-of-fit on F ²	1.138
Final R indices [I > 2σ(I)]	R ₁ = 0.0606, wR ₂ = 0.1065
R indices (all data)	R ₁ = 0.0878, wR ₂ = 0.1152
Largest diff. peak and hole [e.Å ⁻³]	0.187 and -0.193

Table A9.2 Atomic coordinates ($\times 10^4$) and equivalent isotropic displacement parameters ($\text{\AA}^2 \times 10^3$) for $\text{C}_{24}\text{H}_{18}\text{B}_2\text{N}_2\text{O}$ (**31**). $U(\text{eq})$ is defined as one third of the trace of the orthogonalized U_{ij} tensor.

	x	y	z	$U(\text{eq})$
C(2)	2170(2)	-2336(4)	-1608(1)	25(1)
C(3)	1376(2)	-800(4)	-1604(1)	25(1)
C(4)	985(2)	-1290(4)	-1197(1)	24(1)
C(5)	1363(2)	-3336(4)	-836(1)	24(1)
C(7)	2459(2)	-1962(4)	-2031(1)	28(1)
C(8)	2013(2)	-119(4)	-2423(1)	32(1)
C(9)	1259(2)	1437(4)	-2404(1)	34(1)
C(10)	943(2)	1089(4)	-2003(1)	30(1)
C(11)	206(2)	175(4)	-1165(1)	30(1)
C(12)	-201(2)	-383(5)	-811(1)	34(1)
C(13)	148(2)	-2459(4)	-476(1)	32(1)
C(14)	921(2)	-3911(4)	-490(1)	29(1)
C(31)	5347(2)	-7879(4)	-1598(1)	25(1)
C(36)	6235(2)	-6263(4)	-1333(1)	24(1)
C(37)	6241(2)	-4317(4)	-959(1)	25(1)
C(42)	5370(2)	-4101(4)	-848(1)	27(1)
C(38)	7097(2)	-2637(4)	-706(1)	29(1)
C(39)	7109(2)	-855(4)	-348(1)	35(1)
C(40)	6276(2)	-683(4)	-222(1)	39(1)
C(41)	5419(2)	-2285(4)	-473(1)	36(1)
C(32)	5340(2)	-9735(4)	-1949(1)	31(1)
C(33)	6207(2)	-10063(4)	-2037(1)	33(1)
C(34)	7093(2)	-8515(4)	-1778(1)	33(1)
C(35)	7103(2)	-6644(4)	-1435(1)	30(1)
B(1)	2669(2)	-4393(4)	-1160(1)	26(1)
B(20)	4400(2)	-5856(5)	-1150(1)	27(1)

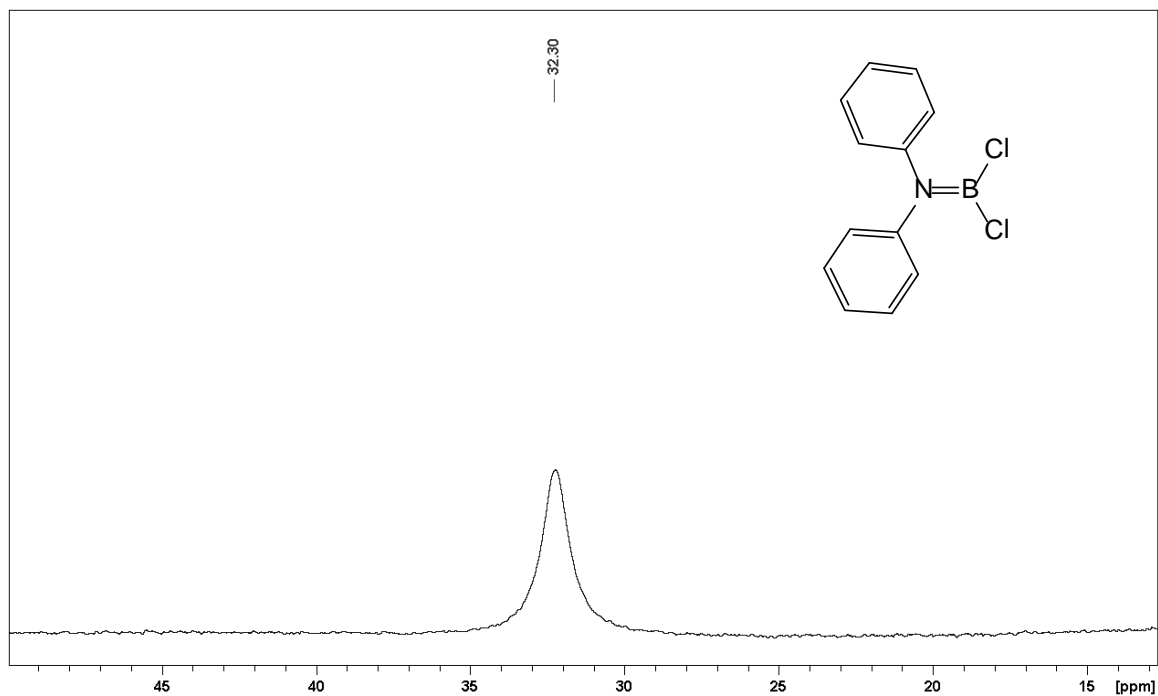
148 A. Crystallographic Data

N(6)	2187(1)	-4767(3)	-818(1)	27(1)
N(21)	4465(1)	-7603(3)	-1510(1)	28(1)
O(1)	3503(1)	-5878(3)	-1080(1)	33(1)

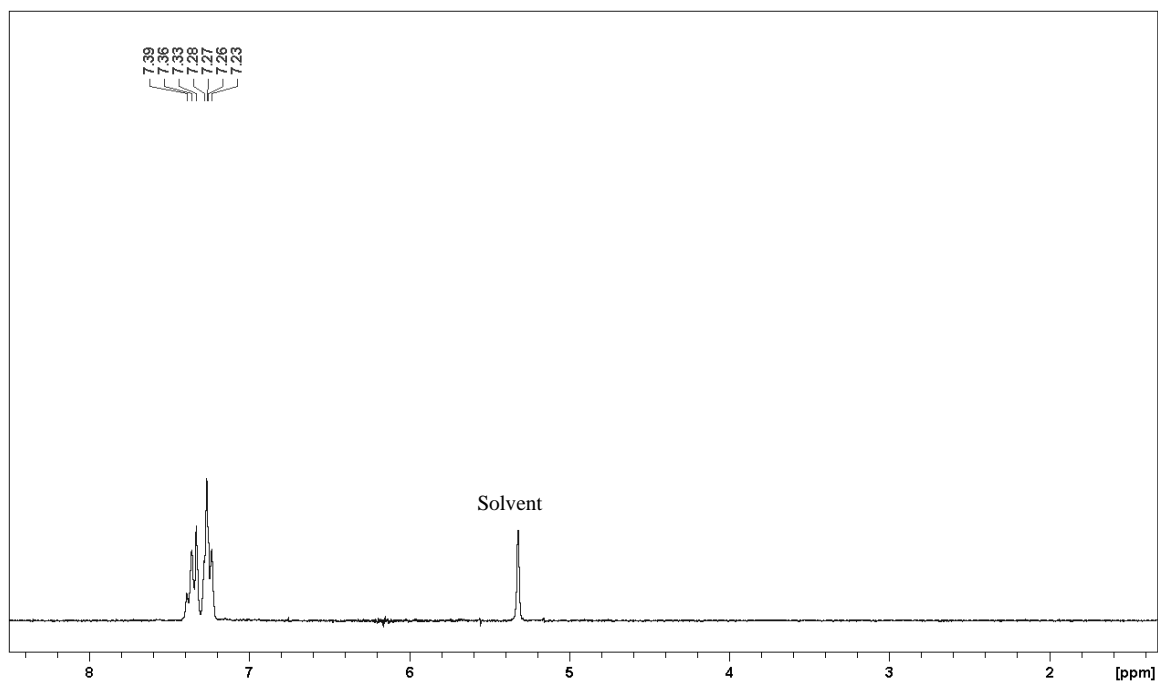
B. Selected NMR Spectra

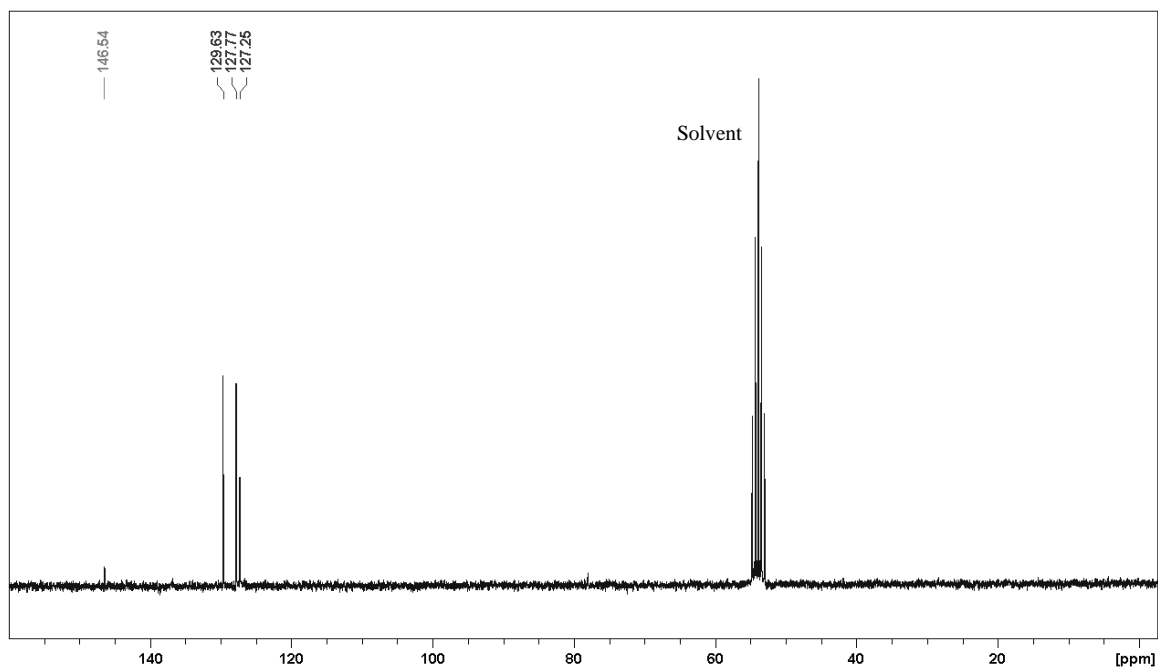
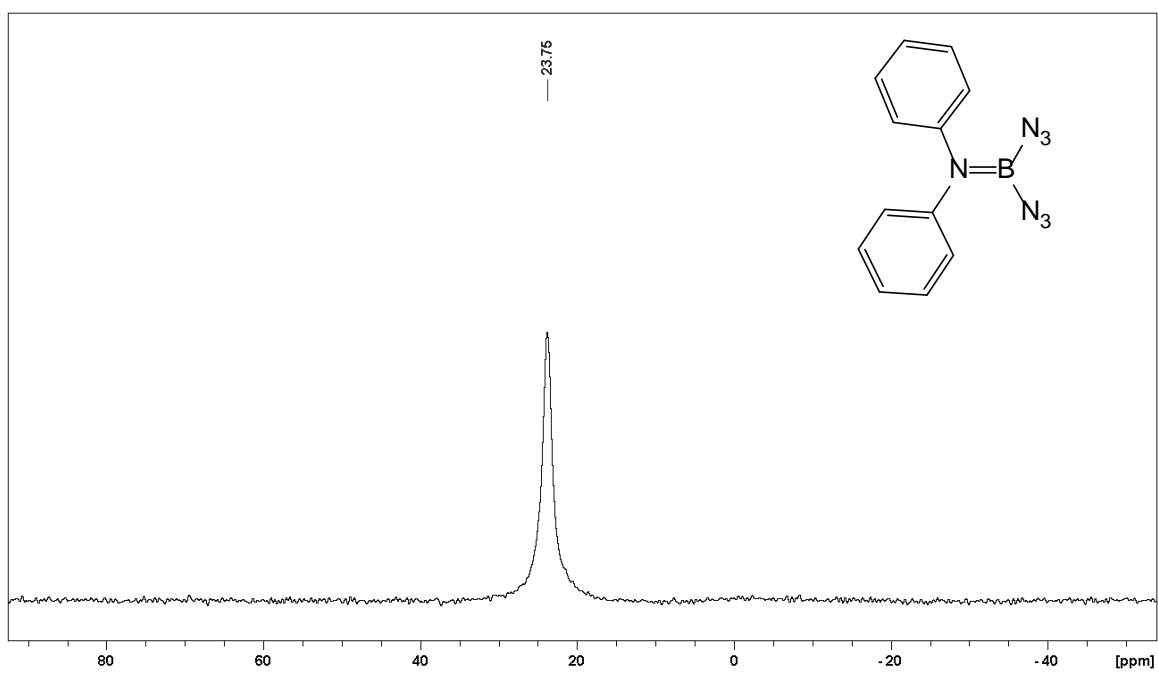
Compound 1 in CD_2Cl_2

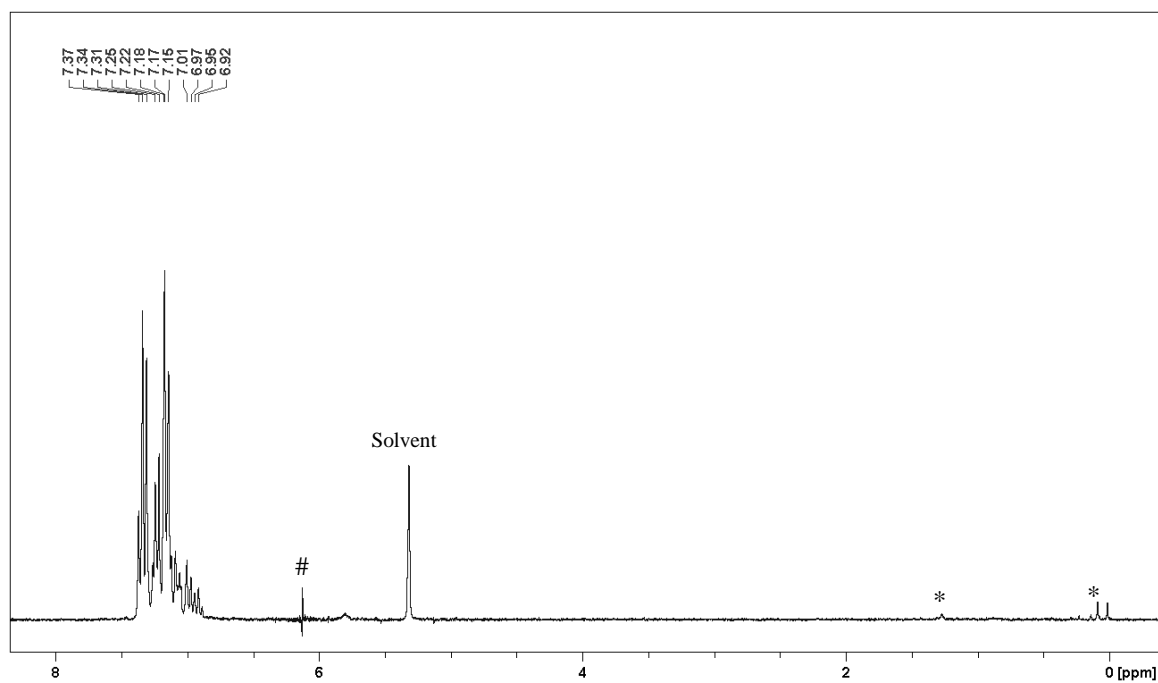
$^{11}\text{B}\{^1\text{H}\}$ (80.3 Mhz, $h_{\nu/2} = 77.7$ Hz)



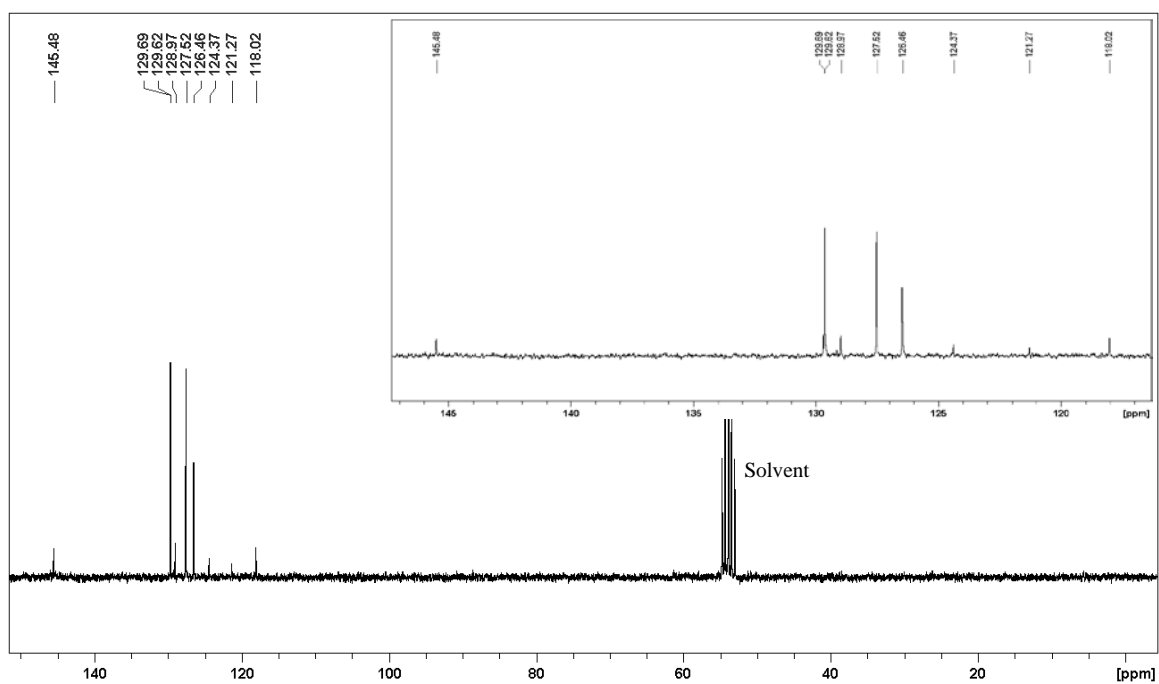
^1H (250 MHz)

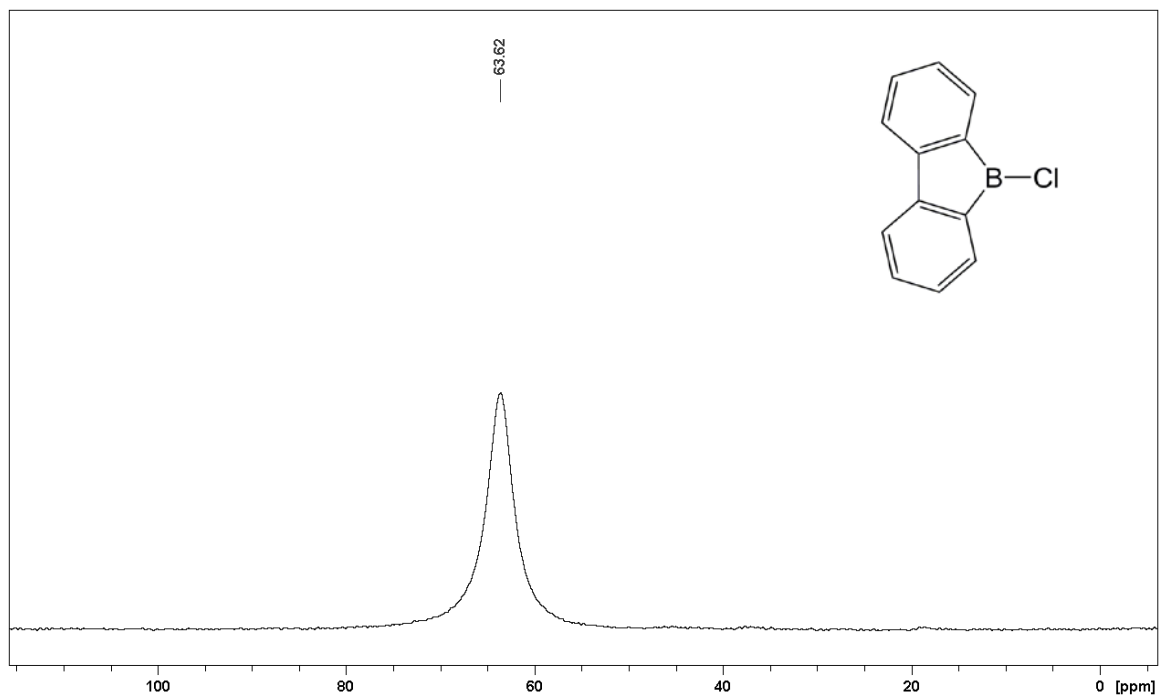
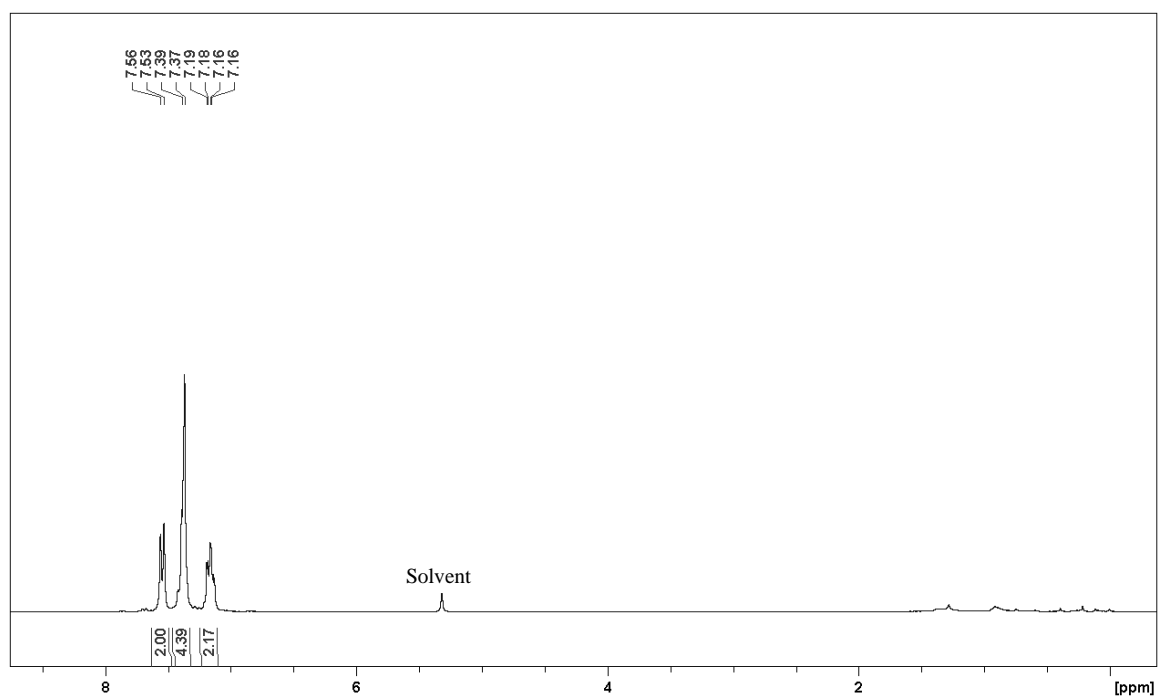


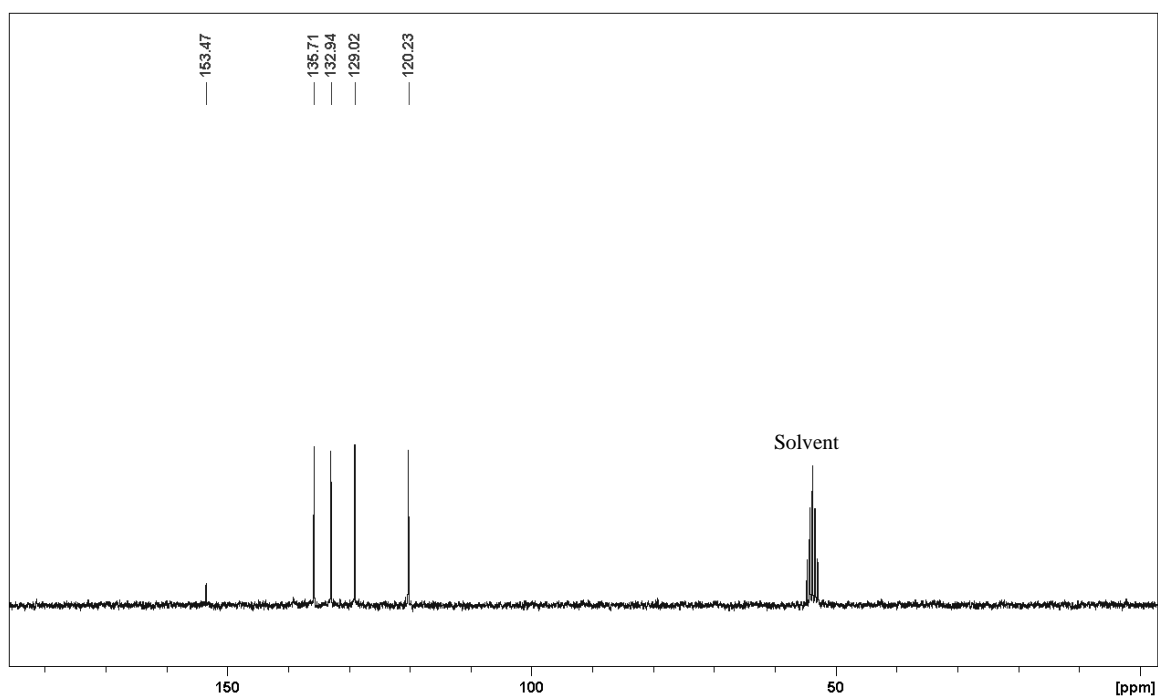
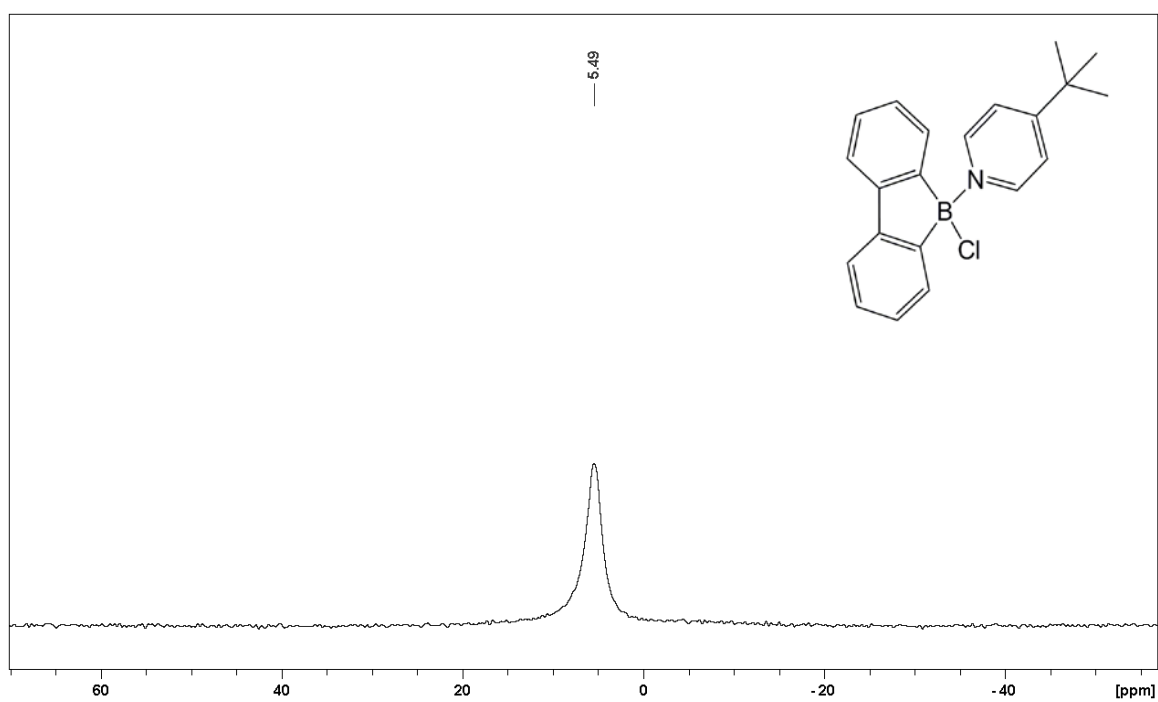
$^{13}\text{C}\{^1\text{H}\}$ (62.9 MHz)Compound 2 in CD_2Cl_2 $^{11}\text{B}\{^1\text{H}\}$ (80.3 MHz, $h_{1/2} = 115.5$ Hz)

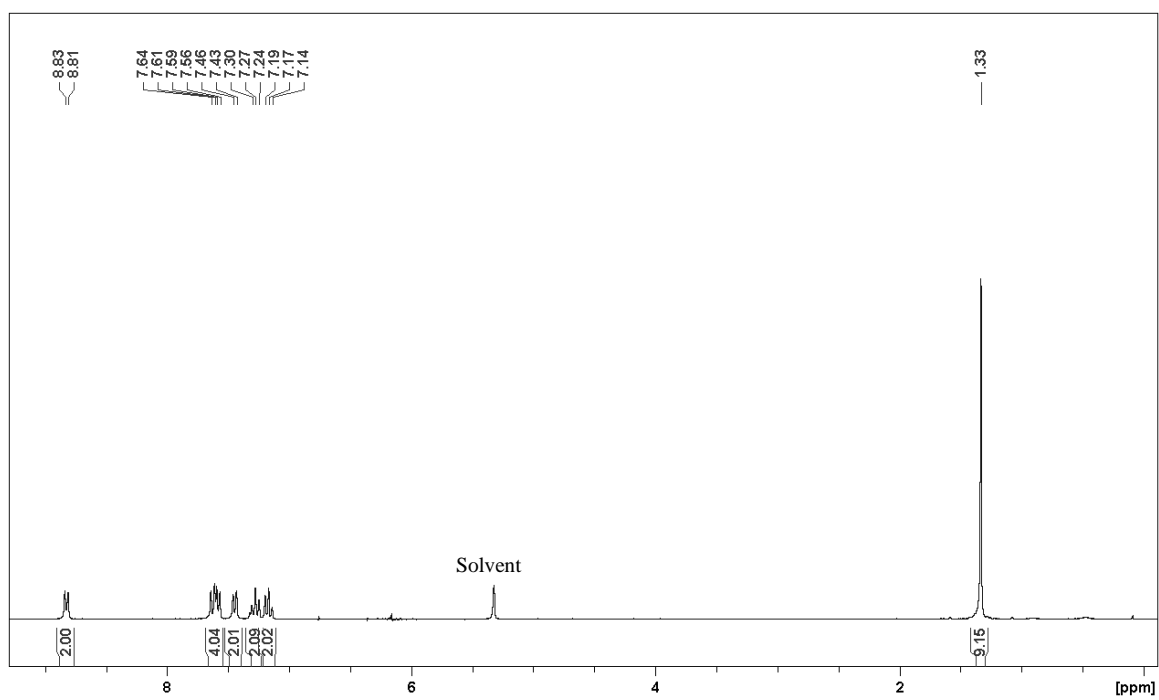
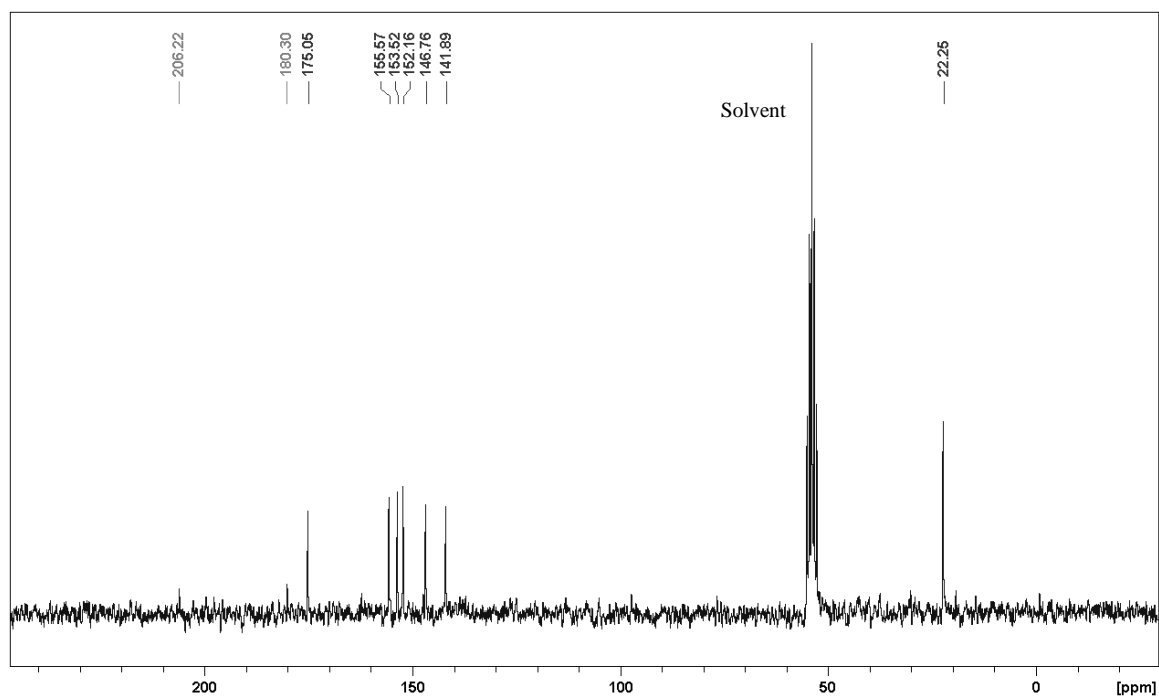
^1H (250 MHz)

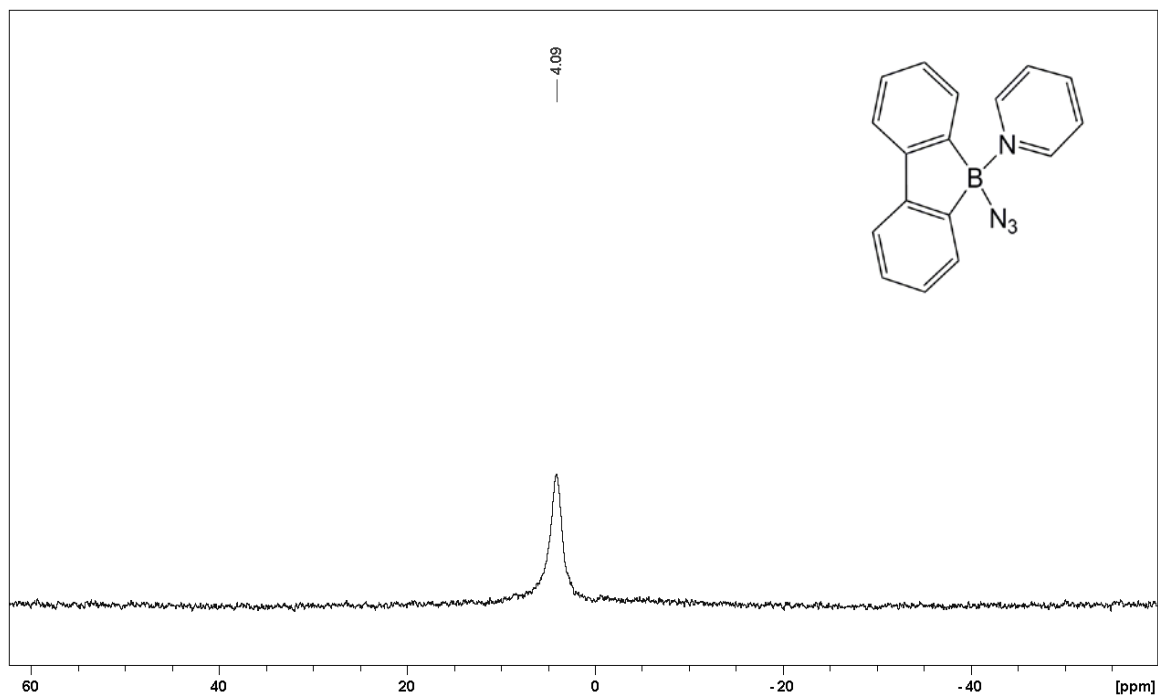
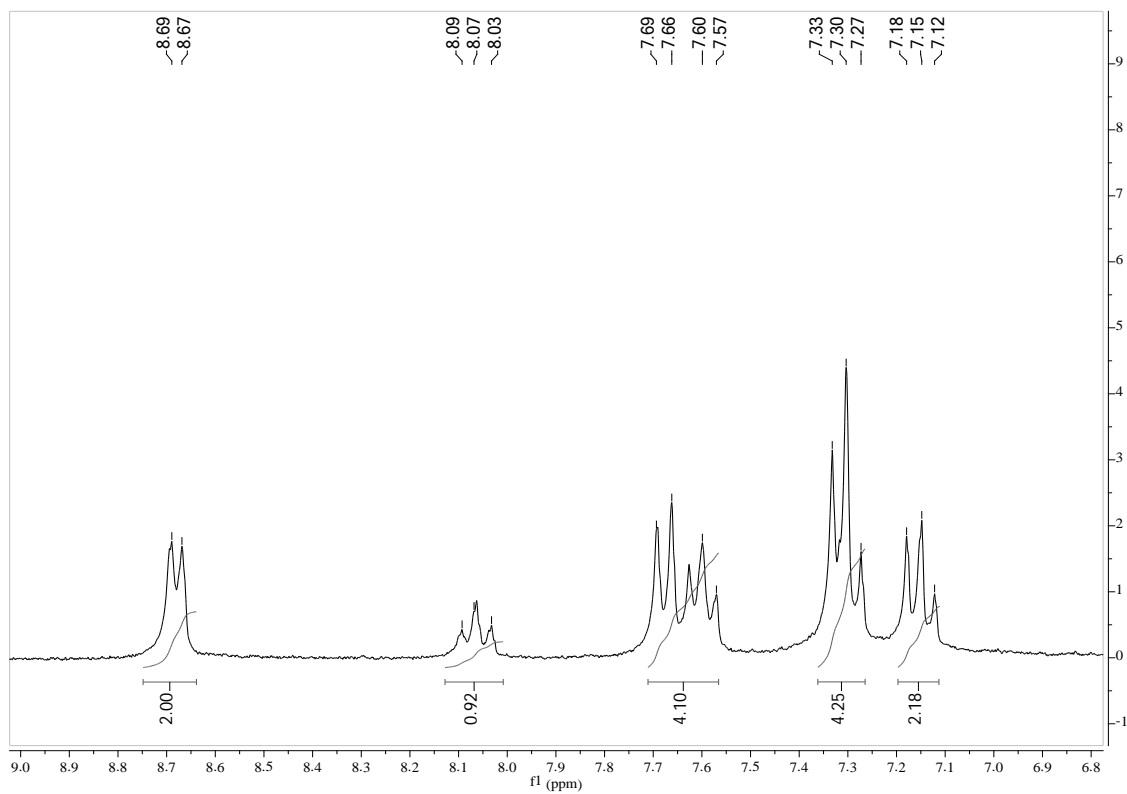
= middle of the spectra, * = Trimethylsilanol

 $^{13}\text{C}\{^1\text{H}\}$ (62.9 MHz)

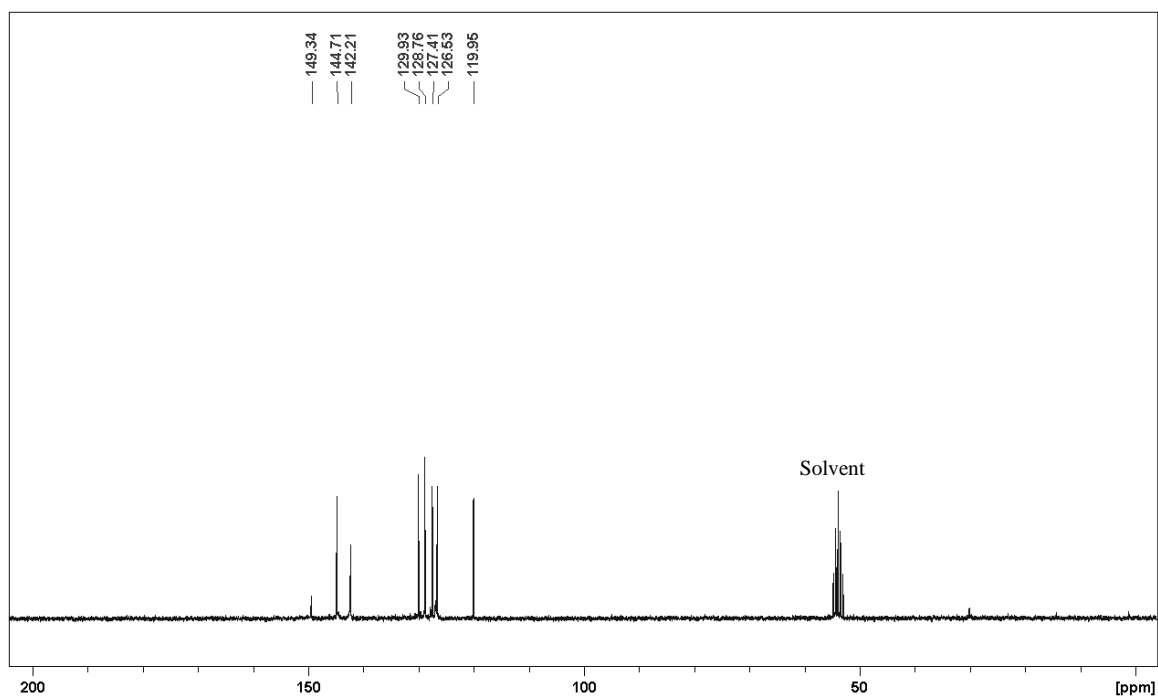
Compound **6** in CD₂Cl₂¹¹B{¹H} (80.3 MHz, *h*_{1/2} = 246.5 Hz)¹H (250 MHz)

$^{13}\text{C}\{^1\text{H}\}$ (62.9 MHz)Compound **6b** in CD_2Cl_2 $^{11}\text{B}\{^1\text{H}\}$ (80.3 MHz, $h_{1/2} = 168.4$ Hz)

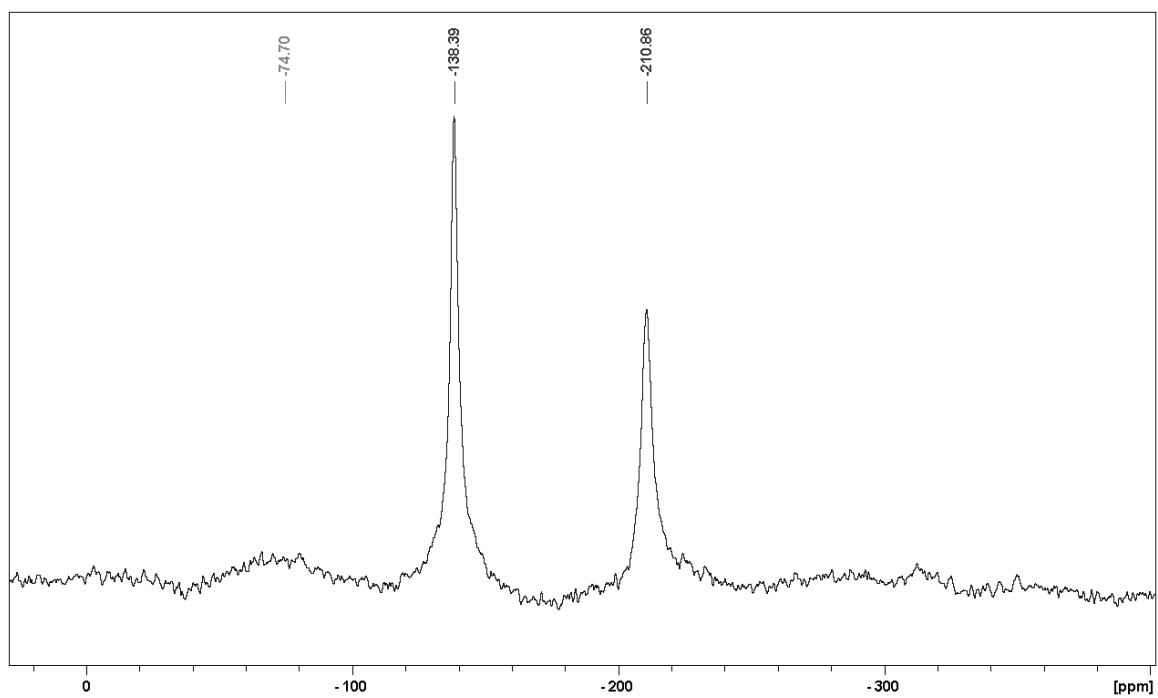
^1H (250 MHz) $^{13}\text{C}\{^1\text{H}\}$ (62.9 MHz)

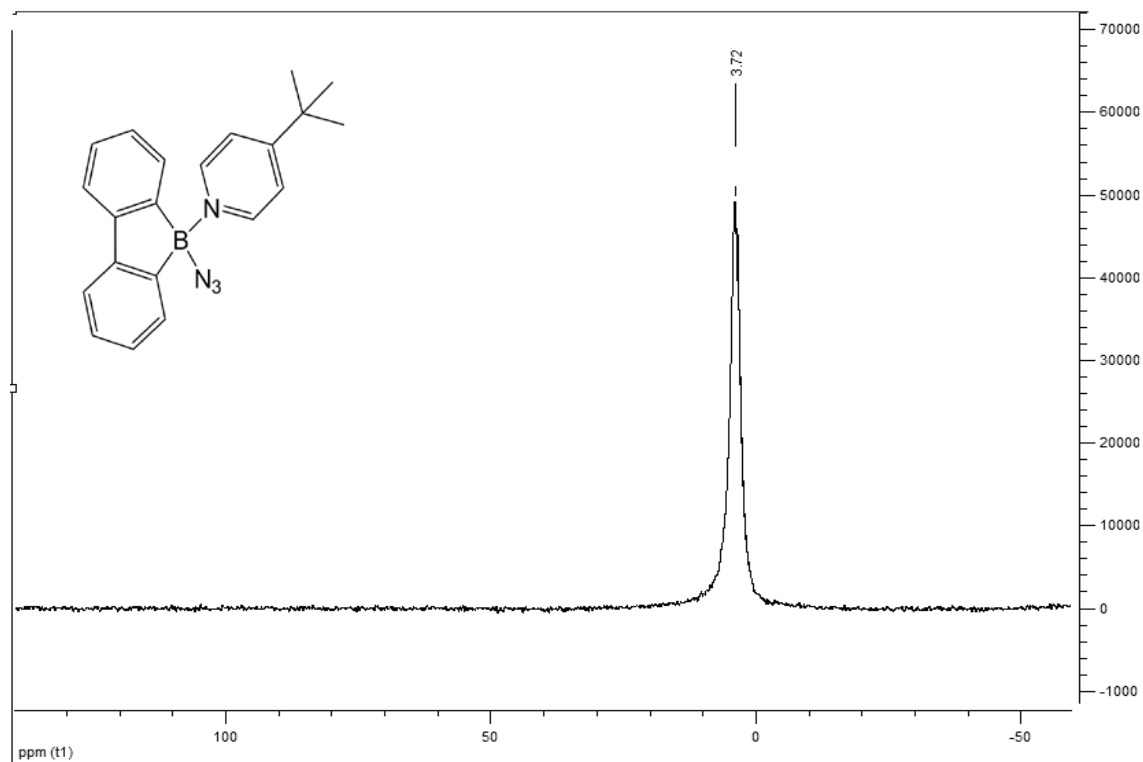
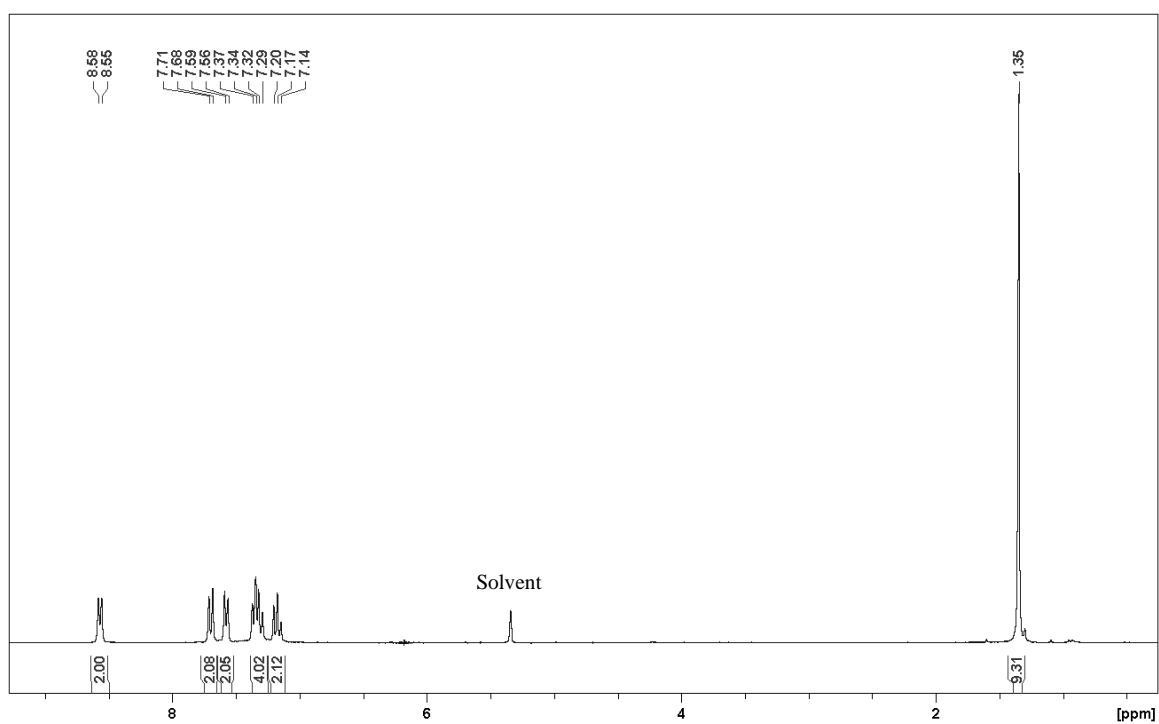
Compound **9** in CD₂Cl₂¹¹B{¹H} (80.3 MHz, *h*_{1/2} = 115.5 Hz)¹H (250 MHz)

$^{13}\text{C}\{^1\text{H}\}$ (62.9 MHz)



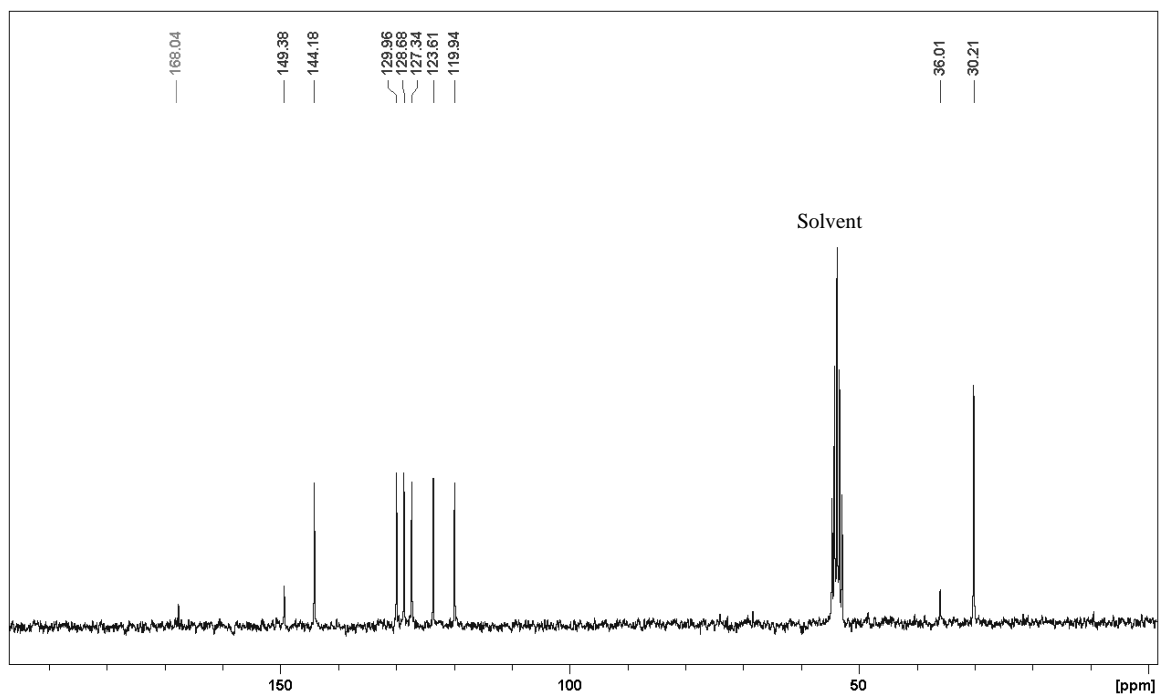
^{14}N (28.9 MHz)



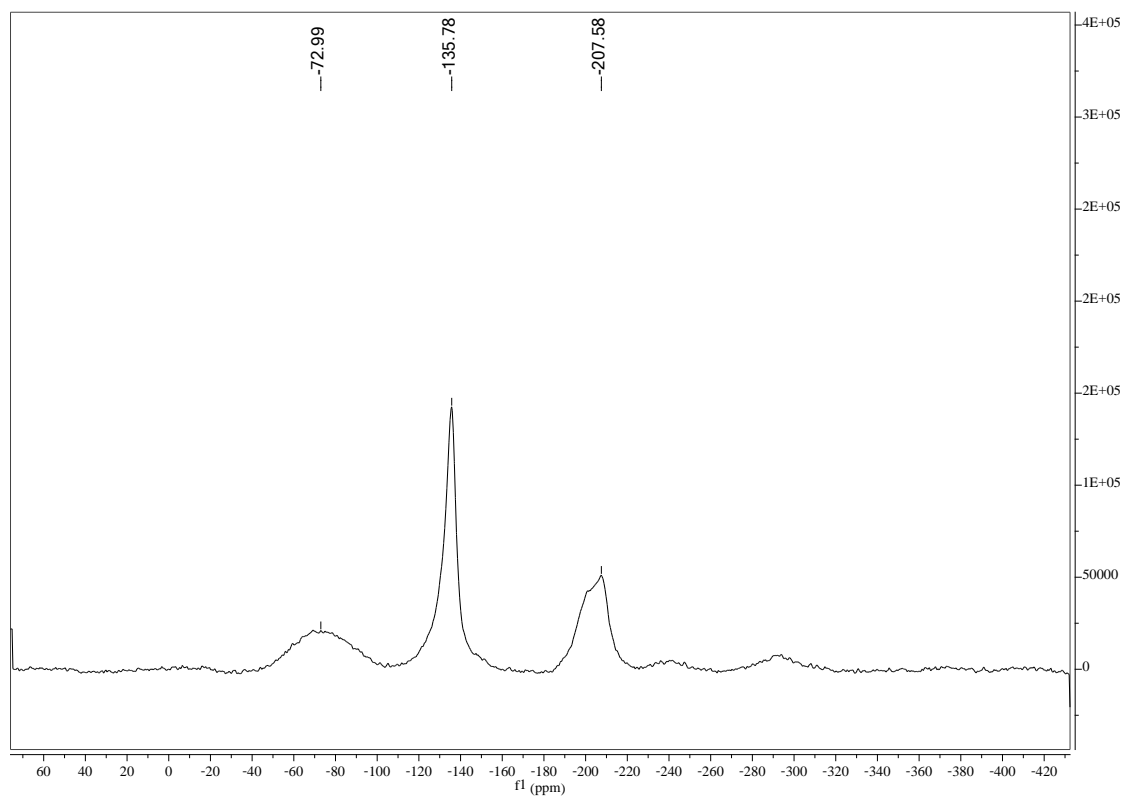
Compound **10** in CD₂Cl₂¹¹B{¹H} (80.3 MHz)¹H (250 MHz)

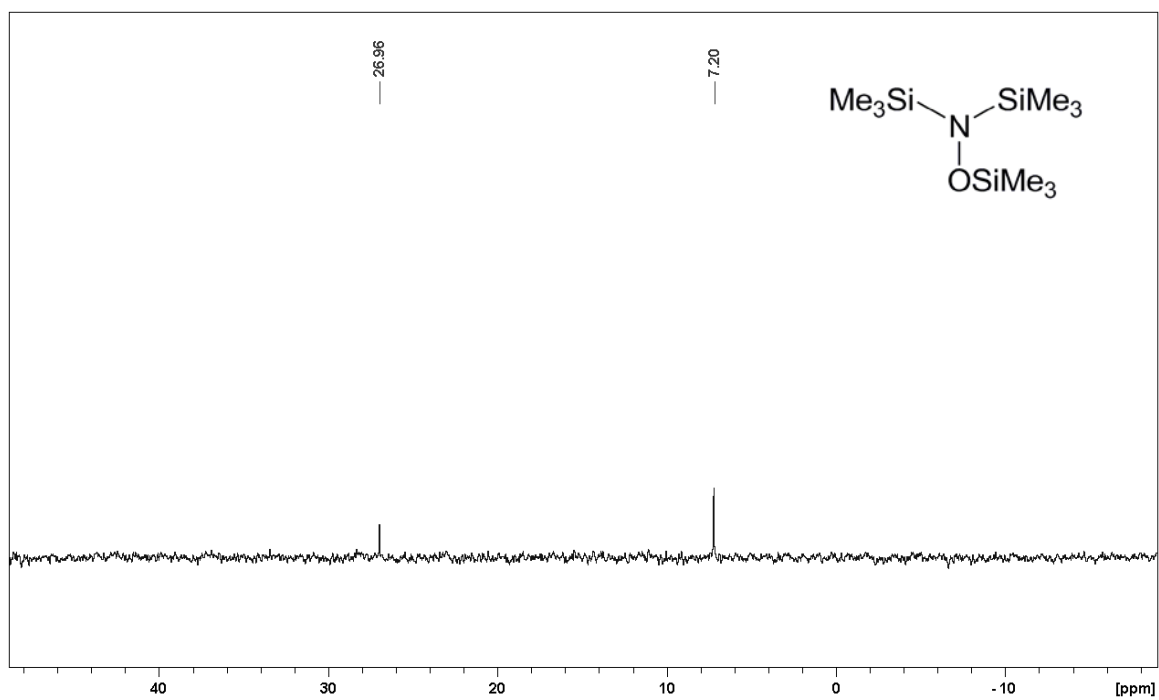
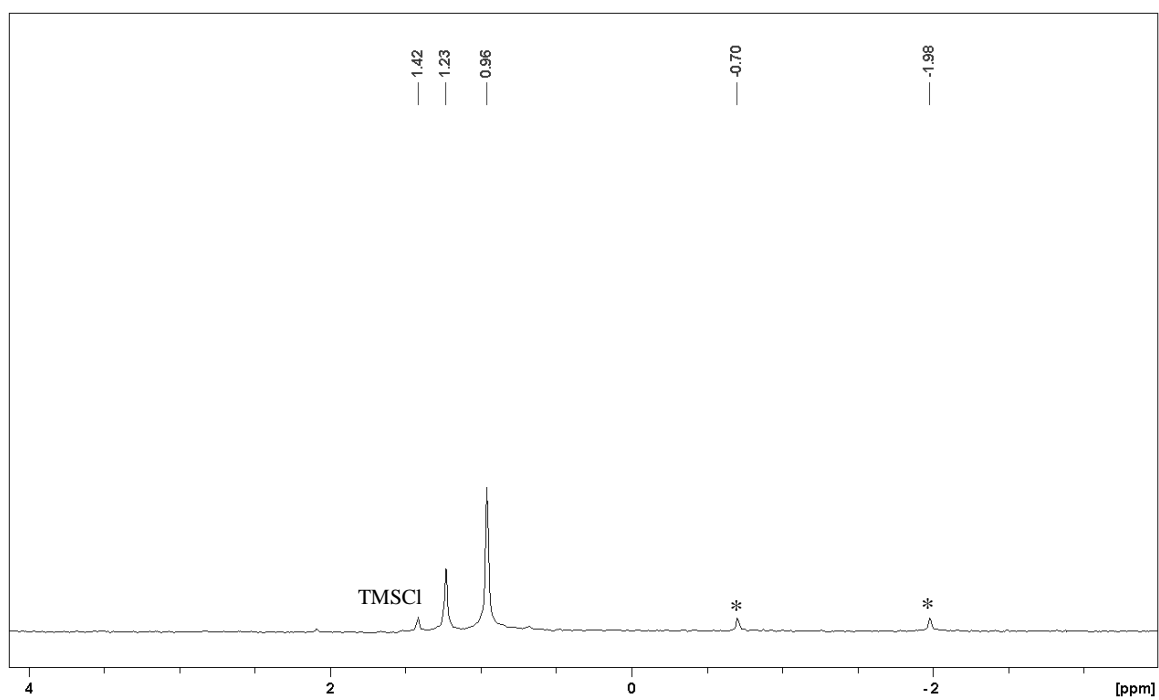
158 B. Selected NMR Spectra

$^{13}\text{C}\{^1\text{H}\}$ (62.9 MHz)

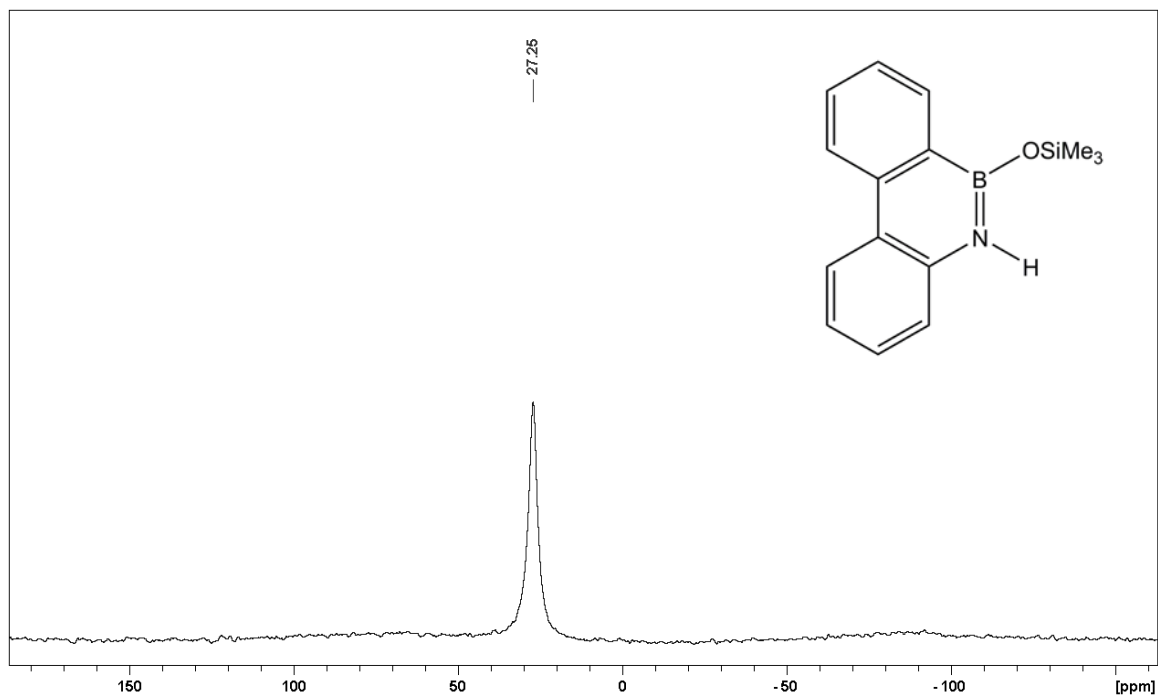
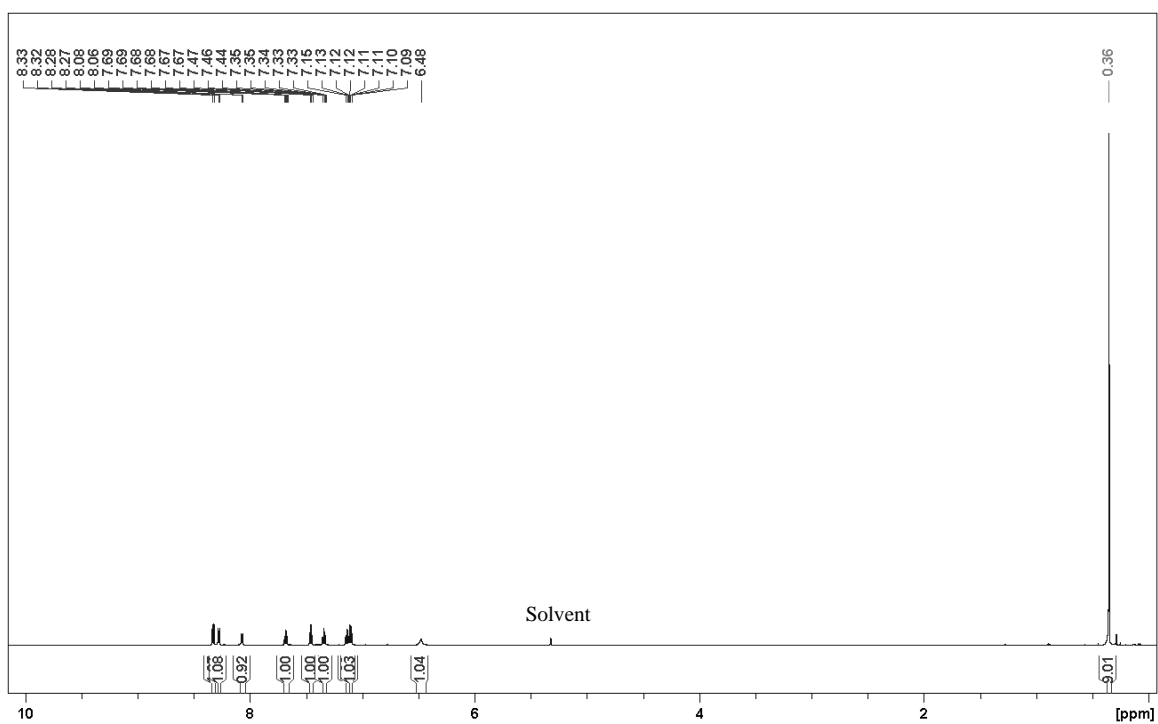


^{14}N (28.9 MHz)

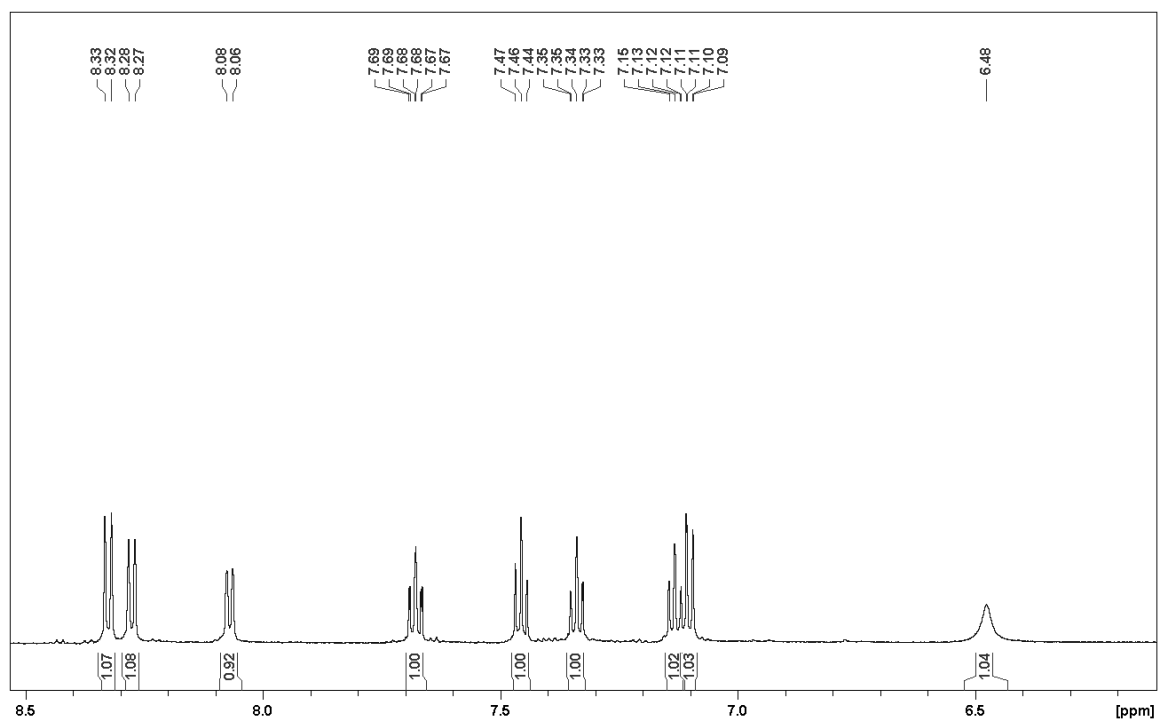
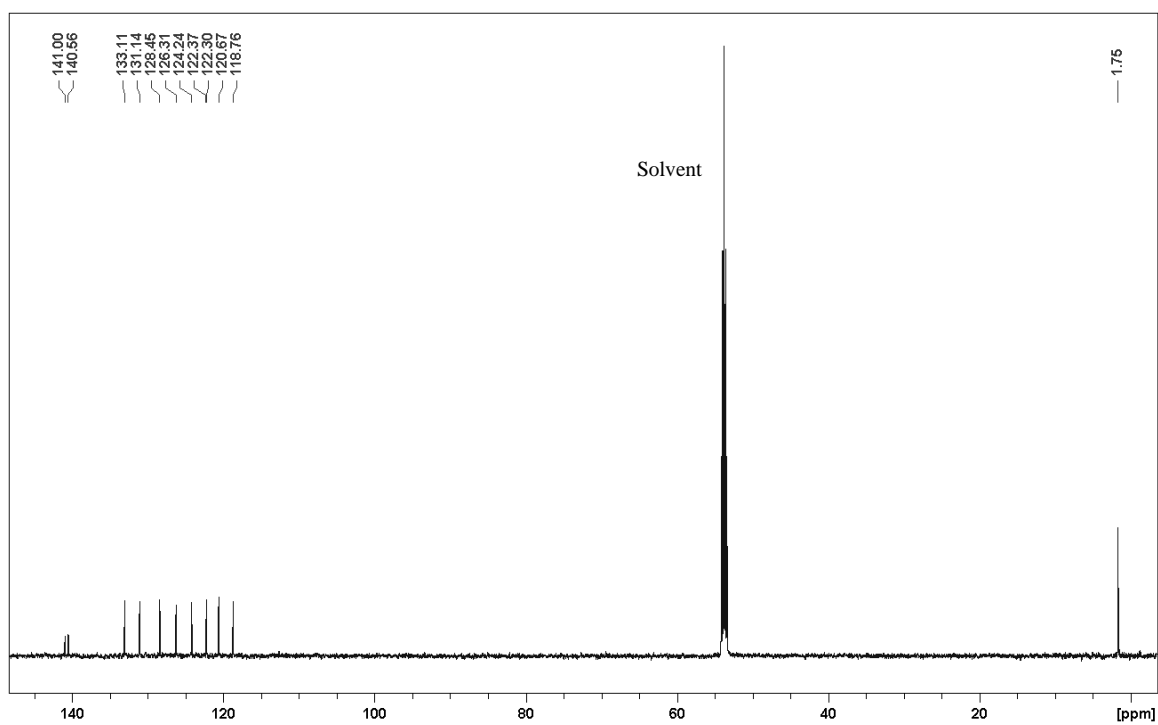


Compound **12** in C_6D_6 ^{29}Si (49.7 MHz) $^{13}C\{^1H\}$ (100.6 MHz)

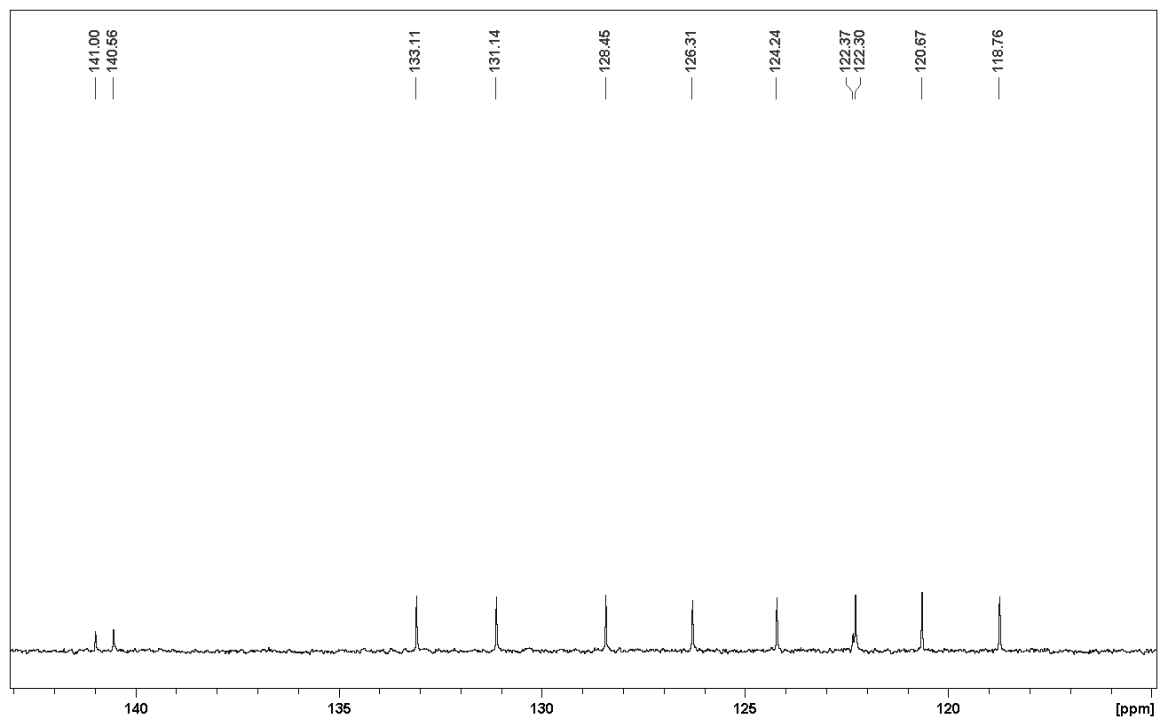
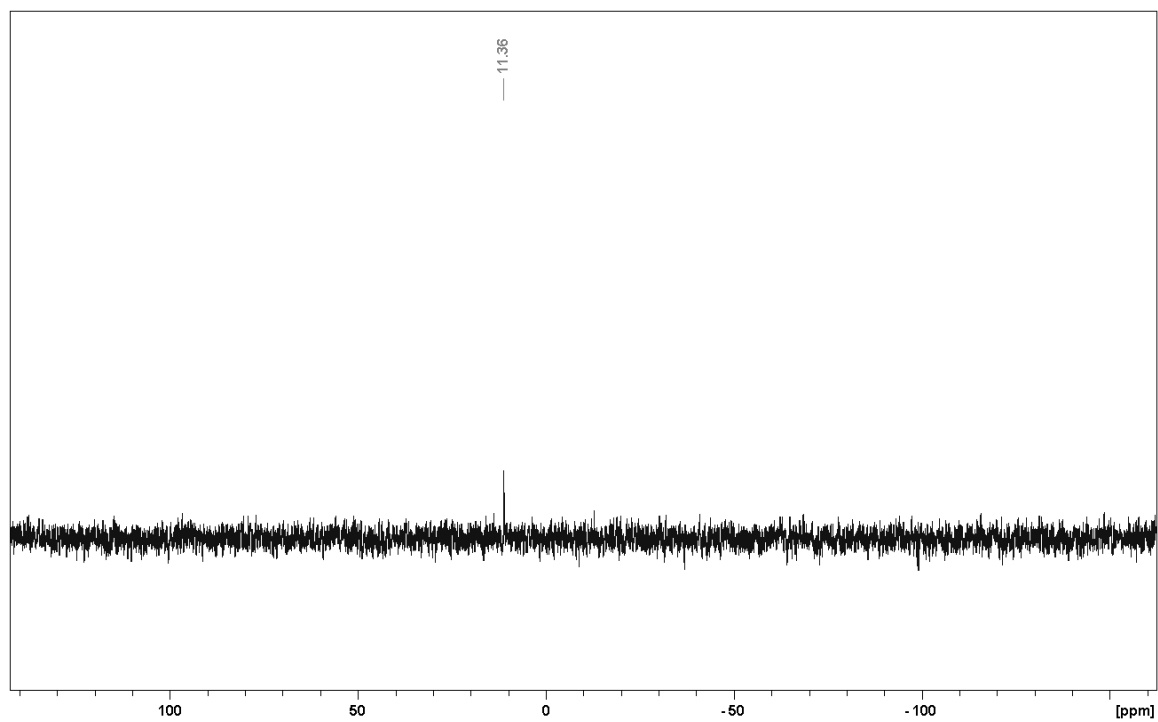
* Unidentified

Compound **15** in CD₂Cl₂¹¹B{¹H} (80.3 MHz, *h*_{1/2} = 239 Hz)¹H (600 MHz)

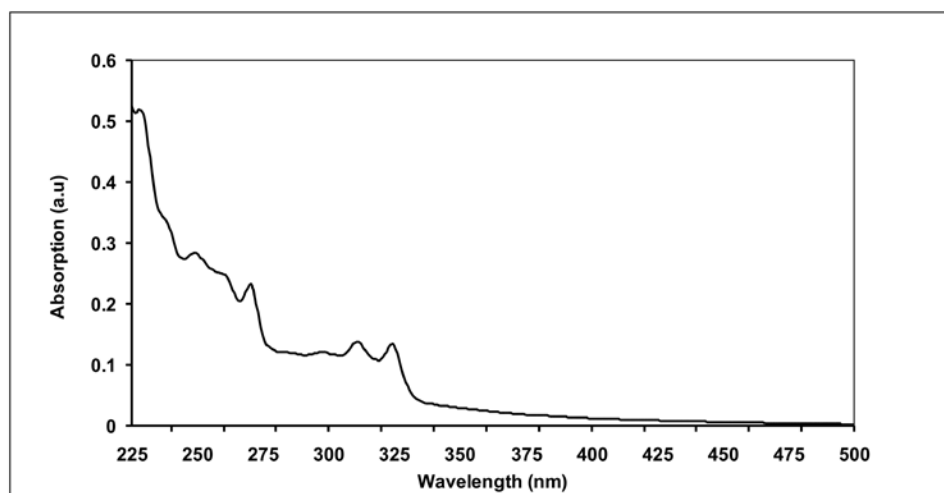
Extended view of aromatic region

 $^{13}\text{C}\{^1\text{H}\}$ (150.9 MHz)

Extended view of aromatic region

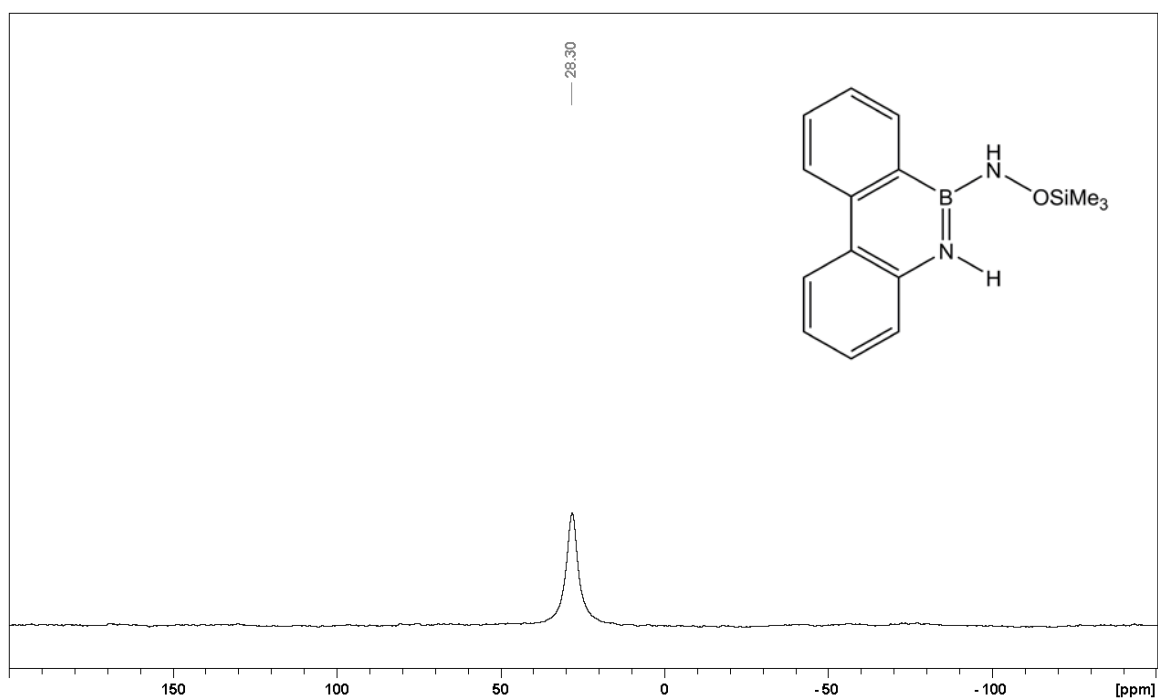
 ^{29}Si (49.7 MHz)

UV-Vis absorption spectrum in *n*-hexane

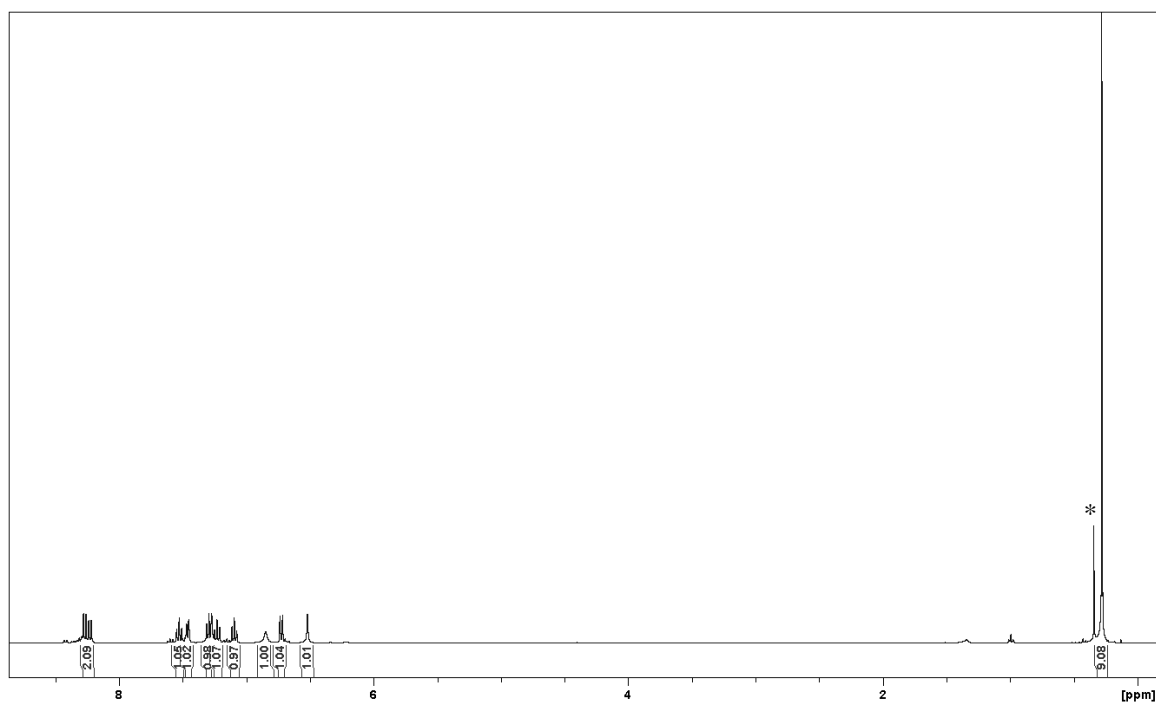


Compound **18** in CD_2Cl_2

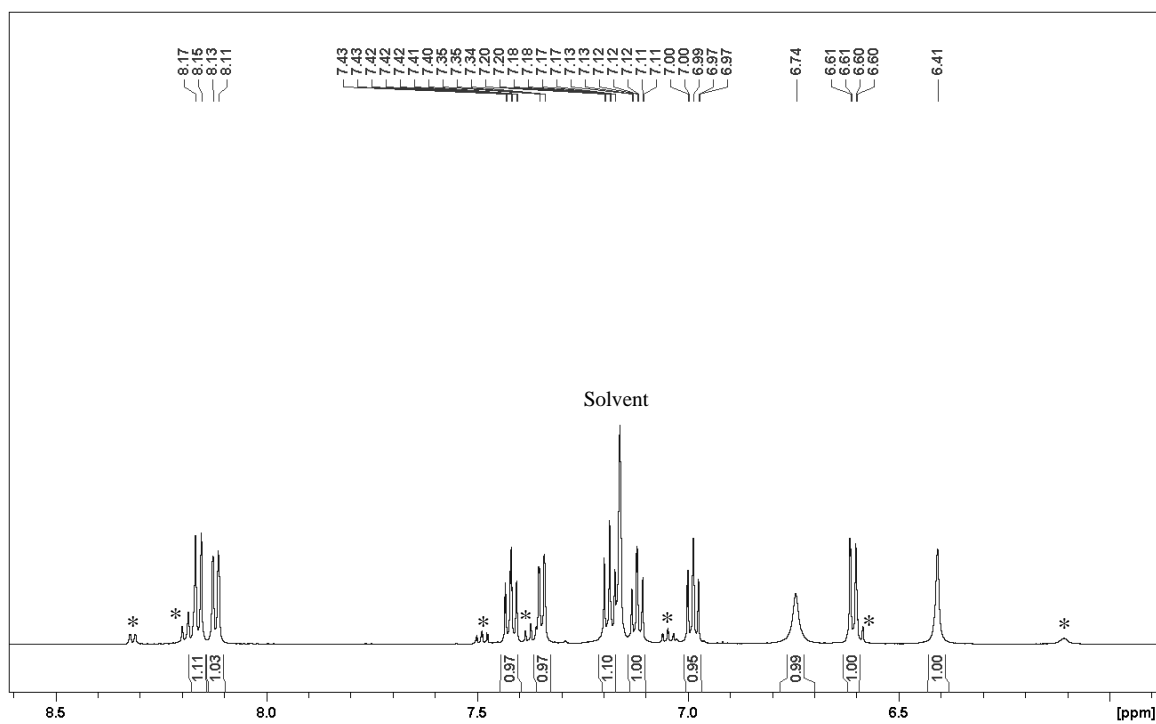
$^{11}\text{B}\{^1\text{H}\}$ (80.3 MHz, $h_{1/2} = 296$ Hz)



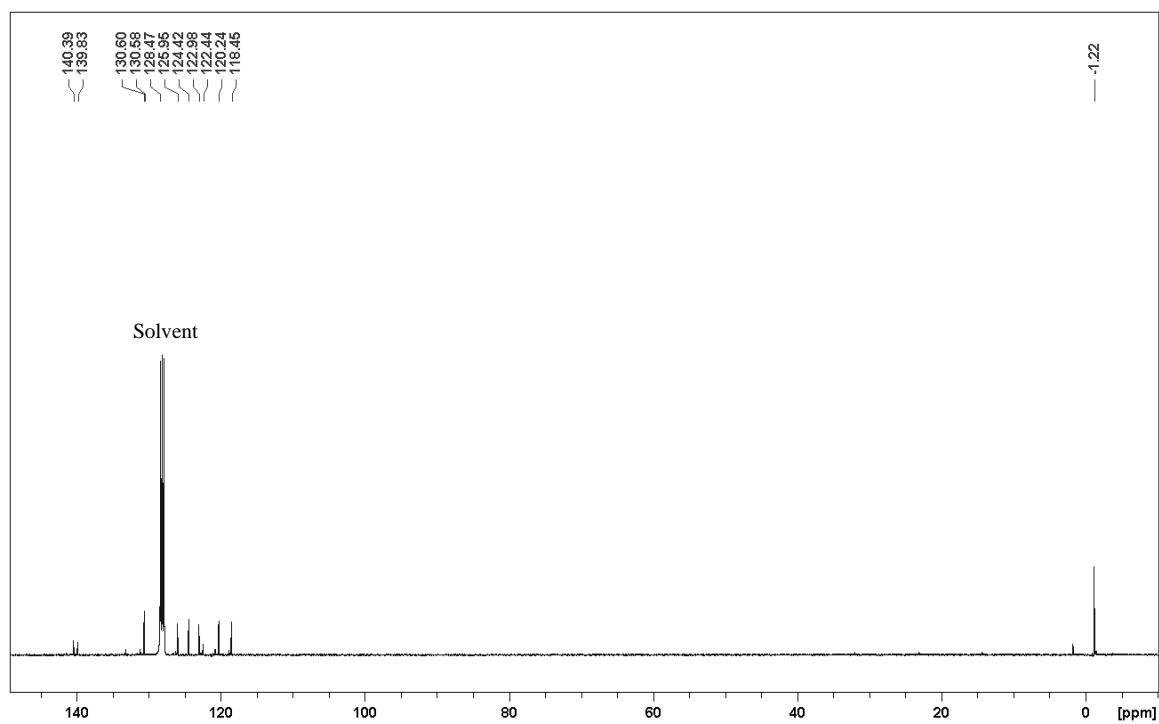
^1H (400 MHz)



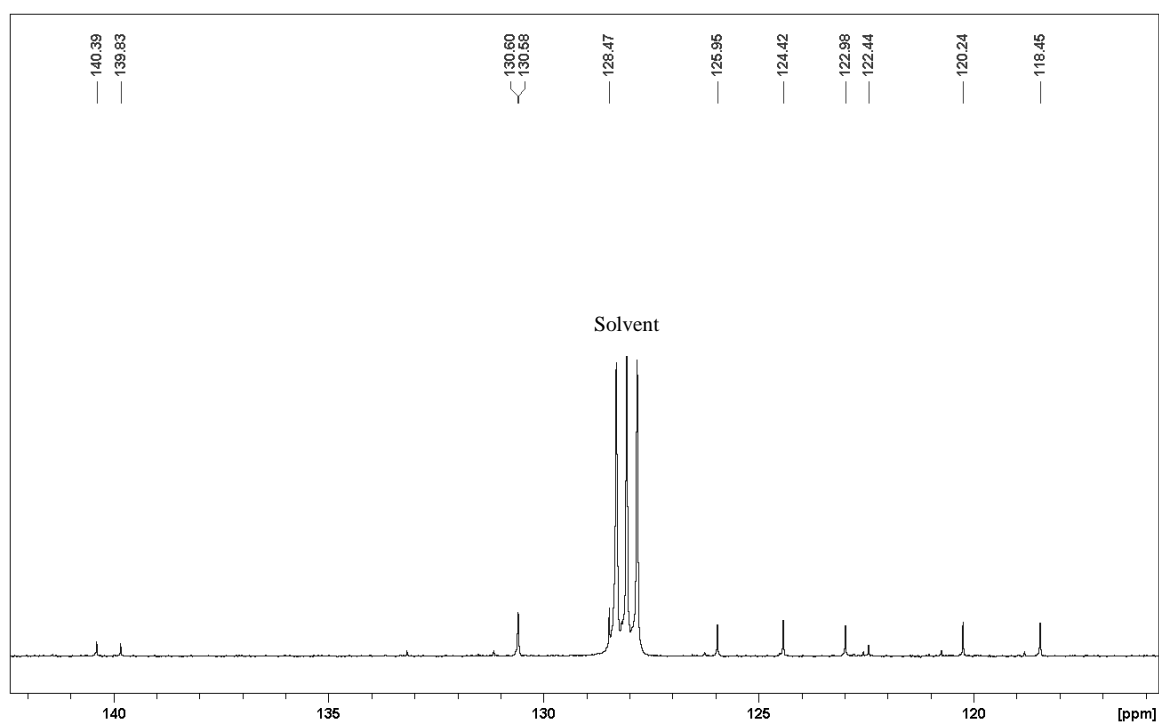
Extended view of aromatic region



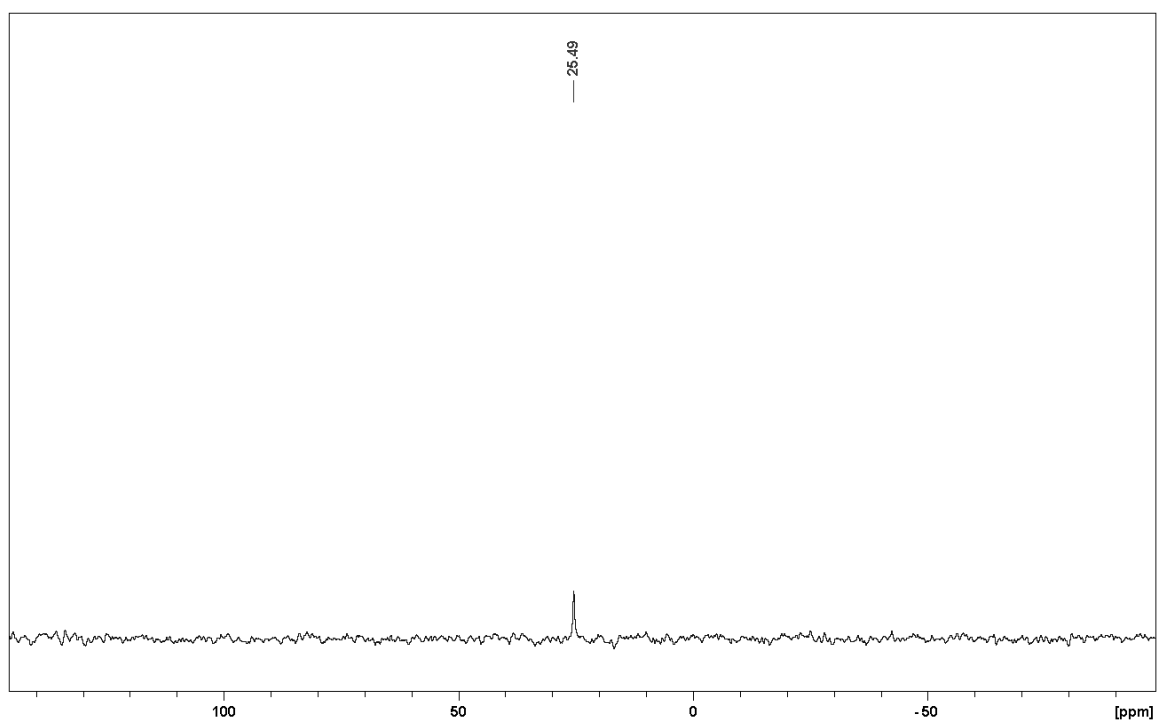
* Marked signals are due to compound **15**

$^{13}\text{C}\{^1\text{H}\}$ (100.6 MHz)

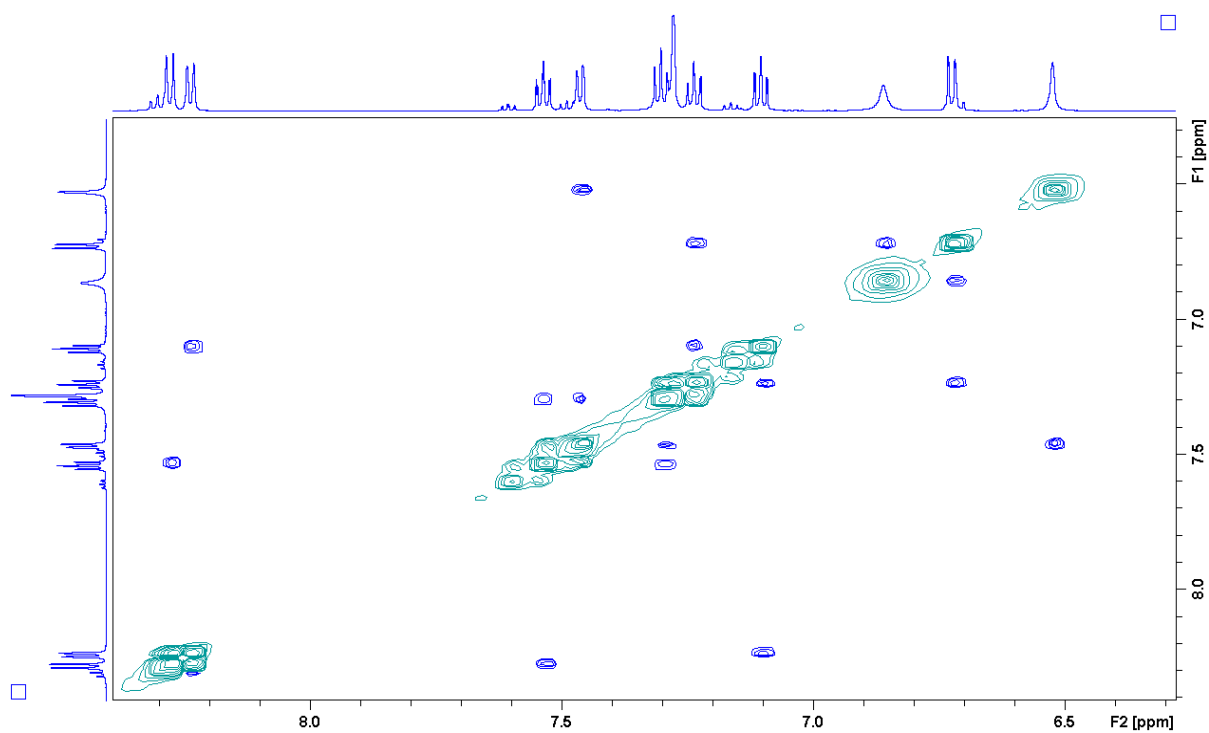
Extended view of aromatic region



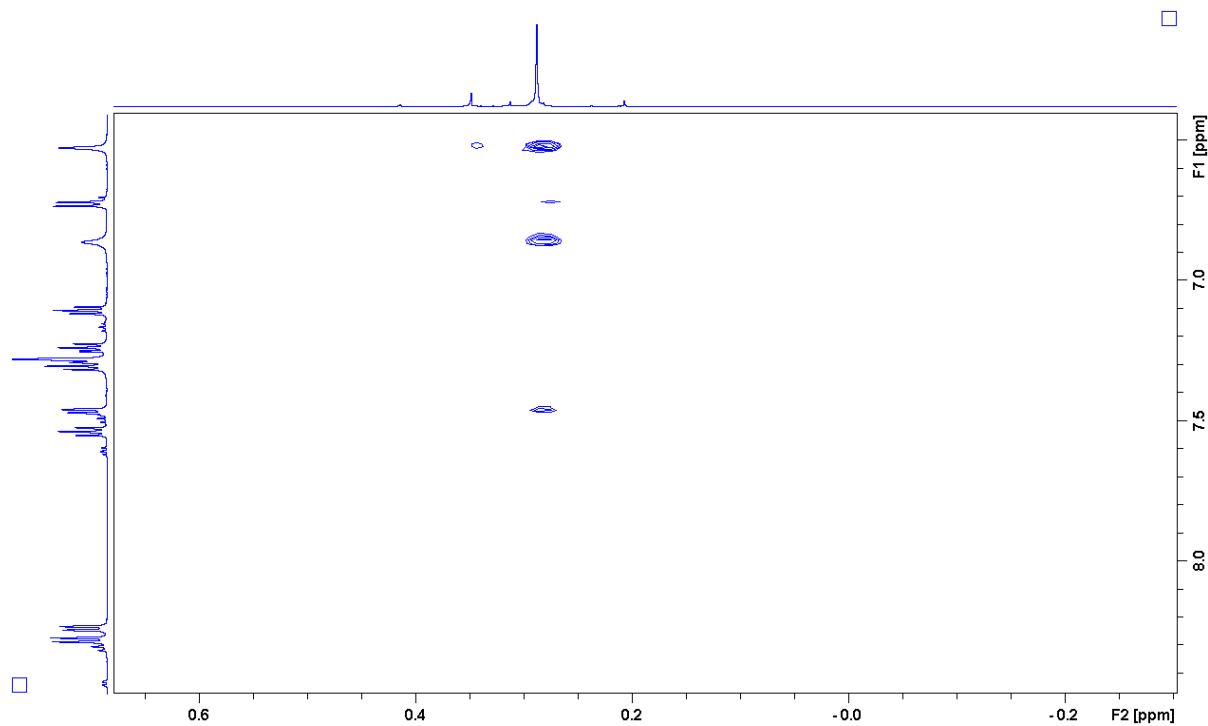
^{29}Si (49.7 MHz)



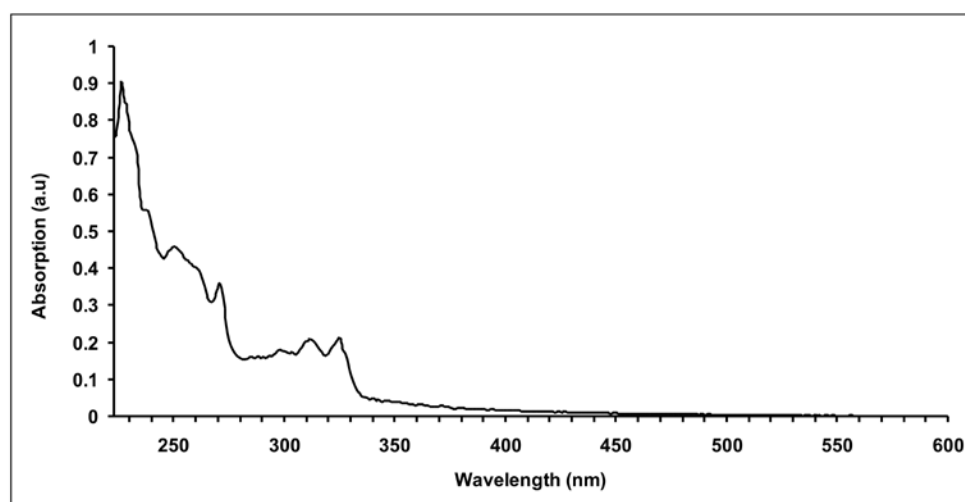
NOESY: measured at 600 MHz; Aromatic region

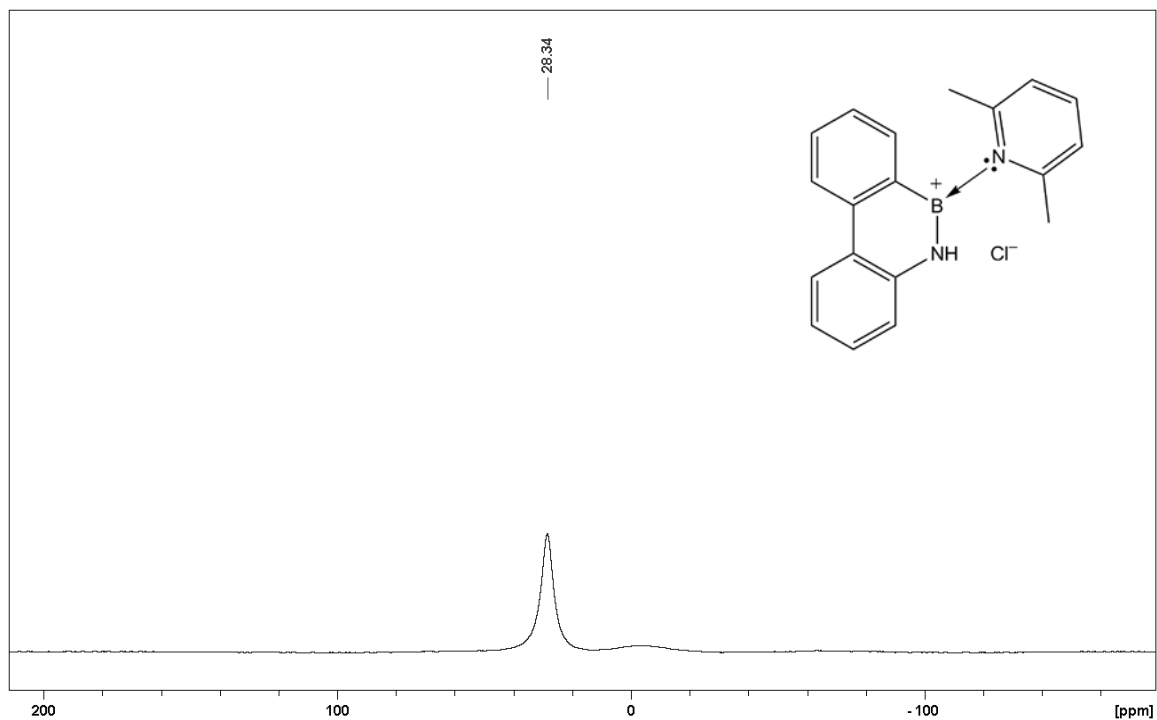
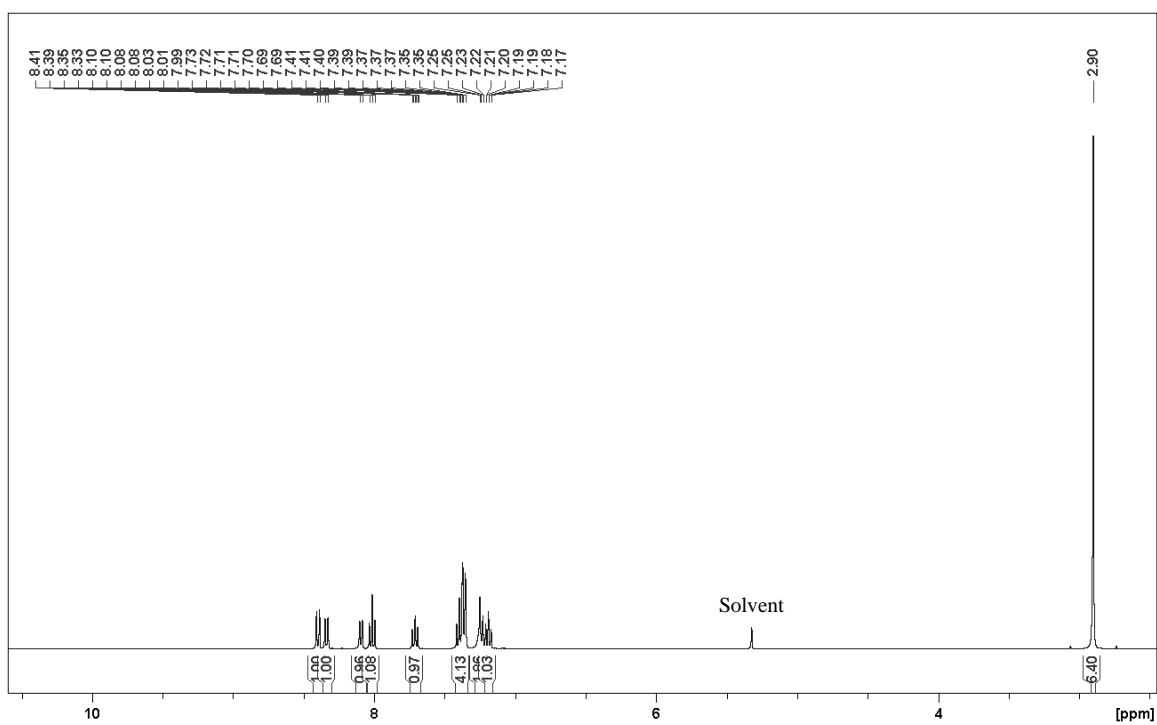


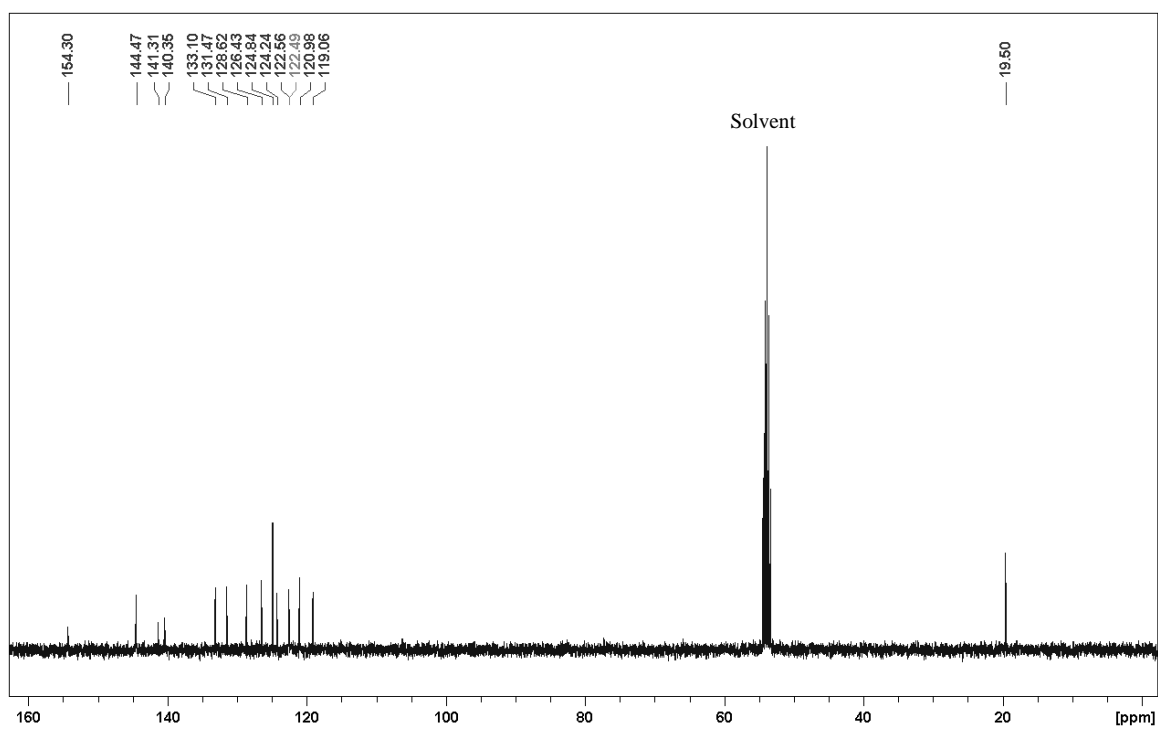
NOESY interaction of TMS protons to aromatic protons



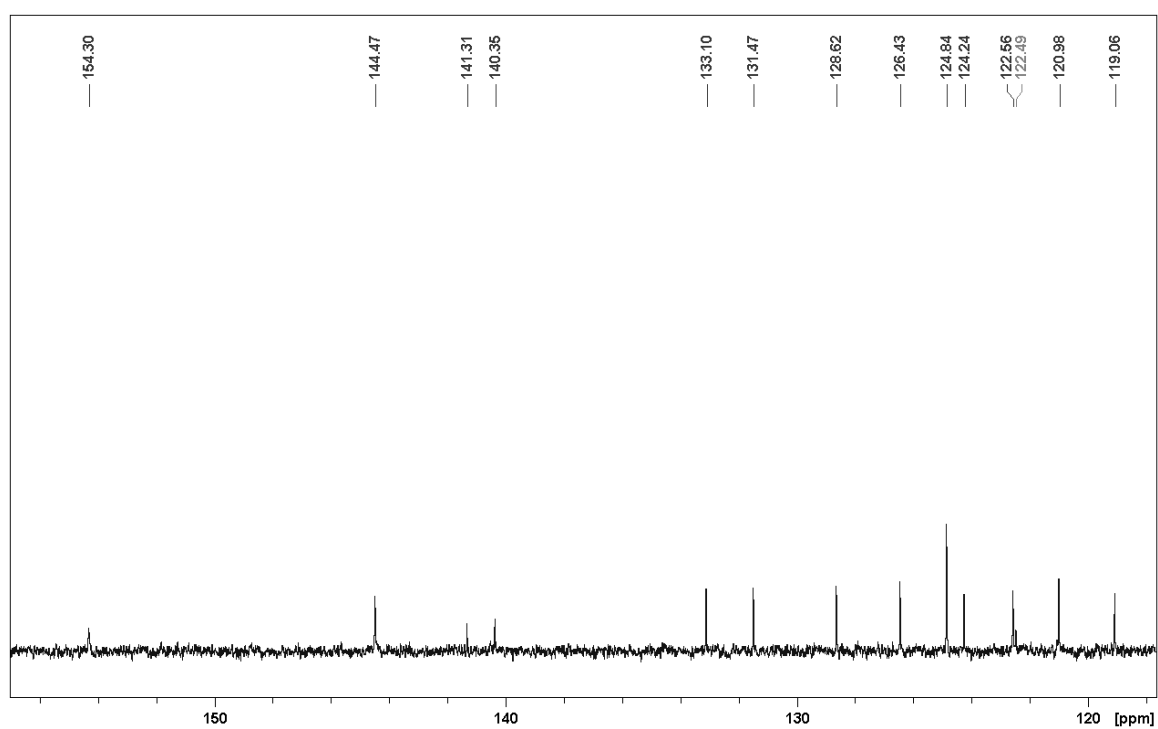
UV-Vis absorption spectrum in *n*-hexane



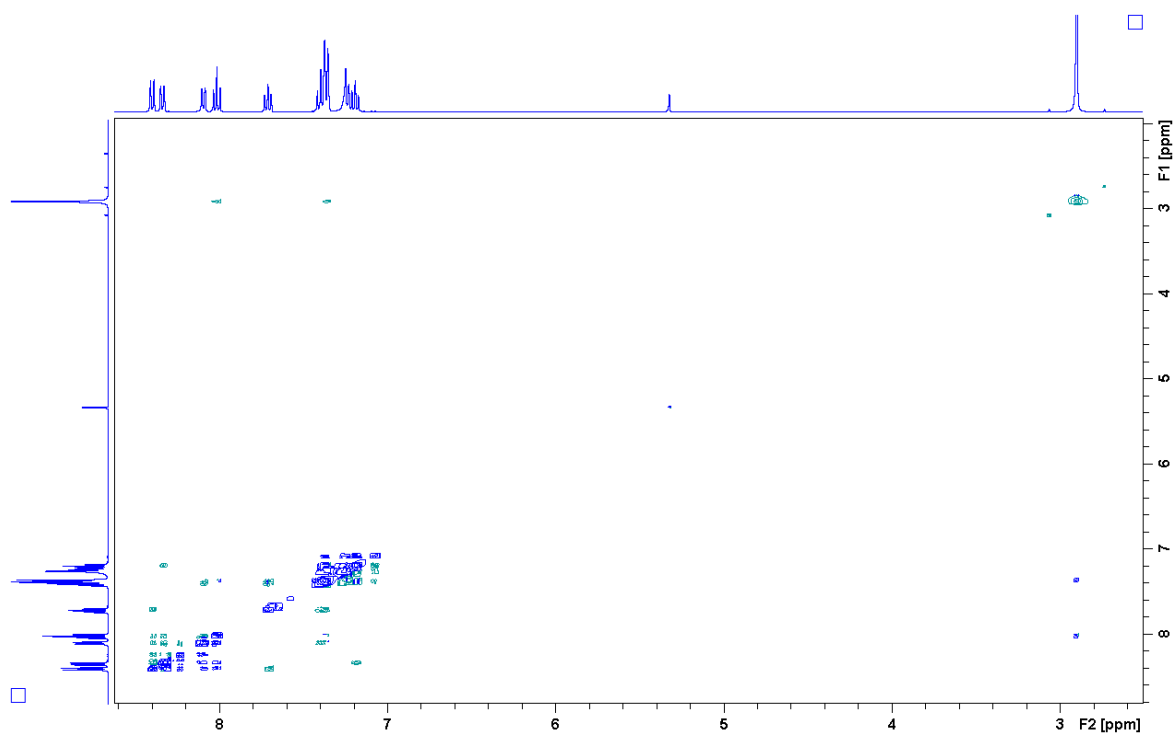
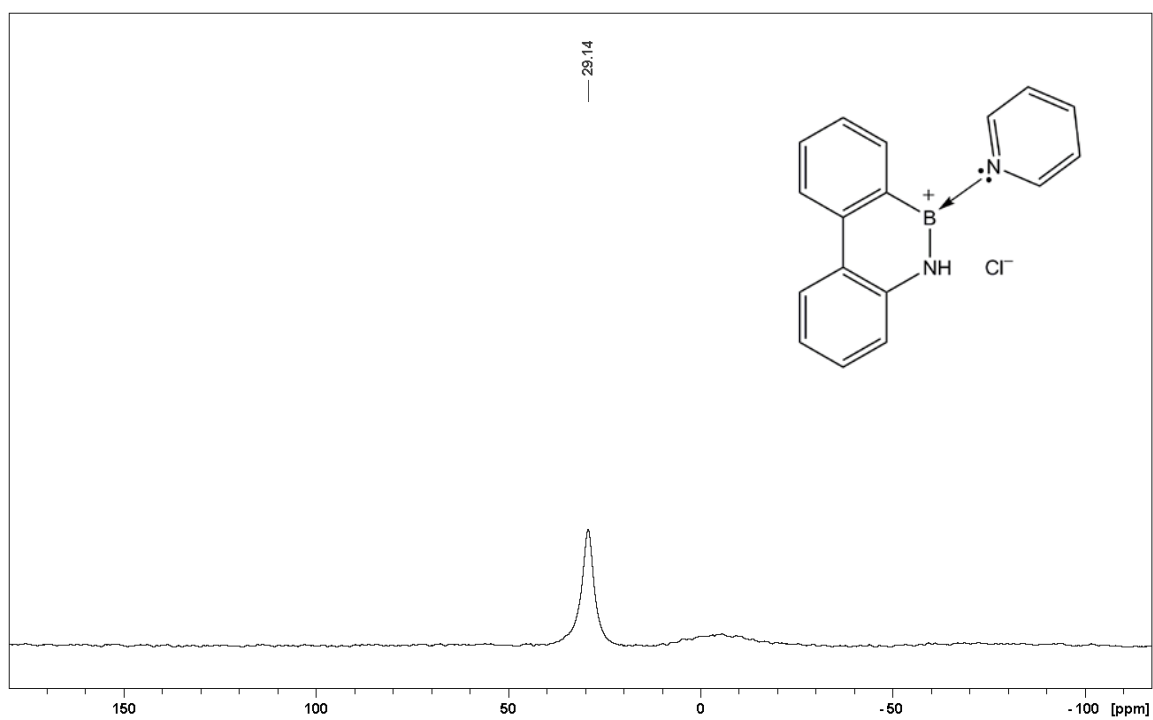
Compound **22** in CD₂Cl₂¹¹B{¹H} (80.3 MHz, *h*_{1/2} = 366.8 Hz)¹H (400 MHz)

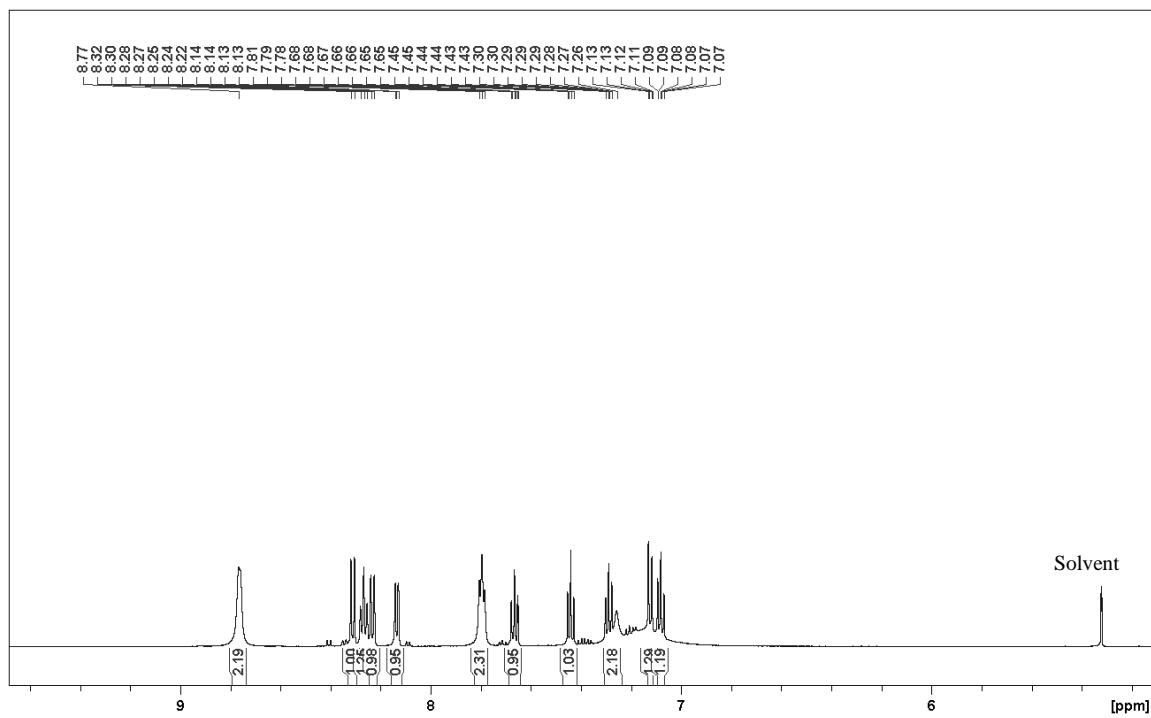
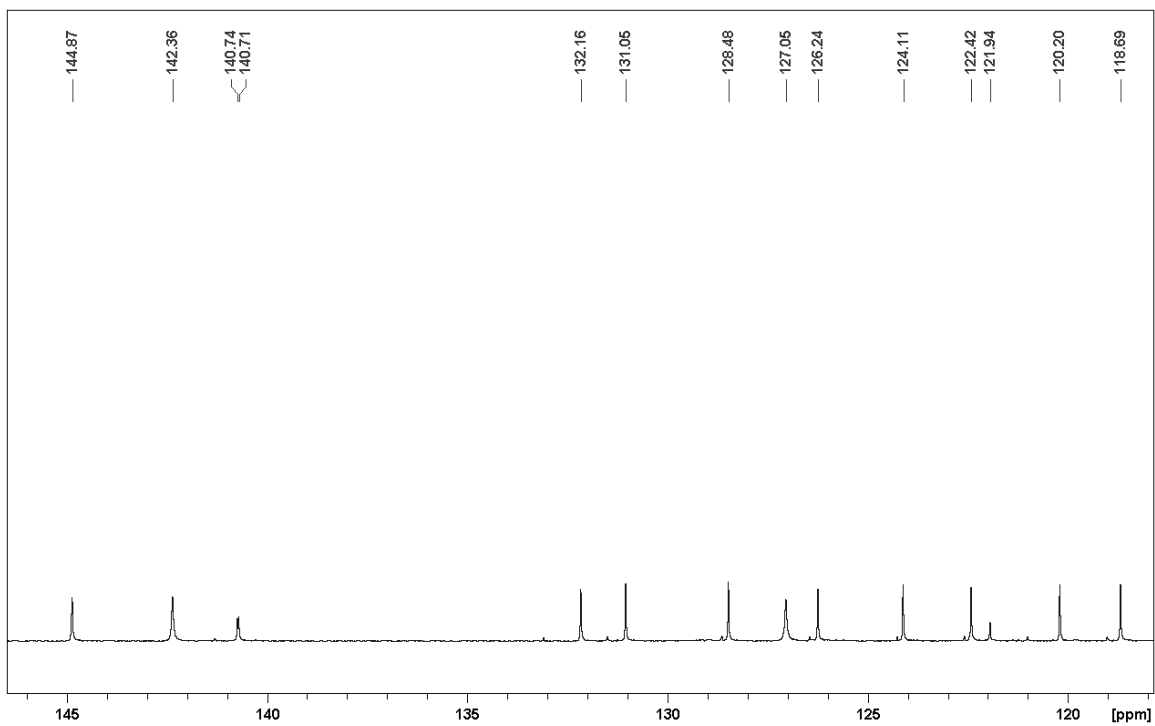
$^{13}\text{C}\{^1\text{H}\}$ (100.6 MHz)

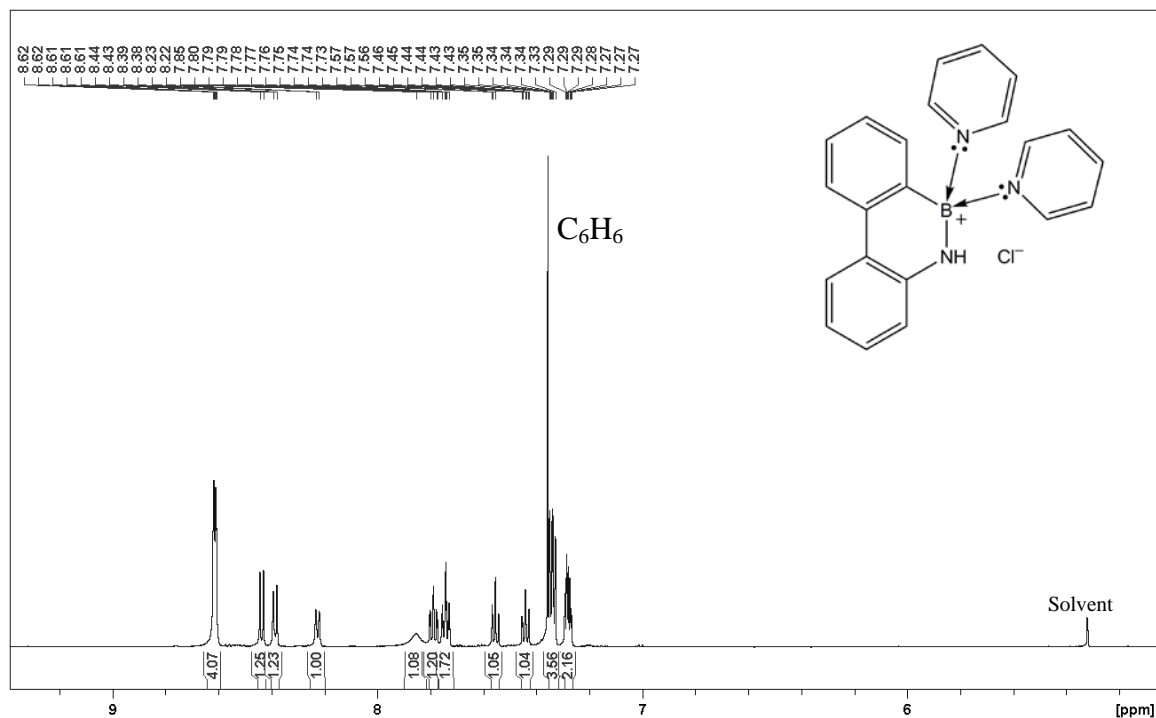
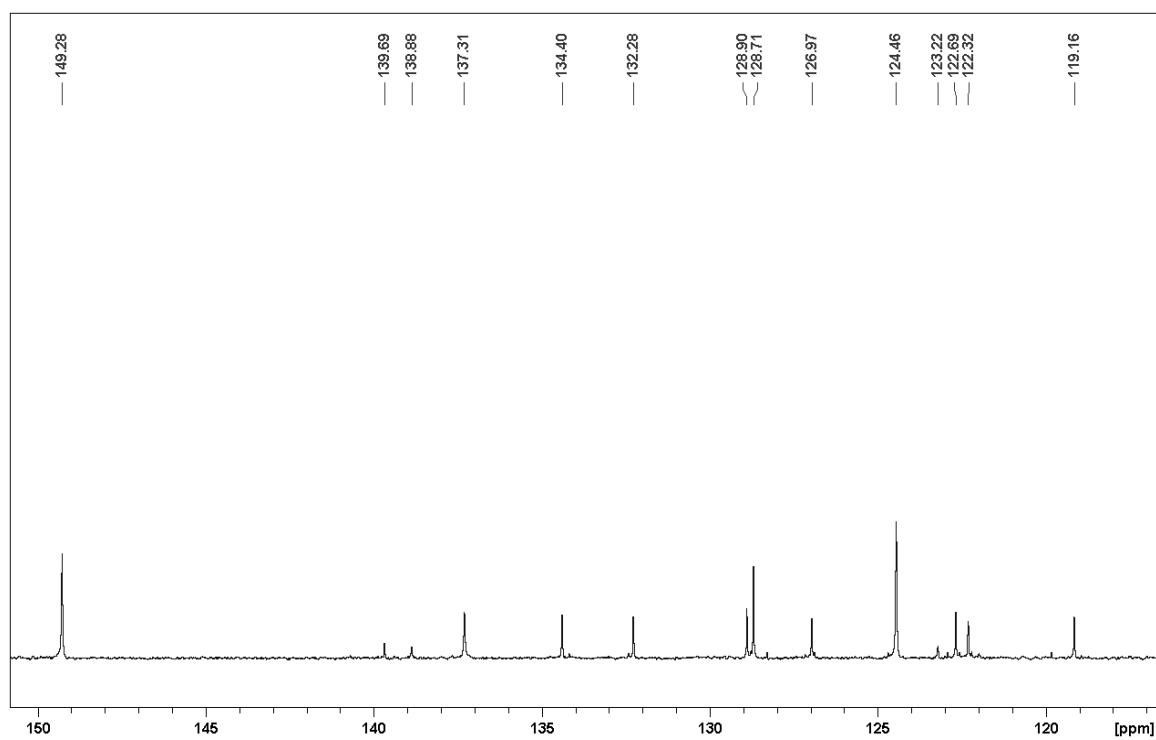
Extended view of aromatic region

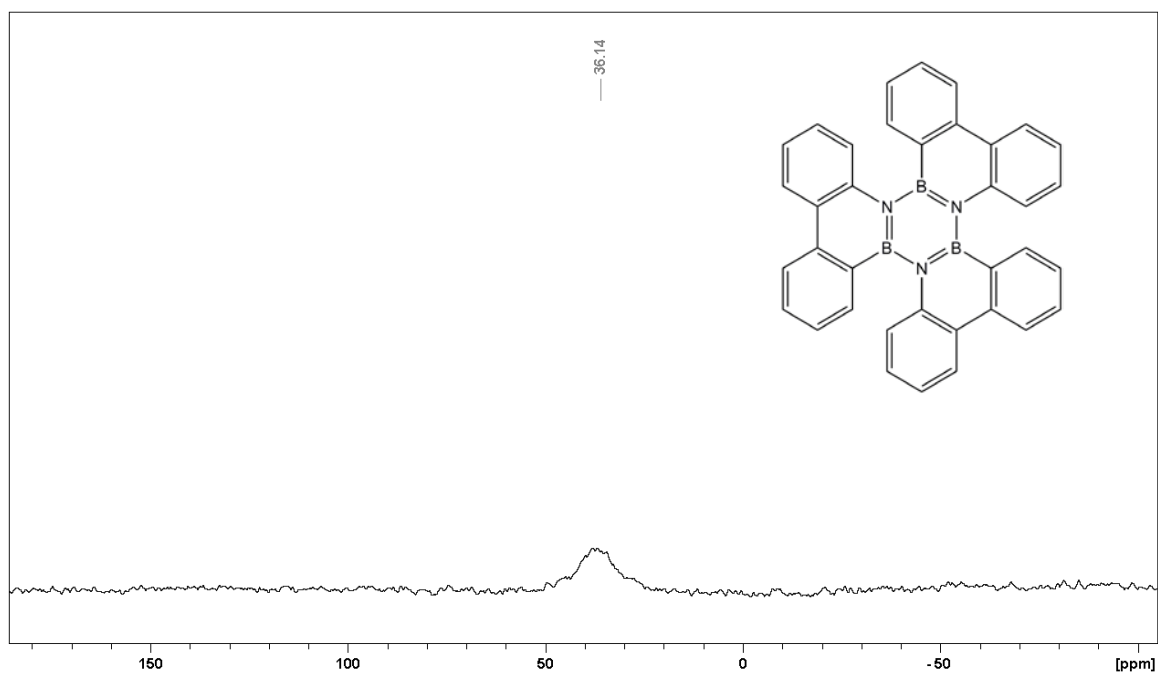
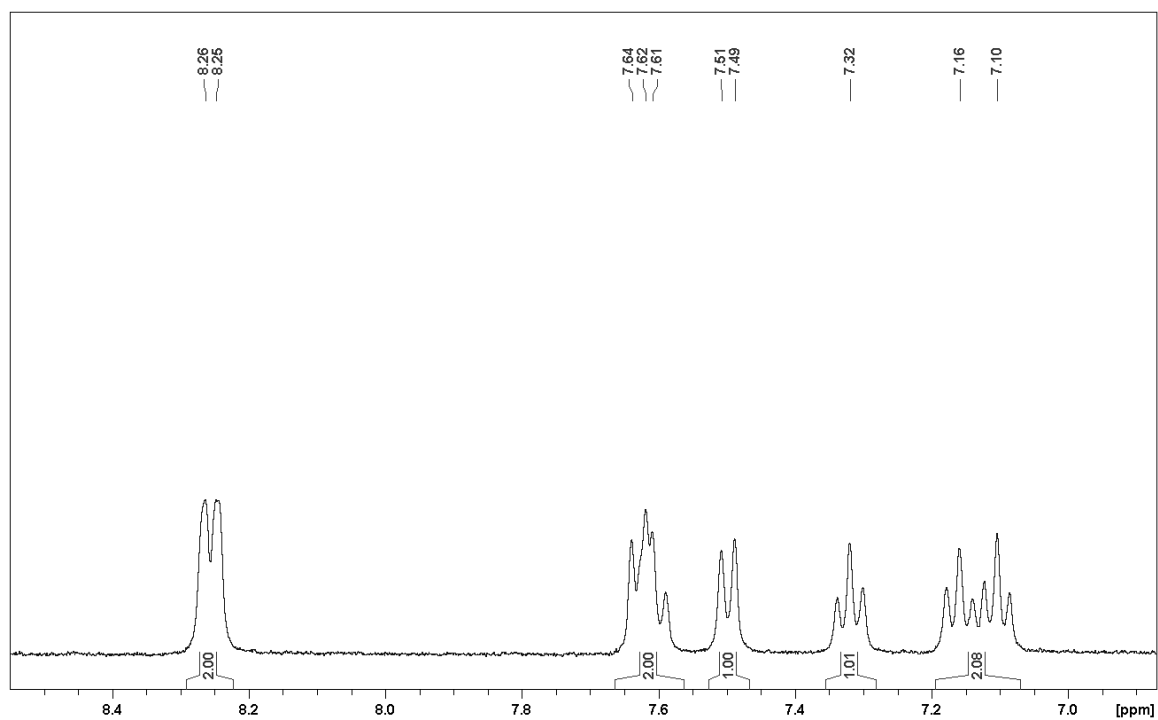


NOESY (400 MHz)

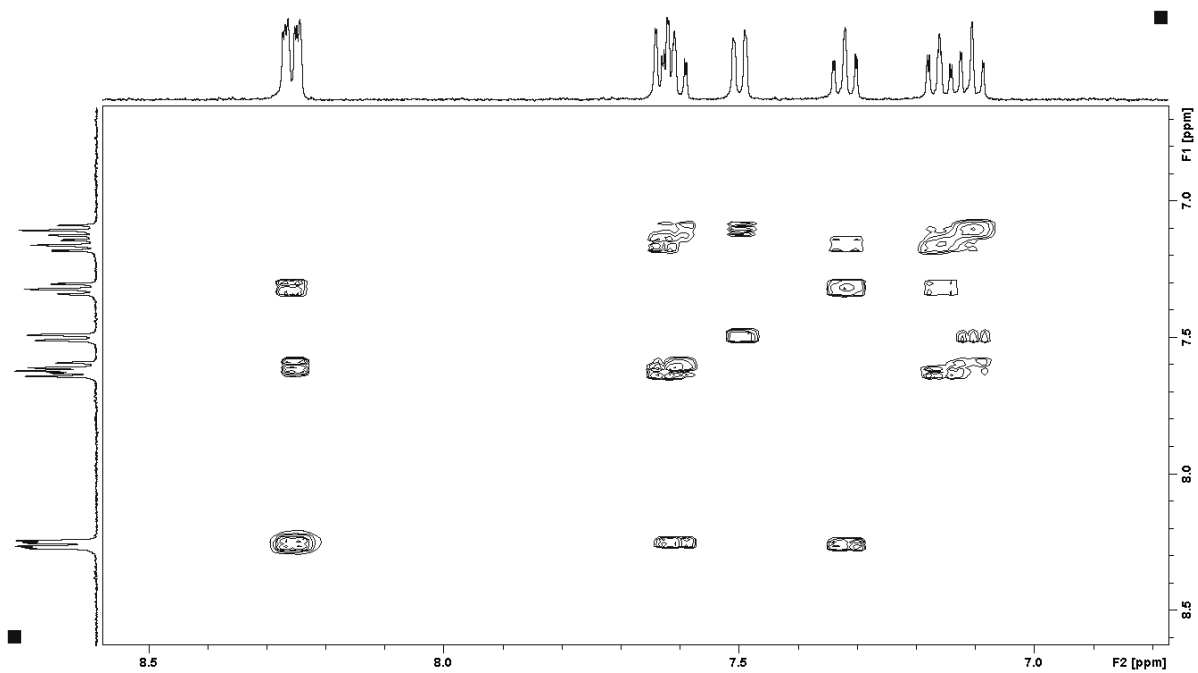
Compound **23** in CD₂Cl₂¹¹B (80.3 MHz, *h*_{1/2} = 250.5 Hz)

^1H (600 MHz) ^{13}C (150.9 MHz)

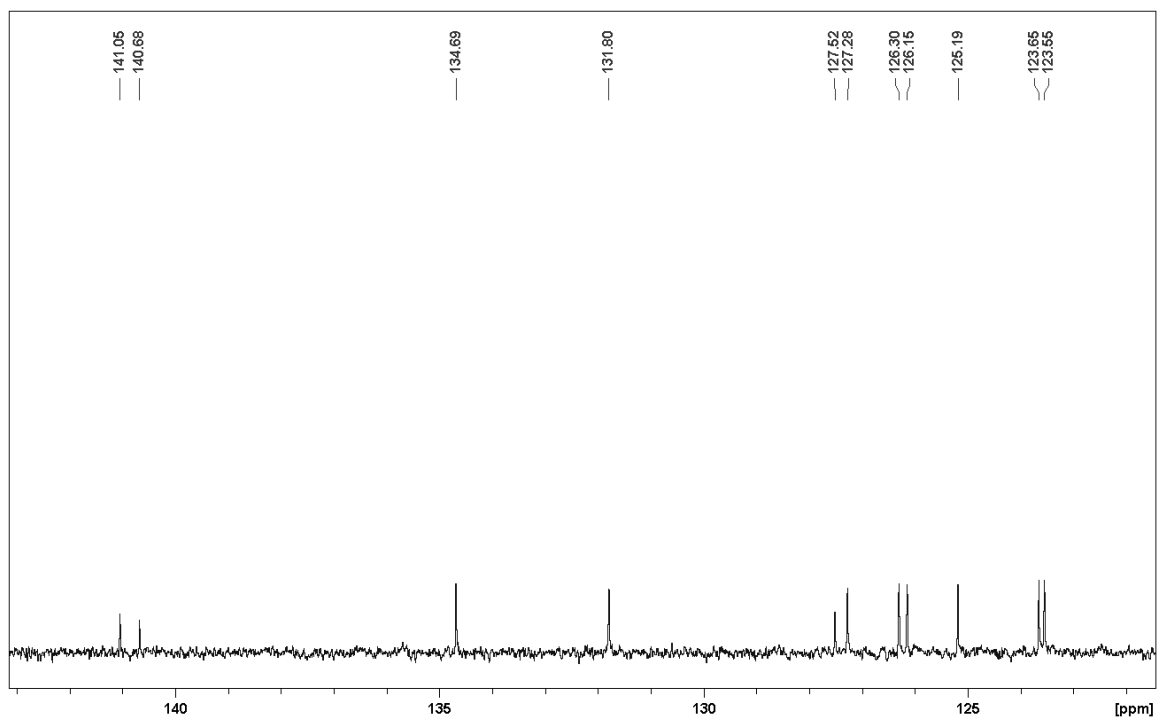
Compound **24** in CD₂Cl₂¹H (600 MHz)¹³C{¹H} (150.9 MHz) (extended view of the aromatic region)

Compound **33** in CD₂Cl₂¹¹B{¹H} (80.3 MHz, *h*_{1/2} = 690.1 Hz)¹H (400 MHz)

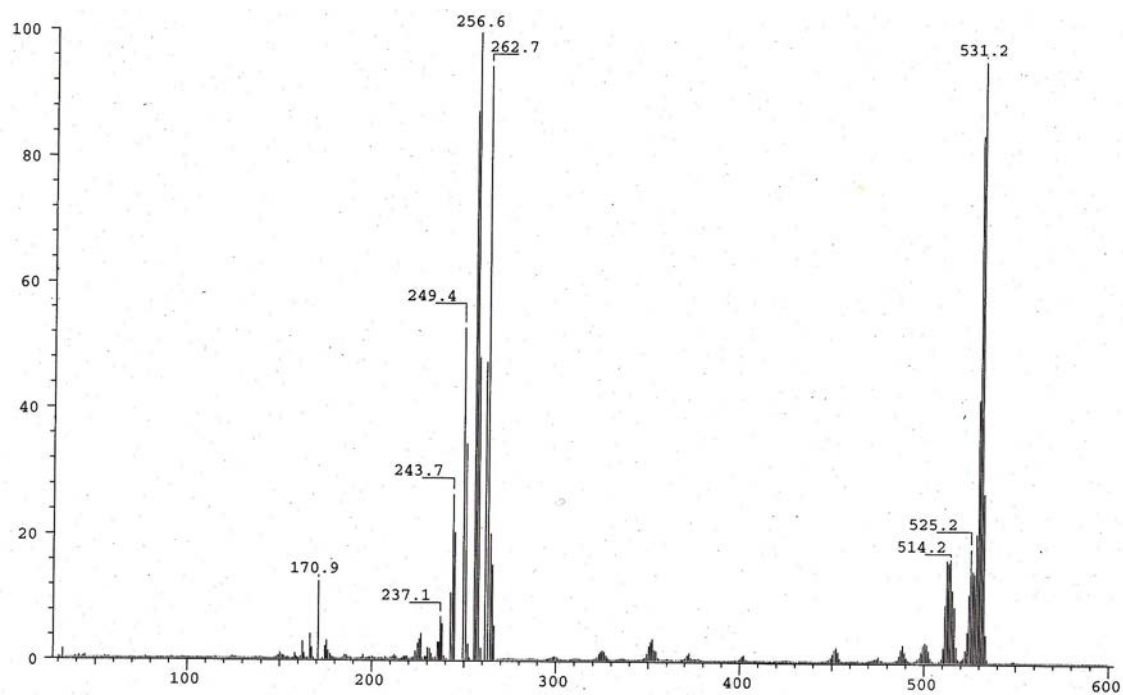
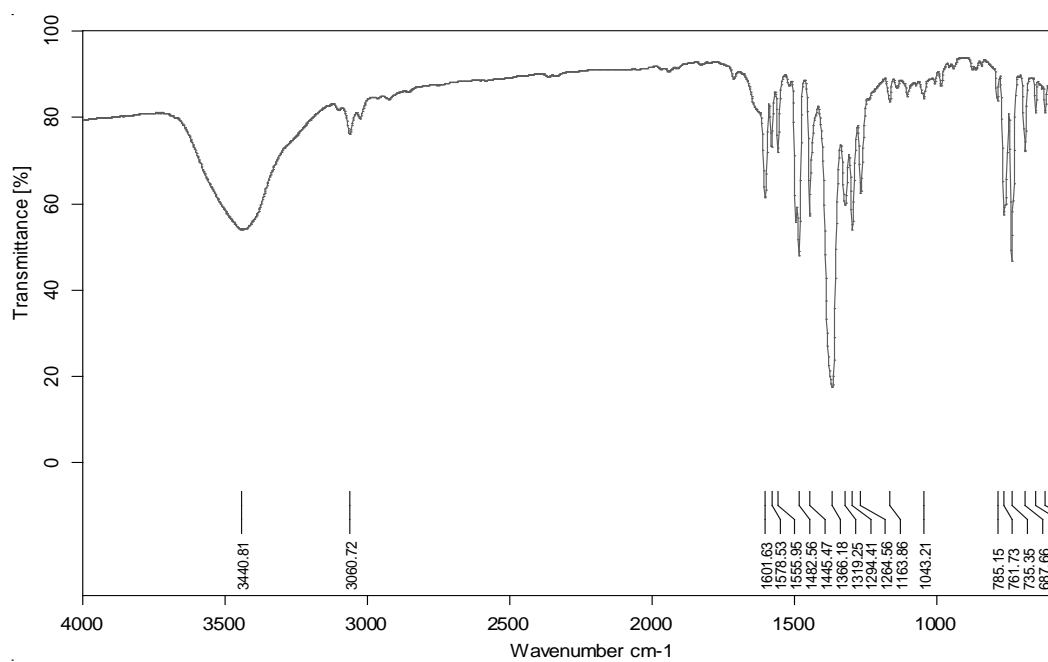
^1H - ^1H COSY (400 MHz)

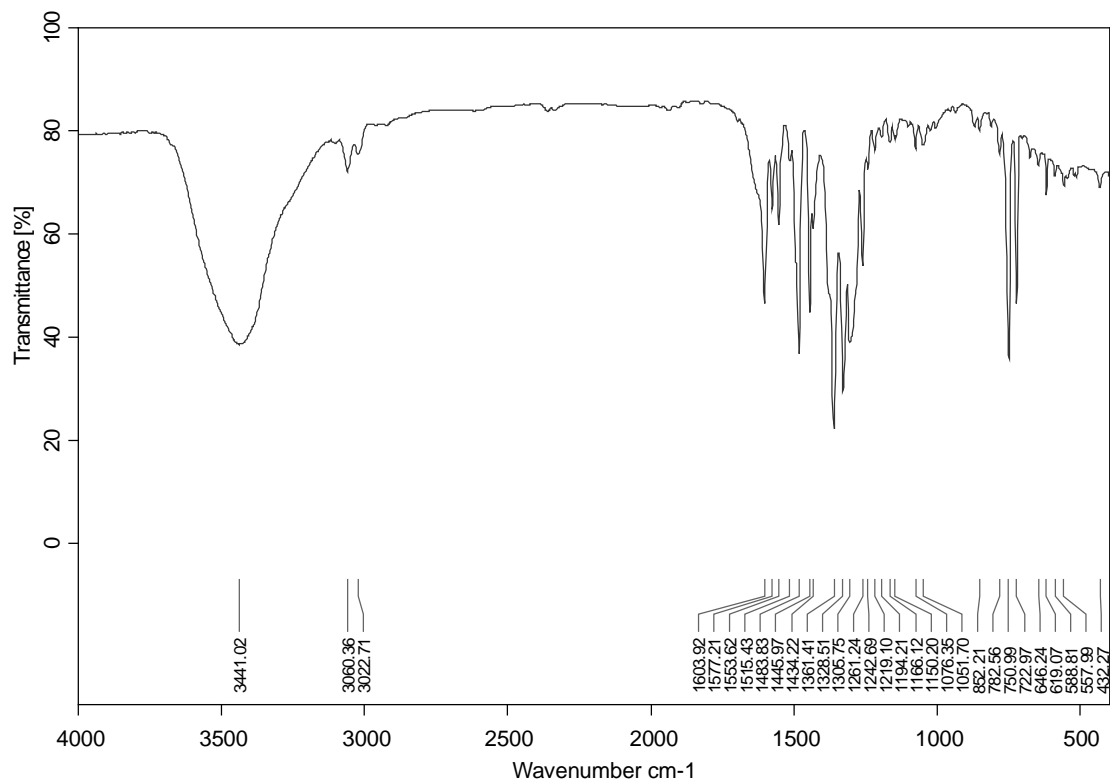


^{13}C (100.6 MHz)

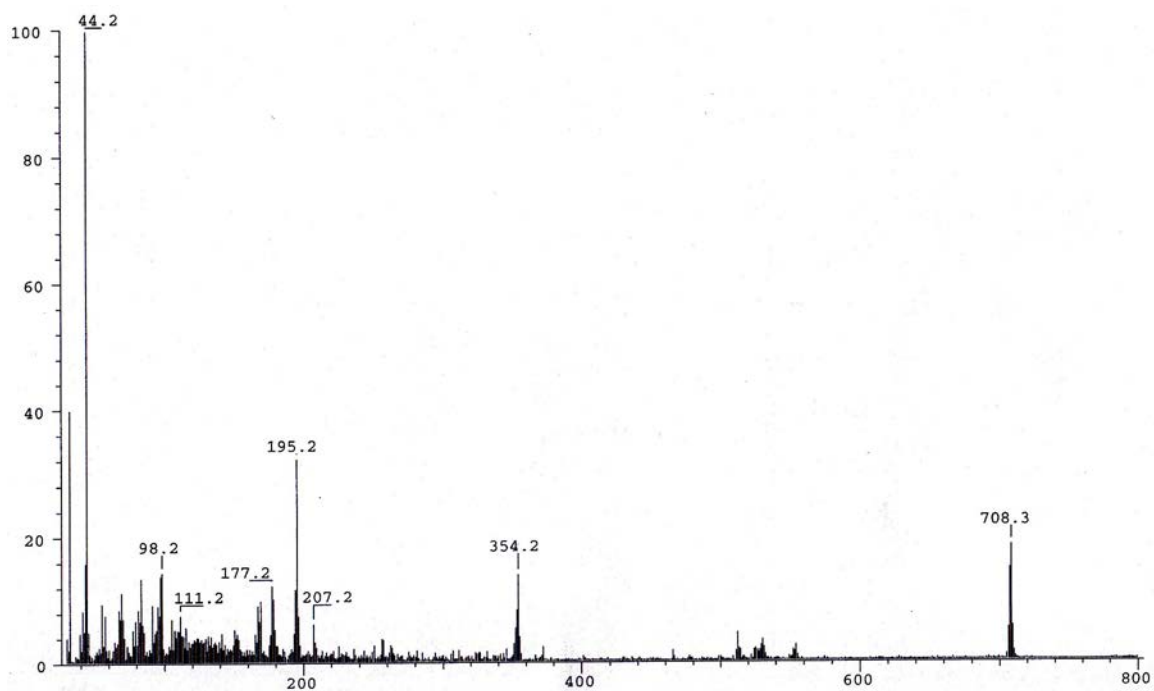


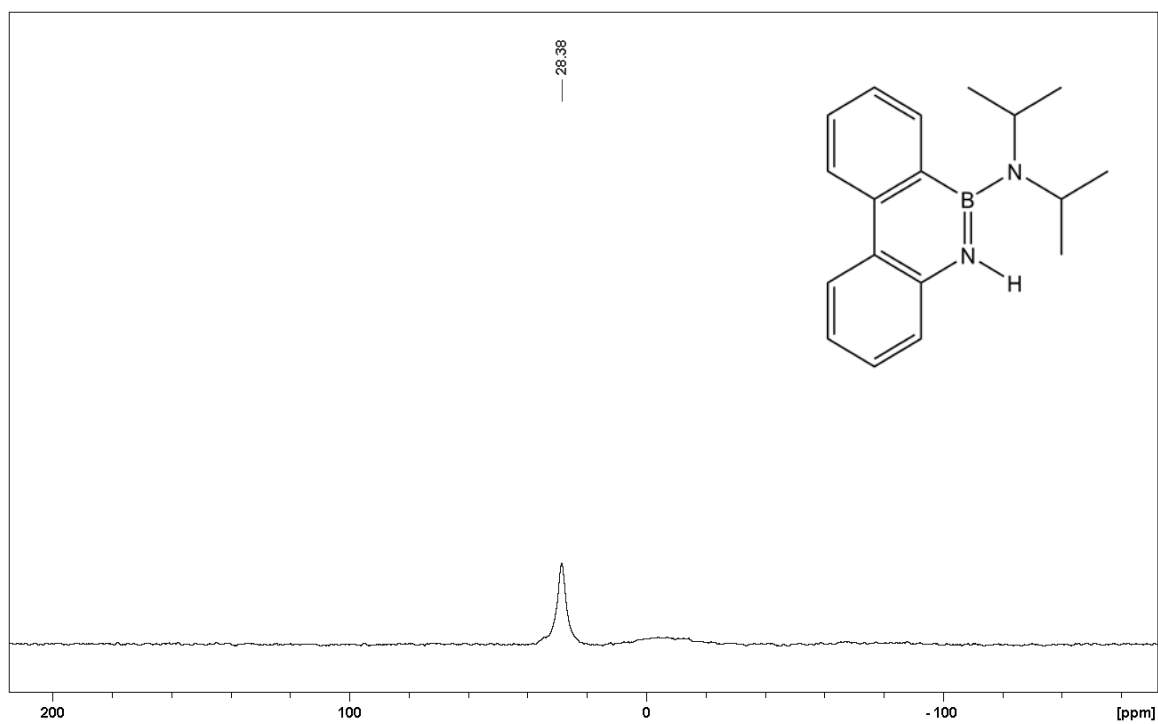
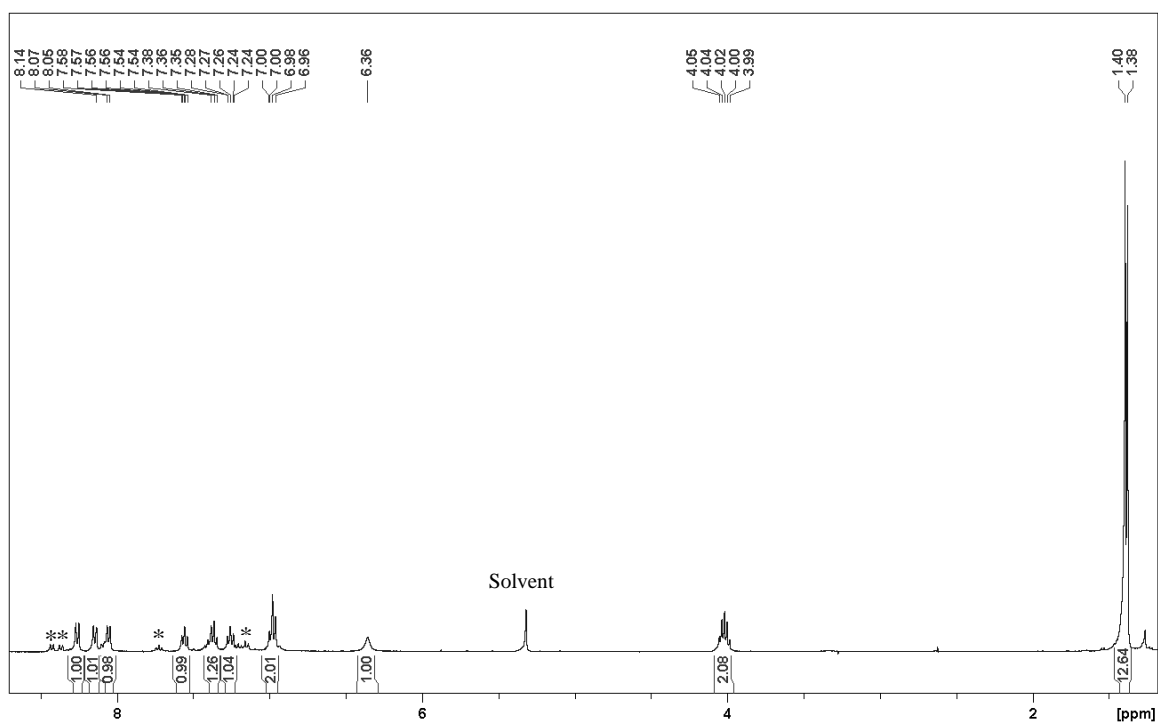
Mass Spectrum: EI (70 eV)

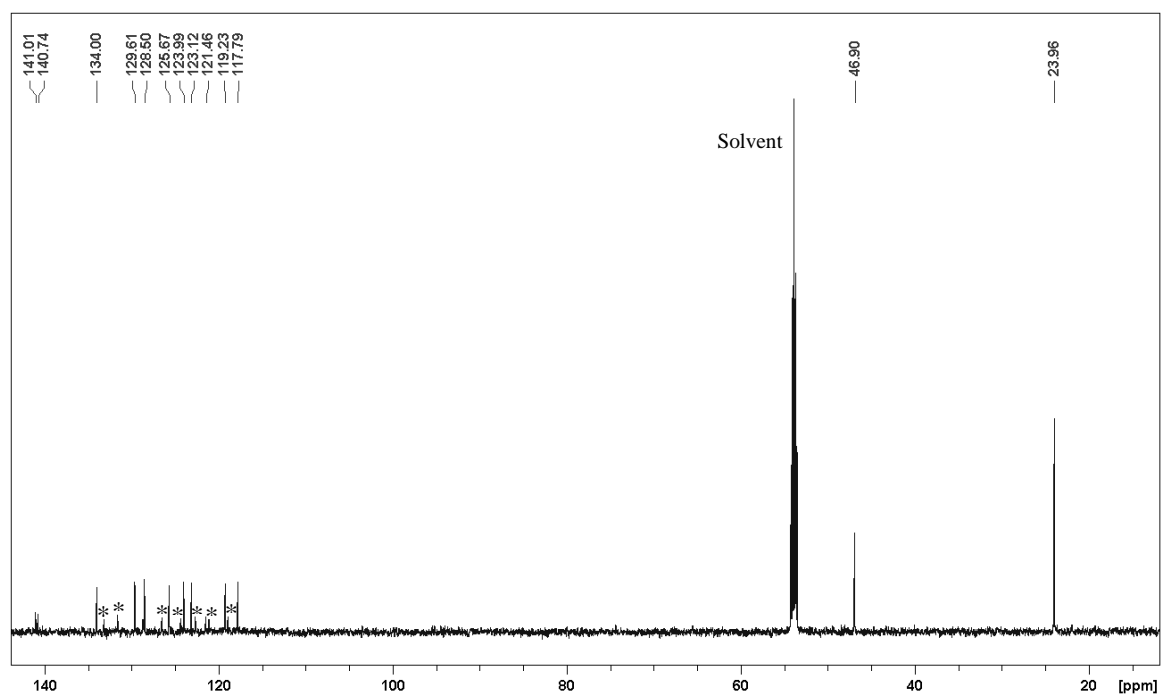
Infrared Spectrum of **33**: in KBr pellet

Infrared spectrum of compound **35**: in KBr pellet

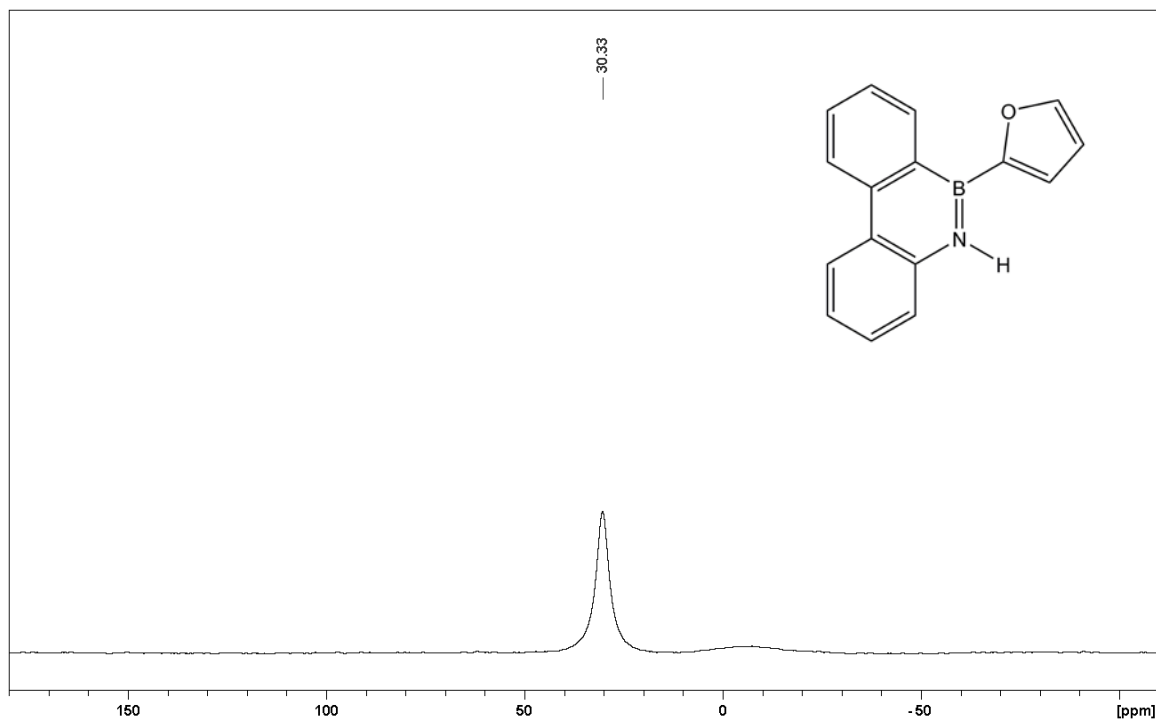
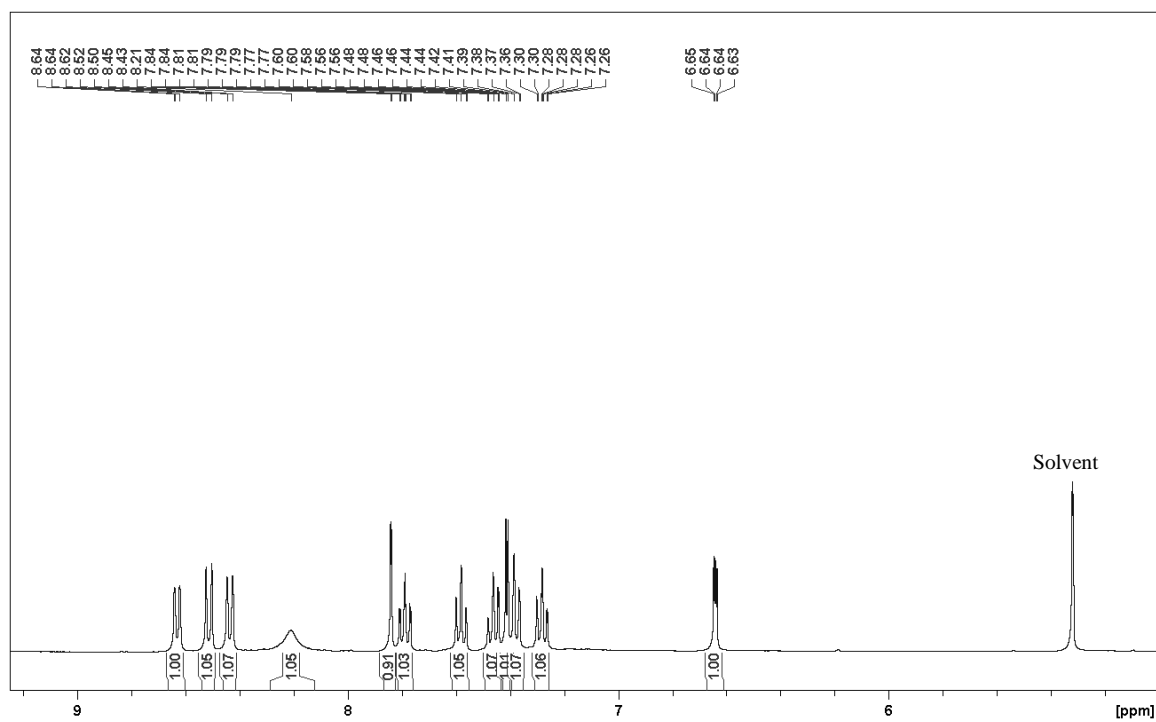
Mass (EI, 70 eV)



Compound **36** in CD₂Cl₂¹¹B{¹H} (80.3 MHz, *h*_{1/2} = 243.2 Hz)¹H (400 MHz)

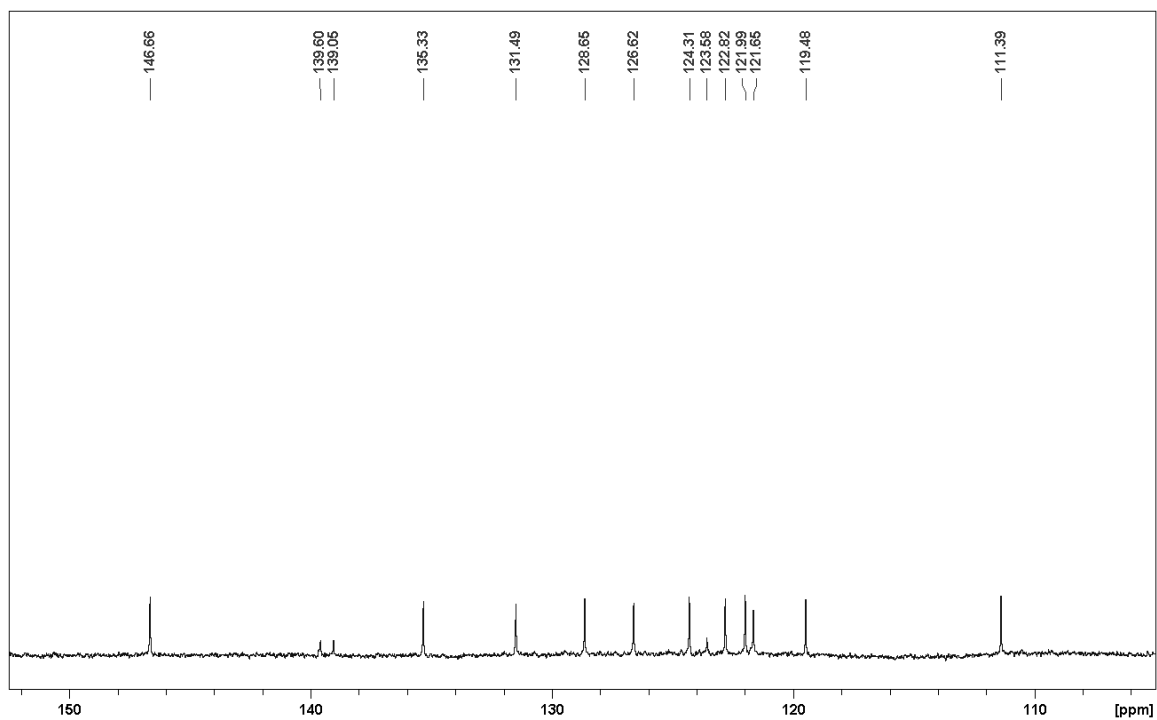
^{13}C (150.9 MHz)

* Marked peaks in the ^1H & ^{13}C spectra are due to the partially hydrolyzed product, bis-(10,9-borazarophenanthryl)ether **31**.

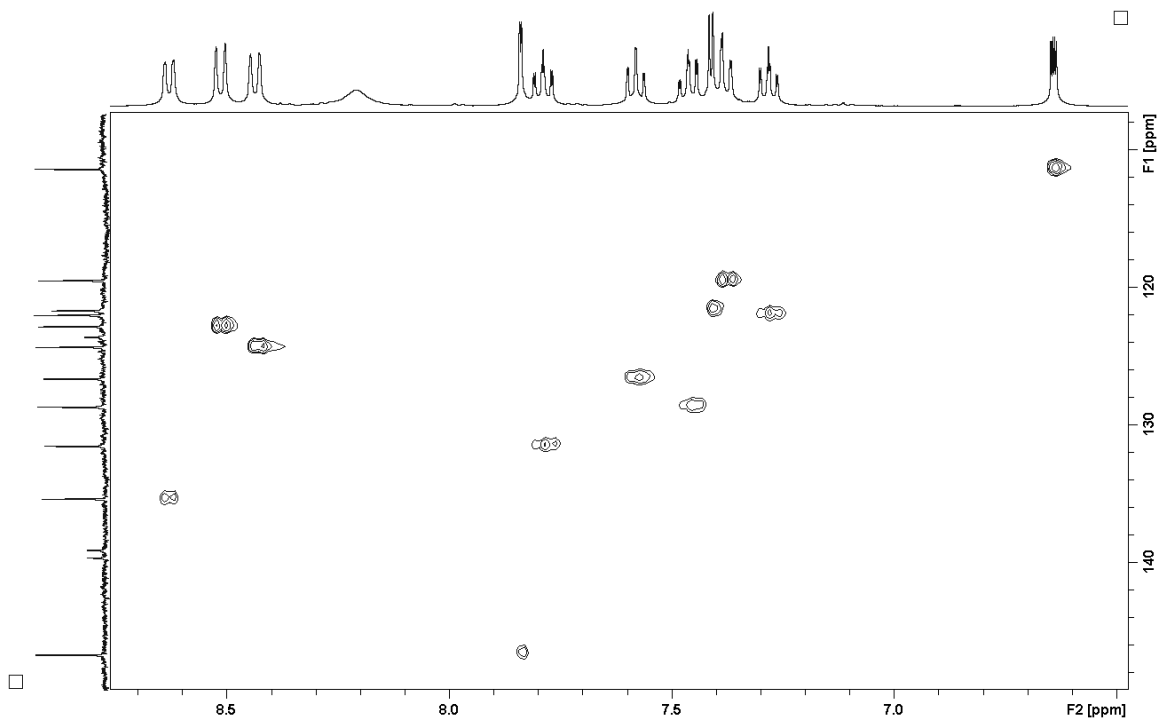
Compound **38** in CD₂Cl₂ $^{11}\text{B}\{^1\text{H}\}$ (80.3 MHz, $h_{1/2} = 287.1$ Hz) ^1H (400 MHz)

180 B. Selected NMR Spectra

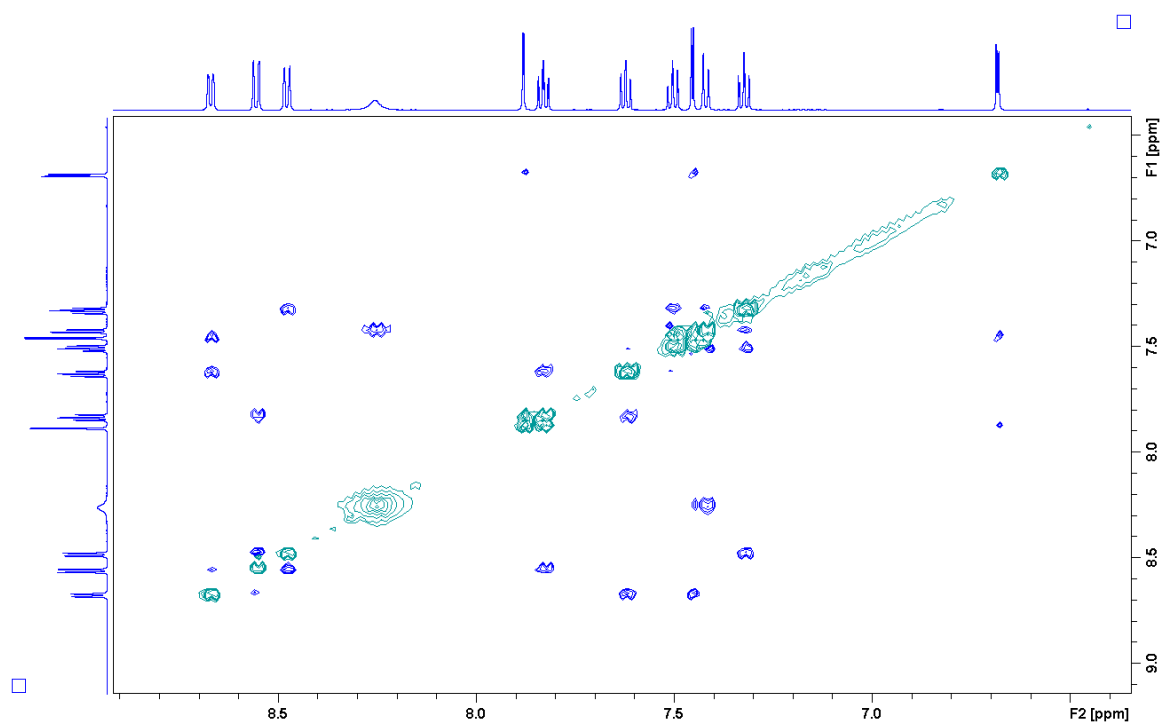
$^{13}\text{C}\{^1\text{H}\}$ (150.9 MHz)



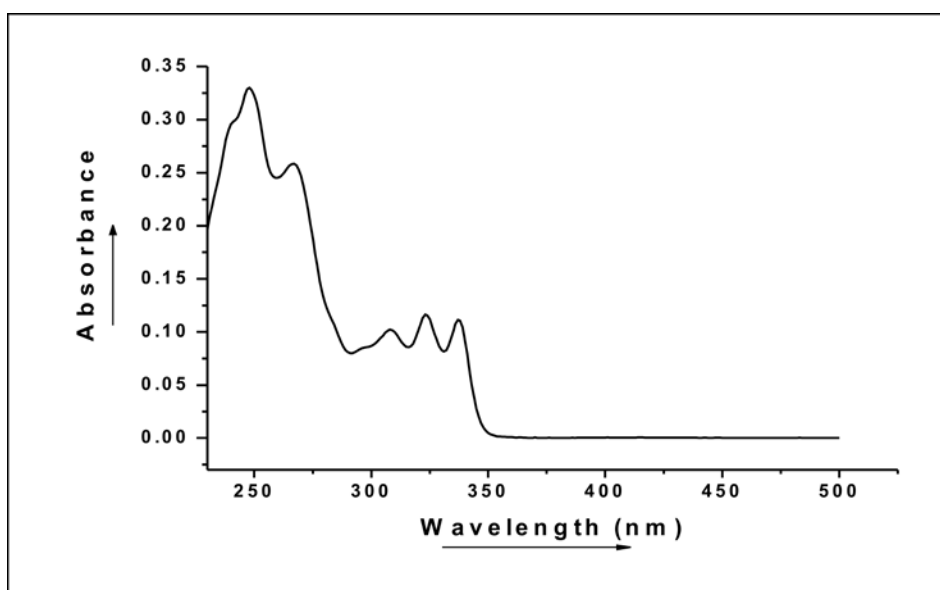
$^1\text{H}-^{13}\text{C}$ HSQC

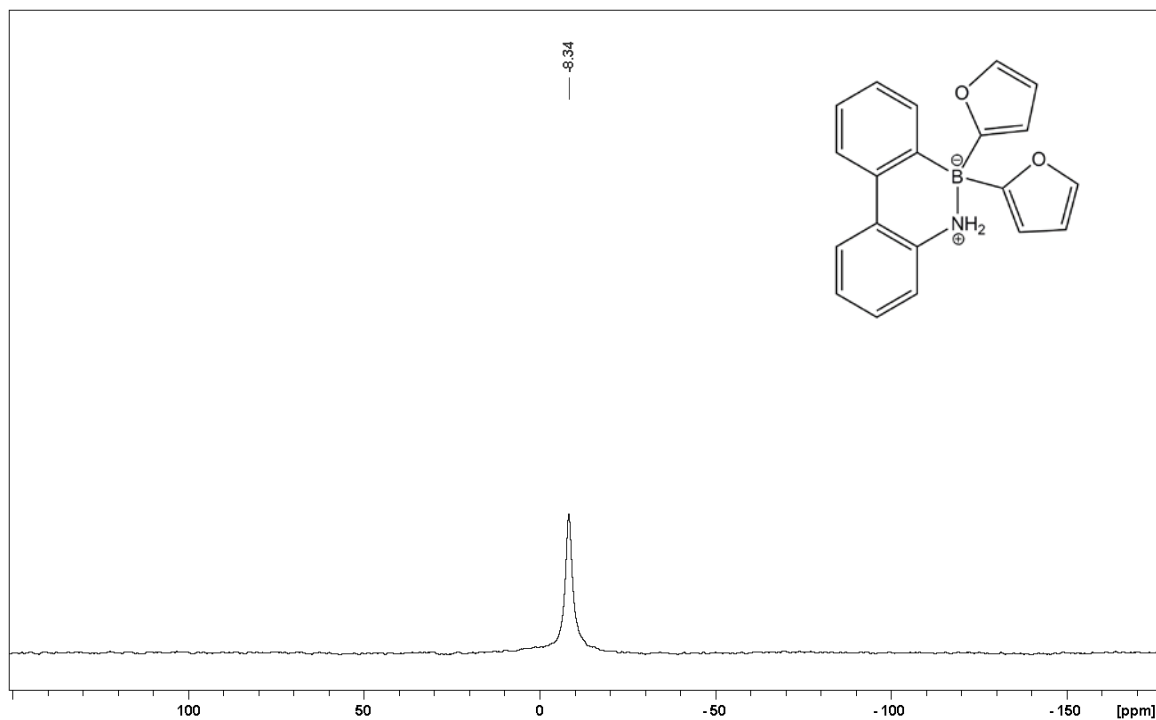
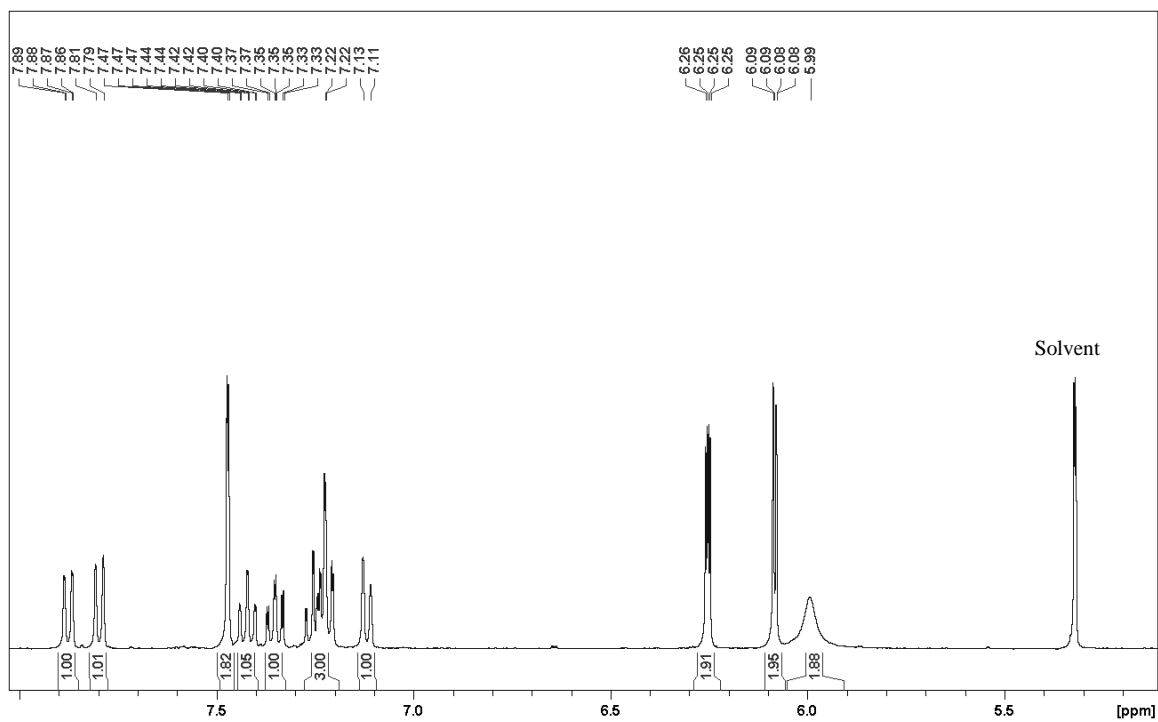


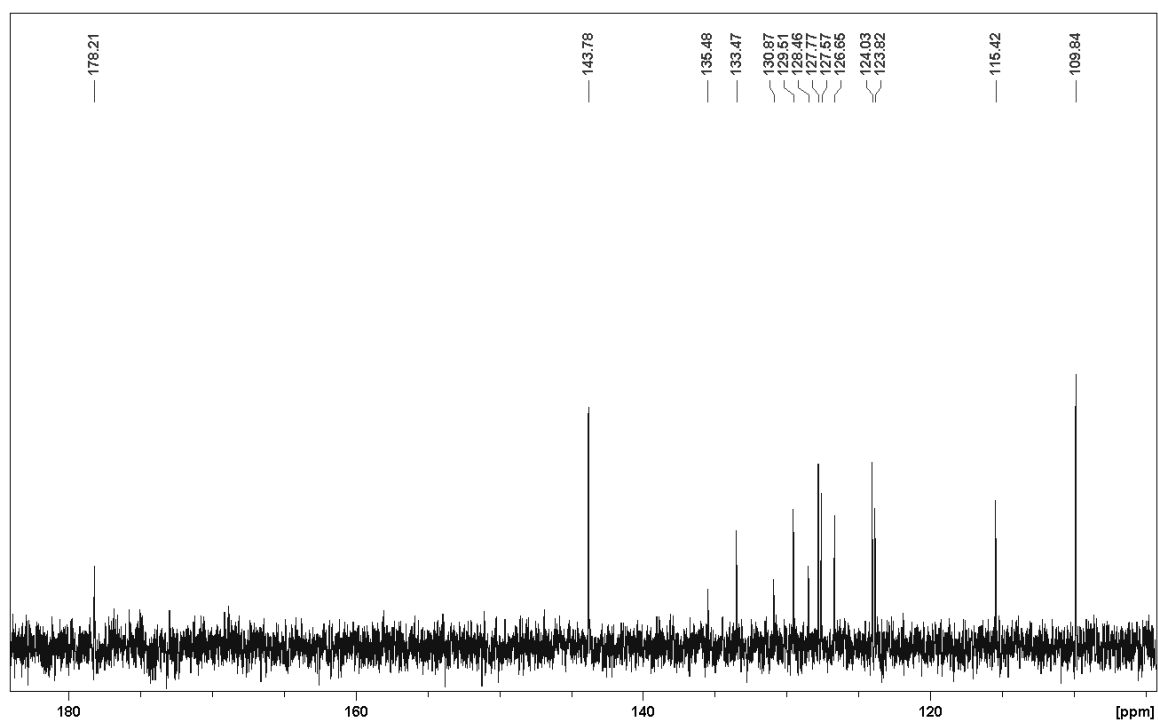
NOESY (600 MHz)



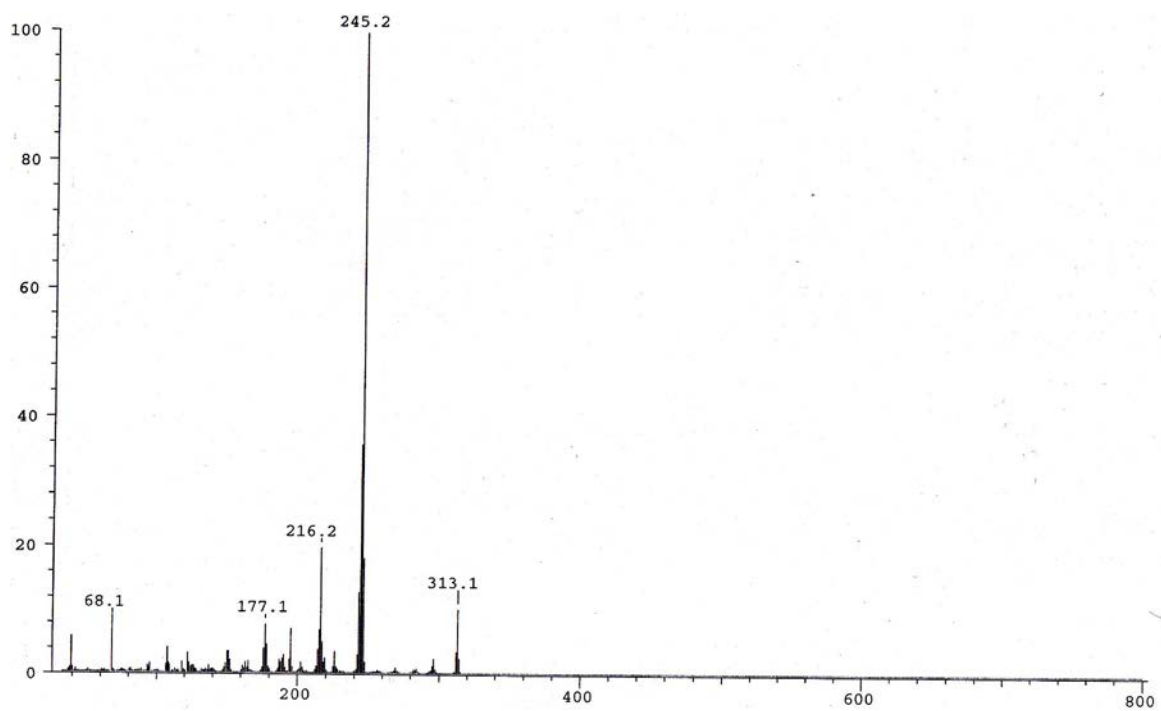
UV-Vis absorption spectrum in dichloromethane



Compound **40** in CD₂Cl₂¹¹B{¹H} (80.3 MHz, *h*_{1/2} = 181.5 Hz)¹H (400 MHz)

$^{13}\text{C}\{^1\text{H}\}$ (100.6 MHz)

Mass (EI, 70 eV)



C. Bibliography

- [1] P. Paetzold, *Adv. Inorg. Chem.* **1987**, *31*, 123.
- [2] P. Paetzold, *Pure & Appl. Chem.* **1991**, *63*, 345.
- [3] W. Pieper, D. Schmitz, P. Paetzold, *Chem. Ber.* **1981**, *114*, 3801.
- [4] M. S. Platz, Wiley-Interscience, Hoboken, **2004**.
- [5] M. T. Nguyen, *J. Chem. Soc., Chem. Commun.* **1987**, 342.
- [6] M. L. McKee, *J. Phys. Chem.* **1994**, *98*, 13243.
- [7] H. F. Bettinger, H. Bornemann, *J. Am. Chem. Soc.* **2006**, *128*, 11128.
- [8] H. F. Bettinger, M. Filthaus, *Org. Biomol. Chem.* **2010**, *8*, 5477.
- [9] H. F. Bettinger, M. Filthaus, H. Bornemann, I. M. Opperl, *Angew. Chem. Int. Ed.* **2008**, *47*, 4744.
- [10] H. F. Bettinger, M. Filthaus, P. Neuhaus, *Chem. Commun.* **2009**, 2186.
- [11] J. Breidung, H. Buerger, C. Koetting, R. Kopitzky, W. Sander, M. Senzlober, W. Thiel, H. Willner, *Angew. Chem. Int. Ed. Engl.* **1997**, *36*, 1983.
- [12] W. Sander, C. Kötting, *Chem. Eur. J.* **1999**, *5*, 24.
- [13] C. Kötting, W. Sander, *J. Am. Chem. Soc.* **1999**, *121*, 8891.
- [14] M. Filthaus, L. Schwertmann, P. Neuhaus, R. W. Seidel, I. M. Opperl, H. F. Bettinger, **2010**, *Submitted*.
- [15] A. Meller, U. Seebold, W. Maringgele, *J. Am. Chem. Soc.* **1989**, *111*, 8299.
- [16] W. Maringgele, U. Seebold, A. Heine, D. Stalke, M. Noltemeyer, G. M. Sheldrick, A. Meller, *Organometallics* **1991**, *10*, 2097.
- [17] W. Maringgele, D. Bromm, A. Meller, *Tetrahedron* **1988**, *44*, 1053.
- [18] A. Meller, W. Maringgele, G. Elter, D. Bromm, M. Noltemeyer, G. M. Sheldrick, *Chem. Ber.* **1987**, *120*, 1437.
- [19] A. Meller, D. Bromm, W. Maringgele, D. Böhler, G. Elter, *J. Organomet. Chem.* **1988**, *347*, 11.
- [20] M. Regitz, *Vol. E19b*, Methoden der Organische Chemie (Houben-Weyl) ed., G. Thieme Vlg. Stuttgart-New York, **1989**.
- [21] C. A. Thompson, L. Andrews, J. M. L. Martin, J. El-Yazal, *J. Phys. Chem.* **1995**, *99*, 13839.
- [22] R. Kinjo, B. Donnadieu, M. A. Celik, G. Frenking, G. Bertrand, *Science* **2011**, *333*, 610.
- [23] P. Bissinger, H. Braunschweig, K. Kraft, T. Kupfer, *Angew. Chem. Int. Ed. Engl.* **2011**, *50*, 4704.
- [24] H. Braunschweig, M. Colling, *J. Organomet. Chem.* **2000**, *614-615*, 18.
- [25] H. Braunschweig, T. Wagner, *Angew. Chem. Int. Ed. Engl.* **1995**, *34*, 825.

-
- [26] H. Braunschweig, B. Ganter, *J. Organomet. Chem.* **1997**, 545, 163.
- [27] H. Braunschweig, C. Kollann, U. Englert, *Eur. J. Inorg. Chem.* **1998**, 465.
- [28] H. Braunschweig, C. Kollann, K. W. Klinkhammer, *Eur. J. Inorg. Chem.* **1999**, 1523.
- [29] H. Braunschweig, C. Kollann, U. Englert, *Angew. Chem. Int. Ed. Engl.* **1998**, 37, 3179.
- [30] D. A. Addy, G. A. Pierce, D. Vidovic, D. Mallick, E. D. Jemmis, J. M. Goicoechea, S. Aldridge, *J. Am. Chem. Soc.* **2010**, 132, 4586.
- [31] H. Braunschweig, M. Colling, C. Kollann, H.-G. Stammer, *Angew. Chem. Int. Ed. Engl.* **2001**, 40, 2229.
- [32] H. Braunschweig, M. Colling, C. Hu, K. Radacki, *Angew. Chem. Int. Ed. Engl.* **2003**, 42, 205.
- [33] E. R. Lory, R. F. Porter, *J. Am. Chem. Soc.* **1973**, 95, 1766.
- [34] P. Paetzold, A. Richter, T. Thijssen, S. Würtenberg, *Chem. Ber.* **1979**, 112, 3811.
- [35] P. Paetzold, G. Stohr, H. Maisch, H. Lenz, *Chem. Ber.* **1968**, 101, 2881.
- [36] J. Kiesgen, J. Münster, P. Paetzold, *Chem. Ber.* **1993**, 126, 1559.
- [37] C. Klöfkorn, M. Schmidt, T. Spaniol, T. Wagner, O. Costisor, P. Paetzold, *Chem. Ber.* **1995**, 128, 1037.
- [38] J. Münster, P. Paetzold, E. Schröder, H. Schwan, T. v. Bennigsen-Mackiewicz, *Z. Anorg. Allg. Chem.* **2004**, 630, 2641.
- [39] B. Kröckert, K. van Bonn, P. Paetzold, *Z. Anorg. Allg. Chem.* **2005**, 631, 866.
- [40] P. Paetzold, *Phosphorous, Sulfur and Silicon and the related Elements* **1994**, 93-94, 39.
- [41] P. Paetzold, C. von Plotho, *Chem. Ber.* **1982**, 115, 2819.
- [42] K. Delpy, H.-U. Meier, P. Paetzold, C. v. Plotho, *Z. Naturforsch. B* **1984**, 39b, 1696.
- [43] K.-H. v. Bonn, T. v. Bennigsen-Mackiewicz, J. Kiesgen, C. v. Plotho, P. Paetzold, *Z. Naturforsch.* **1988**, 43b, 61.
- [44] P. Paetzold, J. Kiesgen, K. Krahe, H.-U. Meier, R. Boese, *Z. Naturforsch.* **1991**, 46b, 853.
- [45] H.-U. Meier, P. Paetzold, E. Schröder, *Chem. Ber.* **1984**, 117, 1954.
- [46] P. Paetzold, T. v. Bennigsen-Mackiewicz, *Chem. Ber.* **1981**, 114, 298.
- [47] G. Elter, M. Neuhaus, A. Meller, D. Schmidt-Bäse, *J. Organomet. Chem.* **1990**, 381, 299.
- [48] W. Luthin, G. Elter, A. Heine, D. Stalke, G. M. Sheldrick, A. Meller, *Z. Anorg. Allg. Chem.* **1992**, 608, 147.
- [49] E. Rivard, W. A. Merrill, J. C. Fettinger, R. Wolf, G. H. Spikes, P. P. Power, *Inorg. Chem.* **2007**, 46, 2971.

- [50] W. Luthin, J.-G. Stratmann, G. Elter, A. Meller, A. Heine, H. Gornitzka, *Z. Anorg. Allg. Chem.* **1995**, 621, 1995.
- [51] H. Nöth, S. Weber, *Z. Naturforsch.* **1983**, 38b, 1460.
- [52] E. v. Steuber, G. Elter, M. Noltemeyer, H.-G. Schmidt, A. Meller, *Organometallics* **2000**, 19, 5083.
- [53] P. Paetzold, E. Eleftheriadis, R. Minkwitz, V. Wölfel, R. Gleiter, P. Bischof, G. Friedrich, *Chem. Ber.* **1988**, 121, 61.
- [54] H. G. Viehe, *Angew. Chem. Int. Ed. Engl.* **1965**, 4, 746.
- [55] P. Paetzold, C. v. Plotho, G. Schmid, R. Boese, B. Schrader, D. Bougeard, U. Pfeiffer, R. Gleiter, W. Schäfer, *Chem. Ber.* **1984**, 117, 1089.
- [56] P. Paetzold, K. Delpy, R. Boese, *Z. Naturforsch.* **1988**, 43b, 839.
- [57] T. Franz, E. Hanecker, H. Nöth, W. Stöcker, W. Storch, R. Winter, *Chem. Ber.* **1986**, 119, 900.
- [58] P. Paetzold, C. v. Plotho, G. Schmid, R. Boese, *Z. Naturforsch.* **1984**, 39b, 1069.
- [59] K. Delpy, D. Schmitz, P. Paetzold, *Chem. Ber.* **1983**, 116, 2994.
- [60] H. Nöth, R. Staudigl, H.-U. Wagner, *Inorg. Chem.* **1982**, 21, 706.
- [61] P. Paetzold, E. Schröder, G. Schmid, R. Boese, *Chem. Ber.* **1985**, 118, 3205.
- [62] P. Paetzold, C. von Plotho, E. Niecke, R. Rüger, *Chem. Ber.* **1983**, 116, 1678.
- [63] P. Paetzold, K. Delpy, R. P. Hughes, W. A. Herrmann, *Chem. Ber.* **1985**, 118, 1724.
- [64] P. Paetzold, R. Truppat, *Chem. Ber.* **1983**, 116, 1531.
- [65] P. Paetzold, C. von Plotho, H. Schwan, H.-U. Meier, *Z. Naturforsch.* **1984**, 39b, 610.
- [66] H. Nöth, S. Weber, *Chem. Ber.* **1985**, 118, 2554.
- [67] E. Bulak, G. E. Herberich, I. Manners, H. Mayer, P. Paetzold, *Angew. chem. Int. Ed. Engl.* **1988**, 27, 958.
- [68] H. Nöth, *Angew. Chem. Int. Ed. Engl.* **1988**, 27, 1603.
- [69] F. A. Cotton, J. D. Jamerson, B. R. Stults, *J. Am. Chem. Soc.* **1976**, 98, 1774.
- [70] P. Paetzold, K. Delpy, *Chem. Ber.* **1985**, 118, 2552.
- [71] P. Paetzold, K. Delpy, R. Boese, *Z. Naturforsch.* **1988**, 43b, 1209.
- [72] P. J. Fazen, L. A. Burke, *Inorg. Chem.* **2006**, 45, 2494.
- [73] I. R. Dunkin, *Matrix-Isolation Techniques A Practical Approach*, Oxford University Press, **1998**.
- [74] H. F. Bettinger, *J. Am. Chem. Soc.* **2006**, 128, 2534.
- [75] H. J. Becher, *Z. Anorg. Allg. Chem.* **1957**, 289, 262.
- [76] W. Gerrard, E. F. Mooney, *J. Chem. Soc.* **1960**, 4028.
- [77] W. Gerrard, H. R. Hudson, E. F. Mooney, *J. Chem. Soc.* **1960**, 5168.
- [78] M. Baudler, A. Marx, *Z. Anorg. Allg. Chem.* **1981**, 474, 18.

-
- [79] P. N. Gates, E. J. McLaughlan, E. F. Mooney, *Spectrochim. Acta* **1965**, *21*, 1445.
- [80] J. Goubeau, M. Rahtz, H. J. Becher, *Z. Anorg. Allg. Chem.* **1954**, *275*, 161.
- [81] K. Niedenzu, J. W. Dawson, *J. Am. Chem. Soc.* **1959**, *81*, 3561.
- [82] F. Zettler, H. Hess, *Chem. Ber.* **1975**, *108*, 2269.
- [83] W. Fraenk, T. Habereeder, A. Hammerl, T. M. Klapötke, B. Krumm, P. Mayer, H. Nöth, M. Warchhold, *Inorg. Chem.* **2001**, *40*, 1334.
- [84] R. L. Mulinax, G. S. Okin, R. D. Coombe, *J. Phys. Chem.* **1995**, *99*, 6294.
- [85] I. A. Al-Jihad, B. Liu, C. J. Linnen, J. V. Gilbert, *J. Phys. Chem.* **1998**, *102*, 6220.
- [86] L. Andrews, P. Hassanzadeh, T. R. Burkholder, J. M. L. Martin, *J. Phys. Chem.* **1993**, *98*, 922.
- [87] P. A. S. Smith, *The Chemistry of Open-Chain Organic Nitrogen Compounds, Vol. 2*, W. A. Benjamin, Inc.:New York, **1966**.
- [88] M. Filthaus, PhD Thesis, Ruhr-Universität Bochum **2010**.
- [89] H. Jiao, P. v. R. Schleyer, B. R. Beno, K. N. Houk, R. Warmuth, *Angew. Chem. Int. Ed. Engl.* **1997**, *36*, 2761.
- [90] S. Sakai, *J. Mol. Struct.-Theochem* **2005**, *715*, 101.
- [91] F. D. Proft, P. v. R. Schleyer, J. H. v. Lenthe, F. Stahl, P. Geerlings, *Chem. Eur. J.* **2002**, *8*, 3402.
- [92] A. C. Scheiner, H. F. Schaefer, B. Liu, *J. Am. Chem. Soc.* **1989**, *111*, 3118.
- [93] J. G. Radziszewski, B. A. H. Jr., R. Zahradnik, *J. Am. Chem. Soc.* **1992**, *114*, 52.
- [94] A. Schweig, N. Münzel, H. Meyer, A. Heidenreich, *Struct. Chem.* **1990**, *1*, 89.
- [95] H. Gilman, B. G. Gaj, *J. Org. Chem.* **1957**, *22*, 447.
- [96] F. Leroux, M. Schlosser, *Angew. Chem. Int. Ed.* **2002**, *41*, 4272.
- [97] R. Köster, G. Benedikt, *Angew. Chem.* **1963**, *75*, 419.
- [98] R. Köster, H.-G. Willemsen, *Liebigs Ann. Chem.* **1974**, 1843.
- [99] C. K. Narula, H. Nöth, *J. Organomet. Chem.* **1985**, *281*, 131.
- [100] H. Hong, T. C. Chung, *J. Organomet. Chem.* **2004**, *689*, 58.
- [101] P. Buchalski, I. Grabowska, E. Kaminska, K. Suwinska, *Organometallics* **2008**, *27*, 2346.
- [102] S. Biswas, I. M. Oppel, H. F. Bettinger, *Inorg. Chem.* **2010**, *49*, 4499.
- [103] C. L. B. Macdonald, J. D. Gorden, A. Voigt, S. Filipponi, A. H. Cowley, *Dalton Trans.* **2008**, 1161.
- [104] T. Wagner, U. Eigendorf, G. E. Herberich, U. Englert, *Struct. Chem.* **1994**, *5*, 233.
- [105] A. J. Ashe, W. Klein, R. Rousseau, *Organometallics* **1993**, *12*, 3225.
- [106] F. Zettler, H. D. Hausen, H. Hess, *J. Organomet. Chem.* **1974**, *72*, 157.
- [107] M. M. Olmstead, P. P. Power, *J. Am. Chem. Soc.* **1986**, *108*, 4235.

- [108] P. A. Chase, W. E. Piers, B. O. Patrick, *J. Am. Chem. Soc.* **2000**, *122*, 12911.
- [109] R. J. Wehmschulte, A. A. Diaz, M. A. Khan, *Organometallics* **2003**, *22*, 83.
- [110] C. K. Narula, H. Nöth, *Inorg. Chem.* **1985**, *24*, 2532.
- [111] H. Braunschweig, I. Fernandez, G. Frenking, T. Kupfer, *Angew. Chem. Int. Ed.* **2008**, *47*, 1951.
- [112] C.-W. So, D. Watanabe, A. Wakamiya, S. Yamaguchi, *Organometallics* **2008**, *27*, 3496.
- [113] J. D. Hoefelmeyer, S. Sole, F. P. Gabbai, *Dalton Trans.* **2004**, 1254.
- [114] B. Schilling, V. Kaiser, D. E. Kaufmann, *Chem. Ber.* **1997**, *130*, 923.
- [115] J. D. Hoefelmeyer, F. P. Gabbai, *J. Am. Chem. Soc.* **2000**, *122*, 9054.
- [116] N. Wiberg, W.-C. Joo, K. H. Schmid, *Z. Anorg. Allg. Chem.* **1972**, *394*, 197.
- [117] W. Fraenk, T. M. Klapötke, B. Krumm, H. Nöth, M. Suter, M. Warchhold, *J. Chem. Soc., Dalton Trans.* **2000**, 4635.
- [118] P. I. Paetzold, *Z. Anorg. Allg. Chem.* **1963**, *326*, 47.
- [119] P. I. Paetzold, M. Gayoso, K. Dehnicke, *Chem. Ber.* **1965**, *98*, 1173.
- [120] W. Fraenk, T. M. Klapötke, B. Krumm, P. Mayer, *Chem. Commun.* **2000**, 667.
- [121] E. Wiberg, H. Michaud, *Z. Naturforsch.* **1954**, *96*, 497.
- [122] P. I. Paetzold, G. Maier, *Angew. Chem.* **1964**, *76*, 343.
- [123] P. Paetzold, H.-J. Hansen, *Z. Anorg. Allg. Chem.* **1966**, *345*, 79.
- [124] W. Fraenk, T. M. Klapötke, B. Krumm, P. Mayer, H. Nöth, H. Piotrowski, M. Suter, *J. Fluorine Chem.* **2001**, *112*, 73.
- [125] P. Paetzold, G. Maier, *Chem. Ber.* **1970**, *103*, 281.
- [126] W. Fraenk, T. Habereeder, T. M. Klapötke, H. Nöth, K. Polborn, *J. Chem. Soc., Dalton Trans.* **1999**, 4283.
- [127] P. I. Paetzold, *Fortschr. Chem. Forsch.* **1967**, *8*, 437.
- [128] U. Müller, *Z. Anorg. Allg. Chem.* **1971**, *382*, 110.
- [129] P. v. R. Schleyer, P. K. Freeman, H. Jiao, B. Goldfuss, *Angew. Chem. Int. Ed.* **1995**, *34*, 337.
- [130] C. Fan, W. E. Piers, M. Parvez, *Angew. Chem. Int. Ed.* **2009**, *48*, 2955.
- [131] G. A. Olah, G. K. S. Prakash, G. Liang, P. W. Westerman, K. Kunde, J. Chandrasekhar, P. R. Schleyer, *J. Am. Chem. Soc.* **1980**, *102*, 4485.
- [132] A. Ledwith, D. G. Morris, *J. Chem. Soc.* **1964**, 508.
- [133] G. W. Cowell, T. D. George, A. Ledwith, D. G. Morris, *J. Chem. Soc. B* **1966**, 1169.
- [134] G. W. Cowell, A. Ledwith, *J. Chem. Soc. B* **1967**, 695.
- [135] T. L. Amyes, J. P. Richard, M. Novak, *J. Am. Chem. Soc.* **1992**, *114*, 8032.

-
- [136] C. F. Rodriguez, D. L. Vuckovic, A. C. Hopkinson, *J. Mol. Struct. (Theochem)* **1996**, 363, 131.
- [137] H. Jiao, P. v. R. Schleyer, Y. Mo, M. A. McAllister, T. T. Tidwell, *J. Am. Chem. Soc.* **1997**, 119, 7075.
- [138] F. Dietz, N. Tyutyulkov, M. Rabinovitz, *J. Chem. Soc. Perkin Trans. 2* **1993**, 157.
- [139] D. R. Armstrong, P. G. Perkins, *J. Chem. Soc. (A)* **1966**, 1026.
- [140] C. P. Brock, R. P. Minton, K. Niedenzu, *Acta Cryst. Sect. C* **1987**, 43, 1775.
- [141] M. A. Beckett, G. C. Strickland, K. S. Varma, D. E. Hibbs, M. B. Hursthouse, K. M. A. Mailk, *J. Organomet. Chem* **1997**, 535, 33.
- [142] R. Boese, M. Polk, D. Bläser, *Angew. Chem.* **1987**, 99, 239.
- [143] G. Alcaraz, L. Euzenat, O. Mongin, C. Katan, I. Ledoux, J. Zyss, M. Blanchard-Desce, M. Vaultier, *Chem. Commun.* **2003**, 2766.
- [144] K. Hoffman, E. Weiss, *J. Organomet. Chem.* **1974**, 67, 221.
- [145] F. P. Tsui, T. M. Vogel, G. Zon, *J. Am. Chem. Soc.* **1974**, 96, 7144.
- [146] F. P. Tsui, Y. H. Chang, T. M. Vogel, G. Zon, *J. Org. Chem.* **1976**, 41, 3381.
- [147] W. H. Atwell, D. R. Weyenberg, J. G. Uhlmann, *J. Am. Chem. Soc.* **1969**, 91, 2025.
- [148] A. G. Brook, P. J. Dillon, *Can. J. Chem.* **1969**, 47, 4347.
- [149] A. G. Brook, D. R. Weyenberg, *J. Am. Chem. Soc.* **1968**, 90, 3438.
- [150] A. G. Brook, D. R. Weyenberg, *J. Organomet. chem.* **1966**, 5, 594.
- [151] T. J. Barton, M. Juvet, *Tetrahedron Lett.* **1975**, 3893.
- [152] Y. H. Chang, F.-T. Chiu, G. Zon, *J. Org. Chem.* **1981**, 46, 342.
- [153] P. Paetzold, H.-U. Meier, H. Schwan, C. v. Plotho, *Z. Naturforsch.* **1988**, 43b, 1676.
- [154] D. Männig, H. Nöth, H. Prigge, A.-R. Rotsch, S. Gopinathan, J. W. Wilson, *J. Organomet. Chem.* **1986**, 310, 1.
- [155] A. Sebald, B. Wrackmeyer, *J. Organomet. chem.* **1986**, 307, 157.
- [156] H. Braunschweig, T. Kupfer, *Chem. Commun.* **2008**, 4487.
- [157] G. E. Herberich, H. Ohst, *Z. Naturforsch. Teil B* **1983**, 38, 1388.
- [158] G. E. Herberich, M. Hostalek, R. Laven, R. Boese, *Angew. Chem.* **1990**, 102, 330.
- [159] G. E. Herberich, H. Ohst, *Chem. Ber.* **1985**, 118, 4303.
- [160] G. E. Herberich, M. Negele, *J. Organomet. Chem.* **1988**, 350, 81.
- [161] G. E. Herberich, U. Englert, M. Hostalek, R. Laven, *Chem. Ber.* **1991**, 124, 17.
- [162] K. Witke, P. Reich, H. Kriegsmann, *J. Organomet. Chem.* **1968**, 15, 37.
- [163] P. Boudjouk, R. West, *Intra-Sci. Che., Rep.* **1973**, 7, 65.
- [164] R. West, *Adv. Organomet. Chem.* **1977**, 16, 1.
- [165] R. Wolfgramm, U. Klingebiel, M. Noltemeyer, *Z. Anorg. Allg. Chem.* **1998**, 624, 865.

- [166] R. Wolfgramm, U. Klingebiel, *Z. Anorg. Allg. Chem.* **1998**, *624*, 1031.
- [167] R. Wolfgramm, T. Müller, U. Klingebiel, *Organometallics* **1998**, *17*, 3222.
- [168] F. Diedrich, U. Klingebiel, F. Dall'Antonia, C. Lehmann, M. Noltemeyer, T. R. Schneider, *Organometallics* **2000**, *19*, 5376.
- [169] F. Diedrich, U. Klingebiel, W. Schäfer, *J. Organomet. chem.* **1999**, *588*, 242.
- [170] R. West, P. Boudjouk, T. A. Matuszko, *J. Am. Chem. Soc.* **1969**, *91*, 5184.
- [171] R. West, P. Boudjouk, *J. Am. Chem. Soc.* **1973**, *95*, 3987.
- [172] U. Wannagat, O. Smrekar, *Monatsch. Chem.* **1969**, *100*, 750.
- [173] P. Nowakowski, R. West, *J. Am. Chem. Soc.* **1976**, *98*, 5616.
- [174] C. Summerford, K. Wade, *J. Chem. Soc. A* **1970**, 2010.
- [175] S. Biswas, C. Maichle-Mössmer, H. F. Bettinger, unpublished work.
- [176] K. D. M. Harris, B. M. Kariuki, C. Lambropoulos, D. Philip, J. M. A. Robinson, *Tetrahedron* **1997**, *53*, 8599.
- [177] J. M. A. Robinson, B. M. Kariuki, D. Philip, K. D. M. Harris, *Tetrahedron Lett.* **1997**, *38*, 6281.
- [178] P. R. Ashton, K. D. M. Harris, B. M. Kariuki, D. Philip, J. M. Robinson, N. Spencer, *J. Chem. Soc., Perkin Trans. 2* **2001**, 2166.
- [179] H. Nöth, W. Storch, *Chem. Ber.* **1976**, *109*, 884.
- [180] J. R. Galsworthy, M. L. H. Green, V. C. Williams, A. N. Chernega, *Polyhedron* **1998**, *17*, 119.
- [181] E. Frainnet, F. Duboudin, F. Dabescat, G. C. R. Vincon, *Acad. Sci., Ser. C* **1973**, *276*, 1469.
- [182] M. T. Reetz, *J. Organomet. Chem.* **1977**, *16*, 33.
- [183] C. Trindle, D. D. Schillady, *J. Am. Chem. Soc.* **1973**, *95*, 703.
- [184] S. Schmatz, F. Diedrich, C. Ebker, U. Klingebiel, *Eur. J. Inorg. Chem.* **2002**, 876.
- [185] T. Albrecht, G. Elter, A. Meller, *Z. Anorg. Allg. Chem.* **1999**, *625*, 1453.
- [186] R. W. Hoffmann, *Dehydrobenzene and Cycloalkynes, Vol. 11*, Verlag Chemie Weinheim/Bergstr; Academic Press New York and London, **1967**.
- [187] G. Wittig, G. Pieper, G. Fuhrmann, *Ber. Dtsch. Chem. Ges.* **1940**, *73*, 1193.
- [188] G. Wittig, *Naturwiss.* **1942**, *30*, 696.
- [189] G. Wittig, L. Pohmer, *Angew. Chem.* **1955**, *67*, 348.
- [190] J. D. Roberts, H. E. Simmons, L. A. Carlsmith, C. W. Vaughan, *J. Am. Chem. Soc.* **1953**, *75*, 3290.
- [191] R. Huisgen, H. Rist, *Naturwiss.* **1954**, *41*, 358.
- [192] M. J. S. Dewar, V. P. Kubba, R. Pettit, *J. Chem. Soc.* **1958**, 3073.
- [193] M. J. S. Dewar, R. B. K. Dewar, Z. L. F. Gaibel, *Org. Synth.* **1966**, *46*, 65.

-
- [194] M. J. D. Bosdet, C. A. Jaska, W. E. Piers, T. S. Sorensen, M. Parvez, *Org. Lett.* **2007**, *9*, 1395.
- [195] J. March, *Advanced Organic Chemistry*, 4th ed., Wiley-Interscience, New York, **1992**.
- [196] W. I. Cross, M. P. Lightfoot, F. S. Mair, R. G. Pritchard, *Inorg. Chem.* **2000**, *39*, 2690.
- [197] B. J. Kim, D. S. Matteson, *Angew. Chem. Int. Ed.* **2004**, *43*, 3056.
- [198] H. C. Brown, E. Negishi, *J. Am. Chem. Soc.* **1971**, *93*, 6682.
- [199] W. E. Piers, S. C. Bourke, K. D. Conroy, *Angew. Chem. Int. Ed.* **2005**, *44*, 5016.
- [200] A. J. V. Marwitz, J. T. Jenkins, L. N. Zakharov, S.-Y. Liu, *Angew. Chem. Int. Ed.* **2010**, *49*, 7444.
- [201] I. Ghesner, W. E. Piers, M. Parvez, R. McDonald, *Chem. Commun.* **2005**, 2480.
- [202] K. Ma, J. W. Bats, M. Wagner, *Acta. Cryst.* **2001**, *E57*, o846.
- [203] T. K. Wood, W. E. Piers, B. A. Keay, M. Parvez, *Chem. Commun.* **2009**, 5147.
- [204] B. M. Mikhailov, M. E. Kuimova, *J. Organomet. Chem.* **1976**, *116*, 123.
- [205] S. Hüinig, I. Wehner, *Heterocycles* **1989**, *28*, 359.
- [206] L. Ding, K. Ma, F. F. Bains, M. Bolte, P. Zanello, M. Wagner, *Organometallics* **2001**, *20*, 1041.
- [207] A. Prokofjevs, J. W. Kampf, E. Vedejs, *Angew. Chem. Int. Ed.* **2011**, *50*, 2098.
- [208] M. J. S. Dewar, V. P. Kubba, *Tetrahedron* **1959**, *7*, 213.
- [209] M. J. S. Dewar, P. Maitlis, *J. Am. Chem. Soc.* **1961**, *83*, 187.
- [210] R. G. Pearson, F. V. Williams, *J. Am. Chem. Soc.* **1953**, *75*, 3073.
- [211] R. H. Linnel, *J. Org. Chem.* **1960**, *25*, 290.
- [212] H. R. Kricheldorf, *Makromol. Chem.* **1974**, *175*, 3325.
- [213] J. Stevens, S. Nasrazadani, *PowerPlant Chem.* **2011**, *13*, 212.
- [214] S. Biswas, M. Müller, C. Tönshoff, K. Eichele, C. Maichle-Mössmer, A. Ruff, B. Speiser, H. F. Bettinger, *Submitted* **2010**.
- [215] R. Köster, K. Iwasaki, S. Hattori, Y. Morita, *Liebigs Ann. Chem.* **1968**, *720*, 23.
- [216] K. Niedenzu, J. W. Dawson, *Boron-Nitrogen Compounds*, Springer, Berlin-Heidelberg-New York, **1965**.
- [217] G. C. Culling, M. J. S. Dewar, P. A. Marr, *J. Am. Chem. Soc.* **1964**, *86*, 1125.
- [218] R. Köster, S. Hattori, Y. Morita, *Angew. Chem. Int. Ed.* **1965**, *4*, 695.
- [219] P. J. Roberts, D. J. Brauer, Y.-H. Tsay, C. Krüger, *Acta. Cryst.* **1974**, *B30*, 2673.
- [220] R. A. Jones, *The Chemistry of Heterocyclic Compounds, Part 1, Pyrroles, Vol. 48*, Wiley-interscience, **1990**.
- [221] R. R. Fraser, M. Bresse, T. S. Mansour, *J. Chem. Soc., Chem. Commun.* **1983**, 620.

- [222] L. Eriksson, K. Vyakaranam, J. Ludvik, J. Michl, *J. Org. Chem.* **2007**, 72, 2351.
- [223] M. Hu, J. Li, S. Q. Yao, *Org. Lett.* **2008**, 10, 5529.
- [224] P. Spagnolo, P. Zanirato, *Tetrahedron Lett.* **1987**, 28, 961.
- [225] P. Spagnolo, P. Zanirato, *J. Chem. Soc. Perkin Trans. 1* **1988**, 2615.
- [226] T. M. Gilbert, *Organometallics* **2003**, 22, 2298.
- [227] J. W. Coe, M. C. Wirtz, C. G. Basore, J. Candler, *Org. Lett.* **2004**, 6, 1589.
- [228] G. R. Fulmer, A. J. M. Miller, N. H. Sherden, H. E. Gottlieb, A. Nudelman, B. M. Stoltz, J. E. Bercaw, K. I. Goldberg, *Organometallics* **2010**, 29, 2176.
- [229] G. M. Sheldrick, *Acta. Crystallogr.* **2008**, A64, 112.
- [230] G. M. Sheldrick, *Acta. Cryst.* **1990**, A46, 467.
- [231] M. J. Frisch, G. W. Trucks, H. B. Schlegel, G. E. Scuseria, M. A. Robb, J. R. Cheeseman, G. Scalmani, V. Barone, B. Mennucci, G. A. Petersson, H. Nakatsuji, M. Caricato, X. Li, H. P. Hratchian, A. F. Izmaylov, J. Bloino, G. Zheng, J. L. Sonnenberg, M. Hada, M. Ehara, K. Toyota, R. Fukuda, J. Hasegawa, M. Ishida, T. Nakajima, Y. Honda, O. Kitao, H. Nakai, T. Vreven, J. A. Montgomery, J. E. Peralta, F. Ogliaro, M. Bearpark, J. J. Heyd, E. Brothers, K. N. Kudin, V. N. Staroverov, R. Kobayashi, J. Normand, K. Raghavachari, A. Rendell, J. C. Burant, S. S. Iyengar, J. Tomasi, M. Cossi, N. Rega, J. M. Millam, M. Klene, J. E. Knox, J. B. Cross, V. Bakken, C. Adamo, J. Jaramillo, R. Gomperts, R. E. Stratmann, O. Yazyev, A. J. Austin, R. Cammi, C. Pomelli, J. W. Ochterski, R. L. Martin, K. Morokuma, V. G. Zakrzewski, G. A. Voth, P. Salvador, J. J. Dannenberg, A. D. D. S. Dapprich, O. Farkas, J. B. Foresman, J. V. Ortiz, J. Cioslowski, D. J. Fox, Rev. A. 02 ed., Gaussian, Inc., Wallingford, CT, **2009**.
- [232] W. J. Hehre, R. Ditchfield, J. A. Pople, *J. Chem. Phys.* **1972**, 56, 2257.
- [233] P. C. Hariharan, J. A. Pople, *Theor. Chim. Acta* **1973**, 28, 213.
- [234] M. J. Frisch, J. A. Pople, J. S. Binkley, *J. Chem. Phys.* **1984**, 80, 3265.
- [235] A. D. Becke, *J. Chem. Phys.* **1993**, 98, 5648.
- [236] C. Lee, W. Yang, R. G. Parr, *Phys. Rev. B* **1988**, 37, 785.
- [237] B. Miehlich, A. Savin, H. Stoll, H. Preuss, *Chem. Phys. Lett.* **1989**, 157, 200.

Curriculum Vitae

Sunanda Biswas

Personal Information

Name Sunanda Biswas
Date of Birth 14th November 1984
Nationality Indian
Marital Status Single

Present Address

Gösstrasse 55, 215
72070 Tübingen,
Germany

Permanent Address

Vill: Subarnapur (Milanpalli)
Post: Subarnapur
P.S.: Haringhata
Dist: Nadia
West Bengal, India.
PIN 741249

Education

09/2007 – 11/2011 PhD student at Eberhard Karls Universität Tübingen, Germany. Dissertation title “*Boron-Nitrogen Derivatives of Organic Reactive Intermediates.*”
07/2005 – 07/2007 Master of Science in Chemistry at Indian Institute of Technology Madras, Tamilnadu, India.
08/2002 – 07/2005 Bachelor of Science (with Honors) in Chemistry at Chakdaha College, University of Kalyani, West Bengal, India.
08/2000 – 06/2002 Higher Secondary at Rajlaksmi Kanya Vidyapith, Barojaguli, Nadia, West Bengal, India.
08/1998 – 06/2000 Secondary Education at Rajlaksmi Kanya Vidyapith, Barojaguli, Nadia, West Bengali, India.